esa bulletin

number 100 - december 1999

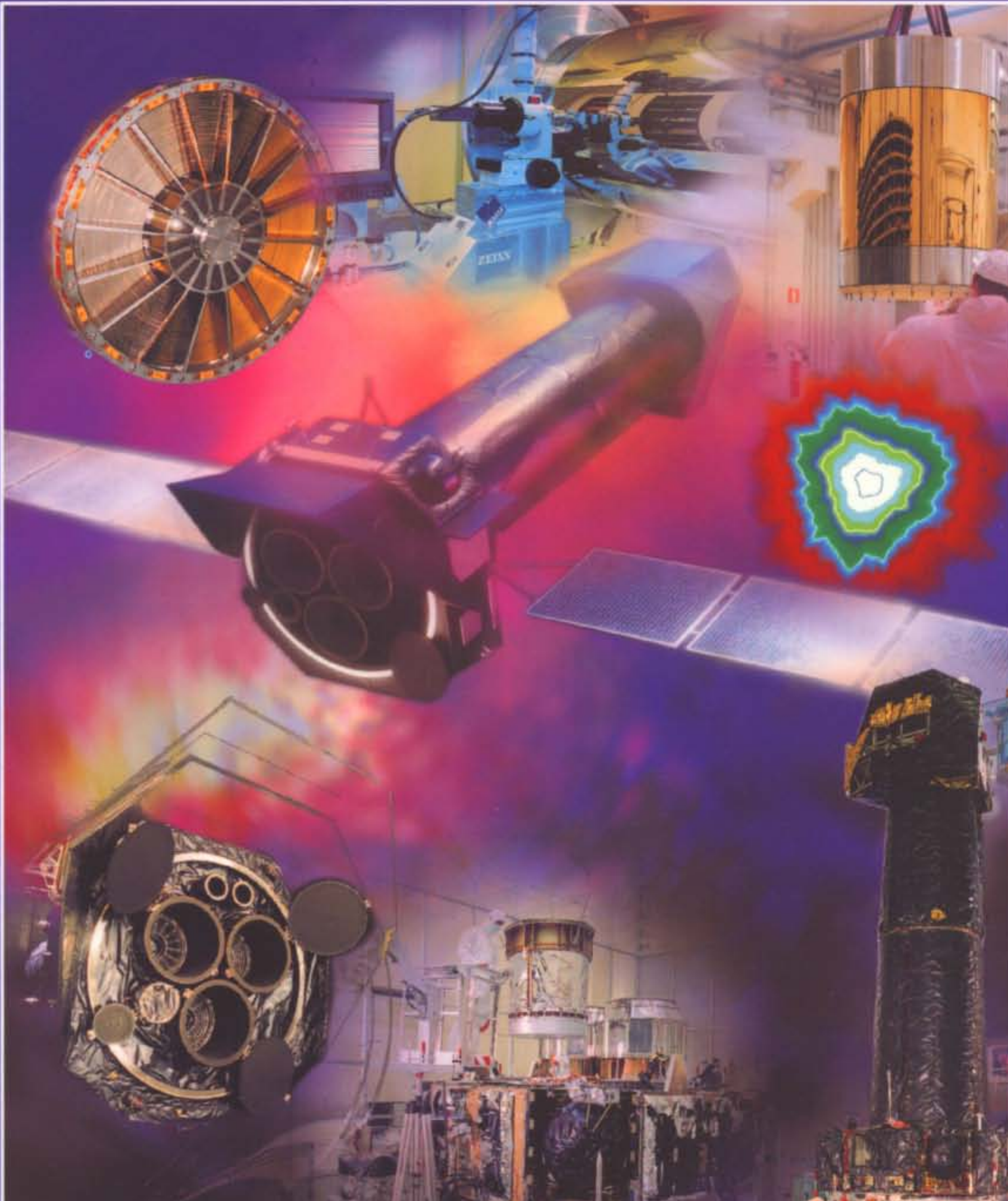

Special Issue

European Space Agency
Agence spatiale européenne

european space agency

The European Space Agency was formed out of, and took over the rights and obligations of, the two earlier European Space Organisations: the European Space Research Organisation (ESRO) and the European Organisation for the Development and Construction of Space Vehicle Launchers (ELDO). The Member States are Austria, Belgium, Denmark, Finland, France, Germany, Ireland, Italy, Netherlands, Norway, Spain, Sweden, Switzerland and the United Kingdom. Canada is a Cooperating State.

In the words of the Convention: The purpose of the Agency shall be to provide for and to promote, for exclusively peaceful purposes, co-operation among European States in space research and technology and their space applications, with a view to their being used for scientific purposes and for operational space applications systems.

(a) by elaborating and implementing a long-term European space policy, by recommending space objectives to the Member States, and by concerting the policies of the Member States with respect to other national and international organisations and institutions;
(b) by elaborating and implementing activities and programmes in the space field;
(c) by co-ordinating the European space programme and national programmes, and by integrating the latter progressively and as completely as possible into the European space programme, in particular as regards the development of applications satellites;
(d) by elaborating and implementing the industrial policy appropriate to its programme and by recommending a coherent industrial policy to the Member States.

The Agency is directed by a Council composed of representatives of Member States. The Director General is the chief executive of the Agency and its legal representative.

The ESA HEADQUARTERS are in Paris.

The major establishments of ESA are:

THE EUROPEAN SPACE RESEARCH AND TECHNOLOGY CENTRE (ESTEC), Noordwijk, Netherlands.

THE EUROPEAN SPACE OPERATIONS CENTRE (ESOC), Darmstadt, Germany

ESRIN, Frascati, Italy.

Chairman of the Council: A. Bensoussan

Director General: A. Rodotà.

agence spatiale européenne

L'Agence Spatiale Européenne est issue des deux Organisations spatiales européennes qui l'ont précédée — l'Organisation européenne de recherches spatiales (CERS) et l'Organisation européenne pour la mise au point et la construction de lanceurs d'engins spatiaux (CECLES) — dont elle a repris les droits et obligations. Les Etats membres en sont: l'Allemagne, l'Autriche, la Belgique, le Danemark, l'Espagne, la Finlande, la France, l'Irlande, l'Italie, la Norvège, les Pays-Bas, le Royaume-Uni, la Suède et la Suisse. Le Canada bénéficie d'un statut d'Etat coopérant.

Selon les termes de la Convention: l'Agence a pour mission d'assurer et de développer, à des fins exclusivement pacifiques, la coopération entre Etats européens dans les domaines de la recherche et de la technologie spatiales et de leurs applications spatiales, en vue de leur utilisation à des fins scientifiques et pour des systèmes spatiaux opérationnels d'applications:

(a) en élaborant et en mettant en oeuvre une politique spatiale européenne à long terme, en recommandant aux Etats membres des objectifs en matière spatiale et en concertant les politiques des Etats membres à l'égard d'autres organisations et institutions nationales et internationales;
(b) en élaborant et en mettant en oeuvre des activités et des programmes dans le domaine spatial;
(c) en coordonnant le programme spatial européen et les programmes nationaux, et en intégrant ces derniers progressivement et aussi complètement que possible dans le programme spatial européen, notamment en ce qui concerne le développement de satellites d'applications;
(d) en élaborant et en mettant en oeuvre la politique industrielle appropriée à son programme et en recommandant aux Etats membres une politique industrielle cohérente.

L'Agence est dirigée par un Conseil, composé de représentants des Etats membres. Le Directeur général est le fonctionnaire exécutif supérieur de l'Agence et la représente dans tous ses actes.

Le SIEGE de l'Agence est à Paris.

Les principaux Etablissements de l'Agence sont:

LE CENTRE EUROPEEN DE RECHERCHE ET DE TECHNOLOGIE SPATIALES (ESTEC), Noordwijk, Pays-Bas.

LE CENTRE EUROPEEN D'OPERATIONS SPATIALES (ESOC), Darmstadt, Allemagne.

ESRIN, Frascati, Italie

Président du Conseil: A. Bensoussan

Directeur général: A. Rodotà.

bulletin

contents/*sommaire*

number 100 - december 1999

Cover: The building and testing of XMM and its payload

Editorial/Circulation Office
ESA Publications Division
ESTEC, PO Box 299, Noordwijk
2200 AG The Netherlands
Tel.: (31) 71.5653400

Editors
Bruce Battrick
Dorothea Danesy

Layout
Carel Haakman

Graphics
Willem Versteeg

Montage
Paul Berkhout
Isabel Kenny

Advertising
Brigitte Kaldeich

Printed in the Netherlands ISSN 0376-4265

European Space Agency
Agence spatiale européenne

FIRST INTERNATIONAL SYMPOSIUM ON

MICROGRAVITY RESEARCH & APPLICATIONS IN PHYSICAL SCIENCES & BIOTECHNOLOGY

10-15 September 2000 Sorrento, Italy

Co-sponsored by
ASI, CNES, CSA, DLR, ESA, NASA and NASDA

Aims and Scope

The Symposium intends to provide a forum for scientists from academia and industry to present and discuss recent advances in their research on gravity-dependent phenomena in Physical Sciences and Biotechnology. Results originating from theoretical work, numerical modelling, ground-based and flight investigations are solicited. The major topics include Fundamental Physics, Fluid Physics, Heat and Mass Transport Phenomena, Physical Chemistry, Fluid Thermodynamics, Thermophysical Properties of Fluids, Combustion, Solidification Physics and the Crystallisation of Inorganic Materials and Biological Macromolecules. Topics in Biology and Bioengineering, which are expected to benefit from cross-fertilisation and synergy with physicists, such as multi-phase flows and surface physical chemistry, including structured deposition of macromolecules, will also be addressed.

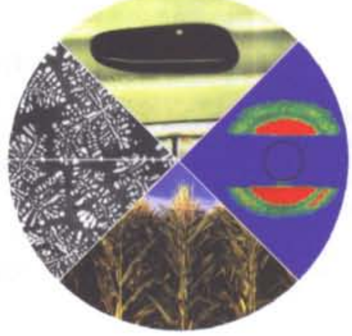

International Scientific Committee Chairman
Prof. Ilya Prigogine, Nobel Laureate in Chemistry
ULB Brussels, Belgium
University of Texas at Austin, USA

Symposium Chairman
Prof. Antonio Viviani
Seconda Università di Napoli
Aversa, Italy

Abstract deadline: 31 January 2000

Conference Secretariat
ESTEC Conference Bureau
P.O.Box 299
2200 AG Noordwijk
The Netherlands
Tel.: +31-(0)71-5655005
e-mail: confburo@estec.esa.nl

http://www.estec.esa.int/CONFANNOUN/

Co-Chairman
Prof. Francesco Gaeta
Microgravity Advanced Research
and Support Centre, Naples, Italy

ESA Coordinator
Dr. Olivier Minster
ESA/ESTEC
Noordwijk, The Netherlands

esa

Seconda Università degli Studi di Napoli
SUN

Alcatel Espacio:

Quality in Time

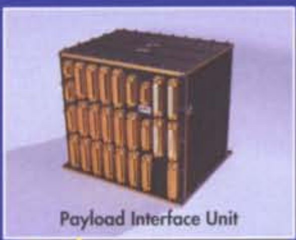

Payload Interface Unit

Antenna Pointing Electronic

Remote Terminal Unit

BPSK Modulator

Main Products

- **Digital Electronic Equipment:**
  - On Board Data Handling
  - Base Band Processing
  - Antenna Pointing and Control System
- **Radiofrequency Equipment:**
  - TTC S-Band Digital Transponder
  - L-Band Transmitter
  - BPSK/QPSK Modulators
  - Filters, Diplexers, Multiplexers, etc.
- **Systems Engineering:**
  - On-Board Processing OBP/ Multimedia
  - Communications Network for air navigation (GNSS)
  - Ground support equipment and automatic test benches

ASIC-Technology

S-band digital Transporder

Ku-band input Multiplexer

C-band Filters

Alcatel Espacio is "your best partner in the Telecommunication Space field" for the design, development, and manufacturing of on-board equipment for multimedia, mobile communication, observation, broadcasting, and others applications.

The company is participating in programs, such as: Aces, Arabsat, Globalstar, Hot Bird, Sesat, Skybridge, Worldstar, Spot 5, Helios 2, Ariane V, Meteosat 2nd Generation, XMM, Integral, Envisat.

ALCATEL

The Hi-Speed Company

Alcatel Espacio, S.A. C/ Einstein, 7 - 28760 Tres Cantos (P.T.M.) Madrid - Spain. Tel. (34 1) 807 79 00 - Fax (34 1) 807 79 99

Space Radiation Alarm

"CEASE"

COMPACT ENVIRONMENTAL ANOMALY SENSOR

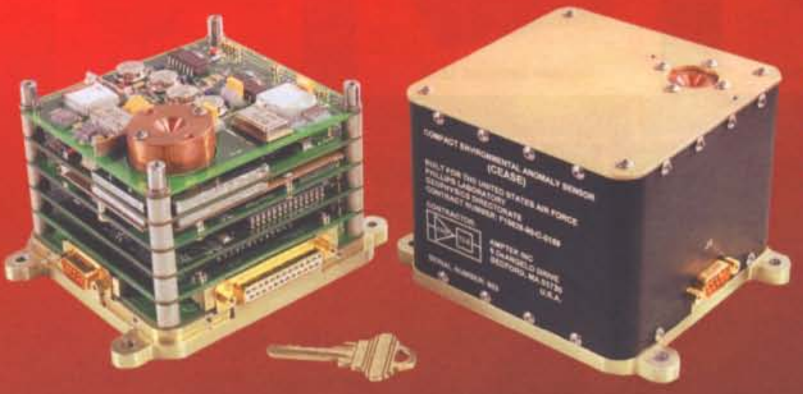

FEATURES:

- Compact: 10 x 10 x 8.1 cm^3, 1 kg
- Low Power: 1.5 W
- Flexible I/O: Supports 1553B and RS422
- Full GSE and operational software
- On-board determination of hazardous conditions

CEASE is a compact, radiation hard, low power, space "weather" hazard sensor developed to monitor the local radiation environment and to provide autonomous real-time warnings of:

- Total Radiation Dose
- Radiation Dose Rate
- Surface Charging
- Deep Dielectric Charging
- Single Event Effects
- Solar Cell Damage.

CEASE detailed radiation data is used to pinpoint causes of spacecraft anomalies, and to forecast hazardous conditions before they affect the mission. The spacecraft, in turn, can re-prioritize its operations, inhibit any anomaly sensitive tasks such as attitude control adjustments, or initiate other prudent actions as indicated by the **CEASE** warning flags. Device degradation mechanisms and radiation tolerance of components can also be monitored.

The US Department of Defense has selected **CEASE** for several missions, including:

- **TSX-5**
- **STRV-1C**
- **SBIRS LADS**

and the **DSP** operational spacecraft.

Amptek has a long and distinguished track record in the manufacture of space instrumentation. Mission examples include: DMSP, TIROS, CRRES, NEAR and APEX.

Current off-the-shelf Amptek sensors measure spacecraft charging, thermal and suprathermal, and high energy particles.

In addition, Amptek provided the X-ray Detector on the Mars PATHFINDER Mission.

High reliability components from Amptek have been the number one choice of many missions, including: GALILEO, CASSINI, GIOTTO, AXAF, SUISEI, CLUSTER, SOLAR, GEOTAIL, SOHO, INTEGRAL, WIND and AMPTE.

AMP TEK ®

AMPTEK INC.

6 DE ANGELO DRIVE, BEDFORD, MA 01730-2204 U.S.A.

Tel: +1 (781) 275-2242 Fax: +1 (781) 275-3470 email: sales@amptek.com http://www.amptek.com


IT'S 30 YEARS SINCE
THIS SPACE BECAME
TOO SMALL FOR US.

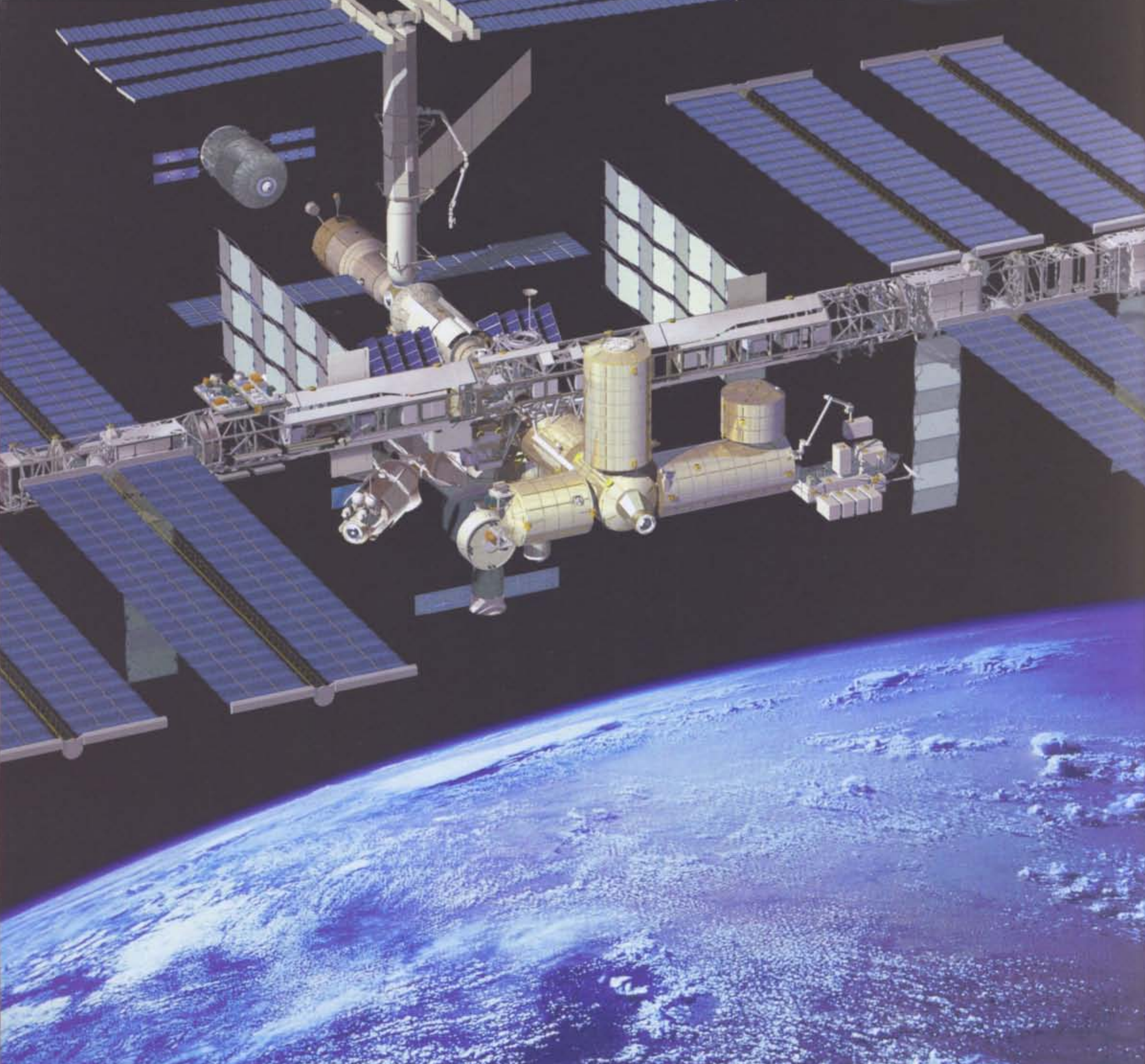

GORE Wires and Cables for Space Applications

Over twenty years of technological experience, Gore has proved competence in space applications for many milestones of space missions, such as Moon Landing, Spacelab, EURECA, ERS1 + 2, Italsat, SAX, SPOT, ISO, Envisat, XMM, Metop, Integral, scientific research in space, Columbus.

As a special cable supplier we support you in planning the next step into space. Call us now.

TEL.:+ 49/91 44/6 01-0 • FAX:+ 49/91 44/60 14 53
W. L. GORE & ASSOCIATES GMBH • NORDRING 1 • D-91785 PLEINFELD / GERMANY

GORE
Creative Technologies Worldwide

Foreword

The launch of the X-ray Multi-Mirror (XMM) telescope on flight V119, the first commercial launch of Ariane-5, will mark another important milestone for European Space and the Agency's Scientific Programme.

The mission, conceived in the late 1970s, entered the assessment-study phase in 1982 and was adopted as a 'Cornerstone Mission' in the then new Horizon 2000 Programme approved by the Science Programme Committee in 1984. The industrial studies were completed in 1988 and the scientific payload selected in 1989.

A major challenge for the mission designers from the outset was the development of the mirror technology enabling the replication of the telescope mirrors to a sufficient accuracy to meet the stringent mission requirements. Development work in industry started in 1984 using carbon fibre reinforced plastic technology, augmented in 1986 with development work on electroformed nickel mirror shells. The latter technology was chosen as the most reliable prior to the start of the spacecraft development programme in 1994. As the mirror technology was being developed, the payload configuration evolved from 19 telescopes in 1983 through several stages to the current three-telescope configuration in 1991.

The industrial phase commenced in 1994, resulting in the current configuration of a 10 m high spacecraft, over 4 m in diameter, and with a launch mass of just under 4 tonnes. This is the largest scientific spacecraft yet developed in Europe.

The spacecraft procurement programme has been extremely successful and all essential elements of the mission are now in place and configured for launch: the spacecraft including its scientific payload; the mission operations centre at ESOC in Germany; the science operations centre at Vilspa in Spain; and finally the Ariane V504 launch vehicle.

As an additional 'first', XMM is the first ESA mission whose launch has been insured under the new ESA corporate policy endorsed by the Administrative and Finance Committee (AFC) at the end of September. The partial insurance of the mission, which will enable the European science community to continue to participate in x-ray astronomy in the case of loss of mission during the launch phase up to injection, is a part of the Agency's corporate risk-assessment policy established as a foundation for the future.

Europe and its scientific community will take a quantum step forward in X-ray astronomy with the launch of XMM.

J. Credland
Head of Scientific Projects
ESA Directorate for Scientific Programmes

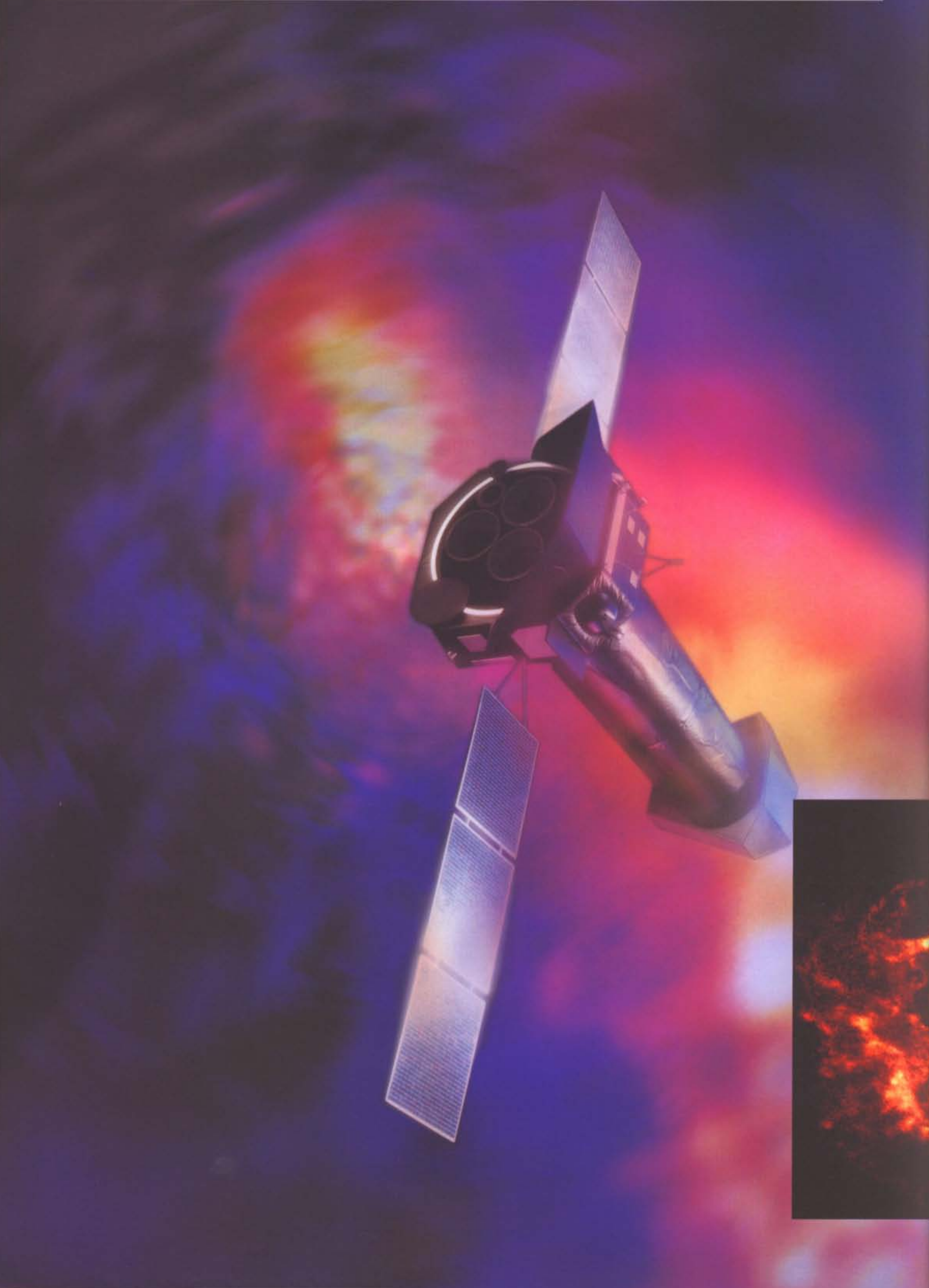

XMM: Advancing Science with the High-Throughput X-Ray Spectroscopy Mission

F.A. Jansen
Space Science Department, ESA Directorate for Scientific Programmes, ESTEC, Noordwijk, The Netherlands

The X-Ray Multi-Mirror Mission (XMM) is an X-ray astrophysics observatory scheduled for launch in December 1999. With a projected lifetime of 10 years, it will enable astronomers to conduct sensitive spectroscopic observations of a wide variety of cosmic sources.

X-ray astronomy primarily involves the study of plasmas having temperatures in the range of 10^6 to 10^8 K. Such plasmas radiate the bulk of their energy at X-ray wavelengths between 100 eV and 15 keV (0.8 - 120 Å). Apart from X-ray continuum emission, produced through such processes as thermal Bremsstrahlung, a significant fraction of the total emissivity may arise from line emission. At these high temperatures, cosmically abundant elements such as hydrogen and helium are stripped of all of their electrons. Only heavier elements can, depending on the temperature, retain their K- or L-shell electrons. The study of transitions from these elements, which are primarily in a hydrogenic or helium-like state, represents an important diagnostic tool for achieving an understanding of the physics of cosmic X-ray sources.

As the mechanisms and the conditions underlying the generation of visible light and X-rays are completely different, comparing the two provides useful complementary information. A comparison of the visible and X-ray emissions for the young supernova remnant Cas A is shown in Figure 1. These images clearly illustrate that there is a lot to be learnt about the highly energetic processes underlying the emission of X-rays from exploding stars, accreting black holes, etc.

XMM is specifically designed to investigate in detail the spectra of cosmic X-ray sources down to a limiting flux of 10^{-15} ergs/cm^2/s. It will be able to detect X-ray sources down to a few times 10^{-16} ergs/cm^2/s. With XMM, it will be possible to routinely perform such measurements, whereas on previous missions this was either impossible or required an excessive amount of observing time.

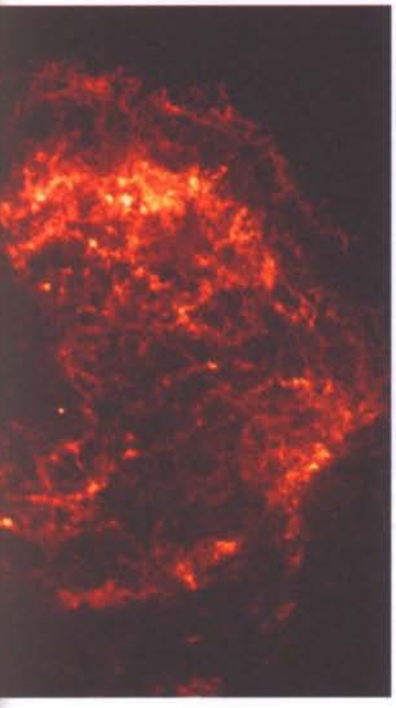

a

Figure 1a. The supernova remnant Cas A, as seen in X-rays. The emission is caused by stellar ejecta, which have been heated to several million degrees by the passage of the blast wave associated with the explosion of the progenitor star ~350 years ago (courtesy of NASA/CXC/SAO)

Figure 1b. The supernova remnant Cas A, as seen in visible light. Although the global structure, as shown in Figure 1a can still be identified, the actual material and conditions of the emitting medium are quite different (courtesy of MDM)

b

Figure 2. The XMM Structural Thermal Model (STM) in the ESTEC clean room

The principal characteristics of XMM (Fig. 2) can be summarised as follows:

- effective collection area 4500 cm^2 at 1 keV (12.4 Å) and 1000 cm^2 at 10 keV (1.24 Å)
- almost constant angular resolution across the full waveband of ~ 15 arcsec HEW (Half-Energy Width)
- X-ray field of view ~30 arcmin
- capability of performing sensitive medium-resolution spectroscopy with resolving powers between 100 and 700 over the wavelength band 5 – 35 Å (350 – 2500 eV)
- broadband imaging spectroscopy from 100 eV to 15 keV (0.8 – 120 Å)
- simultaneous sensitive coverage of the wavelength band 1600 – 6000 Å (~17 arcmin field of view) through a dedicated optical monitor, co-aligned with the X-ray telescopes
- continuous coverage of a source for up to 42 h (except for a small gap around apogee).

A suite of complementary instruments on board the XMM mission brings about these characteristics.

The European Photon Imaging Camera (EPIC) instrument provides an X-ray imaging camera for each of the three telescope modules of XMM. The detectors are based on cooled Charge-Coupled Devices (2 MOS-CCD cameras, 1 p-n CCD camera), operating in a photon-counting mode to provide simultaneous imaging and non-dispersive spectroscopy (spectral resolving power ~7 at 0.2 keV to ~70 at 15 keV) for every field that XMM observes. These powerful diagnostics will have a significant impact on every branch of X-ray astrophysics. An example of the very high performance of these instruments is shown in Figure 3.

The mission's aim of providing a medium-resolution spectroscopic capability is achieved by means of two Reflection Grating Spectrometers (RGSs). The grating arrays are placed directly behind two of the three Mirror Modules, in front of the EPIC MOS cameras, and each intercepts about 50% of the converging beams. Position- and energy-sensitive readout at the spectroscopic (secondary) focus is performed by strip arrays of nine MOS CCDs each. The energy resolution of these CCDs is used to separate the overlapping diffraction orders –1 and –2, and to reject background arising from diffuse X-rays as well as from particle radiation or internal detector effects (Fig. 4).

These X-ray instruments are placed behind one of the major achievements of XMM, the X-ray mirrors. Having set out to achieve a performance of 30 arcsec Half-Energy Width (HEW) at 2 keV, the actual achieved performance is a factor of 2 better (Table 1).

*Table 1. XMM Mirror Module measured X-ray imaging performance**

In arcsec:	FM1	FM2	FM3	FM4
FWHM @ 1.5 keV	8.4	6.6	6.0	4.5
FWHM @ 8.0 keV	7.7	6.6	5.1	4.2
HEW @ 1.5 keV	15.2	15.1	13.6	12.8
HEW @ 8.0 keV	14.4	14.8	12.5	12.2
W90 @ 1.5 keV	56.8	57.2	48.1	58.0
W90 @ 8.0 keV	161.0	182.0	153.0	130.0

* The actual Mirror Modules mounted on XMM for flight are FM2, 3 and 4.

The Optical Monitor (OM) enables XMM to provide simultaneous coverage of the telescope field in the waveband 1700 to 6000 Å. The 30 cm Cassegrain telescope will cover a 17 by 17 $arcmin^2$ field with an angular resolution of ~1 arcsec through the use of photon-counting detectors. This instrument is also equipped with a standard set of U, B and V filters, as well as specific UV-wavelength band filters and two grisms for low-resolution dispersive spectroscopy over the full wavelength band.

The XMM orbit will be a 40 deg, southern-inclination orbit which allows for > 95 % visibility of the sky over the first two years of the mission's lifetime.

The XMM Science Operations Centre (SOC) is located at ESA's Vilspa (Villafranca del Castillo) facility, near Madrid (E), and supports the scientific part of the XMM operations:

- Issuing Announcements of Opportunity (AOs) and coordinating the peer-review process to arrive at the scientifically optimum XMM observing programme.
- Writing the XMM User's Handbook, which is the guide to be used by guest observers in preparing their proposals.
- Performing the mission planning.
- Distributing the observation files to the observers.
- Performing the calibration of the instruments.
- Defining and writing the software required to scientifically simulate the performance of the full XMM observatory (SciSIM). This component is actively used in determining and predicting the calibration of the instruments on-board the XMM observatory. Examples of the use and capabilities of the SciSIM are shown in Figures 3 and 4.

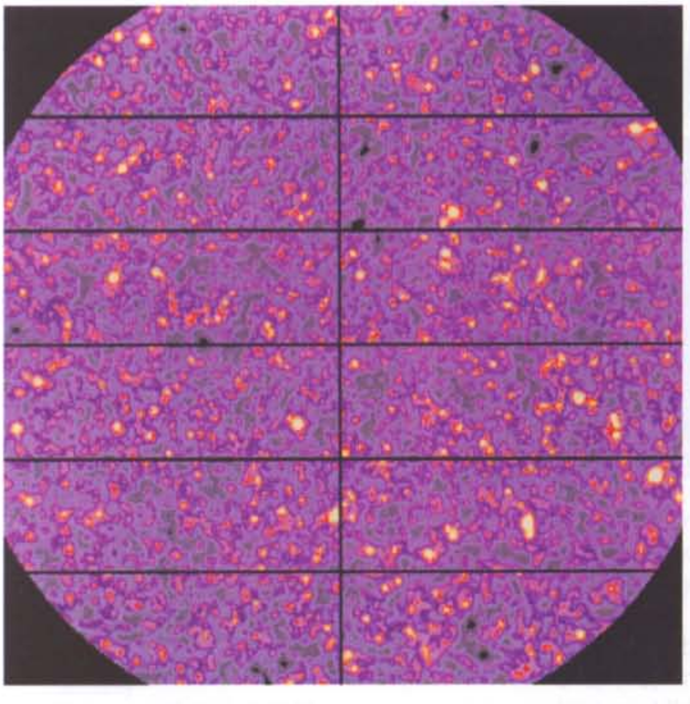

Figure 3. A simulated EPIC p-n camera deep-field exposure. A 200 000 sec deep-field exposure has been simulated using the source number versus source strength (log N - log S) relationship extrapolated down to 10^{-16} erg/cm²/s. The full 30 arcmin field of view is shown (courtesy of D. Lumb, ESTEC)

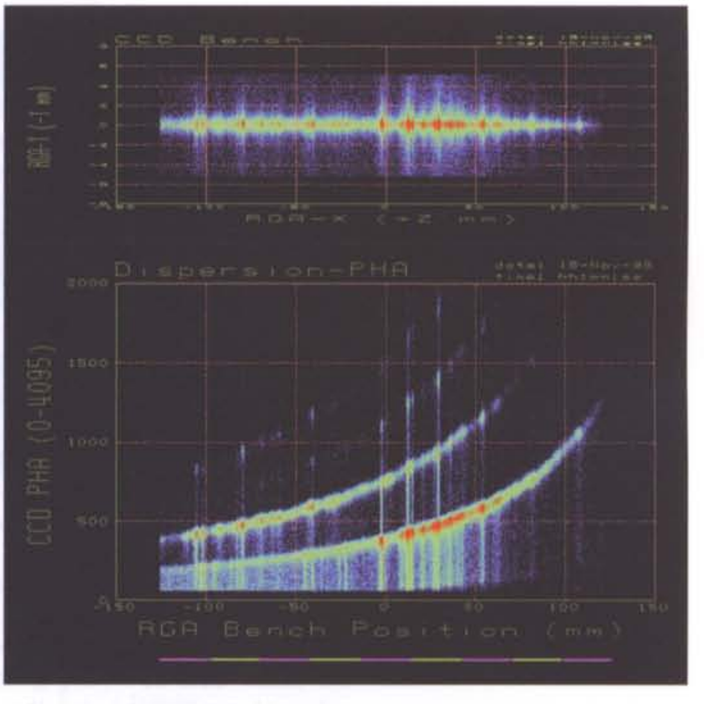

Figure 4. Simulation of an XMM RGS observation of Capella. The top panel shows the image in the spectroscopic focus with the dispersion direction along the abscissa. The lower panel shows the same information on the abscissa, but here the ordinate uses the CCD energy information, thus illustrating the mechanism separating the grating orders. All the bright features are resolved spectral lines in the spectrum of Capella

- Defining and writing the software required to analyse XMM data (SAS). This is a collaborative effort with the AO-selected, Survey Science Consortium (SSC).
- Ensuring the public availability of the standard analysis results, as made available by the SSC.

The first XMM Announcement of Opportunity (AO-1) attracted the attention of an astonishing number (~2000) of professional astronomers worldwide, which approximately amounts to 25% of the World's astronomical community. The number of proposals received was seven times higher than the volume that could be accommodated.

One of the major areas of development has been the XMM Scientific Analysis System (SAS). This comprises both the interactive analysis and the pipeline software used by the SSC to routinely process all XMM data. In this area, the SOC has developed a set of software layers known as the Data Access Layer (DAL) and Calibration Access Layer (CAL), which largely simplify the (re-)use of XMM software by other analysis systems and also allow simpler interfaces between the SAS development teams at the different sites. All of these features are present in the third release (internal to ESA and SSC) of the full SAS software package, which also is available for limited external testing.

Another part of the work performed by the SOC was the description of the calibration of the XMM instruments. This is especially difficult for traditional items like the Response Matrix File (RMF). For detailed analysis of data of the quality and spectral resolution to be generated by XMM, it is no longer sufficient to store a (limited) set of RMFs that could be made available to the observers. A full set of RMFs would require so much disk storage that it would be prohibitive for the XMM observers to use them. Instead, it is generally recognised that software will have to be written which generates these response matrices instantly, taking into account all details of the dataset and instrument being analysed. By using prototype versions of this software, this approach has proven to be a viable and promising option.

The SOC has developed, in coordination with the XMM Science Working Team (SWT), a coherent programme for the XMM in-orbit calibration and performance verification phase. This phase is going to take three months to execute, rather than the two months originally proposed. The extra time is required to compensate for some of the instrument calibration, which could not be performed on the ground due to time pressures.

In its preparation of operational activities, the SOC has run through a number of science cases and compared XMM to other missions. An important feature of XMM is how it complements the NASA Chandra mission. The main features of XMM (compared to Chandra) are:
- Point spread function nearly independent of energy.
- Point spread function nearly constant over full FOV (30 arcmin).
- Effective area: at 2 keV, 5 times Chandra; at 10 keV, ~50 times Chandra.
- All instruments operate simultaneously, which gives XMM a large multiplexing advantage over many previous and contemporaneous missions.
- Optical Monitor available, which will allow for simultaneous optical coverage of most XMM observed fields without having to revert to logistically complex, ground/space-based co-ordinated observations.
- No degradation of the RGS spectral resolution for slightly extended (~10 arcsec) sources. This is important as it will allow for unprecedented high-spectral-resolution studies of slightly extended objects.

The science best performed with Chandra will focus on the use of its high spatial resolution and very high-resolution spectroscopy of bright X-ray sources, whereas XMM will, inter alia, excel in the study of faint extended high-temperature plasmas, where its capabilities are unrivalled and unique.

In summary, XMM will bring the opportunity to greatly expand the number of known X-ray sources and extend our knowledge on the already known population of X-ray sources.

X-Ray Telescope for Sky Mapping

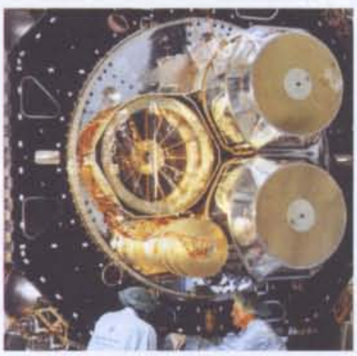

The three mirror modules and the optical monitor

The focal plane assembly with cameras and spectrometers

A major breaktrough in the generation of a sky map of X-ray sources was achieved by the German X-ray satellite Rosat, which was built under the leadership of Dornier Satellitensysteme GmbH.

XMM with a far better resolution will substantially advance the "decoding" of X-ray sources. A marked increase in the number of detected sources is also expected. The XMM telescope contains three identical X-ray mirror assemblies. With a total of 174 mirror shells, this new telescope has an enormous throughput and high sensitivity compared to all previous projects.

Under a contract of ESA, Dornier Satellitensysteme GmbH leads the consortium of 35 European companies which developed and built the satellite.


Advanced System Engineering & Proven Solutions
for Spacecraft AIT & Ground Infrastructure
A prime Dutch Aerospace System Engineering, Telecommunication, Simulation, Data Processing & EGSE Solution Provider
Satellite Services BV
Scheepmakerstraat 40
2222 AC Katwijk aan Zee
The Netherlands
Tel: +31-(0)71-402-8120
Fax: +31-(0)71-402-7934
www.satserv.nl
info@satserv.nl

An Overview of the XMM Observatory System

H. Barré
XMM Project, ESA Directorate for Scientific Programmes,
ESTEC, Noordwijk, The Netherlands

H. Nye & G. Janin
XMM Ground Segment, ESA Directorate for Technical and Operational Support,
ESOC, Darmstadt, Germany

XMM is the largest scientific observatory developed by ESA and dedicated to exploring the Universe in the soft-X-ray portion of the electromagnetic spectrum. This article presents XMM as a complete system, composed by the space segment (the satellite and its launch vehicle) and the ground segment (all of ground-based infrastructure needed to control the satellite and gather the scientific data). The definition of the XMM orbit, which is also described, is a key element in meeting the primary mission objectives and satisfying the project programmatic requirements and constraints.

The XMM system

XMM is a powerful end-to-end space observatory system that will enable astronomers around the world to obtain directly processed and calibrated scientific results based on their own observation proposals. This means that the XMM system has been designed to:

- process the observation requests, proposals and targets of opportunity
- plan and schedule the sequence of observations in an optimal manner, taking into account their duration, the orbital position and the satellite control and maintenance
- carry out the observations by pointing the satellite precisely in the right direction
- gather, evaluate, process and calibrate the scientific data in a format suitable for the end user
- archive all mission products for the complete mission lifetime.

In order to serve those functions, the XMM observatory is composed of:

- the XMM satellite, a very powerful X-ray space telescope mainly characterised by its three mirror modules focusing the X-ray radiation towards the five scientific cameras located at the other extremity of the satellite at a focal distance of 7.50 m
- the Ariane-5 launcher system, the most powerful European launch vehicle, needed to inject the XMM satellite into a dedicated highly elliptical orbit (HEO) perfectly suited to the space observatory
- the ground segment, comprising all components necessary to control and communicate in real time with the XMM satellite, i.e. ground stations and associated communication systems, control centres and ground facilities.

Figure 1 shows the overall XMM mission architecture.

The XMM satellite

Designed around the X-ray telescope system, the XMM satellite is configured modularly and is composed of four main elements:

- The Focal-Plane Assembly (FPA), consisting of the Focal-Plane Platform (FPP) carrying the focal-plane instruments, the European Photon and Imaging Camera (EPIC) and the Reflection Grating Spectrometer (RGS), and the data-handling and power distribution units for the cameras. The EPIC and RGS instruments are fitted with radiators, which cool the CCD detectors via cold fingers.
- The Telescope Tube (TT), maintaining the relative position between the FPA and the MSP. Due to its length of 6.80 m, the Telescope Tube is physically composed of two halves: the upper and lower tubes. The upper tube includes two reversible venting and outgassing doors (VOD), and supports the outgassing baffle (OGB).
- The Mirror Support Platform (MSP), consisting of the platform itself and carrying the three mirrors assemblies (Mirror Modules + entrance and exit baffles + doors + two RGS grating boxes), the Optical Monitor (OM) and the two star-trackers.

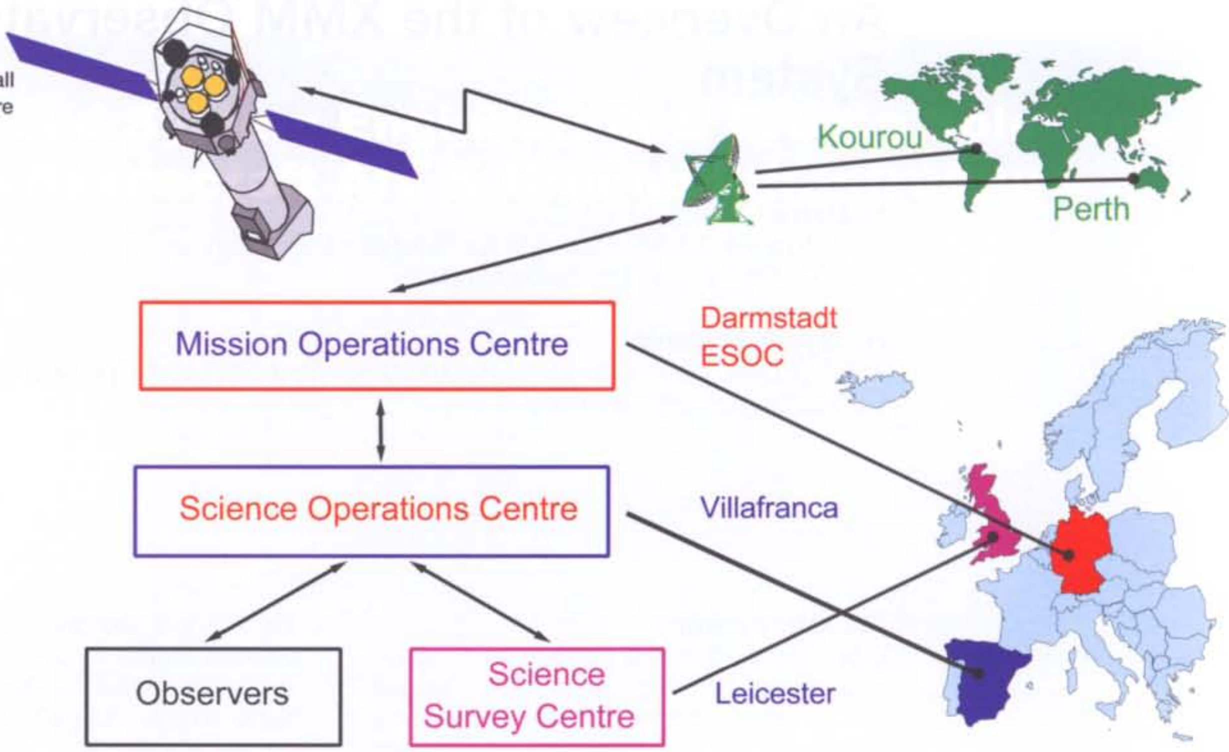

Figure 1. The overall mission architecture

- The Service Module (SVM), which carries the spacecraft subsystems and associated units providing the necessary resources to the satellite. Also attached to the SVM are the two solar-array wings, the Telescope Sun Shield (TSS) and the two S-band antennas mounted on their booms.

Figure 2 presents an exploded view of XMM, highlighting the spacecraft's modular configuration. Figure 3 indicates the physical implementation of the XMM telescopes, showing the X-ray mirror assemblies and the focal-plane cameras at the two ends of the Telescope Tube.

The Focal-Plane Assembly and the Service Module are designed as self-contained modules, so that they can be fully integrated and tested independently from each other. During the qualification and acceptance programmes, most environmental tests (vibration, thermal vacuum) have been conducted at satellite assembly level:
- the Lower Assembly, comprising the SVM, MSP and lower Telescope Tube
- the Upper Assembly, comprising the FPA and upper Telescope Tube.

The Service Module consists of a closed box, shaped around a hollow central cone, and comprises the lower and upper platforms as well as four side panels, on which all satellite bus units are installed.

The functions provided by the Service Module are:
- the primary and secondary structures to interface with the launcher adapter, to support the subsystem units, and to interface with and support the Mirror Support Platform and the Telescope Tube
- the thermal control to maintain the SVM units and equipment within specified temperature limits, and to provide a very strictly controlled thermal environment for the mirror assemblies via the Mirror Thermal Control Unit (MTCU)
- the Attitude and Orbit Control System (AOCS) for precise pointing/slewing in all operational modes, and for the performance of orbit acquisition/maintenance via the RCS propulsion system (Reaction Control System)
- the On-Board Data Handling (OBDH) for the decoding of ground telecommands, the distribution of ground or on-board commands, the sampling and formatting of telemetry data, and central on-board time distribution
- the Radio Frequency System (RFS), operating in S-band, ensuring communications (uplinking of telecommands, downlinking of telemetry) with the ground stations and providing a ranging mode for orbit determination
- the Electrical Power Subsystem (EPSS) for the generation and distribution of regulated power to all equipment via a 28 V main bus.

Figure 4 is an exploded view of the XMM Service Module, with its side panels open. Thanks to its particular shape, with a large central hole of 2.10 m diameter, the XMM bus can be used to accommodate a large variety of

Figure 2

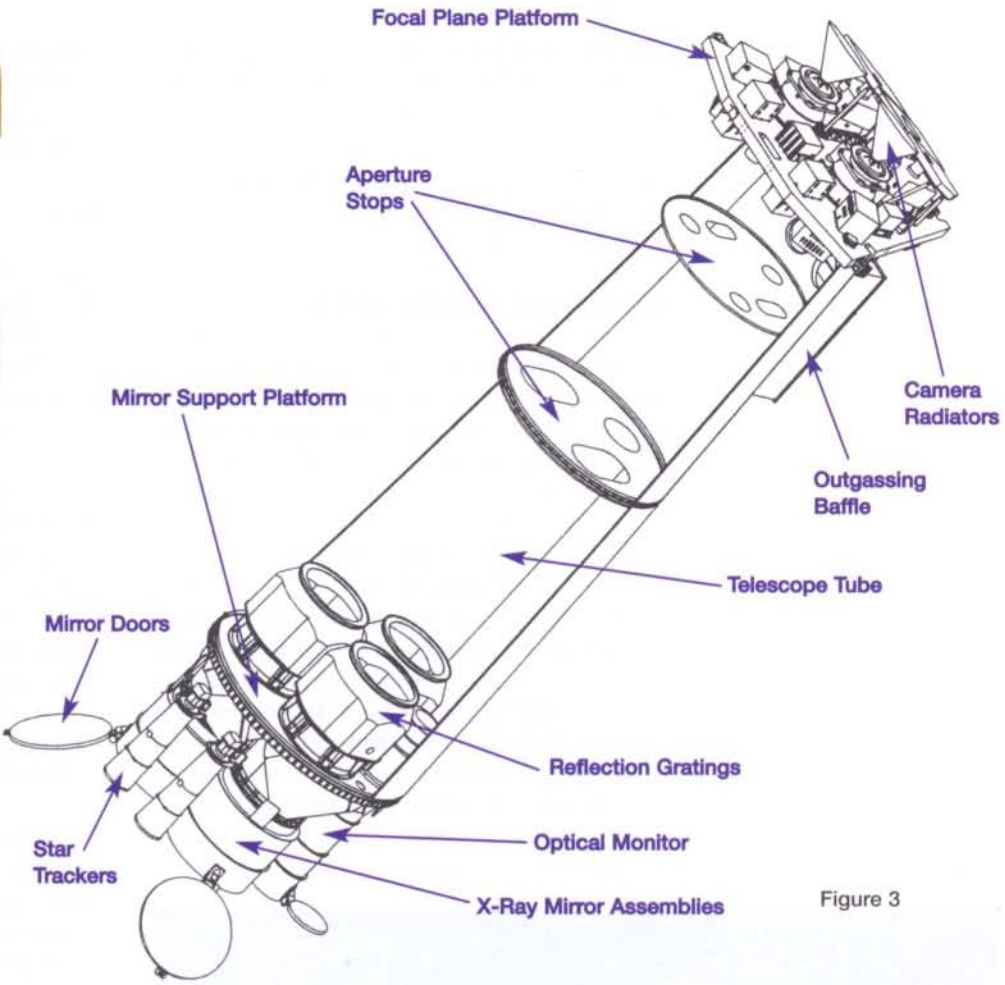

Figure 3

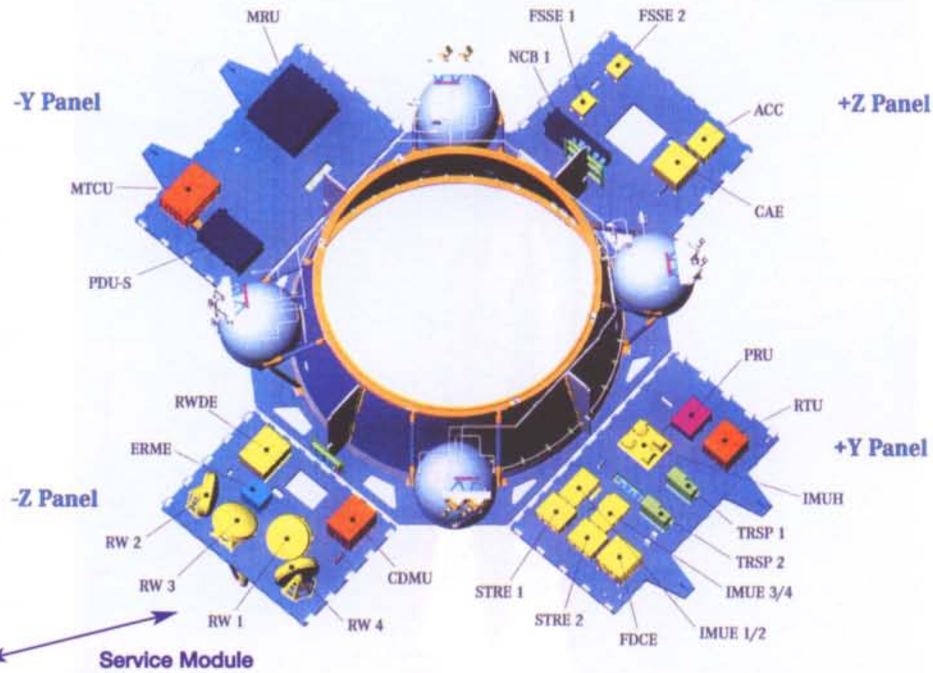

Figure 4

payloads. ESA's Integral satellite is reusing the complete XMM Service Module and the majority of its equipment.

Complete descriptions of the XMM subsystems are to be found in the articles dedicated to them in this ESA Bulletin.

The Ariane-5 launcher system

Throughout the XMM development phases, the launch vehicle has permanently been taken into account as a major component in the definition of the XMM system. The launch-vehicle capabilities have had a direct influence on all elements of the mission, such as:

- The achievable orbit, which in turn has an impact on the scientific return (percentage of the mission time dedicated to scientific observations), as well as the infrastructure needed on the ground (number and location of ground stations, communications networks).
- The performance (payload dimensions and mass) and features (ballistic phase; delayed injection) that drive the satellite design mainly in terms of: loads and structure; orbit-acquisition and reaction-control systems; and mass, propellant and power budgets.

Figure 5. Ariane-5

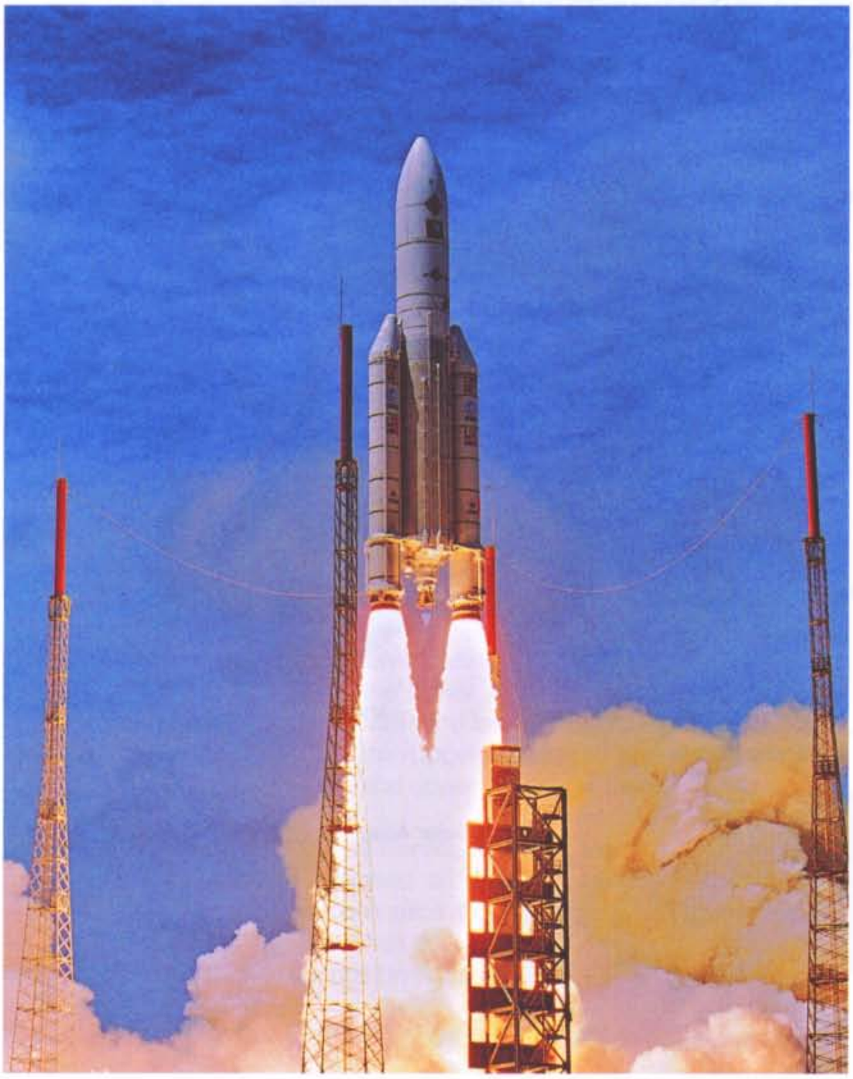

Initially – during the Phase-A studies – it was planned to launch XMM on an Ariane-44L vehicle. XMM has evolved rapidly since Phase-B, the design phase, to take advantage of the benefits of a launch by Europe's most powerful launcher, Ariane-5.

During Phase-C/D, the main development phase, the detailed designs for the satellite, the orbit and the ground segment have been traded-off and adjusted to take optimal advantage of Ariane-5's capabilities in terms of performance, trajectory, and qualification features. By now, therefore, the XMM satellite and its launcher form a truly tailored pair, characterised by:

- Full usage of the available volume under the Ariane-5 short fairing (the upper corners of the satellite have been 'tailored' to fit inside the conical part of the fairing).
- Full usage of the launcher's performance in terms of launch mass and target orbit.
- Optimised launch trajectory and injection orbit and sequence.

In December 1999, XMM will be injected by Ariane-5 into a Highly Elliptical Orbit (HEO) defined by the following orbital parameters:

- Perigee altitude 850 km
- Apogee altitude 114 000 km
- Inclination 40 deg
- Argument of perigee 55 deg
- Longitude of ascending node (measured from Kourou meridian) - 5.513 deg.

The injection of XMM will take place some 1610 sec (almost 27 min) after lift-off from ESA's launch base in Kourou, French Guiana, at a true anomaly angle of 42.25 deg. Figure 5 shows an earlier Ariane-5 launch.

The XMM orbit

As a major engineering activity, the selection of XMM's orbit has been the subject of numerous system studies and trade-offs to optimise the top-level XMM mission objectives, whilst taking into account all other components of the system. The following requirements were thereby derived:

- to maximise scientific observation time in an undisturbed environment
- to ensure an orbital lifetime of at least 10.25 years (3 months commissioning + 2 years nominal + 8 years extended lifetime)
- to maximise ground coverage during scientific observations (real-time mission, no on-board data storage)
- to make optimal use of the available launcher
- to respect the requirements applied to the satellite and its design limitations and constraints such as: maximum eclipse duration compatible with the satellite power

autonomy (battery capacity); separation and first orbit (satellite activation/checkout) in sunlight; solar aspect angles during perigee-raising manoeuvres at subsequent apogees.

The analysis of those requirements led to the selection of an orbit that is:
- highly elliptical, allowing maximum time above the radiation belts, i.e. higher than 40000 km
- geosynchronous, with a period that is multiple of 24 hours, giving optimal coverage from dedicated ESA ground stations.

Further trade-offs between eclipse duration, visibility from ground stations and launch-window size led to the optimal definition of the remaining orbital parameters (inclination, argument of perigee, minimum altitude of perigee) and allowed the calculation of the complete launch-window scenario by combining the derived constraints. As an example, the perigee altitude will remain higher than 6000 km throughout the 10.25 year mission lifetime.

The resulting XMM launch window has the following specific characteristics:
- There are two seasonal windows per year: a summer and a winter window, each with a typical length of about 70 days.
- Each seasonal window is bounded by the orbital stability requirement at the opening (lower limit), and by the eclipse duration at the closing (upper limit).
- The daily window has a duration of between 30 and 60 minutes.

The operational XMM orbit (Fig. 6), reached about 8 days after lift-off, has the following initial parameters:

– Perigee altitude	7000 km
– Apogee altitude	114 000 km
– Inclination	40 deg
– Argument of perigee	55 deg
– RA of ascending node	240 deg
– Period	47.86 h.

These parameters will evolve as the mission progresses. As an example, the perigee altitude will vary between 7000 km and 22 000 km, while the apogee altitude will vary between 115 000 km and 100 000 km.

Such an orbit gives more than 44 hours of direct contact with the ground stations, of which some 40 hours will be dedicated to scientific observations above 40 000 km.

Another significant system-engineering activity has been to adequately use the system margins to increase flexibility at project-management level and to find optimal solutions in terms of technical performance, cost and schedule.

By continuous and rigorous control of the XMM satellite mass budget, it has been possible to preserve positive mass margins, which have mainly been exploited on two occasions:
- Installation of bigger batteries (24 Ah, instead of 18 Ah). This was induced by the non-availability of the delayed injection capability of the launcher, which in turn led to the selection of an orbit with an apogee in the

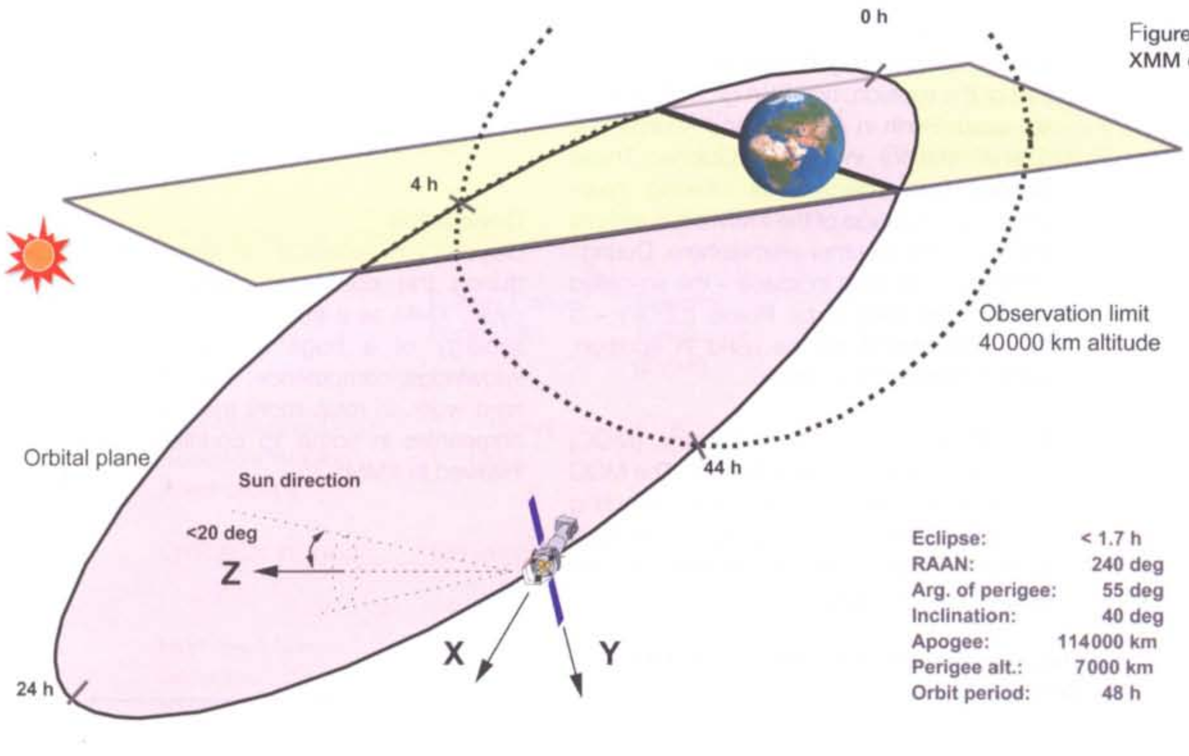

Figure 6. The operational XMM orbit

Southern Hemisphere, rather than in the Northern Hemisphere.
- Loading of additional propellant (some 52 kg) into the spacecraft's four tanks. Part of this extra fuel allowed the launch date for XMM to be advanced by about 1.5 months (from 21 January 2000, to 8 December 1999).

Dedicated manoeuvres have been defined in order to relax the above constraints for XMM orbit definition, namely:
- Sub-optimal attitude during the three Perigee Raising Manoeuvres (PRMs), thus relaxing the Solar Aspect Angle (SAA) requirements
- Raising of the initial altitude of the perigee above 7000 km, thereby getting around the orbital stability limit.
- Final acquisition of the operational orbit via an Apogee Correction Manoeuvre (ACM), to maintain the mandatory period of 48 h.

As a result of this interactive engineering process, four XMM reference orbits were baselined throughout the project development cycle.

The XMM ground segment

The ground segment consists of all of the infrastructure and systems needed on Earth to communicate with, monitor and control the XMM satellite in real time, as well as to gather, process and archive the scientific data harvested by the X-ray cameras on board.

The major components of the XMM ground segment are:

- The ground stations to track the satellite and communicate at S-band with the on-board transponders. During the operational scientific part of the mission, two ESA ground stations are used: Perth in Australia and Kourou (the 'Diane' station) in French Guiana. These stations were selected as offering near-complete coverage of the XMM orbit, with its apogee in the Souther-Hemisphere. During XMM's first 10 days in space – the so-called Launch and Early Orbit Phase (LEOP) – a third ESA station will be used in addition, namely Villafranca in Spain.

- The Mission Operations Centre (MOC) located at ESOC in Darmstadt (D). The MOC is responsible for monitoring and controlling the satellite: all telecommands will be sent from the MOC, and all telemetry will be received at the MOC.

The main elements of the Mission Operations Centre are:

- The XMM Mission Control System (XMCS), in charge of receiving, decoding and processing the telemetry, as well as assembling the telecommands to the satellite.
- The XMM Simulator (called the MOC-SIM), a software model of the satellite platform, used for pre-validation of commands and procedures.
- The Flight Dynamics System, in charge of orbit determination and attitude re-constitution. The FDS also defines all of the attitude and orbit control manoeuvres in an optimal way to maximise the duration of the scientific observations, whilst still respecting the XMM-imposed in-orbit constraints, such as avoidance of bright celestial bodies in the telescope field of view.

- The Science Operations Centre (SOC), located at Vilspa (Villafranca) in Spain. The SOC is responsible for preparing all scientific observations, and analysing and processing the corresponding scientific data The main elements of the SOC are:

  - The XMM Science Control System (XSCS) in charge of defining the planning of the scientific observations and monitoring their execution
  - The XMM Simulator (called the SOC-SIM), a software model of the satellite experiments, used for validation of ground procedures, as well as validation of instrument on-board software
  - The XMM Archive Management System (AMS), which stores and allows retrieval of all XMM data and associated products.

- The Science Survey Centre (SSC), located in Leicester (UK), in charge of pipeline processing the XMM observations data, as well as performing serendipitous sky surveys.

Conclusion

Besides the technical achievements realised during the complete project development cycle, XMM as a true system results from the synergy of a huge amount of expertise, knowledge, competence, motivation and sheer hard work. In total, more than 50 institutes or companies in some 15 countries have been involved in XMM.

The Scientific Instruments On-board XMM – Technical Highlights

G. Bagnasco, H. Eggel, F. Giannini & S. Thürey
XMM Project, ESA Directorate for Scientific Programmes,
ESTEC, Noordwijk, The Netherlands

The payload carried by the X-Ray Multi-Mirror Mission (XMM), the second Cornerstone of the ESA Horizon 2000 Science Programme, consists of three scientific instruments: the Reflection Grating Spectrometer (RGS), the European Photon Imaging Camera (EPIC), and the Optical Monitor (OM). This article provides a general overview of the main characteristics of all three instruments.

Introduction

At the end of 1999, when the XMM satellite is put into its 48-h highly elliptical orbit by an Ariane-5 vehicle from the European launch base in Kourou, French Guiana, X-ray astronomers from all over the World will have the opportunity to exploit the most powerful X-ray observatory ever built.

For the first time, they will have the unique possibility to perform simultaneously:

- high-throughput non-dispersive spectroscopic imaging, with the EPIC instrument
- high-resolution dispersive spectroscopy, with the RGS instrument, and
- optical/ultraviolet imaging with the OM instrument.

An exploded view of the XMM payload, with the main elements labelled, is shown in Figure 1.

Three Mirror Modules, co-aligned with the OM telescope, and equipped with two RGS grating assemblies, lie at the heart of the XMM telescope. Each Mirror Module, with a focal length of 7.5 m, will provide an unprecedented collecting area, thanks to its 58 nested Wolter-I-type shells*, designed to operate in the soft X-ray energy band between 0.1 and 10 keV (1-100 Å).

The XMM telescope is completed by three EPIC cameras, placed in the foci of the three Mirror Modules, and by two RGS cameras, suitably positioned to collect the spectrum created by the two grating assemblies. A Telescope Tube, which is equipped with two aperture stops for stray-light suppression and with an outgassing baffle for cleanliness and decompression purposes, separates the Cameras from the Mirror Modules.

* For a detailed description of the Mirror Modules, see the companion article in this Bulletin titled 'XMM's X-ray Telescopes' on page 30.

Table 1. Main characteristics of the XMM instruments

Instrument	Main Purpose	Energy Range/ Bandwidth	Spectral Resolution (E /ΔE)	Spatial Resolution (arcsec)	Sensitivity	Total Mass/Power
EPIC	High-throughput non-dispersive imaging/ spectroscopy	0.1 - 15 keV 1 - 120 Å	5 - 60	14 (Half Energy Width)	10^{-14} erg/cm^2 sec	235 kg 240 W
OM	Optical/UV imaging	160 - 600 nm	50 -100 (with grisms)	1	< 24 magnitude	82 kg 60 W
RGS	High-resolution dispersive spectroscopy	0.35 - 2.5 keV 5 - 35 Å	200 - 800 (400/800 at 15 Å in 1st/2nd order)	N.A.	3×10^{-13} erg / cm^2 s	248 kg 140 W

Figure 1. The main elements of the XMM payload

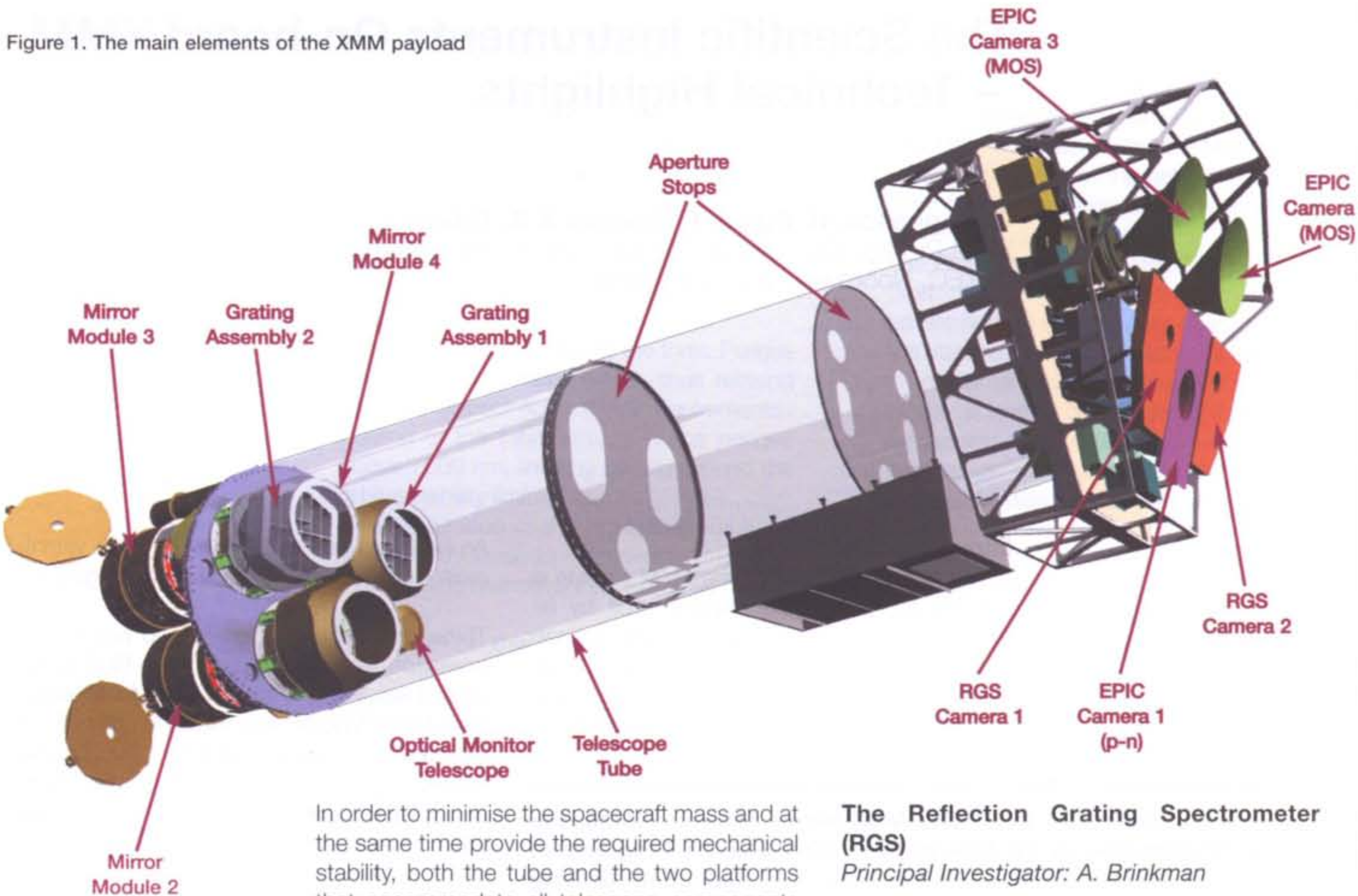

In order to minimise the spacecraft mass and at the same time provide the required mechanical stability, both the tube and the two platforms that accommodate all telescope components are made of Carbon Fibre Reinforced Plastic (CFRP), with an aluminium honeycomb core.

Each instrument on board XMM has been designed and built by a multi-national consortium of institutes and industries, directly funded through the resources of the countries involved and under the leadership of a Principal Investigator (PI). Figure 2 (opposite) provides an overview of the industrial participants and the three instrument consortia. The main scientific performances and technical characteristics of the EPIC, OM and RGS instruments are listed in Table 1.

The Reflection Grating Spectrometer (RGS)

Principal Investigator: A. Brinkman

Instrument concept

The conceptual idea behind the RGS instrument is depicted schematically in Figure 3. The incoming X-ray radiation, collected and focused by the Mirror Module, is partly intercepted by a set of reflection gratings which, like a prism, disperse the various wavelengths at different angles so that a spectrum can be collected and analysed by a strip of Charge Coupled Device (CCD) detectors. The X-ray radiation that passes undispersed through the set of gratings is focused onto the EPIC cameras for imaging purposes.

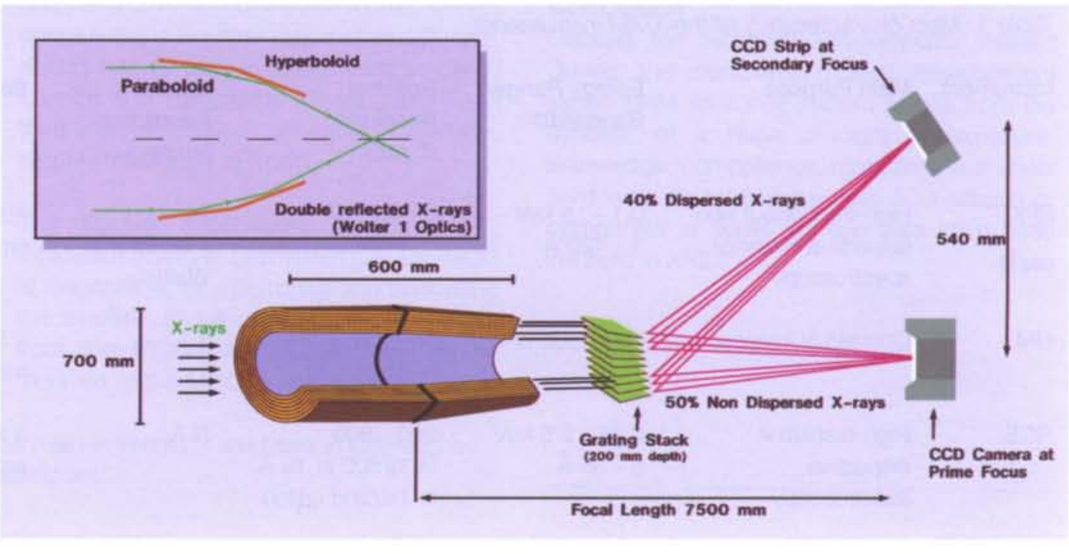

Figure 3. Schematic of the concept underlying the RGS instrument

Figure 2. The industrial structure (above) and participants in the three Instrument Consortia

Institute	Instrument	Country
Mullard Space Science Laboratory	OM (PI)/RGS	UK
University of Leicester	EPIC (PI)	
School of Physics, Birmingham	EPIC	
University of California, Santa Barbara	OM	USA
Los Alamos and Sandia National Labs.	OM	
Columbia University, New York	RGS	
University of California, Lawrence Livermore National Lab.	RGS	
Centre Spatial de Liège	OM	B
Space Research Organisation of the Netherlands, Utrecht	RGS (PI)	NL
Service d'Astrophysique, Saclay	EPIC	F
Centre d'Etude Spatiale des Rayonnements	EPIC	
Institut d'Astrophysique Spatial, Orsay	EPIC	
Paul Scherrer Institute, Villigen	RGS	CH
Istituto di Fisica Cosmica, Milan	EPIC	I
Istituto di Tecnologie e Studio delle Radiazioni Extraterrestri, Bologna	EPIC	
Istituto di Astronomia, Palermo	EPIC	
Max-Planck-Institut für Extraterrestriche Physik, Garching	EPIC	D
Institut für Astronomie und Astrophysik, Tübingen	EPIC	

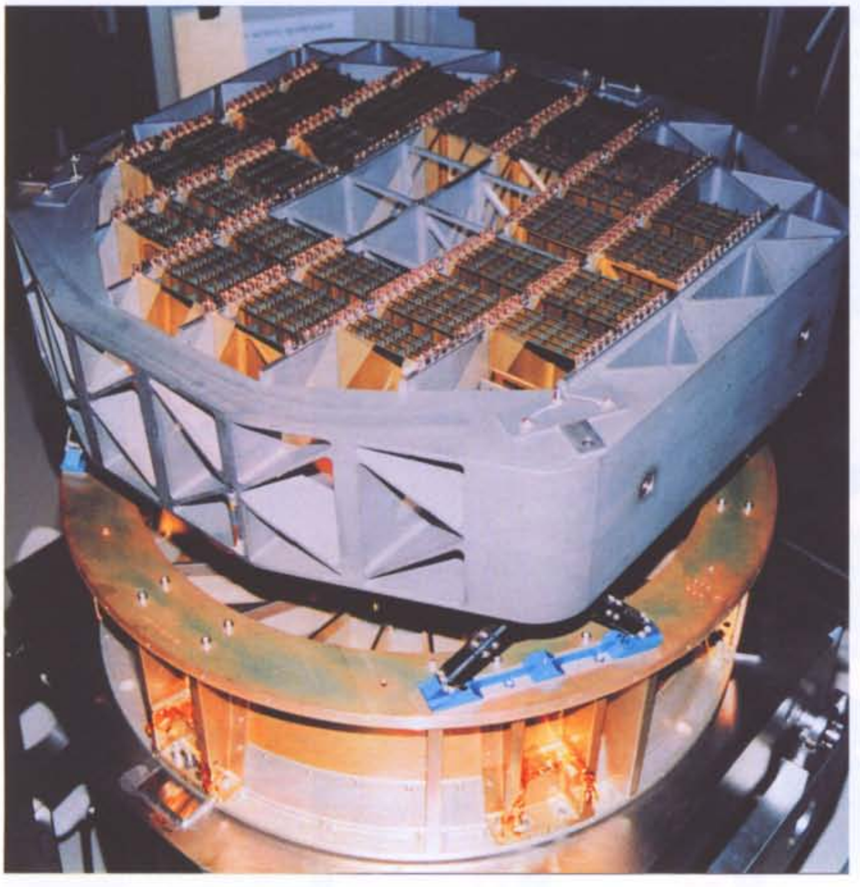

Figure 4. The grating array of the RGS instrument

Instrument description

Many of the design parameters – such as the number, size, type of gratings and CCD, and their relative positions – have gone through a long and complex optimisation process aimed at maximising the three main RGS scientific drivers: bandwidth, spectral resolution and sensitivity. This process has led to an instrument configuration featuring two identical independent instrument chains, each consisting of five units:
- a grating array
- a CCD camera
- one analogue electronics unit
- two digital electronics units, which are cold-redundant.

Some of their characteristics are described below.

The grating array, shown in Figure 4, is made up of a stiff lightweight monolithic beryllium structure, which houses 182 reflection gratings. In order to achieve its X-ray dispersing capabilities, each reflection grating features more than 600 groves/mm ruled on a 200 micron-thick gold layer, deposited on top of a 20 cm x 10 cm silicon-carbide substrate. Linear and angular positioning accuracies between gratings of the order of a few microns and a few arcseconds have been achieved by means of sophisticated manufacturing techniques, like precision diamond grinding and interferometric alignment. Finally, precise and stable mounting of the grating array onto the Mirror Module is achieved by means of three V-shaped titanium flexures.

Figure 5. The flight model of the RGS Camera (courtesy of SRON)

The need to maximise the instrument's sensitivity and at the same time optimise its optical characteristics has driven the RGS camera design and dictated the choice in terms of the number, type and working temperature of the CCD detectors that lie at its heart. Figure 5 shows the flight model of the RGS camera.

Passive cooling to about -80°C for optimal CCD performance is achieved by connecting the CCD bench inside the camera, via an aluminium cold finger, to a flat two-stage radiator viewing cold space. Six glass-fibre struts provide a robust support and at the same time minimise the conductive heat inputs on the radiator itself. Further thermal insulation of the cold CCDs from the warm external environment is accomplished by two separate heat shields, which by means of a sophisticated 'labyrinth' structure, achieve stable CCD positioning, satisfactory thermal de-coupling and substantial radiation shielding.

The choice of 'back-illuminated' CCD technology enables a high quantum efficiency to be achieved throughout the 5 - 35 Å instrument bandwidth. Each CCD has 768 x 1024 pixels, 27 x 27 microns in size. A strip of nine of these devices have been chosen so that the 253 mm-long spectrum created by the grating array can fit onto the detector focal plane, shown in Figure 6. Both the CCD strip and the centre of the grating array are positioned on an imaginary circle about 7 m in diameter, to minimise the aberrations of the optical system.

Among other tasks, the 'front-end' electronics inside the camera performs the CCD read-out, its conditioning and the signal amplification by distributing a suitable clock sequence and setting the correct bias voltages and gains for the preamplifiers.

The remainder of the electronics is distributed inside the analogue and the digital units. The former processes the pre-amplified signals coming from the nine CCDs, converts them into digital signals using a 12-bit Analogue-to-Digital Converter (ADC) and passes them, together with the set of housekeeping parameters, to the digital electronics. This unit is substantially in charge of the overall control of the instrument by, for example, choosing the appropriate operating mode for the instrument and configuring it accordingly, as well as formatting the data into suitable telemetry packets following data reduction. It also handles the incoming telecommands and provides appropriate power to the instrument.

The European Photon Imaging Camera (EPIC)

Principal Investigator: M. Turner

Instrument concept

The EPIC instrument is made up of three independent instrument chains, each one consisting of a camera unit with a Charge Coupled Device (CCD) detector assembly, an analogue electronic unit for camera control and signal conditioning, a digital signal-processing unit, and a data-handling unit, responsible for overall instrument control, data formatting, and interfacing to the spacecraft.

The three CCD cameras, positioned in the primary foci of the Mirror Modules, can be configured in a wide range of observation modes, which affect their sensitivity, and their spatial, spectral and time resolution. In this way, a large variety of time-correlated imaging and spectral measurements of one or more celestial objects can be gathered in a single observation.

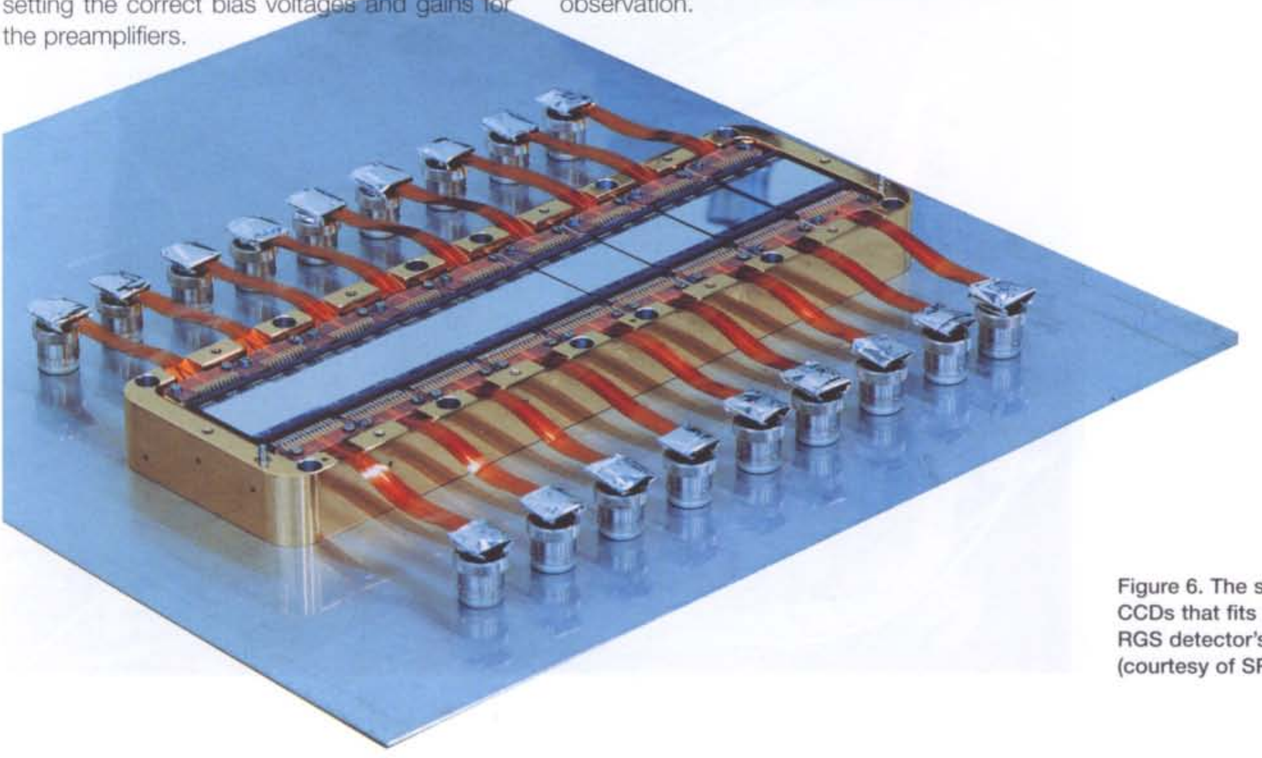

Figure 6. The strip of nine CCDs that fits within the RGS detector's focal plane (courtesy of SRON)

A Radiation Monitor completes the EPIC instrument set-up. It will continuously monitor the particle radiation environment to which XMM will be exposed, thereby providing us with valuable supporting data on the actual performances of the sensors and electronics.

Instrument description

Two cameras consist of an arrangement of seven metal-oxide (MOS) CCD arrays covering the 30 arcmin field of view of each Mirror Module. Each CCD is mounted on a ceramic carrier, which in turn is integrated on an Invar support structure for the complete focal-plane assembly.

Figure 7. One of the two EPIC instrument MOS CCD assemblies during integration

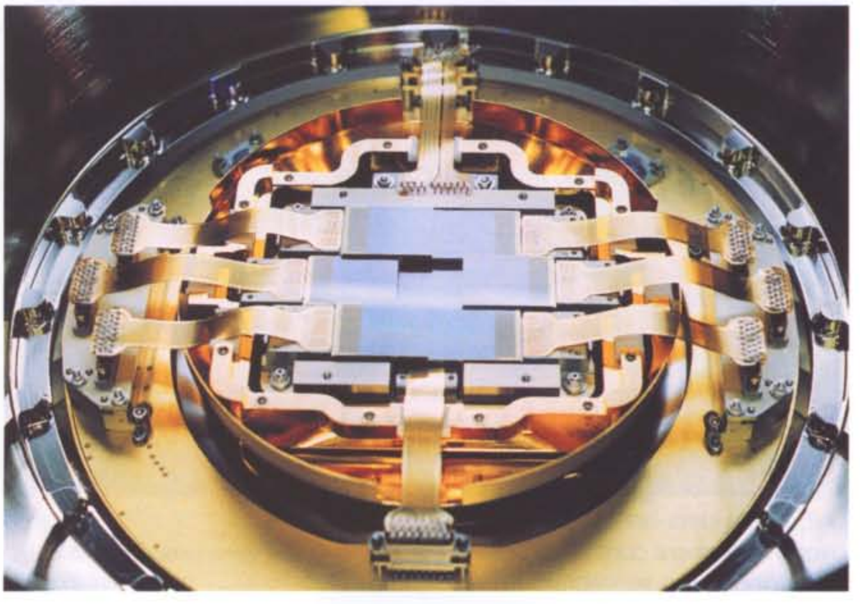

Figure 7 shows a MOS CCD assembly during integration at Leicester University (UK). Each MOS CCD features an imaging area of 600 x 600 pixels, 40 microns in size, capable of detecting X-rays in an energy band ranging from 0.1 to 15 keV, with a maximum timing resolution of 1 ms. In a typical observation mode, the full focal plane, consisting of seven CCDs, is read out in 2.7 s.

The third CCD camera, shown in Figure 8, differs from the first two MOS cameras mainly in terms of the semiconductor technology used, and the CCD size, number and layout.

Figure 9 shows an integrated p-n focal-plane layout. Twelve back-illuminated CCDs are all generated on a single 10 cm-diameter wafer. Each of them is organised as a 64 x 200 matrix of 150 micron-sized pixels. The use of p-n technology has resulted in a higher quantum efficiency than comparable instruments, particularly for energies around or below 0.5 keV and above 6 keV. Typical full-frame readout times of 48 ms can be achieved, with a maximum timing resolution of 40 microsec.

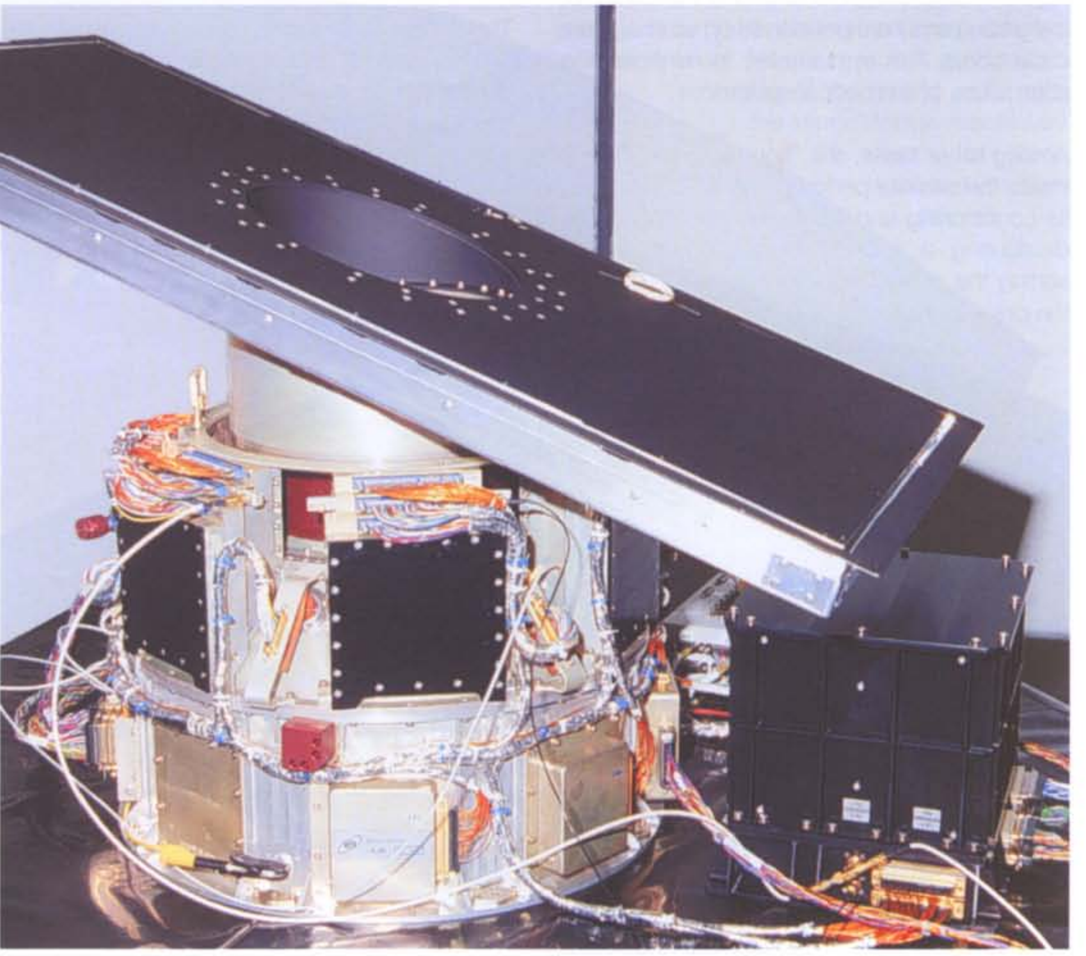

Figure 8. The p-n CCD camera of the EPIC instrument

Electrically, the CCDs are divided into four quadrants of three CCDs each, which can be controlled and read out separately by four electronic sections that provide for direct driving and buffering of all CCD signals.

Both the MOS and p-n focal-plane assemblies are enclosed in a vacuum-tight camera housing, which provides suitable shielding from the particle radiation environment.

In order to maximise instrument sensitivity, the three CCD detector assemblies are passively cooled to -100°C by means of a cold finger thermally coupled to a radiator system facing cold space. Figure 10 shows a top view of the Focal Plane Assembly in which the two MOS camera conical (white) radiators and the flat p-n camera rectangular radiator (black) between the two RGS camera radiators, can be identified.

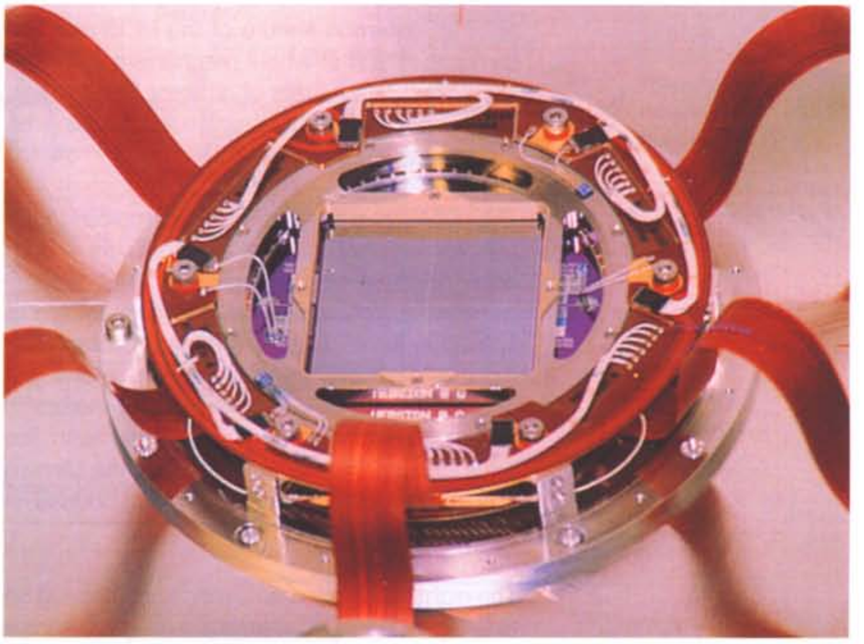

Figure 9. An integrated EPIC p-n CCD focal-plane layout

Figure 10. XMM's Upper Module during final MLI installation, showing the Focal-Plane Assembly

Another common feature of the MOS and p-n cameras is a filter-wheel mechanism with four aluminised Mylar filters of different thicknesses, which can be suitably selected depending on the intensity of the source.

The MOS Analogue Electronics Unit accommodates all programmable CCD sequencers, clock drivers, and bias voltage generators. The CCD output signals are fed to analogue signal chains with multiplexers and eight ADCs with 12-bit resolution, allowing a single CCD to be read out via two nodes in certain operational modes, together with the other CCDs. The thermal control for the camera and filter-wheel electronics is also housed in this box.

The eight CCD raw data streams are passed on to a digital signal-processing unit, which serves for high-speed data pre-processing and reduction. Eight Event Detection Units with pattern libraries and offset maps provide for the discrimination of X-ray events from gamma rays, particle events, and background noise.

The Event Analyser and the Control Electronics Units carry the equivalent functions of these two MOS units in the p-n chain. The Event Analyser is responsible for generating all CCD clock signals, reading the analogue signals of the 12 CCDs, digitising the data and making the basic noise and offset subtraction and event discrimination.

The Control Electronics accommodates various control and interface functions which are needed within the p-n camera system, such as camera-temperature and filter-wheel control. The bias voltages of the CCDs are also controlled and a large set of CCD parameters is made available for incorporation into the instrument's housekeeping telemetry.

The formatted output data from the MOS and p-n chains are passed on to the respective data-handling units. They represent a general-purpose 16-bit microprocessor architecture, with high-speed interfaces for handling the science data. All science and housekeeping data are formatted into telemetry packets according to ESA standards. The unit also decodes, checks and executes all tele-command packets.

The data-handling units select and control the various operating modes of the cameras: Full-Frame mode allows the readout of all CCDs; Window mode reads out only a selected area of the CCDs; Fast/Timing mode is selected for high time resolution, while Burst mode is selected for high-speed readout. Additionally, various Diagnostic modes can be commanded in order to support instrument calibration or to check CCD performance parameters before commencing an observation.

The Radiation Monitor detector is mounted on the outside of the XMM satellite and features three redundant silicon detectors. Two are sensitive to high-energy particles, such as electrons above 200 keV and protons above 10 MeV, while the third can detect low-energy electrons above 30 keV. Count rates and spectra of the particle radiation are accumulated in an electronics unit, which formats the raw data in either a Fast mode, with a time resolution of 4.0 sec, or in a Slow mode with an accumulation period of 512 sec.

The Optical Monitor (OM)

Principal Investigator: K. Mason

Instrument concept

The Optical Monitor is a modified Ritchey-Chrétien optical/ultraviolet telescope with a 30 cm diameter primary mirror, co-aligned with the three X-ray Mirror Modules, so that simultaneous observations in the X-ray and in the optical/UV regime can be carried out. The OM is a powerful instrument that will be capable of detecting sources with a sensitivity limit of magnitude 24 in its 17 arcmin field of view. It can provide images in the wave band from 160 to 600 nm with a resolution of about 1 arcsec, spectra of X-ray sources by means of low-resolution grisms (optical devices that combine the characteristics of a grating and a prism), and high-time-resolution photometry.

Instrument description

Three units compose the OM instrument: the telescope unit and two cold redundant digital electronic units. Figure 11 identifies the main constituents of the telescope, which can be summarised as follows:

- A long baffle with internal radial vanes for minimising stray-light from off-axis sources.
- A door fitted on the baffle to protect the optics from contamination whilst on the ground and during launch.
- The telescope module, made up of a 30 cm-diameter primary mirror and a 7 cm-diameter secondary mirror.
- The blue module which houses a beam deflector, and the two redundant detectors equipped with their respective filter wheels.
- The detector processing electronics.
- The telescope power supply.

The incoming light is focussed by the telescope module onto a 45 deg flat mirror mechanism, which can deflect the beam onto either of the

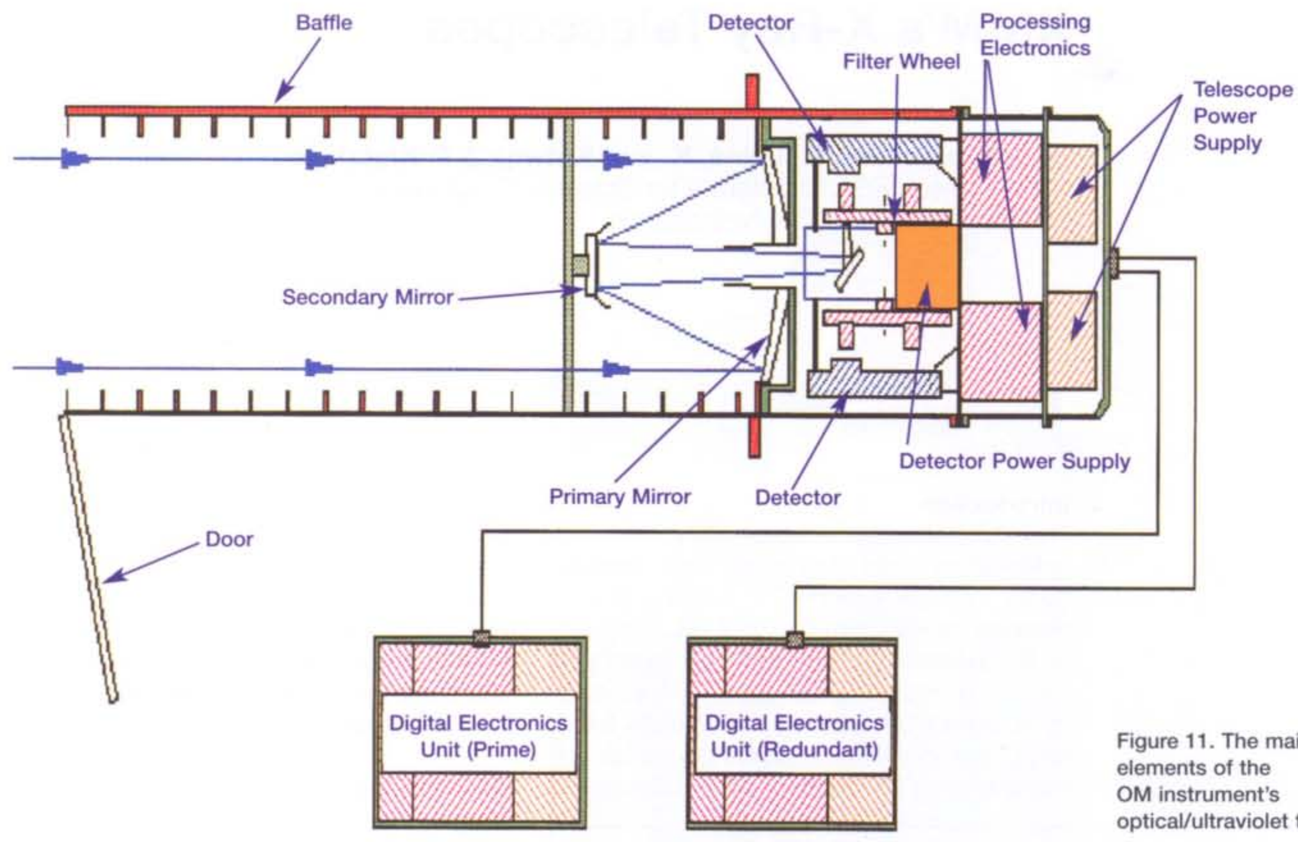

Figure 11. The main elements of the OM instrument's optical/ultraviolet telescope

two detectors by a 180 deg rotation around its longitudinal axis. Two filter wheels with seven filters, two grisms, a magnifier and a blocked position are positioned in front of the detector entrance aperture. Each detector assembly consists of an image intensifier with a photo-cathode, a micro-channel plate, a tapered fibre optics and a CCD.

The detector electronics reads out the CCD every 10 msec and centroids the photo-electron cloud with a resolution of 1/8th of a CCD pixel. This allows reconstruction of the angular position of the photons within a 0.5 arcsec circle over a 2048 x 2048 grid.

In order to maintain the detector temperature at around 30°C and to provide cooling to the rest of the electronics at the back of the telescope, four heat pipes transfer the heat to the front baffle, which acts as a radiator. The optics are maintained at 20°C by means of control heaters.

Each digital electronic unit consists of three parts: a digital-processing, an instrument-control and a power supply. The first one performs science data processing, including image accumulation over typically 1000 sec. Four digital signal-processing microprocessors and 11 Mbyte of memory are used to perform this function. It is also possible to store all of the time-stamped events for a small area of the detector in order to study the time-variability of sources.

In order to maintain the 1arcsec resolution over the complete exposure, the digital-processing electronics performs tracking every 10-20 sec on the acquired image and corrects the position of the detected photons accordingly.

Before being passed to the spacecraft's On-Board Data-Handling System, data are sent to the processor inside the instrument controller for proper packet reformatting. The instrument controller also provides the basic instrument control function, telecommand processing, housekeeping monitoring and code up-linking. Finally, the power-supply provides conditioned power for both the digital-processing electronics and the instrument controller.

Conclusion

XMM, with its simultaneous observation capabilities provided by dispersive high-resolution X-ray spectrometers (RGS) and by high-throughput non-dispersive X-ray imagers (EPIC) in combination with optical/ultraviolet images (OM), will guarantee a substantial leap forward in the X-ray astronomy of the next millennium.

Acknowledgement

The authors wish to acknowledge the enormous efforts of the Principal Investigators and their teams responsible for the three instruments on-board XMM, on whose work this article has been based.

XMM's X-Ray Telescopes

D. de Chambure, R. Lainé, K. van Katwijk & P. Kletzkine
XMM Project, ESA Directorate for Scientific Programmes,
ESTEC, Noordwijk, The Netherlands

Introduction

The XMM spaceborne observatory has been designed as a high-throughput X-ray spectroscopy mission covering a broad band of energies, ranging from 0.1 to 12 keV. The heart of the payload consists of three telescopes (Fig. 1), developed under direct ESA contract by a consortium of several European firms, each with particular technical expertise for manufacturing specific parts of the telescopes.

The XMM observatory has, at its heart, three large X-ray telescopes, which will provide a large collecting area (1430 cm^2 each at 1.5 keV, and 610 cm^2 each at 8.0 keV) with a spatial resolution of around 14-15 arcsec. At the end of 1998, three months ahead of schedule, the three flight and the two spare models of the X-ray telescope were handed over to the XMM Prime Contractor Daimler Chrysler Aerospace (D). The three flight models were integrated onto the spacecraft's optical platform at ESTEC at the end of March 1999.

The X-ray telescopes show mechanical and optical performances much better than specification, which will undoubtedly bring important benefits for astronomers. The most challenging parts of their development phase were the design, manufacture and testing of the X-ray mirrors, which required four intensive years of work under ESA's direct management (see ESA Bulletin No. 89, Feb. 1997).

This article focusses on the telescope design, with emphasis on the X-ray mirrors and baffles, and the X-ray and optical test results achieved with the flight models of the telescope, including stray-light reduction. Based on the lessons learnt from the XMM experience, the prospects for the next generation of ultra-thin X-ray mirrors are also addressed.

The optics for each telescope consist of 58 nested Wolter-I grazing-incidence mirrors, or Mirror Modules, chosen to maximise the effective collecting area within the volume allocated. This highly nested design calls for the manufacture of a large number of X-ray-quality mirror shells. In 1993, after a competitive development programme, nickel electroforming technology was selected for the mirror production, with Media Lario (I) as Prime Contractor. Two years later, the yield ratio for the nickel mirrors was sufficient to successfully undertake the massive task of producing 311 X-ray-quality mirror shells – representing a total of 200 m^2 of high-quality optical surface – required for the start of the Qualification Model (QM) and Flight Model (FM) production phases. After the timely delivery of the QM Mirror Module, and after the completion of optical and environmental testing, the XMM Mirror Module was pronounced 'qualified' in October 1996.

By September 1998, the first four FM Mirror Modules had been delivered to ESA, and the acceptance and calibration tests were completed at Centre Spatial de Liège, the Max-Planck Institute and Dornier's facilities near Munich. At the end of 1998, three months ahead of schedule, the three selected flight models and the two spare models of the X-ray telescope were handed over to the XMM Prime Contractor, Daimler Chrysler Aerospace (Dornier). The three flight models were integrated onto the optical platform of the spacecraft in the clean tent in the ESTEC integration area at the end of March 1999.

The telescopes with the best optics have been chosen for flight, namely the FM2, FM3 and FM4 flight models. The two telescopes with the best resolution (FM3 and FM4) were allocated to the spectrometers (gratings + RGS detectors) and the EPIC MOS imaging camera, which have a better resolution than the EPIC p-n imaging camera. FM5 was not included in the selection since, being a spare, its delivery was foreseen after the date of selection and integration.

The X-ray baffle development, contracted to Sener (E), had to be completed in a short time, at a late stage in the XMM programme (after the start of the main development phase, C/D). Once the decision had been taken to reduce the X-ray stray light by including an X-ray baffle, it took the XMM Project only seven months to design it, to demonstrate manufacturing feasibility, and to verify that the telescope's performance was not degraded in terms of resolution, effective area and optical stray light.

Telescope design

The three telescopes consist of the following elements (Fig. 2):

- mirror assembly door: closes and protects the X-ray optics and the telescope's interior against contamination during integration, testing, transport, launch and the early orbit phase
- entrance baffle: provides the stray-light suppression capability in the visible wavelength range at angles larger than 47°. It consists of a cylindrical aluminium shell with an outer diameter of 870 mm. The inside is covered by 12 circumferential vanes and is optically black. Due to volume constraints under the Ariane-5 launcher fairing, the baffle length is limited to 900 mm, including the protrusion of 200 mm below the separation plane into the launch adapter. They are mounted after the integration of the Mirror Modules on the spacecraft
- X-ray baffle (XRB): blocks X-rays from just outside the nominal field of view, which would otherwise reflect on the hyperboloid section of the mirrors, resulting in stray light
- Mirror Module (MM): the X-ray optics of the telescope
- 'electron deflector' (produces a toroidal magnetic field): located right behind the mirrors (in the shadow of the Mirror Module spider), for diverting 'soft' electrons (with energy up to 100 keV)

Figure 1. Integration of the three X-ray telescopes on the XMM spacecraft inside the class-100 area of the ESTEC Test Centre (Noordwijk, NL)

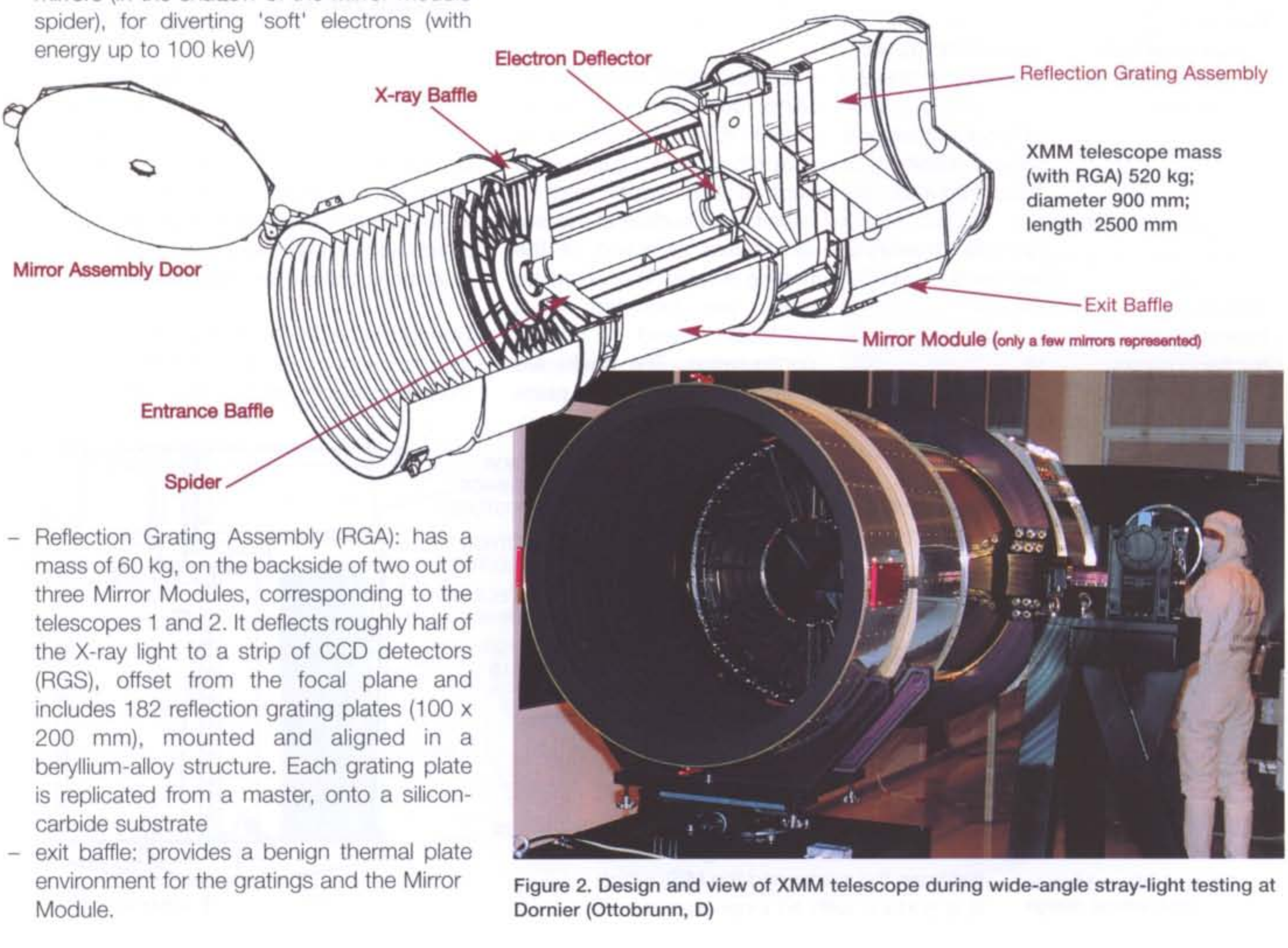

- Reflection Grating Assembly (RGA): has a mass of 60 kg, on the backside of two out of three Mirror Modules, corresponding to the telescopes 1 and 2. It deflects roughly half of the X-ray light to a strip of CCD detectors (RGS), offset from the focal plane and includes 182 reflection grating plates (100 x 200 mm), mounted and aligned in a beryllium-alloy structure. Each grating plate is replicated from a master, onto a silicon-carbide substrate
- exit baffle: provides a benign thermal plate environment for the gratings and the Mirror Module.

Figure 2. Design and view of XMM telescope during wide-angle stray-light testing at Dornier (Ottobrunn, D)

Mirror Module

A Mirror Module is a grazing-incidence telescope (Wolter-I type) which is designed to operate in the X-ray energy range of 0.1-12 keV with a focal length of 7.5 m and with a resolution of 16 arcsec. A Mirror Module consists of 58 nested mirror shells bonded at one end to a spider (or spoked wheel) and their supporting structure. The grazing angle of the X-rays ranges from 17 arcmin for the smallest mirror to 40 arcmin for the largest. The optical concept of the XMM Mirror Module is shown in Figure 3.

740 mm and an outer diameter of 770 mm, needs to be better than 5 µm. Heaters and thermistors, mounted on the spokes and the outer ring of the spider, provide the thermal control for the Mirror Module at 20°C ± 2°C, with transverse and radial gradients not exceeding 2°C.

The X-ray mirrors are thin monolithic gold-coated nickel shells. The mirror shell manufacturing is based on a replication process (Fig. 5), which transfers a gold layer deposited on the highly-polished master

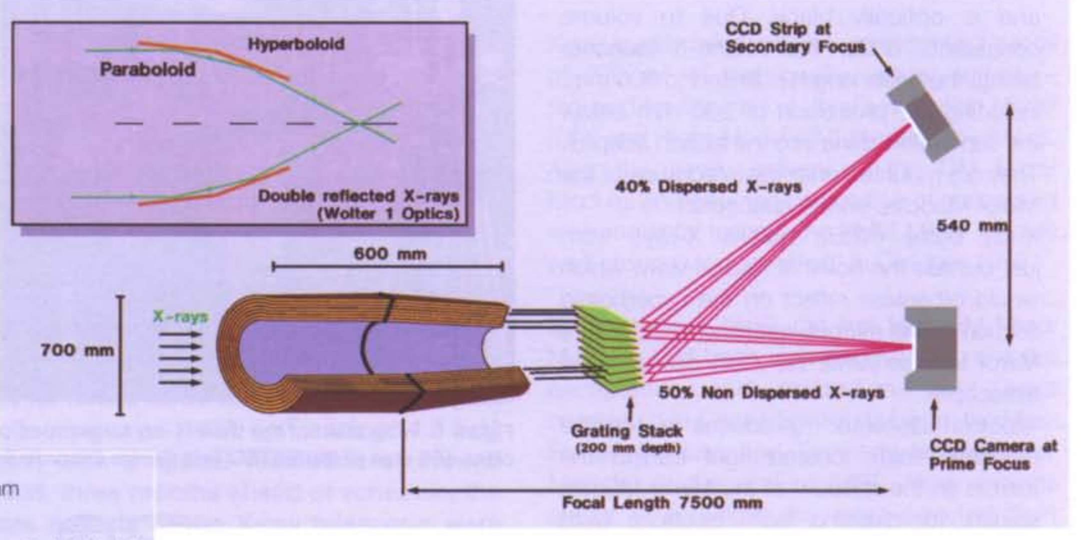

Figure 3. Optical design of the XMM Mirror Module with the EPIC and RGS detectors

Focal length	7500 mm
Resolution	
Half Energy Width	16 arcsec (0.1-12 keV)
Full Width Half Max	8 arcsec (0.1-12 keV)
Effective area	
	1475 cm^2 (1.5 keV)
	580 cm^2 (8 keV)
	130 cm^2 (12 keV)
Mirror diameter and thickness	
Outermost	700 mm (1.07 mm)
Innermost	306 mm (0.47 mm)
Mirror length	600 mm
Packing distance	1- 5 mm
Number of mirrors	58
Reflective surface	Gold (250 nm layer)
Mirror Module mass	420 kg

The mechanical design of the Mirror Module is shown in Figure 4. Each mirror is shaped to a paraboloid surface in front and a hyperboloid surface at the rear for double reflection of the grazing X-rays. The 58 mirror shells are mounted in a confocal and coaxial configuration. The shells are glued at their entrance plane to the 16 spokes of a spider (spoke wheel) made out of Inconel. This material was chosen for its thermal expansion, which is close to that of the electrolytic nickel of the mirrors. The spider is connected to the platform of the XMM spacecraft via an aluminium interface structure, the Mirror Interface Structure (MIS), which consists of a double conical surface reinforced by stiffeners and an interface ring. To minimise the mechanical deformations of the mirrors and therefore the optical degradation, the flatness of the mounting interface between the spider and the MIS, which is a surface with an inner diameter of

mandrel to the electrolytic nickel shell, which is electroformed on the gold layer. The production of the required 58 master mandrels was contracted to Zeiss (D). They are initially made out of double conical aluminium blocks coated with Kanigen nickel, then lapped to the exact shape and, finally, super-polished to a surface roughness better than 4 Å (0.4 nm).

Due to the sensitivity of the mirrors in the way they are supported, the most critical steps in the manufacturing of the Mirror Module are the

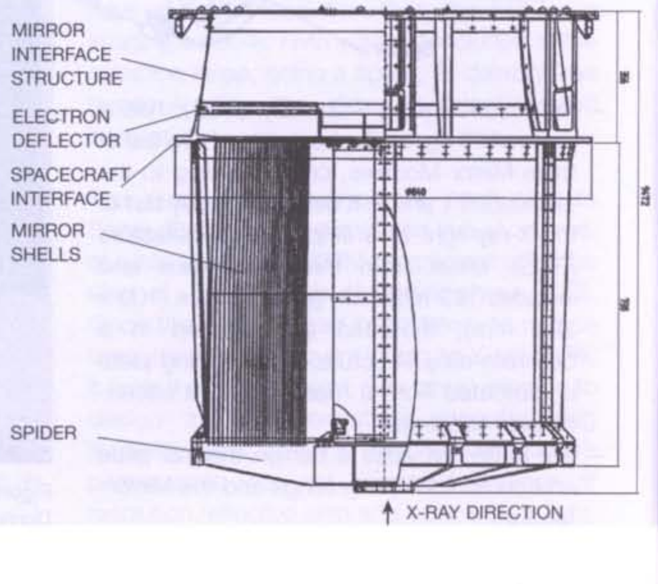

Figure 4. Mirror Module mechanical design

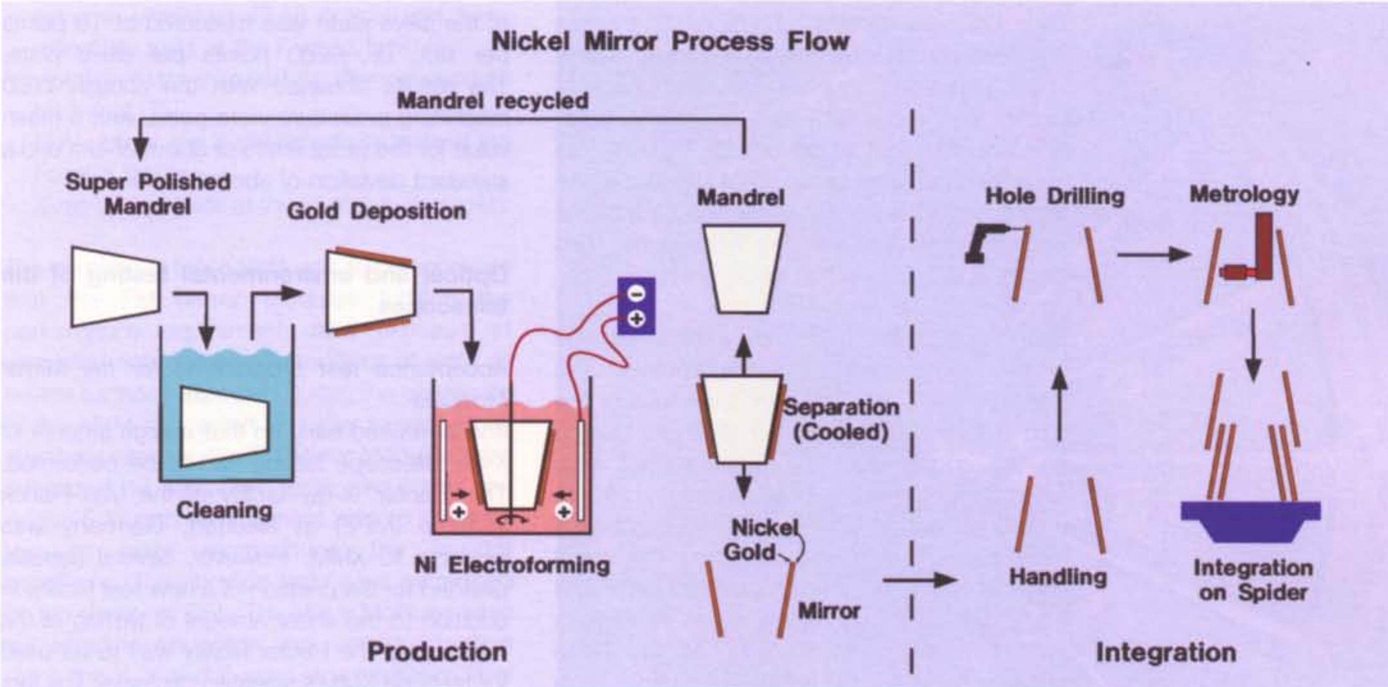

production of the mirror shells and their integration onto the spider. Indeed, the XMM mirrors are very fragile, their diameter-to-thickness ratio being in the order of 324, ten times as large as for SAX or JET X telescopes.

The technological development and the management of the XMM X-ray mirror programme have been detailed in a previous issue of the ESA Bulletin (No. 89, February 1997).

X-ray baffle

Single reflections from one or more of the hyperboloid surfaces introduce a high level of confusing stray flux in the Field of View (FOV) of the detectors. This occurs for objects located close to, but outside, the FOV (cone angle of 15 arcmin). Previous X-ray telescopes with a small number of mirrors could be protected from such effects by individual shells in front of each mirror. However, highly nested telescopes, such as ASCA, are not baffled due to the limited space between the mirrors. This represents an important limitation for ASCA that produces significant stray light and complicates the evaluation of the observation data. This stray light can only be suppressed by using a 'pre-collimator' (or X-ray baffle) consisting of thin cylindrical shells, which extend the mirror shells forward. In order to reduce reflection and scattering from the cylindrical surfaces, cylindrical sections can be removed leaving thin circular annular rings (strips) in front of each mirror (Fig. 6).

Figure 5. Mirror production and integration process

Figure 6. Principle and 3D view of the X-ray baffle

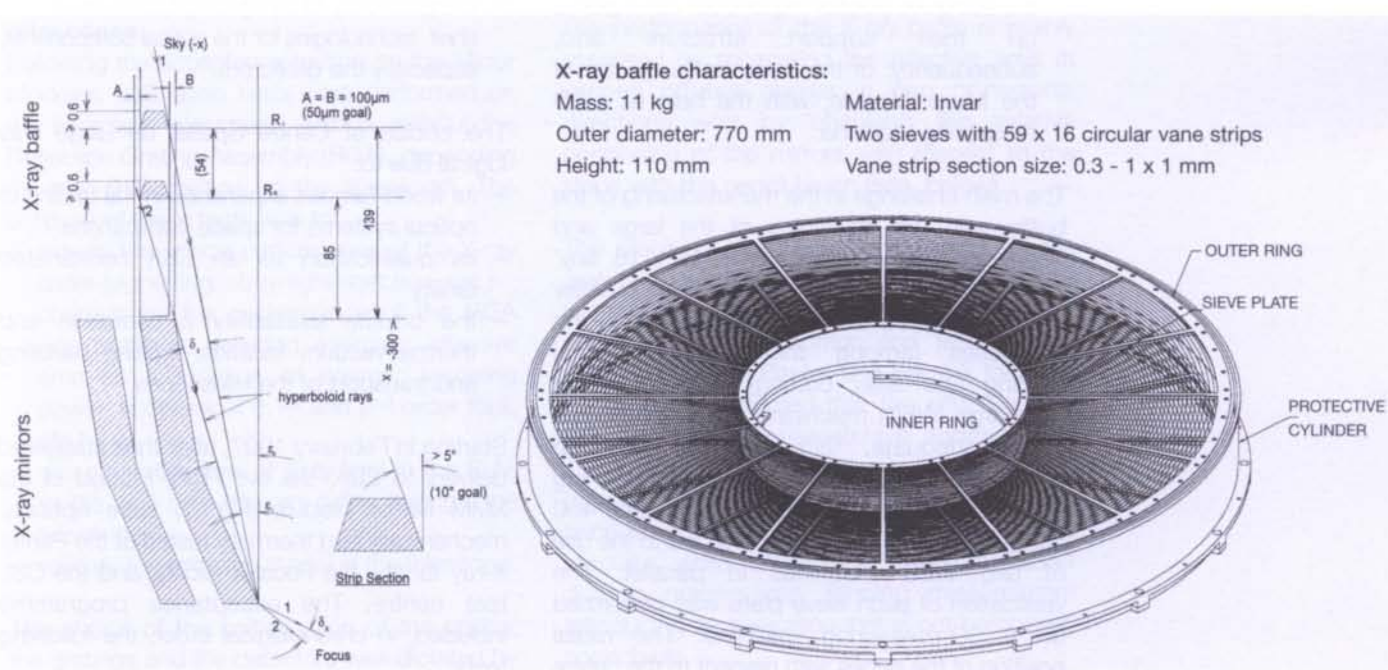

Thus, the X-ray baffle is constructed as a series of 'sieve plates', made out of circular strips. These plates are mounted in line with the front face of the mirrors, such that they block single-reflection rays, but do not eclipse the bona fide two-reflection rays. In the XMM telescope, the axial space available allows for two such plates to be incorporated into the X-ray baffle. This blocks about 80% of the single-reflection flux.

Each sieve plate is basically a disc, with 59 circular strips and 16 radial spokes, and therefore 59 x 16 slots. The thickness of the disc is 1 mm, except for the stiffeners located on the spokes and the outer annular ring, where the thickness is locally 5 mm. In order to reduce the optical stray light, introduced by the X-ray baffle, to a maximum extent, the lateral surfaces of the strips are chamfered by 5° and the edges of the strips are made very sharp (radius smaller than 20 µm). All the baffle surfaces (including the edges of the vane strips) facing the mirrors are blackened.

The main requirement placed on the X-ray baffle is the accuracy of the radial position of the edges of the vane strips of the sieves with respect to the position of the mirrors. It must be better than 100 µm, including manufacturing, assembly and integration errors, and displacement due to thermal conditions (-10°C to +10°C).

The fulfilment of this high tolerance requirement relies on:
- the selection of a high-quality Invar material, with a very low coefficient of thermal expansion ($< 10^{-6}\ ^{\circ}C^{-1}$), for the sieve plates and their support structure (inner and outer ring)
- the accurate machining of each sieve plate
- the accurate positioning of both sieve plates on their support structure and, subsequently, of the X-ray baffle on top of the Mirror Module, with the help of a 3D measuring machine.

The main challenge in the manufacturing of the baffle was the machining of the large and flexible Invar sieve plate, with its 59 x 16 'tiny' strips, with a precision better than 65 µm. After having analysed several potential machining processes (among them photochemical etching and laser cutting), Wire Electrical Discharge (WED) machining proved to be the most adequate, although it has the disadvantage of involving long machining times. Each sieve plate needed between 400 and 500 machining hours, which led to the use of two WED machines in parallel. The verification of each sieve plate was performed on a 3D-measuring machine. The radial position of the edges with respect to the centre of the sieve plate was measured at 10 points per slot, i.e. 9280 points per sieve plate. The results obtained with the chosen WED machining procedure were good, with a mean value for the radial errors of about 25 µm and a standard deviation of about 35 µm.

Optical and environmental testing of the telescopes

Acceptance test programme for the Mirror Modules

It was realised early on that a large amount of X-ray telescope testing had to be performed. The 'Panter' X-ray facility of the Max-Planck Institute (MPE) at Neuried, Germany was available to XMM. However, several aspects pleaded for the creation of a new test facility. In addition to the sheer amount of testing of the telescopes, the Panter facility was to be used for tests on XMM's scientific cameras. The fact that the telescopes tested at Panter had to be in the horizontal position was not insignificant for such thin mirror shells, and parasitic gravity effects could not be excluded. Most importantly, for the measurement of the optical performance, a third of the mirror shell surface could not physically be properly illuminated because of the slight divergence of the X-ray beam. The ESA XMM Project office therefore decided, in 1994, to complement the Panter facility by building a custom-designed, vertical facility equipped with an 800-mm EUV collimator and two thin X-ray beams, adapted to the dimensions of the telescopes. This facility, called 'Focal-X', is located at Centre Spatial de Liège (CSL) in Belgium. Two aspects motivated the choice of EUV light (at 58 nm):
- the negligible level of diffraction effect
- the possibility of using fairly standard off-the-shelf technologies for the optical components, especially the detectors.

The choice of Centre Spatial de Liège was logical due to:
- its world-famous experience in the testing of optical systems for space applications
- its qualification as an ESA coordinated facility
- the on-site availability of vibration and thermal-vacuum facilities, limiting handling and transport of the telescopes.

Starting in February 1997, after their staggered delivery to ESA, the five Flight Models of the XMM Mirror Module (Fig. 7) were optically, mechanically and thermally tested at the Panter X-ray facility, the Focal-X facility, and the CSL test centre. The acceptance programme included, in chronological order, the following tests:

- extreme ultraviolet (EUV) optical and X-ray reflectivity tests at the Focal-X facility
- vibration tests followed by thermal-vacuum testing at CSL
- EUV optical and X-ray reflectivity tests at the Focal-X facility
- X-ray optical tests at the Panter X-ray facility.

The purpose of these tests was to demonstrate that the FM Mirror Modules fulfilled the performance requirements after exposure to simulated environmental conditions at least as severe as those expected during the service life of the XMM spacecraft. In order to verify their structural integrity, the FM Mirror Modules were subjected to vibration tests simulating the Ariane-5 launch environment and to thermal-vacuum tests representing the in-orbit conditions. The vibration tests were performed on the shaker at CSL. The Mirror Modules were subjected to sinusoidal and random vibration along the X, Y and Z-axes at acceptance level (10 g axial and 6.7 g lateral). The thermal tests (3 cycles between –20°C and 40°C) were performed in the Focal-2 thermal-vacuum test chamber at CSL.

The environmental tests on the FM Mirror Modules were successful because the following criteria were fulfilled:
- the specified test input loads were applied
- the fundamental frequencies were within specification and did not vary significantly after the high-level vibration tests
- no visual damage was observed after the environmental tests
- the optical performance had not deteriorated due to the vibration and the thermal tests (see below).

Calibration test programme for the telescopes

Following the acceptance testing on the Mirror Modules, calibration tests were performed on the complete telescopes, with or without the Reflection Grating Assembly (RGA), depending on their final position on the spacecraft. The purpose of these tests was to:
- assess the optical performance of the X-ray baffle (vignetting, stray-light rejection, etc.)
- characterise the performance of the RGA (line profile at selected energies; effective area as a function of energy; resolving power, positions of 0,1st and 2nd order focii, etc.)
- determine the level of stray light in the EUV, visible and near-infrared going through the telescope
- validate the software model of the telescope.

The choice of the combination of the optics, the gratings and the detectors was dictated by the scientific objectives of the XMM mission. In view of the lower resolution of the EPIC p-n detector (pixel size 140 µm) compared to the RGS and the EPIC MOS detectors (pixel sizes 27 and 40 µm), the two Mirror Modules with the best resolution were combined with the RGS and EPIC MOS instruments. Therefore, these two Mirror Modules (currently FM3 and FM4) are equipped with the RGAs.

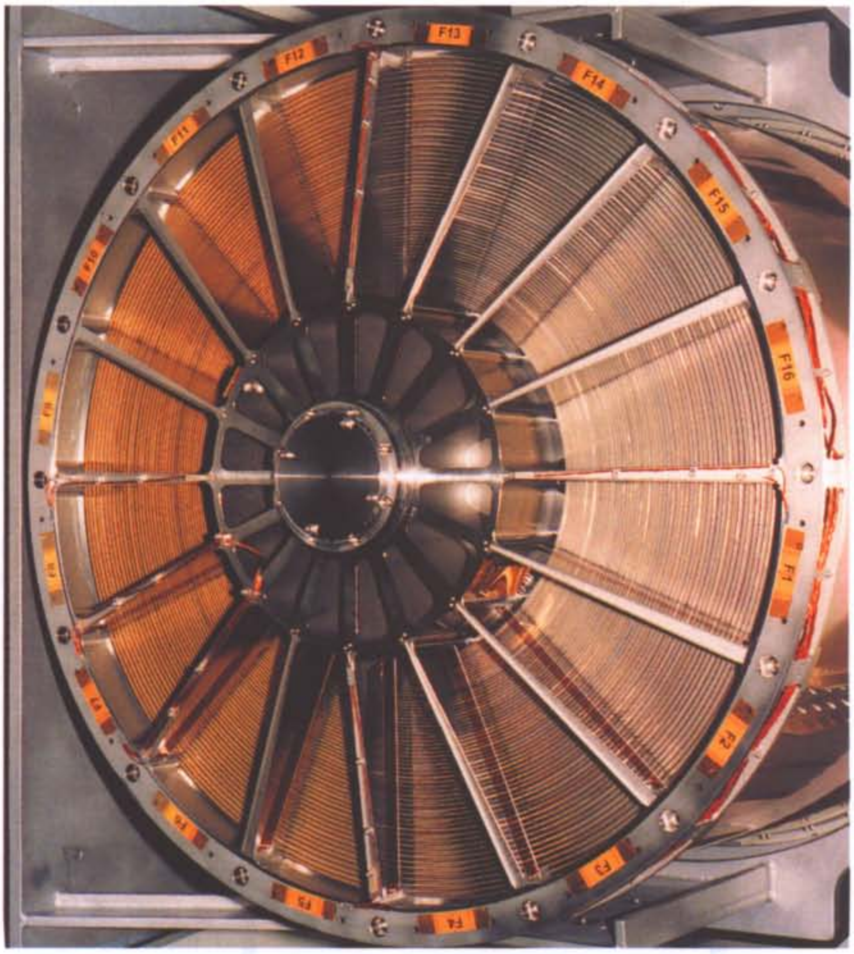

Figure 7. Mirror Module entrance plane with the 58 X-ray mirrors

The performance of the X-ray baffle is mainly assessed by measuring the effective area at various off-axis angles in two orthogonal directions and by checking the relative positioning of the mirrors with respect to the strips with the pencil beam (see below).

The precision alignment and assembly of the grating elements of the RGA were performed at Columbia Astrophysics/Nevis Laboratory, and the end-to-end calibration and testing were performed at the Panter and Focal-X facilities. These tests confirmed that the effective area for both RGS spectrometers is approximately 150 cm^2 at 0.15 nm. The measured resolving power of RGA2 has exceeded predictions because of the high performance of the Mirror Modules, while it falls short slightly for RGA1 due to grating-array fanning misalignment introducing an aberration that is not completely correctable.

Stray-light tests were performed in the EUV, visible and near-infrared spectral ranges, in order to verify the predictions obtained from the stray-light calculations. These tests were carried out at small angles, up to 7.5°, with the Mirror Module plus X-ray baffle and at large angles, from 10° up to at least 47°, with the complete telescope. At small angles, the entrance baffle was not tested because it is not a stray-light contributor (not illuminated by the Earth). Other spacecraft components (i.e. telescope Sun shield; telescope tube) were not present in the stray-light tests due to their large dimensions. Also, they are not considered as important verification subjects, since optical analysis has shown that the corresponding stray paths lead to negligible stray-light levels.

Small-angle stray-light tests were performed at the Focal-X facility. They acquired images for sources located between 20 arcmin and 7° in the visible and in the EUV. This was achieved by tilting the optical bench (supporting the tested telescope), the tower and the upper optical focal bench with the detectors (made as a single structure) and by translating the CCD at different locations to completely cover the EPIC or the RGS Field of View (FoV). Indeed, the CCD is 18 mm x 25 mm, the EPIC FoV has a diameter of 66 mm, and the RGS FoV is rectangular and 25 mm x 250 mm. The images were then analysed and compared to simulations performed with a ray-tracing programme. For all off-axis angles at all azimuthal positions, the test results confirmed the simulations, both qualitatively in terms of image quality and quantitatively in terms of integrated collecting area in the EPIC and RGS FoV.

Large-angle stray-light tests were performed in the large clean room (class 100) at Dornier in August 1998. The test set-up included the light source with a xenon arc lamp, the collimator, the telescope to be tested and a light trap in the direction of the telescope FoV. The test detector was moved to the position of the EPIC and of the RGS camera, where the Point Source Transmittance (PST) was measured and compared with the analysis results. The PST is defined as the integrated stray-light irradiance at the detector divided by the source irradiance at the entrance of the telescope. The measurement of the signal-to-noise ratio (S/N) has shown that the complete optical chain with the source, the optics, the telescope and the chosen CCD test detector is not noise-limited. In fact, it is limited by the scattering of the air and particles, and by the backscattering from the walls of the test facilities within the direct FoV of the telescope. Both are responsible for a background PST in the order of 10^{-9}. Therefore, the stray-light calculations were verified for a large range of angles of incidence of the incoming radiation, except for angles close to 70 - 90°, where the residual PST in the test configuration was too high.

EUV and X-ray results at Centre Spatial de Liège (CSL)

Image quality and effective area in the EUV

The image quality (Full Width Half Maximum (FWHM), Half Energy Width (HEW), 90% Encircled Energy (W90)) of the five Flight Models of the Mirror Module, measured in EUV (58 nm) at CSL, is summarised in Table 1. The EUV tests showed no significant differences in the Encircled Energy Function (EEF) before and

Table 1. Image quality of the Flight Model Mirror Modules from CCD measurements at CSL before (pre-env) and after (post-env) environmental tests compared to the Qualification Model of the Mirror Module at 58 nm

Mirror Module model	MM QM	MM	FM1	MM	FM2	MM	FM3	MM	FM4	MM	FM5
Position on S/C	N/A	Flight	spare	No	RGA	with	RGA2	with	RGA1	Flight	spare
Optical test (58 nm)	Post-env	Pre-env	Post-env	Pre-env	Post-env	Pre-env	Post-env	Pre-env	Post-env	Pre-env	Post-env
HEW at best focus (arcsec)	19.5	15.8	15.5	16.1	15.4	14.2	14.0	13.7	13.9	11.7	11.7
FWHM at best focus (arcsec)	10.2	6.7	6.7	6.9	6.3	5.5	4.5	4.9	4.9	4.9	4.9
W90 at best focus (arcsec)	110	62	63	63.5	62	58	59	62	63	53	55
Focal length (mm)	7496.0	7493.0	7493.0	7493.2	7493.2	7493.7	7493.6	7493.4	7493.4	7494.7	7494.7

Table 2. Measurements of X-ray reflectivity (in %) of mirror sizes 1, 20 & 58 (incidence angles respectively 40, 30 & 17 arcmin) of the 3 telescopes to be flown

Model	FM2			FM3			FM4			Theory (Henke 93)		
Mirror size	1	20	58	1	20	58	1	20	58	1	20	58
Reflectivity at 1.5 keV	68	75	87	69	76	85	63	74	83	76	81	89
Reflectivity at 8 keV	0.5	38	74	0.3	39	73	0.3	37	69	<0.5	43	78

after environmental tests. The overall performance in terms of resolution indicates an important improvement compared to the QM Mirror Module:

- the core of the Point Spread Function (PSF) is very sharp (no double peak as for the QM Mirror Module), especially for Mirror Modules FM3 and FM4 with a FWHM of 4.5 arcsec (Fig. 8)
- the resolution (HEW) is better than for the QM Mirror Module (measured at 20 arcsec) and has been continuously improved
- the W90 has been improved compared to the QM Mirror Module, which was at 100 arcsec, due to reduced deformation of the edges of the mirrors.

The focal images of Mirror Modules FM1 and FM2 (Fig. 8) show a 'triangular' shape, which comes from the distortion of the outer mirror shells (see below). This distortion, responsible for a performance loss estimated to be in the order of 1-2 arcsec for FM1 and 2 arcsec for FM2, occurred during the integration of the Mirror Module. Indeed, several analyses have confirmed that the deformation of the outer mirrors is the result of the unevenness between the spider and the Mirror Interface Structure (flatness of 15 - 25 µm instead of the specified 5 µm), aggravated by small deformations of the integration adapter, on which the spider was mounted during the integration of the mirrors. This point was not identified for the QM Mirror Module as no large X-ray-quality mirror could be integrated in that model. A shimming method was developed and tested, which has been successfully implemented on FM3 and, to a lesser extent, on FM4 and FM5.

X-ray reflectivity tests

The X-ray reflectivity (double reflection) of the five Flight Models of the Mirror Module was measured at several energy levels. Reflectivity measurements were performed in the middle of the mirrors along two azimuths with a pencil beam (diameter 0.5 mm at the entrance of the mirrors with a maximum divergence of 8 arcsec half angle). For each mirror, the reflectivity is the ratio of the integrated counts in the area of interest of the reflected and the incident beam, on a germanium solid-state detector, closed by a beryllium window. The measurement accuracy of the method is estimated to be ± 1-2%. In Table 2, the X-ray reflectivity values have been indicated at 1.5 and 8 keV, for some representative mirrors (largest size #1; smallest size #58 and one with an incidence angle close to critical angle, size #20) of the 3 telescopes to

Figure 8. Point Spread Function of the QM and FM Mirror Modules (log scale of intensity)

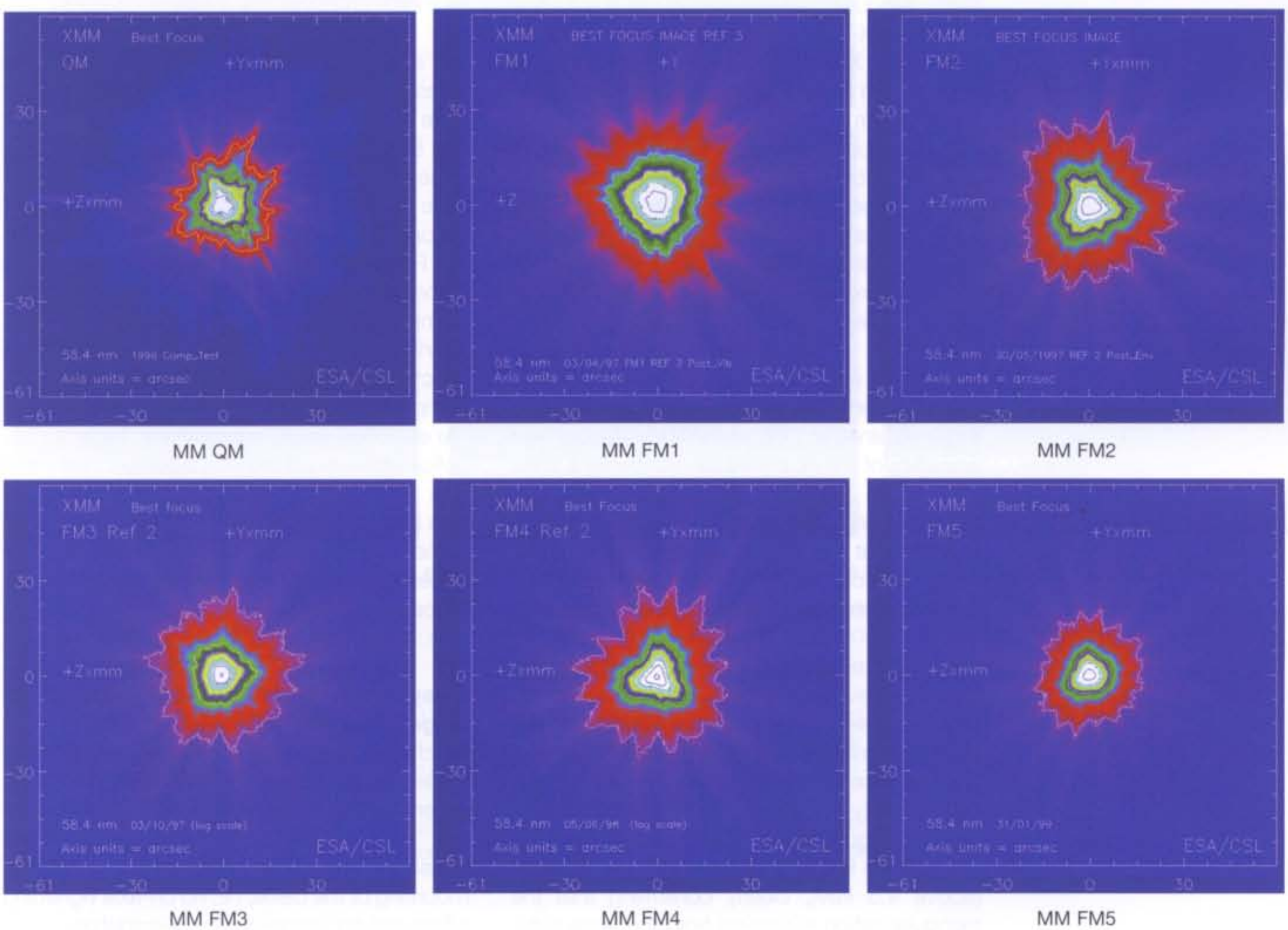

be flown. It shows that the reflectivity of the mirror is good, representing a loss per reflection of only 2 - 3% at 1.5 keV and 3 - 4% at 8 keV. The values take into account corrections for the loss of reflectivity due to scattering of the incident beam outside the detector field (detector diameter 20 mm): 0.6% at 1.5 keV and 6% at 8 keV.

At all energy levels, there was no degradation after each optical/environmental test: values were stable within the measurement accuracy with the exception of the shells (sizes #54, #49 and #45) with high fluctuations (about 10 - 20%). These mirrors are known to have a locally poor micro-roughness (around 0.8 nm measured with Promap interferometer), due to some mandrel surface degradation after a certain number of replications.

X-ray test results at Max-Planck Institute (MPE)

The image-quality figures (Full Width Half Maximum (FWHM), Half Energy (HEW), 90% Encircled Energy (W90)) of the five FMs of the Mirror Module measured at the Panter facility in the period April 1997–July 1999, are summarised in Table 3 and in Figure 9. The Mirror Modules were tested in full illumination (horizontal X-ray beam with a source at 124 m) at different X-ray levels between 0.1 keV and 10 keV, with two different detectors: a Position-Sensitive Proportional Counter (PSPC) and a Charge-Coupled Device (CCD). The PSPC has a diameter of 76 mm, equivalent to a diameter of 980 arcsec in the focal plane, whereas the CCD has a size of 20 mm x 13 mm, which does not cover the wings of the PSF completely. Therefore, reliable W90 measurements could only be obtained with the PSPC.

The X-ray results of the HEW and FWHM measurements give values almost identical to those obtained at CSL, within the measurement accuracy of the facility, which was not the case for the QM Mirror Module. This confirms that the improvements made to the mirror geometry, especially at the edges (affecting 10% of the mirror surface), which are not 'seen' at Panter due to its finite source distance, were successful.

Performances at X-ray energy levels higher than 6.4 keV were slightly better than at 1.5 keV because of the small contribution of the large size mirror shells (effect amplified by the finite source distance) and because of the better quality of the inner mirror shells. In Figure 9, the triangular shape of the core of the focal image is no longer visible at high energy levels (above 4.5 keV), clearly confirming that the triangularisation is coming from the large outer mirrors. The shadowing structures are entirely due to the spider spokes. The images in Figure 9 and the data in Table 3 clearly show that the power in the wings increases at energies between 0.9 keV and 6.4 keV, while the central part does not change significantly. For the higher energy levels, the core and the wings get smaller, since the outer mirrors are no longer contributing, due to the finite source distance and the lower reflectivity of the large mirrors. In conclusion, the mirror scattering, which is expressed in the W90 at high energies, is much better for FM Mirror Modules than for the QM Mirror Module, which was measured at about 240 arcsec at 8 keV.

The determination of the effective area was based on a relative measurement. The same detector (PSPC) was used to measure the count rate of the flux with and without the Mirror Module in the beam. This method has the advantage that most of the properties of the detector do not need to be taken into account for the computation of the effective area. The measurements were done at full illumination with the PSPC moving slightly laterally (few mm) in intra-focal position (100 mm) to avoid obstruction by the wire mesh that supports the detector entrance window. The method's precision was better than ±2%.

For all the FM Mirror Modules, the effective areas measured with full-aperture illumination were systematically 15% lower (both at 1.5 keV and 8.0 keV) than the 'theoretically' achievable value. The results of these full illumination tests have been difficult to analyse because of secondary shadowing due to the geometry of the Panter facility (finite source distance) with respect to the tight nesting of the mirrors. Complementary tests with a reduced beam aperture gave a more reliable estimate of the effective area, with a loss of less than 10% compared to theory. The area is very close to the specified value, as shown in Table 4. The deficit observed in the quasi-parallel beam test was partly due to the reflectivity of the mirrors (see section 'X-ray refectivity tests'), but also to some over-thickness of the mirrors at their edges (protruding burrs from the electroforming process).

X-ray baffle tests at Centre Spatial de Liège (CSL) (Fig.10)

To check the correct positioning of the X-ray baffle on the spider of the Mirror Modules, several optical tests were carried out to ensure that the on-axis optical performance of the telescope remained unchanged after the mounting of the baffle, i.e. no on-axis vignetting effect and no image-quality degradation.

Table 3. X-ray image quality of the five Flight Models of the Mirror Module at best focus, in arcsec (HEW data corrected by quadratic subtraction of the intrinsic resolution of the PSPC at the corresponding energy)

	FM1			FM2			FM3			FM4			FM5		
	PSPC		CCD	PSPC		CCD	PSPC		CCD	PSPC		CCD	PSPC		CCD
Energy (keV)	W90	HEW	FWHM	W90	HEW	FWHM	W90	HEW	FWHM	W90	HEW	FWHM	W90	HEW	FWHM
1.5	57	15.2	8.4	57	15.1	6.6	49	13.6	6	58	12.8	4.5	55	11.1	4.3
4.5	117	15.4	8.3	139	15.8	7.3	-----	-----	-----	135	13	4.5	-----	-----	-----
6.4	169	15.2	8.2	147	15.3	6.6	-----	-----	-----	158	12.5	4.4	-----	-----	-----
8.0	161	14.4	7.7	182	14.8	6.6	153	12.5	5.1	130	12.2	4.2	211	10.9	4.7
9.9	-----	14.3	7.3	-----	-----	-----	-----	-----	-----		12.3	4.4	-----	-----	-----

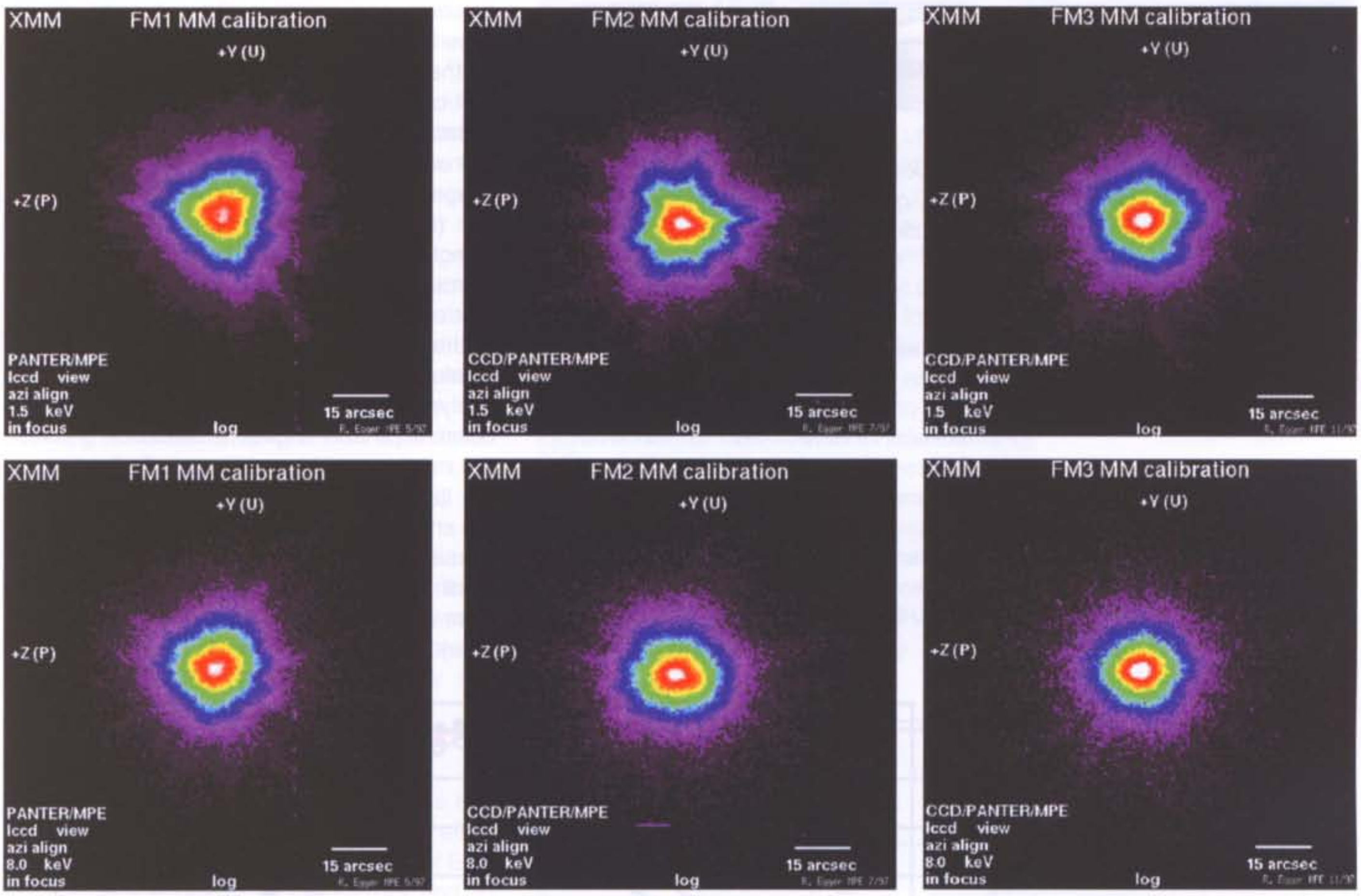

Figure 9. Close-ups of the focal image of the FM1, FM2 and FM3 Mirror Modules at 1.5 and 8 keV. (Courtesy of MPE, Neuried, Germany)

Table 4. On-axis effective area measurements (in cm²) at 1.5 and 8.0 keV (compared to specification and theoretical measurements)

	Energy	FM1	FM2	FM3	FM4	FM5	Specification	Theory	
Full illumination	1.5 keV	911	900	932	905	906	N/A	1074	Theory
(i.e. divergent beam)	8 keV	270	275	284	284	301	N/A	341	using
									B.L. Henke
Reduced beam aperture	1.5 keV	not done	1430	1445	1403	On-going	1475	1560	constants
(i.e. quasi parallel beam)	8 keV	not done	618	600	593	On-going	580	686	July 93

Figure 10. Test of XMM Mirror Module with its X-ray baffle at Centre Spatial Liège (CSL), B

Table 5. X-ray baffle performance in terms of image quality, effective area and stray-light rejection

	FM2	FM3	FM4
Stray-light rejection at 60 arcmin in %	80	80	80
PSF difference for HEW/90W (in arcsec) before and after mounting	0/2	0.1/3	0.1/2
On-axis effective area difference (in %) before and after XRB mounting	2.2	1.1	0.2

The following tests were performed before and after the mounting of the X-ray baffle:

- effective-area measurement at various off-axis angles (between –20 arcmin and +20 arcmin) in two orthogonal directions at 58 nm
- on-axis effective area and Point Spread Function measurement at 58 nm
- X-ray pencil-beam scanning on the Mirror Module aperture to check for possible misalignment between the mirrors and the baffle.

Four Flight Models were equipped and tested with their X-ray baffles. The test results (for the three telescopes to be flown) are indicated in Table 5 and in Figures 11, 12 and 13.

In Figure 11, the evaluations of the images taken with the CCD at the EPIC detector position confirm that the intensity of the hyperboloid reflections was clearly attenuated by the presence of the baffle. Only the central part of the EPIC area is shown (EPIC diameter corresponds to the width of the image). This corresponds to a combination of 9 CCD images taken at CSL. In the left-hand image, the (shiny white) rings are due to single reflection on the hyperboloids of the outer mirrors. In the right-hand image, their intensity is strongly attenuated because of the presence of the X-ray baffle. The true (paraxial) focus is located below and outside the image. When analysing, more closely, several images at different off-axis angles, a difference between the mirrors could be observed. Reflections on the large mirrors were more blocked than on the small mirrors due to the chosen position of the sieves of the baffle. Indeed, some rays (at a small off-axis angle of about 15 - 20 arcmin) were able to pass through the sieves of the X-ray baffle and reflect directly on the

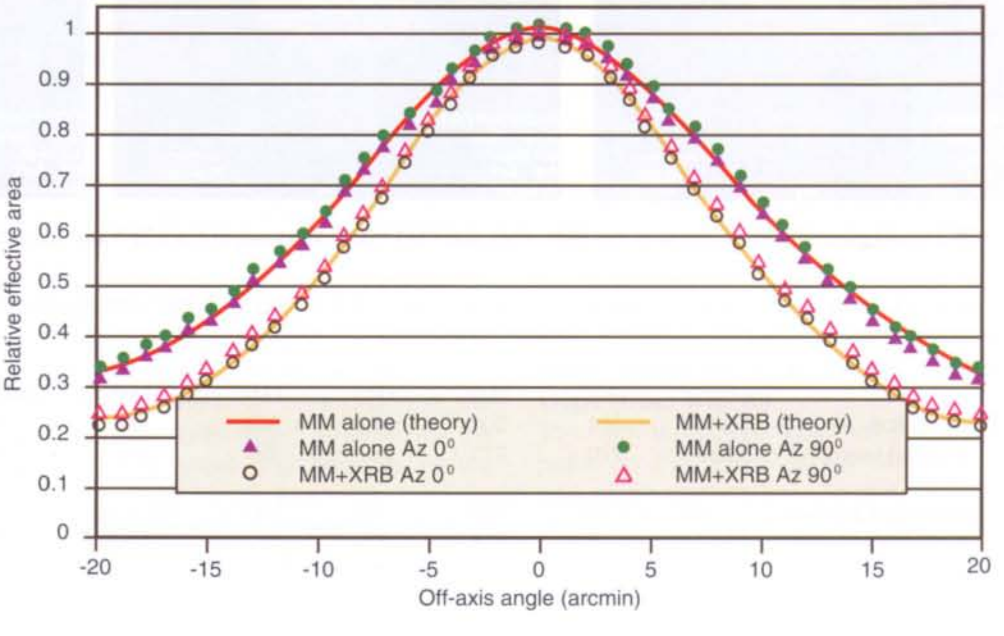

Figure 11. X-ray baffle performance in terms of image quality, effective area and stray-light rejection

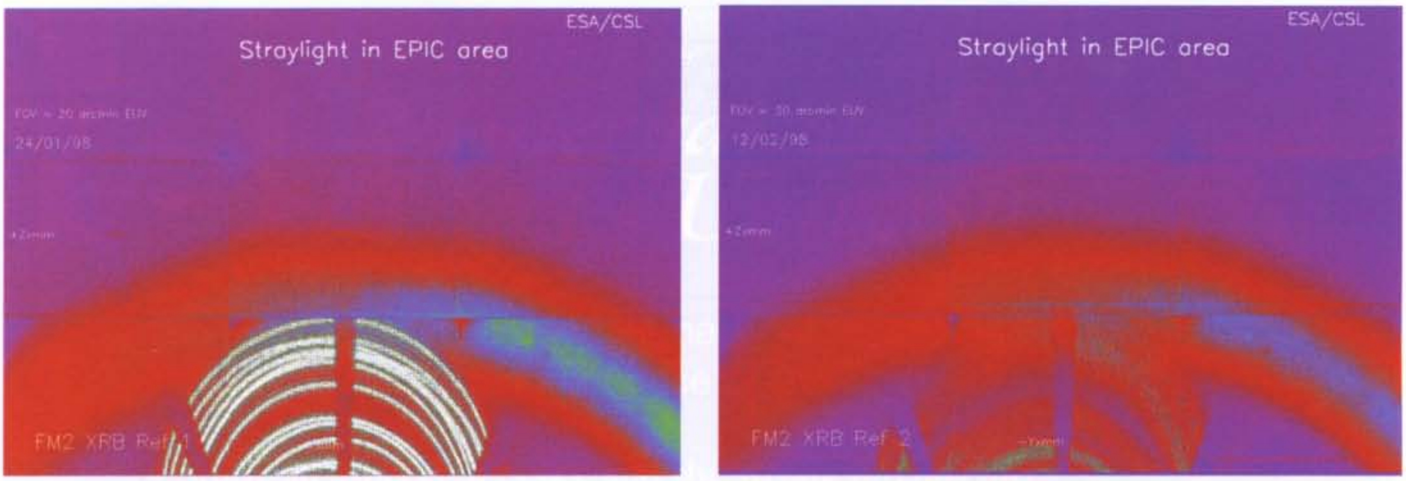

Figure 12. EPIC focal image during EUV stray-light tests on the FM2 Mirror Module without (left) and with X-ray baffle (right) for an off-axis angle of 30 arcmin

hyperboloids of these mirrors. This is because it was not possible to mount a sieve close enough to the mirrors due to the shape of the Mirror Module spider. This was clearly confirmed by the various simulations.

Table 5 shows that for the integrated X-ray baffles, there was no measurable degradation of image quality (PSF) and of the effective on-axis area. The normalised relative effective-area measurements of the Mirror Module with and without the baffle (performed in two orthogonal directions) matched the predictions with a precision better than ±2% (Fig. 11). The stray-light rejection, which is defined as the ratio of the intensity of the image of the single hyperboloid reflections before and after the mounting of the baffle was close to the prediction of 80% for all measured off-axis angles between 20 and 70 arcmin (Figs. 12 & 13).

The X-ray pencil-beam scan tests have also quantitatively confirmed that the position of the vane strips is in the 'shadow' of the mirrors. The measurements were performed with an accuracy better than 100 µm along the two scanned azimuth directions.

Conclusion and future perspective

The development of the XMM telescopes has been very successful. The continuous effort executed under the direct management of ESA to improve the quality of the mirrors and to develop the X-ray baffle has led to excellent results:

- all Flight-Model Mirror Modules have a resolution performance around 14 arcsec (HEW) at energies between 0.9 keV and 12 keV, values that are consistent with the 20 arcsec in-orbit requirement
- measurements on the Qualification-Model Mirror Module with the EPIC p-n camera, made at the Panter facility, have indicated that the Mirror Module is able to collect and sharply focus X-rays up to 17 keV (few cm^2) with a resolution (HEW) of around 15 arcsec
- the performance of the X-ray baffle is according to prediction: it rejects 80% of the stray light (coming from small-angle off-axis sources) without affecting the on-axis performance of the telescope.

The Flight-Model XMM X-ray telescopes, with their superb performance, will undoubtedly bring an important benefit to astronomers, especially for the spectroscopic part of the mission. The addition of the X-ray baffle will also considerably improve the scientific value of the XMM mission by reducing most of the X-ray and optical stray-light sources located just outside the field of view of the detectors.

The effort spent on the production of the five Flight Models of the XMM Mirror Modules (Fig. 14) and the systematic analysis of all of the mirrors produced (about 700 in total including dummies) has led to mirror shells of which the quality is largely determined by the performance of the master mandrels (i.e. HEW = 4 - 5 arcsec). Based on current knowledge, nickel-electroforming technology has been

Figure 13. Integrated collecting area (in log scale) of telescope 3 (no RGA) as a function of off-axis angle

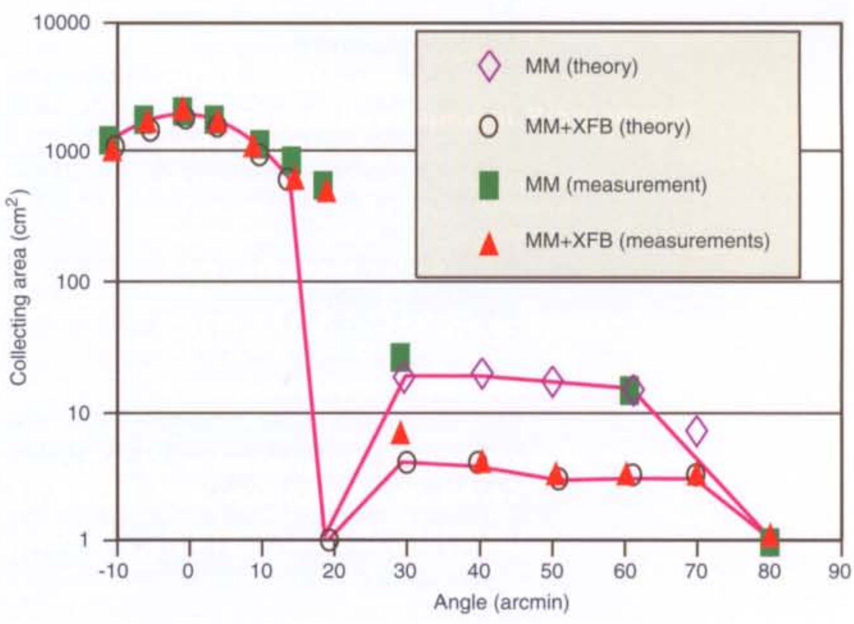

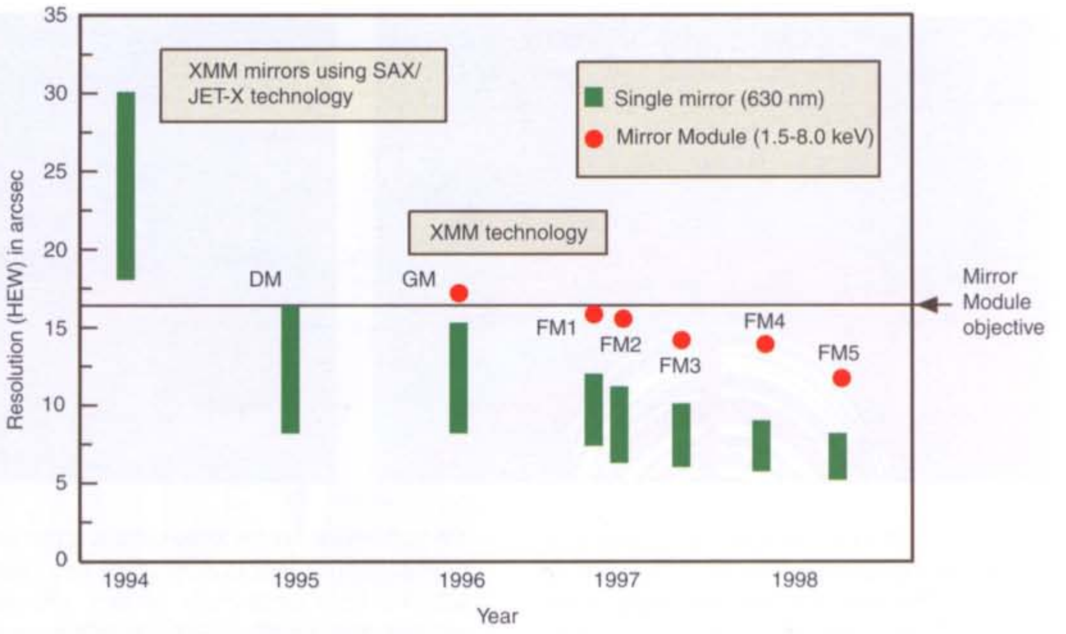

Figure 14. XMM mirror and Mirror Module performance

further improved to deliver lightweight thin mirrors with still better resolutions than those obtained for the XMM mission. Areas of investigation include the improvement of the mechanical properties of the electrolytic nickel. Some promising results have already been obtained by producing thin mirrors with a thickness of 200 µm for a diameter of 700 mm (i.e. 1/5th of the current XMM mirror thickness).

In Europe we now have a very advanced understanding of the production of thin optics using the nickel-electroforming replication technique. Such technology can, of course, be used not only for future X-ray missions (e.g. Xeus, Constellation X), but also for normal-incidence optics such as thin flexible mirrors for adaptive-optic systems, microwave high-accuracy reflectors or cavities.

Acknowledgement

The XMM mirrors were developed and manufactured by ESA and Media Lario (Bosisio Parini, Italy) with the support of:

- APCO (Vevey, Switzerland) for the manufacture of the structural parts and the containers
- BCV-Progretti (Milan, Italy) for the optical and structural analysis
- Kayser Threde (Munich, Germany) for the mechanical design and the analysis.

The optical and X-ray stray-light work was conducted by ESA and Dornier (Friedrichshafen, Germany) with the support of:

- Breault Research Organization (BRO) Inc. (Tucson, Arizona, USA) for the optical stray-light analysis
- Dornier (Ottobrunn, Germany) for the large-angle stray-light tests (including the test-setup development)
- Contraves (Zurich, Switzerland) for the design and manufacture of the entrance baffles
- Sener (Las Arenas, Spain) for the design and manufacture of the X-ray baffles.

The two Reflection Grating Assemblies (RGAs) were developed and manufactured by Columbia University, the University of California (Berkeley), Lawrence Livermore National Laboratory and Space Research Organisation Netherlands (SRON), with financing from NASA.

Our congratulations go to the industrial team for the work achieved, especially to P. Radaelli and G. Grisoni from Media Lario, Y. Gutierrez from Sener, and E. Hölzle, D. Schink and W. Rühe from Dornier. The members of the Telescope Advisory Group, Dr. B. Aschenbach and Dr. H. Bräuninger from the Max-Planck Institute in Garching, Dr. P. de Korte from Space Research Organisation Netherlands in Utrecht, and Dr. R. Willingale from the University of Leicester, as well as ESA staff are thanked for their continuous support during the mirror development effort. Our thanks also go to the testing teams at the Max-Planck Institute, at Centre Spatial de Liège and at Dornier-Ottobrunn, with special mention of R. Egger, J.P. Tock, H. Hansen, I. Domken, Y. Stockman, C. Wührer and R. Birkl. The contributions of P. Gondoin and A. Hawkyard in the early phase of the mirror development effort are also gratefully acknowledged.

Mechanical and Thermal Design of XMM

K. van Katwijk, T. van der Laan & D. Stramaccioni
XMM Project, ESA Directorate for Scientific Programmes,
ESTEC, Noordwijk, The Netherlands

The XMM spacecraft has a conventional structure and thermal design. Due to the long focal length of the telescopes (7.5 m), the mirrors are far removed from the instruments. On the ground and during the launch, the structure has to maintain the integrity of the whole spacecraft. The thermal control does not make use of onboard software. In orbit, the functions of the structure and the thermal control are mixed. Their global common requirement is to relate and align the set of mirrors at one end of the spacecraft with the set of instruments at the other.

Some parts of the instruments will be kept at cryogenic temperatures, but most of the spacecraft will be kept at about room temperature. It is the task of the thermal control to maintain these diverse requirements by passive and active means. Under inevitably varying thermal conditions, the structure has to stay very 'straight'.

Introduction

Once the scientific requirements (and goals) for a spacecraft are set, the system-level requirements follow. A global configuration is then selected that would, in principle, allow the realisation of the spacecraft within these constraints. So far, the constraints are mainly geometrical. The satellite should fit in a launcher, the (focal) distance between optics and detectors should be respected, mechanisms should be moving in the right direction, etc. At this early stage, the structural elements have no real size and the thermal-control elements have no real performance specifications. However, both for structural elements and for thermal-control elements, there is from the start a mass-allocation not to be exceeded. Geometrical constraints and functional requirements lead to an iterative design process that takes into account the realisation of such elements in real hardware. However, the design process gets more complex due to the fact that structural and thermal-control functions are completely coupled. In addition, the thermal control is strongly coupled to the power subsystem. This often makes it difficult to single out the constraints and requirements for the individual subsystems.

Structural design constraints and requirements

The spacecraft structure, like any other structure, is there primarily to guarantee the integrity of the spacecraft under any loading, such as during handling, testing and launch. In addition, it must allow the spacecraft to serve as an optical bench for a telescope and therefore the structure must provide the necessary thermo-elastic stability in orbit. In the case of XMM, this led immediately to the selection of ultra-high-modulus carbon-fibre composites (low thermal expansion) for the main structural elements. Another advantage of this material is its very high modulus of elasticity, which limits structural mass for a structure like this, which is (also) designed for stiffness.

These two favourable qualities of this carbon-fibre material, plus its low mass, have led to its widespread use on XMM, albeit for different reasons in different parts. For instance, for the telescope tube and the mirror support platform, a carbon-fibre composite was necessary for thermo-elastic reasons. A strongly directional lay-up made it possible to meet the requirements, whereas the mass could be kept low. On the other hand, for the central cone of the Service Module, the stiffness required was the main reason for using a carbon-fibre composite.

In complex items, such as the mirror support platform, the joints that are necessarily made out of metal degraded the intended high thermo-elastic stability to such a level that active thermal control was necessary. Here, a carbon-fibre composite had been selected for its high stiffness and strength. Other parts outside the optical path were made of aluminium for reasons of thermal conductivity (honeycomb for Service Module side panels), light-tightness and ease of production (telescope Sun shield, outgassing baffle).

In order to meet the system-level requirements, such as thermo-elastic stability or stiffness for minimum structural resonance frequencies, a system analysis (budget) was performed, from which subsystem apportionments could be made. This was, in particular, needed for those requirements where a number of parts or subsystems contribute. Margins were added to the subsystem apportionments in order to account for uncertainties and interferences of the interfaces.

Mechanical environment

The XMM structure is sized mainly against the launch environment. Only dedicated pick-up points are sized for ground handling and transportation loads.

The launch environment can be subdivided into the following elements:

a. launcher (quasi-static) acceleration loads – necessary to reach orbit
b. launcher dynamic loads – caused by solid-booster ignition, passage through zones of high winds and engine-thrust termination (both solid boosters and liquid stage)
c. launcher-separation shocks
d. acoustic pressure – mainly caused by engine noise reflecting from the ground.

As design parameters, (quasi-static) acceleration and dynamic loads are combined to form worst-case scenarios, and taken as static loads for sizing purposes. The dynamic component of the loading is amplified in the spacecraft and the result taken into account in the dimensioning. For XMM, the amplification in the lateral direction was particularly important. An interesting case has been the lift-off (booster ignition), where the maximum lateral acceleration is about 0.4g at the lower interface of the spacecraft and about 4.5 g at the top of the spacecraft.

The highest axial amplification occurs at the end-of-thrust phase of the booster. The lower interface of the spacecraft 'sees' 0.44g, whereas important masses such as the mirror modules and the focal plane are subjected to 1.1g. In this case, the quasi-static acceleration of 3.8g is more important.

For the Ariane-5 launcher, the shocks due to the separation of the payload shroud and the liquid upper stage from the rest of the launcher are more severe than the shocks due to the (classical) clamp-band separation. Ground tests have demonstrated that the higher level is not critical for the structure, and therefore it was not applied as a dimensioning criterion.

Acoustic pressure from Ariane-5 is high in the low-frequency range. This strongly loads the structures with low mass density (mass per unit area). The telescope Sun shield is a good example of such a case. For the main structure, this type of environment has not been critical.

The in-orbit environment was characterised by the low accelerations coming from the attitude control system. For the main structure, these accelerations are never critical, but the dynamic inputs from the reaction wheels may affect telescope performance. However, this jitter turned out not to be critical.

Structural qualification

The size of the spacecraft prevented a classical system-level approach in the structural qualification programme. A splitting into an upper and a lower module was a logical choice; it splits the telescope tube into two parts. The elements of each module were to be tested separately before integration. This was done by the element supplier to a level that integrity was sufficiently demonstrated. In this way, the risks of module-level testing would be minimised. Of course, mechanical and thermal analysis were performed beforehand, to show adequate de-coupling between modules and to confirm the validity of the modular approach.

The telescope tube was a special case in this sequence, since it contained the boundary between the two modules. In order to prove the integrity of the complete tube, it was loaded in its assembled state. An important aspect of the mechanical testing of these parts was the load level. This was selected to be well above the level to be expected in flight, because most of the parts were sized against stiffness requirements. This meant that in many areas the material thickness was larger than necessary to meet the strength requirements. This margin was exploited by increasing the load levels above the official initial flight loads. Later changes in expected flight loads, coming from module-level testing and updated launcher coupled-load analysis, could thus be absorbed without hardware changes.

Primary structural parts, such as the telescope tube, the tank support struts and the service module cone, were subjected to relatively simple static load tests prior to their delivery for integration into the spacecraft system. These were, of course, worst cases selected from a multitude of loading combinations. Items carrying a lot of equipment did not lend themselves to such simple tests. They were sufficiently over-designed to safely undergo and pass the module-level dynamic tests later in the programme. Such items were typically the focal-plane platform and Service Module side panels.

The telescope Sun shield, as a large and lightly-loaded structure, was a special case. It was felt that dynamic and acoustic loading of the shield was necessary at parts level, because of its complex nature and because of the need to verify its flawless deployment after loading.

Module-level dynamic testing was the next activity, in which shaker limitations were of interest. This was particularly the case for the lower module, due to its high mass (about 3100 kg). However, the modular testing did not prevent the application of loads on the internal interfaces between various equipment items. Of special interest here was the dynamic interaction between the large masses, such as the Mirror Modules, the Optical Monitor and the Service Module side panels full of equipment. Upper Module testing provided sufficient focal-plane loading (not previously tested) and allowed the verification of the cameras, the equipment and the interface with the telescope tube. Finally, the two modules were brought together for modal-survey and acoustic testing at system level.

The modal-survey test was extended with a 'boosted' test to verify the overall stiffness and strength of the telescope tube internal and external interfaces. Even after a loading up to about 1.6 times the flight load, the telescope tube did not show any anomalies.

Acoustic testing was performed to demonstrate overall structural integrity and alignment stability against this type of environment. The light labyrinth of the telescope Sun shield showed (repairable) damage. Additionally, the random vibration responses of equipment, resulting from the acoustic testing, were compared with the corresponding qualification levels. The result was an exceeding of the random qualification level for ten units, all on the side panels of the Service Module with relatively low-mass density. Nine units were successfully re-qualified. For the reaction wheels, a detailed analysis showed that the critical parts (bearings) had not been overloaded during the system-level acoustic test.

A new situation originated from the high shock loading defined for the launcher interface (see above). It was clear that a classical clamp-band release test (which was nevertheless performed) would not produce the required environment. Since no test hardware was available to do an adequate system-level shock test, it was already decided earlier in the programme to perform shock testing at equipment level. Previous system-level tests of Ariane for Cluster had produced equipment-level responses that would be relevant for XMM. The equipment-level responses were enveloped and integrated into the unit-level specifications. All equipment items that contain sensitive parts and those that are close to the launch interface were tested to this specification. A so-called 'ringing plate' test setup was used and no failures occurred.

Mission thermal constraints

The thermal control of XMM must fulfil two basic requirements: it must keep equipment and payload within the required temperature ranges, and it must provide a stable and uniform temperature of the telescope system when scientific observations are performed. The precise geometry and alignment of a telescope system imposes very strict and demanding temperature requirements, so that not only do temperature gradients have to be kept to a minimum, but also, and more importantly, variations of the gradients over time have to be minimised.

In particular, the mirror shells of the Mirror Modules have to be kept at an average temperature of 20°C, with spatial maximum temperature differences of ± 2°C in order to limit thermo-elastic deformations. The three Mirror Modules are mounted on the Mirror Support Platform, which also carries the Optical Monitor and the two star trackers. The optical boresights of all of these instruments have been carefully aligned on the ground and, in order to maintain that alignment, thermal distortions of the platform have to be minimised. Therefore, the platform is maintained almost isothermal, with deviations of less than ± 2°C. On the other hand, the Service Module equipment presents quite standard temperature ranges and attention is therefore mainly paid to simplicity and reliability.

Orbital thermal environment

The thermal design of XMM takes full advantage of the stable environment provided by its high-altitude, long-period orbit and by the limited variation of solar attitude angles that it will experience during observation phases (± 20° pitch combined with ± 20° roll). In fact, the Earth albedo and infrared heat fluxes are negligible along the largest part of its high-altitude orbit. Only at perigee passes, when the altitude reduces to 7000 km, will XMM's thermal stability be slightly affected by the influence of the Earth.

The largest thermal perturbations occur during the eclipse seasons, when the satellite does not receive the Sun's energy for a maximum period of 1.7 h (although, on average, the eclipses are much shorter). However, eclipses always occur below the minimum altitude that is required for observation (40 000 km), leaving time for the spacecraft to recover its temperature stability. Boost heating performed before and after the eclipses by means of heaters helps to reduce the time needed for recovery of the temperature drop caused by eclipses.

In order to cope with all orbital perturbations and with changes of satellite attitude, the telescope tube is completely insulated from the external environment and the heater power that is dissipated inside it can be almost continuously adjusted to compensate for changes.

Overall thermal-control approach

The XMM satellite relies on a combination of passive and active means of thermal control. The passive thermal control is mainly achieved by using classical highly-insulating multi-layer blankets. Typically, blankets are made internally of 20 double-sided aluminised layers separated by Dacron nets. The external layer of all blankets is made of carbon-loaded kapton, which gives the satellite its characteristic black appearance. This kind of kapton has been chosen because of its electrical conductivity, which avoids electrostatic-discharge problems. In addition, the thermo-optical properties of the black finish will not change during the satellite's ten-year lifetime, helping again to maintain temperature stability.

The thermal blankets of the telescope tube and of the hydrazine tanks have the additional task of acting as bumper shields against micro-meteoroid impacts. For this, they are kept at a distance of 2 cm from the structure by means of special spacers.

Telescope tube (Fig. 1)

The insulation performance that has been achieved by the XMM blankets is exceptionally good, especially for the large, undisturbed blankets that insulate the telescope tube. Together with the black lining of its internal surface, they keep the temperature gradient across the tube diameter small and stable. In fact, the measured temperature difference across the tube was only 3°C. The telescope tube is not equipped with heaters and its temperature control is purely passive.

Focal-plane assembly compartment (Fig. 2)

The focal-plane assembly compartment, located on top of the telescope tube and which contains the payload cameras, is controlled during operations in a totally passive way. This is made possible by the power dissipated by the instruments, which remains fairly constant during the mission observation periods. Consequently, the compartment's heat losses are trimmed such that the dissipated power (about 150 W) can keep the temperatures at the required level. Whenever an instrument chain is switched off, an appropriate 'substitution' heater line is switched on in order to replace the missing dissipated power and keep the heat power balance constant. In non-operative and emergency modes, mechanical thermostats will switch these heaters if the temperature falls close to the non-operation temperature limits of the equipment.

Figure 1. Insulated telescope tube

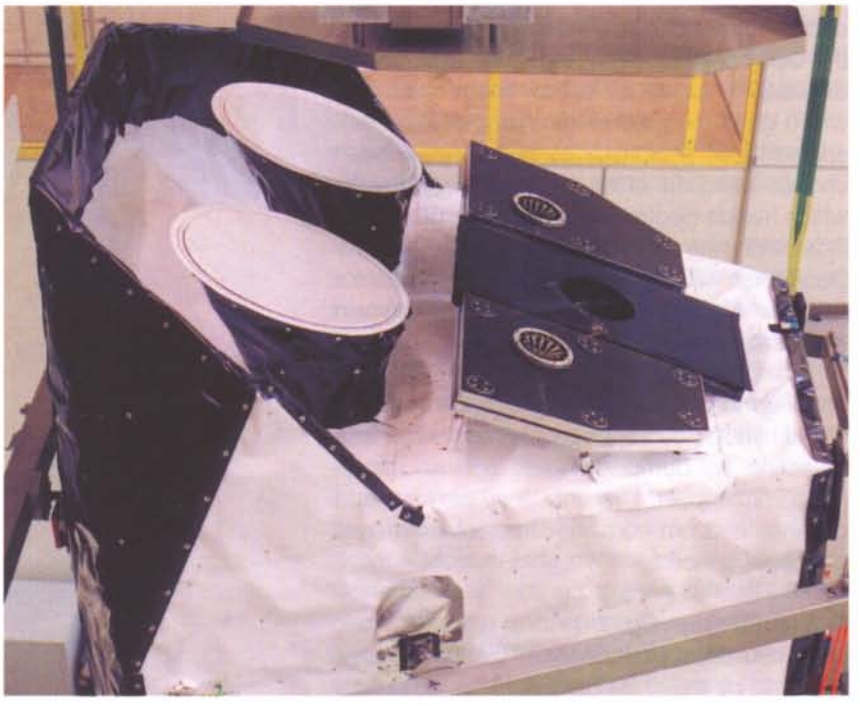

Figure 2. The focal-plane assembly compartment houses the payload cameras. Temperatures are passively controlled by the power dissipated by the instruments

The external shape of the focal-plane assembly compartment minimises the variation of Sun input, caused by changes in attitude of the satellite with respect to the Sun. In fact, the side surfaces and the top plane are canted 20° away from the Sun, so that they are always in shadow. The illuminated face is fully blanketed and acts as a Sun shade. The white-painted areas function as 'foil radiators' through which the heat can leave the compartment. Black and aluminium stripes are applied on their internal side, in order to calibrate their thermal impedance. The five camera radiators are connected by means of 'cold fingers' to the camera detectors to cool down detectors to cryogenic temperatures. Detectors can be heated by using local camera heaters.

Service Module (Fig. 3)

The Service Module, at the other end of the telescope tube, is also fully blanketed with the exception of panel radiators. On the Sun-side they are covered by mirror solar reflectors, while those on the anti-Sun side of the satellite are painted white. Where passive measures are not sufficient to meet the temperature requirements, heaters controlled by thermostats are implemented. No on-board software is used to activate and control heaters. Ground control can configure the heater lines to be powered, while mechanical thermostats perform the actual heater switching. In a typical mission observation phase, about 330 W are dissipated by the equipment and 80 W are provided by the heaters to maintain an internal average temperature of 15°C.

Mirror Modules and mirror support platform (Fig. 4)

The heaters used for fine temperature control of the Mirror Modules and the mirror support platform are powered by the 'Mirror Thermal Control Unit' (MTCU). The MTCU pulse-modulates the current of the heaters according to duty-cycle values stored in its memory. The ground station updates the duty-cycle values when necessary. This kind of control is possible due to the large thermal inertia of the mirrors,

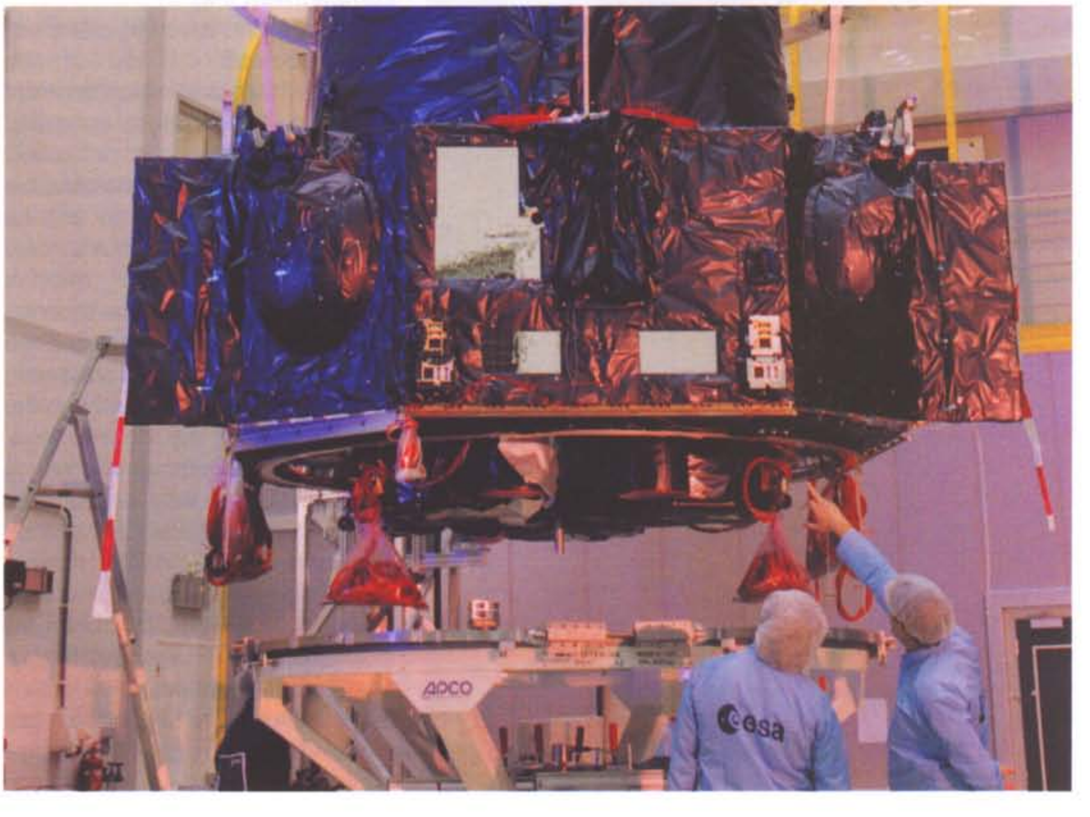

Figure 3. On the Service Module ground control configures heater lines, while mechanical thermostats perform heater switching

Figure 4. The heaters used for fine temperature control of the Mirror Modules and the mirror support platform are powered by the 'Mirror Thermal Control Unit'

the environmental stability of the orbit, and because all observations, for which strict temperature control is required, are always performed under ground control. A pulse-modulation cycle of 1 min allows adjustment of the heater power with a very fine resolution.

Each Mirror Module is thermally insulated from its surroundings and exchanges heat through its entry baffle to space and through its exit baffle to the telescope tube's interior. In order to compensate for the heat lost to space, each module is equipped with pulse-modulated heaters that can deliver up to 100 W. Also, the exit baffles are equipped with pulse-modulated heaters for the compensation of heat lost into the telescope tube. The exit baffle also has the task of thermally controlling the high-precision grating assemblies that need to be kept at 20°C with virtually no spatial temperature gradients. The heat radiated into the telescope-tube cavity keeps the tube at the right temperature level (between 15° and 20°C). The mirror support platform is completely covered by pulse-modulated heaters that can deliver up to 85 W of power. The various heater lines are individually set in order to avoid thermal distortion and to keep the boresight lines of the Mirror Modules, optical monitor and star trackers parallel with each other. The platform also ensures that the Mirror Modules are correctly aligned with the cameras.

Autonomy and failure management

The functioning of XMM's thermal-control subsystem has been designed such that it does not depend on any information from other subsystems. Each function can tolerate a single fault without the need for on-board failure management software, and any failure can be withstood for a maximum period of ground-station outage of 36 h. Each function can be performed by a nominal or by a redundant heater line powered by separate power-distribution units. The nominal and redundant lines of all essential heaters are powered throughout the mission, so that in the event of malfunctioning of the nominal line, the redundant one can automatically take over (triggered by thermostats or by the MTCU).

Verification of the thermal control

The thermal-control design was validated by means of a Sun-simulation thermal-balance test performed on the structural-thermal model of the satellite. The test was conducted in the Large Space Simulator (LSS) at ESTEC. Despite its large dimensions, the LSS facility could not accommodate the complete XMM satellite, which was therefore split into two modules that were tested separately. This modular approach was advantageous from a thermal point of view because it allowed testing of the lower module with the Mirror Module apertures correctly exposed to space (see also ESA Bulletin No. 94, May 1998). In addition, it was demonstrated by analysis that the interaction between the modules is small and well defined. The test allowed the validation of the thermal mathematical models used to design the thermal-control system and to identify its deficiencies. After trimming and final correction of the thermal design, a second thermal-balance test was performed during the thermal-vacuum system test on the flight model which ultimately confirmed the thermal design.

The Attitude and Orbit Control of XMM

A. Elfving
XMM Project, ESA Directorate for Scientific Programmes,
ESTEC, Noordwijk, The Netherlands

Attitude and orbit control of the XMM spacecraft relies on two subsystems on-board: the Attitude and Orbit Control Subsystem (AOCS) and the Reaction Control Subsystem (RCS). Together they must provide:
- **stable Sun-pointing after the spacecraft's separation from the launcher and during solar-array deployment**
- **increase the spacecraft's perigee altitude by means of a chemical propulsion delta-V of about 210 m/s**
- **provide undisturbed, high-accuracy, three-axis pointing during scientific observations lasting up to 40 h**
- **slew the spacecraft between observations, and before and after perigee**
- **ensure that the Sun remains more than 15 deg away from the telescope at all times.**

The Attitude and Orbit Control Subsystem (AOCS)

The AOCS on XMM supports six different operational modes, as indicated in Figure 1. The first three acquisition modes are transitional. The Initial Sun Acquisition mode is used exclusively after XMM's separation from the launcher, to support rate damping, Sun acquisition and solar-array deployment. The Sun Sensor Acquisition mode handles transitions from the use of the wide-angle Sun Acquisition Sensors to the Fine Sun Sensor. It is also used for recovery from the Emergency Sun Acquisition mode (an entirely hardware-supported mode activated by particular failure detection criteria). Finally the Star Tracker Acquisition mode supports the transition from gyroscope to star tracker and from thrusters to reaction wheels.

The two main modes for routine operations, described in more detail in the following paragraphs, are the Inertial Pointing and Slew mode and the Thruster Control Manoeuvre mode.

The various units of the AOCS are shown in Figure 2. In addition, it makes use of the propulsion capabilities of the Reaction Control Subsystem (RCS), which is described below.

The attitude and orbit control design is influenced by four main drivers:

- the high-accuracy inertial pointing
- the delta-velocity injection of about 210 m/s
- no failure or ground-control error may point the telescope closer than 15 deg to the Sun
- 'gyro-lean' operations.

High-accuracy inertial pointing

The high-accuracy attitude information is provided by a star tracker, co-aligned with XMM's telescope, giving accurate star-position data on up to five stars every 0.5 sec. In addition, there is an accurate Sun sensor for precision Sun-line determination around the telescope line-of-sight. The sensor information is processed by the attitude-control computer, on which the operation mode logic and control algorithm software is executed. The resulting control demand is achieved by accurate spin-rate control of three extremely well-balanced reaction wheels. Since the telescope must be inertially pointed in all three axes, a so-called 'Sun steering law' is implemented to compensate for the orbit progression around the Sun.

Thanks to the low noise in the star-tracker measurements, a narrow-bandwidth controller and accurate momentum control of the reaction wheels, the pointing is very stable, being ~1 arcsec over a 2 minute period. The absolute accuracy of the reconstructed attitude based on star-tracker measurements is also very high, at typically 1 arcsec.

Slew manoeuvres are used to reorient the telescope between observations and before and after perigee passages. For large slews outside the star-tracker field of view of 3 x 4 deg, a so-called 'open-loop slew' strategy is implemented. Based on the ground slew tele-commanding, the on-board software generates a three-axis momentum reference profile and a two-axis Sun-sensor reference profile. During the slew, a roll and pitch controller is super-imposing momentum correction onto the reference momentum profile, based on the actual Sun-sensor measurements.

Since no absolute measurements are available for the yaw axis, a residual yaw attitude error

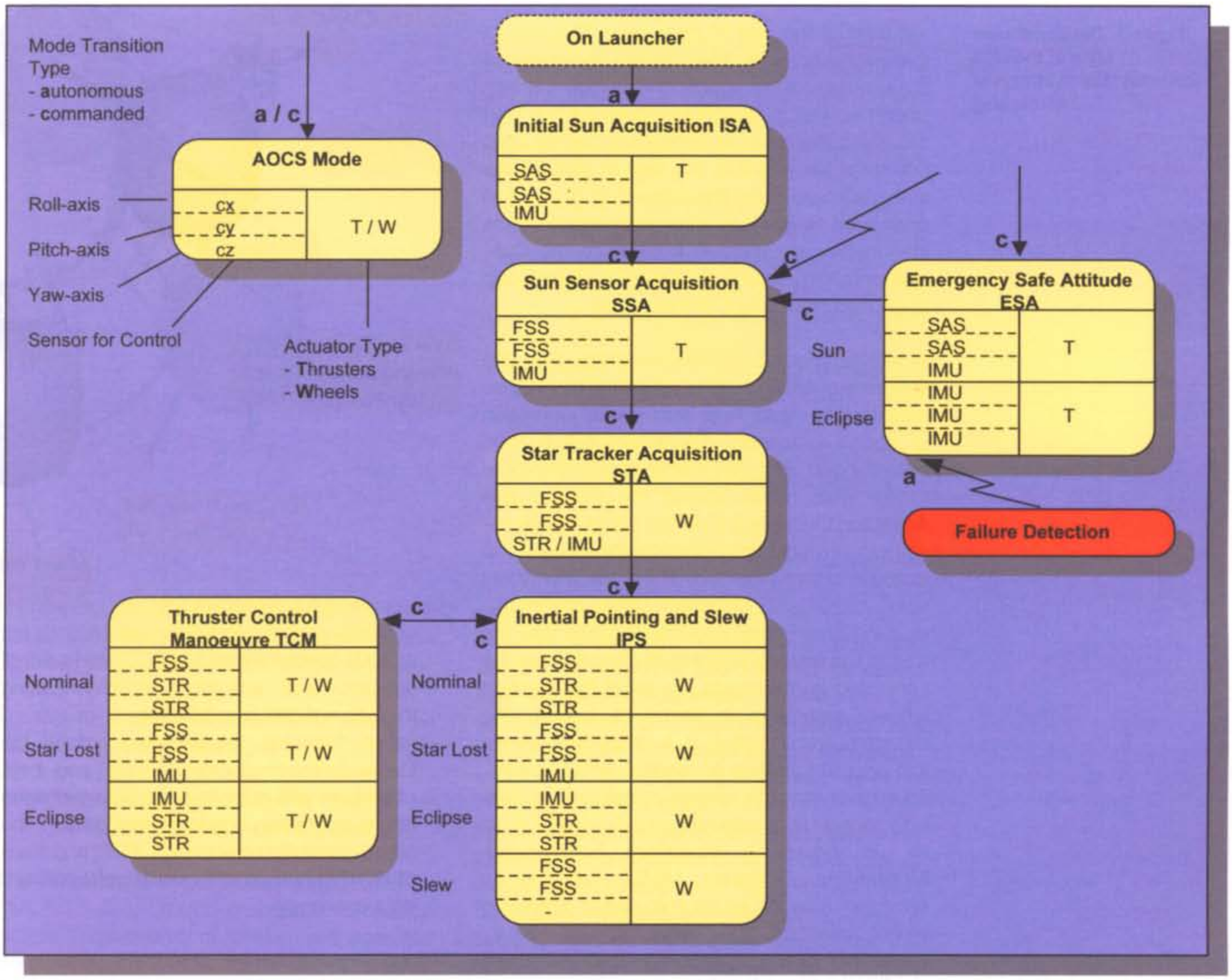

Figure 1. The AOCS operational modes

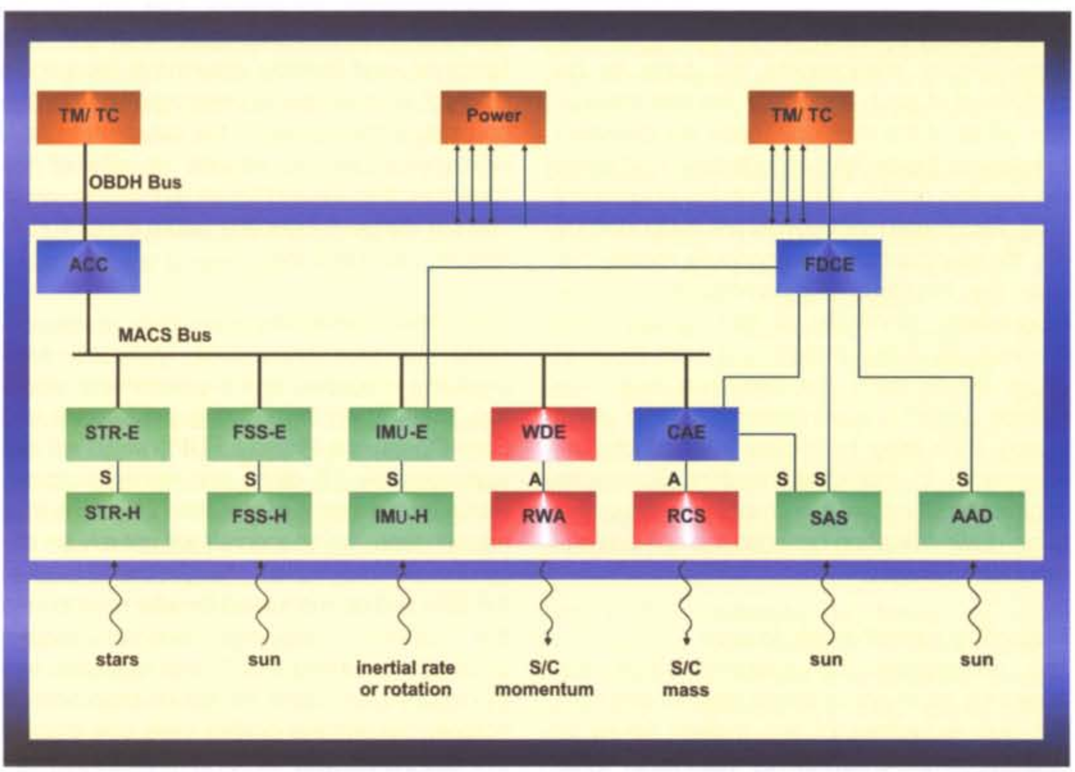

Figure 2. The constituent units of the AOCS

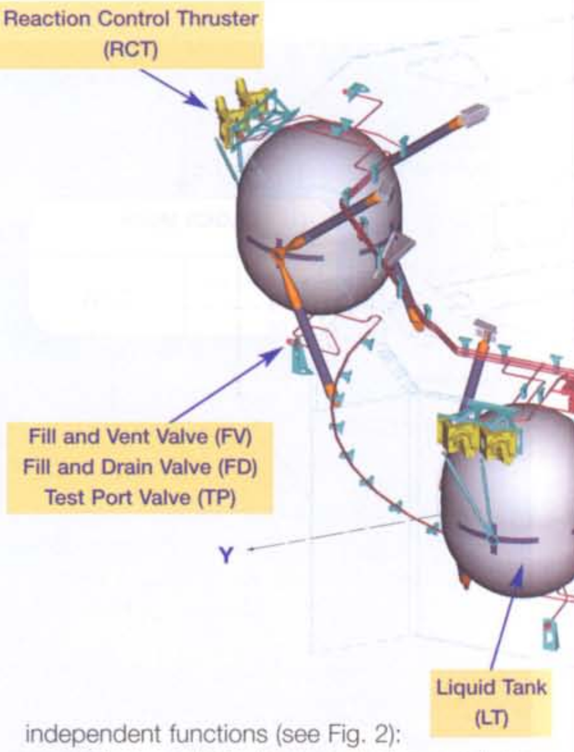

Figure 3. The constituent units of the RCS (courtesy DaimlerChrysler Aerospace)

will exist at the end of each slew. The size of this error is primarily driven by the uncertainty in the estimate of the spacecraft yaw inertia, with uncertainties in reaction-wheel inertia and mounting alignment as secondary contributors. For small slews within the field of view of the star tracker and for the correction of residual open-loop slew errors, measurements from the star tracker are used in addition to the Sun-sensor measurements to provide a closed-loop controlled slew about all three axes.

At regular intervals, typically twice per orbit, the spin rate of each reaction wheel will have to be adjusted, to avoid 'near-zero-speed' operation or speed saturation. The spacecraft is then commanded into thruster-control manoeuvre mode. This mode utilises the Control and Actuation Electronics (CAE) to command (in so-called 'on-modulation') the four thrusters of the propulsion subsystem whilst the reaction-wheel spin rates are changed. The minimum-opening-time limitation of the thrusters sets the limit to the residual spacecraft rates that can be controlled in this mode. To avoid the reaction wheels saturating in terms of torque, the thrusters are operated in a cross-firing mode just prior to transition to reaction-wheel control. To ensure that the wheels remain within their operational range also for ground outages of up to 36 hours, a so-called Autonomous Momentum Dumping (AMD) function is provided. As soon as the spin rate of a reaction wheel reaches its 'near-zero' or 'near-saturation' region, appropriate thruster pulses are fired in 'open loop' to restore the spin rate to the nominal region.

Delta-velocity injection

Delta-velocity manoeuvres will have to be performed at each apogee of the first three or four orbits of the mission. These are designed to increase the perigee altitude from 850 km in the injection orbit to 7000 km in the operational orbit. Also these manoeuvres are supported by the thruster-controlled manoeuvre mode, but here the thrusters are commanded in 'off-modulation'. Nominally all four thrusters are continuously firing, providing a total force of about 90 N along the telescope axis. The attitude control is super-imposed on top of the steady-state firing by means of short closure commands to individual thrusters. To ensure control stability, there is a smooth ramp-up and ramp-down transition between the on- and off-modulation stages.

Protecting against single failures

The requirement to guarantee that the telescope never points closer than 15 deg from the Sun regardless of any system failure or operator error is fulfilled by means of three independent functions (see Fig. 2):
- nominal control, implemented around the attitude control computer (ACC) and a set of sensors and actuators communicating through a digital bus (MACS)
- failure detection, implemented around the failure-detection electronics (FDE) and a set of sensors with point-to-point data exchange
- failure correction, implemented around the failure-correction electronics (FCE) and a set of sensors and actuators with point-to-point data exchange.

These three functions are implemented via independent hardware and software and commanded from the ground by independent telecommands to ensure that any single anomaly cannot propagate between the functions, and thereby ensure the telescope's safety. If, for example, a gyroscope used by the nominal control is faulty, the failure detection, which monitors the attitude or rate of the telescope through a different gyroscope, will in case of danger trigger the failure correction to restore a safe attitude.

'Gyro-lean' operations

XMM has four gyroscopes on-board, each providing integrated rate measurements about two axes. Apart from during the Launch and Early Operations Phase (LEOP), which will last approximately 10 days, and during eclipses, with a total duration of less than 2% of the total mission time, the spacecraft will not rely on any gyroscope information. As described above, the slew and on-modulated thruster manoeuvres are carefully designed not to require gyroscopes. During LEOP and eclipses, two gyroscopes are used for failure detection. In eclipse, the nominal control uses one channel of these gyroscopes for roll control. Throughout

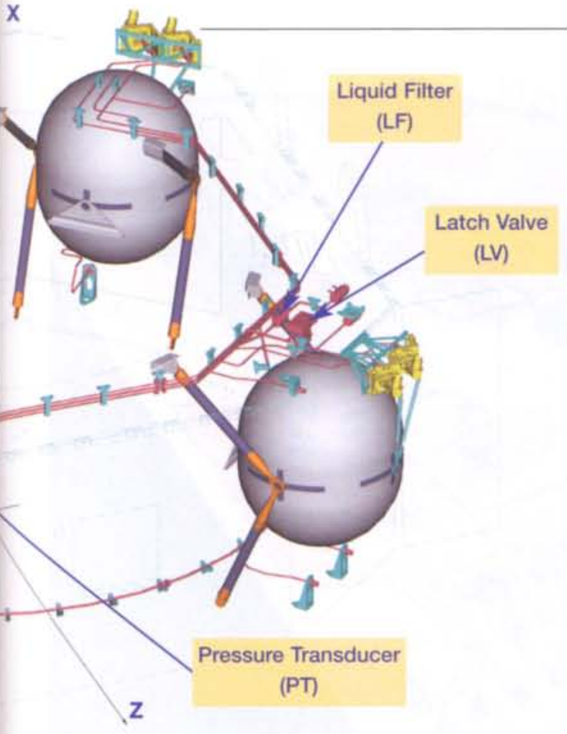

the mission, two other gyroscopes are available in cold stand-by to be used by the safe-attitude controller in case of identified danger.

For the full mission lifetime of 10 years, the estimated in-orbit operating time for 'the most used' gyroscope is less than 1600 h and 700 on/off cycles. Each gyroscope is qualified for well over 4000 h and 4000 on/off cycles.

The Reaction Control Subsystem (RCS)
The RCS is a mono-propellant hydrazine system made entirely of titanium and operated in 'blow-down' mode. Its layout, shown in Figure 3, is characterised by four tanks and two branches, each with four thrusters, a pressure transducer, a liquid filter and an isolation latch valve. The tanks have a maximum capacity of 530 kg of N_2H_4 and the fuel expulsion is achieved through surface-tension techniques. Three of the tanks feed their fuel into the fourth main tank, which acts as the main supplier to the thrusters. The flow-control valve of each thruster has dual seats and is self-closing when electrical power is removed.

Subsystem verification
The functionality of XMM's AOCS has been verified by testing at all levels, i.e. unit, subsystem and spacecraft. Performances have been verified by testing at unit level and by analysis and simulation at subsystem and spacecraft level. The operational procedures have been verified by review at subsystem level and by testing at spacecraft level.

Functional 'closed-loop' testing
In order to test all of the functions of such a complex control system, there is a need to provide the sensors with representative stimuli, either electrically or optically. These stimuli must be a reflection of the dynamic spacecraft motion under the influence of the actuators. For this purpose, a dedicated test environment, the AOCS-SCOE, was constructed which performs the following main sequence of tasks 40 times per second:
- Monitoring of the drive-current requests to the reaction wheels and the thrusters, signals marked 'A' in Figure 2.
- Calculation of the dynamic motion of the spacecraft as a result of these drive requests.
- Translation of this motion into angles and angular rates relevant to each of the different sensors.
- Electrical stimulation of the respective sensor electronics, signals marked 'S' in Figure 2.

In addition, the test environment developed supports a powerful test language that enables repetitive execution of complex test scenarios. Telecommands can be called-up from the operational database and the test execution flow can be made dependent on the results of actual telemetry processing. A version of this test environment was used by the subsystem contractor for the subsystem function verification before delivery to the spacecraft. Figure 4 shows the subsystem tests in progress at Matra Marconi Space (UK) in Bristol with all AOCS flight hardware and flight-representative harnesses mounted on a test table. Later, a second version has been used by the spacecraft prime contractor to support subsystem integration onto the spacecraft and to verify functional integrity before and after various environmental tests. Finally, the test environment has also been extensively used for operational-procedure validation and to support System Validation Tests conducted by ESOC.

Schedule constraints and achievements
In line with the original schedule, the total time taken to design, procure, integrate and verify the AOCS as a subsystem has been 44 months. Three main phases can be distinguished; subsystem design and engineering-model unit procurement (23 months), electrical-model integration and testing (10 months), and flight-model integration and testing (11 months). A total of 88 hardware units have been produced, including 30 flight units and three types of units containing a considerable amount of software.

The main challenges in terms of unit procurement have been to ensure correct interpretation of the unit specifications, timely access to high-reliability EEE parts, and maintaining a continuous focus on schedule-critical tasks. Not surprisingly, the electrical-

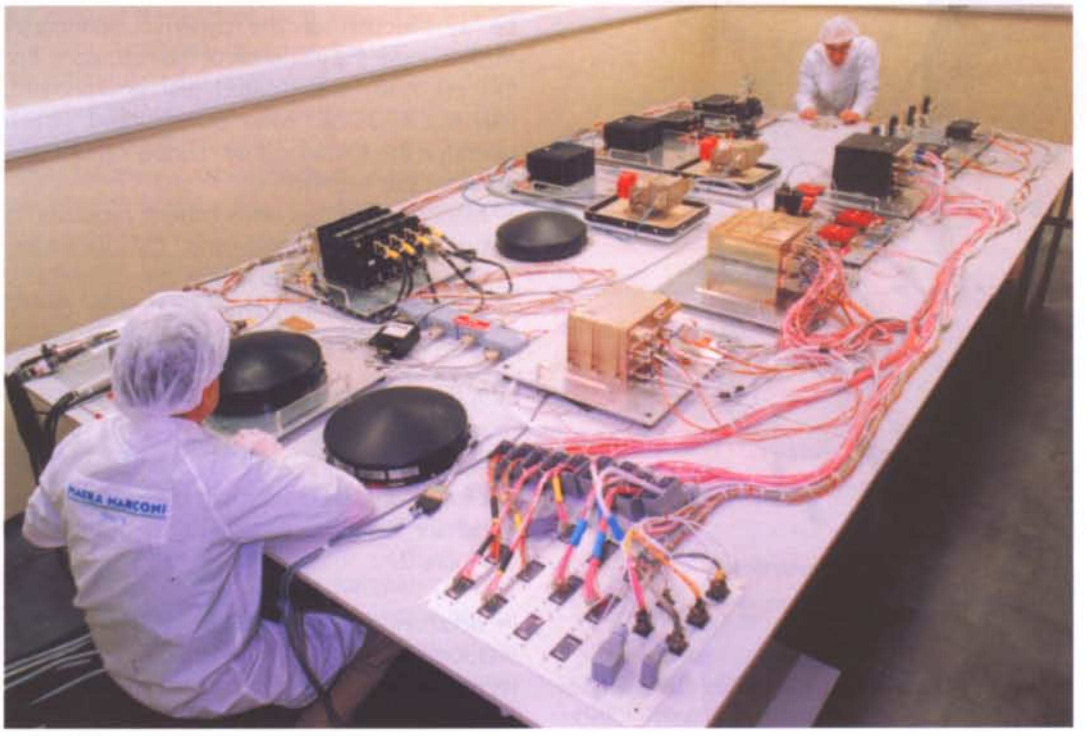

Figure 4. Subsystem testing in progress at Matra Marconi Space, in Bristol (UK)

model integration phase was characterised by 'debugging' of the electrical ground-support equipment (EGSE) to get it operationally stable, and the discovery of a number of short-comings in the on-board software logic. Ultimately, however, the flight-model integration and testing phase clearly demonstrated the completeness of the test coverage and confirmed the subsystem's functionality.

Knowledge transfer from design to operation

One lesson learned is the importance of early involvement of the ground operations team in the AOCS design and verification process, and in particular in the development of flight procedures. The concept of three independent functions for nominal operations, for failure detection and for failure correction relies on the ground segment ensuring a context-consistent configuration on-board. This is a demanding task for the ground segment and has been a focal point during the system verification tests and the mission-rehearsal campaign.

The importance of correct, consistent and complete documentation must not be underestimated. In a project of this size, the only effective means of ensuring adequate knowledge transfer is through proper documentation. This was particularly so in this case because the contractor's site in Bristol was closing during the flight-model delivery phase and access to many key engineers could not be maintained. The AOCS and RCS user manuals, comprising well over 200 documents, have been collected on a dedicated CD-ROM with full-text retrieval capability. Having all design and procedure documentation 'to hand' has been essential during the test campaign, and will be no less important during the launch campaign and LEOP phases.

Acknowledgement

The author would like to extend his gratitude to all personnel in the more than 16 companies who have contributed to the timely delivery, testing and launch readiness of the AOCS and RCS subsystems for XMM. Without detracting from the value of any individual's contribution, I would like to mention a few key colleagues by name: T. Strandberg of Dornier for his infinite energy in fulfilling his responsibilities as subsystem manager; A. Kolkmeier of Dornier, W. Holmes of SATASINT, and W. Davis of CAPTEC for their total, around-the-clock dedication to getting every aspect of the AOCS tested; R. Harris, D. Jukes and M. Backler of Matra Marconi Space (UK) for having conceived and flawlessly implemented a complex AOCS within an unprecedented short time; P. Henry, P. Chapman and M. Neal of Matra Marconi Space for their unselfish contributions in a difficult labour situation; B. Scheurenberg of Dornier for his eagerness to get a good propulsion system delivered on time; A. Schnorhk of ESTEC for his expertise and experience in every aspect of the propulsion system; J. Wohlfart of Dornier and C. Carnevale of Fiat Avio for getting the propulsion system through the CSG safety acceptance and safely fuelled; A. Ferretti of Fiat Avio for his well thought out propulsion system design and technical supervision of its suppliers.

esa

The Pointing and Alignment of XMM

A. Elfving & G. Bagnasco
XMM Project, ESA Directorate for Scientific Programmes,
ESTEC, Noordwijk, The Netherlands

The pointing and alignment performance of the XMM spacecraft will have a very strong influence on the quality of the scientific results obtainable. The pre-launch unit and subsystem tests and subsequent analyses have shown that the scientific requirements will indeed be met with comfortable margins and the performance goals will be met for more than 90% of all anticipated observations.

XMM's optical system

The exploded view of the XMM spacecraft shown in Figure 1 identifies the main elements of the optical system*. Three Mirror Modules (MM-1, 2 and 3), equipped with two Reflecting Grating Assemblies (RGA-1 and 2), and the self-contained Optical Monitor (OM) are mounted at the heart of the spacecraft. The optical system is completed by five Charge Coupled Device (CCD) detector cameras, of which three (EPCH and EMCH-2 and 3) are placed at the 'primary focus' of the respective Mirror Modules. The remaining two cameras (RFC-1 and 2) are suitably positioned at a 'secondary focus' on the imaginary 'Rowland circle', where the spectrum created by the two grating assemblies can be collected.

* More detailed descriptions of the Scientific Instruments and the Mirror Modules on-board XMM can be found on pages 21 and 30 of this Bulletin.

Requirements and goals

Pointing

The pointing requirements originate from the scientists and have been thoroughly defined and negotiated between the Project and the instrument Principal Investigators early in XMM's design phase (Phase-B). Since a stringent pointing requirement is a direct cost driver, it was decided to split the scientists' demands into:

- requirements, which make the mission worthwhile, and

- goals, which would enable each instrument to achieve its ultimate performance.

The requirements must still be fulfilled by the spacecraft under all worst-case conditions, for example at end-of-life and immediately after an eclipse or a slew manoeuvre. The goals, on the other hand, may only be fulfilled under certain conditions but then for the majority of the observation time, e.g. a bright guide star.

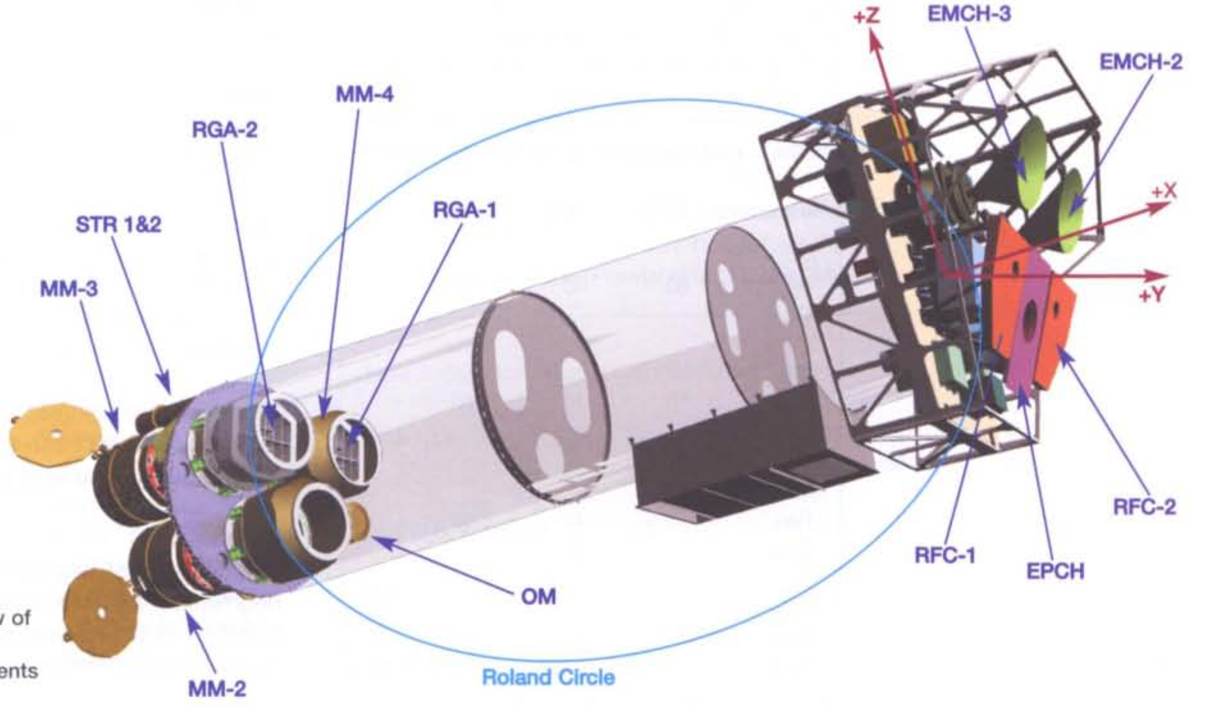

Figure 1. Exploded view of the XMM spacecraft, showing the main elements of the optical system

Figure 2. Pointing definitions for XMM's instruments

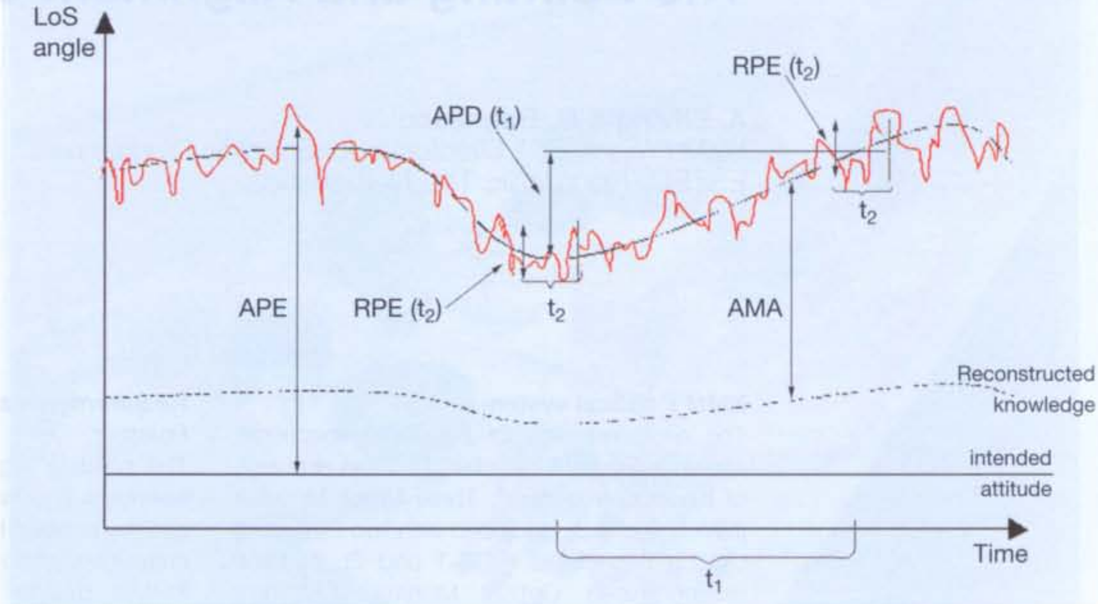

There are typically four requirements that are of particular interest to the scientists (Fig. 2):

The Absolute Pointing Error (APE), defined as the angular separation between the actual direction and the intended telescope line-of-sight. The APE must be such that the image of the observed target will fall onto the instrument detector. Since all of the instrument detectors on XMM are relatively large, being at least ~6 arcmin, in practice this requirement is not very stringent.

The Absolute Measurement Accuracy (AMA), defined as the angular separation between the actual direction and the reconstructed (a posteriori) direction of the telescope. The RGS instrument, and to some extent also the EPIC instrument, uses the location of a photon event on the CCD relative to the observed target as an indication of the energy of the photon. The AMA is therefore a very important performance parameter to allow the investigator to accurately reconstruct the energy spectrum of an X-ray source.

The Absolute Pointing Drift over 16 hours (APD), defined as the change in the angular separation between the actual direction and the intended direction of the telescope over the observation time. The APD is an indication of how well data from individual exposures can be superimposed without further processing in order to establish an integrated image. For XMM, images are superimposed a posteriori, on-board for the OM instrument and on the ground for RGS and EPIC, and thus the APD requirement is not too stringent.

The Relative Pointing Error over 2 minutes (RPE), defined as the angular separation between the actual direction of an axis and a reference axis, over the instrument exposure time. The allowed magnitude of RPE is usually defined as less than half of the instrument angular resolution, in order to ensure that the exposure is not 'blurred' by the instrument/ spacecraft motion. The RPE requirement for the OM is very stringent, since this instrument has very high resolution in the visible/UV spectrum, ~1 arcsec.

The applicable pointing requirements and goals for each instrument's line of sight in arcseconds at 95% confidence level are shown in Table 1.

Table 1. Instrument pointing requirements and goals

Instrument	*EPIC*	*RGS*	*OM*
APE			
Req.	60	60	60
Goal	-	-	-
AMA			
Req.	10	10	10
Goal	1	4	-
APD			
Req.	45	45	45
Goal	-	2	-
RPE			
Req.	5	5	5
Goal	1 (5 sec)	2 (30 sec)	0.25 (10 sec)

Alignment

In the case of alignment as well, thorough negotiation with the scientists has led to the definition of the relevant payload requirements, driven by the characteristics of the XMM optical system.

The alignment requirements for each EPIC 'primary focus' camera are expressed in terms of its maximum allowed translation and rotation with respect to the Mirror Module focus position and bore-sight. Because of the long Mirror Module focal length (7.5 m), its focal depth, which is a measure of the sensitivity of the optics to de-focussing, is of the order of several millimetres. Such insensitivity, combined with CCD detector dimensions of the order of several centimetres, led to maximum allowed translation and rotation requirements of the order of some millimetres and arcminutes, respectively.

Somewhat more complex has been the definition of the alignment requirements in the case of the 'secondary focus' RGS CCD cameras combined with the grating assemblies, mounted on the Mirror Modules. In order to minimise optical aberrations for this 'three-body' optical configuration, it is required that the three units involved - MM, RGA and RFC - lie on an imaginary 6.7 m-diameter 'Rowland circle'. Consequently, a careful apportionment of the alignment requirements had to be established early in the programme.

Another important consequence of the 7.5 m distance between the X-ray mirrors and the CCD cameras is that related to the stability requirements imposed on the structure in-between, which in the case of RGS camera, for example, must be <0.1 mm over 16 hours and <0.2 mm over 3 months.

Analysis and Verification

Pointing and alignment budget

Having defined the requirements and goals applicable to each instrument, an exhaustive pointing and alignment budget was established. The initial use of this budget was to make error allocations to the relevant subsystems, i.e. structure, thermal, AOCS, instruments, AIV alignment and ground processing. It became apparent that there are two dominating error contributors to the challenging measurement accuracy (AMA) goals:

- the thermo-elastic stability between the star trackers and the Mirror Modules and between the latter and the focal-plane cameras, and
- the star position-determination accuracy of the star tracker, i.e. the bias error.

To achieve the short-term pointing stability (RPE) goals, it is essential to reduce the following two effects as much as possible:

- the measurement noise of the star tracker
- the micro-vibrations originating from subtle imbalances or imperfections within the reaction wheels.

After a first round of error-budget iterations, the requirement and goal type of specifications were again carried forward into the subsystem and unit specifications, to obtain the best price/performance procurement.

Pointing verification

The pointing verification process has been based on a combination of analysis, simulations and direct testing of the actual performances of the most critical contributors, namely:

- bias and noise performance measurements of the star tracker
- micro-vibration measurements of the reaction wheels
- thermal gradient test of the mirror support platform and of the telescope tube
- telescope-tube characterisation by deflection measurements under an imposed temperature gradient.

As an example, Table 2 shows the specifications and actual performance of the star tracker.

Calibration campaign and alignment verification

An end-to-end test of the complete XMM spacecraft in order to check the X-ray performances and the correct alignment of all the elements is not possible due to its sheer dimensions. For this reason, already before the start of Phase-B, the alignment-related Assembly, Integration and Verification (AIV) strategy was developed along two main directions, with the aim of avoiding 'late surprises' during the spacecraft alignment. It was decided to:

- carry out an extensive characterisation of the Mirror Modules, both in stand-alone configuration and in integrated configuration together with the grating assembly. Such a calibration campaign allowed the verification at an early stage in the programme that the main parameters of the optical system were within the allocated alignment budget, i.e. the focal length and the 'Rowland circle' diameter

Table 2. Star-tracker specifications and performances

Error type	*Requirement end-of-life*	*Measured begin.-of-life*	*Estimated end-of-life*
Bias (2 σ, in arcsec)	3.5	1.5	1.5
Noise (1 σ, in arcsec):			
Magnitude 8.5	2.5	1.5	1.6
Magnitude 6.5	2.5	0.3	0.3

Figure 3. The alignment set-up used to check the axial positioning of all units at spacecraft level

- establish detailed and consistent alignment procedures starting from unit level (CCD cameras, grating assemblies and Mirror Module), to module level (MM with grating assemblies), up to spacecraft level. This in turn led to the implementation of specific features in the designs of all of the constituents of the optical system, the spacecraft and the Optical Ground Support Equipment to allow simple and precise checking of alignment. As an example, the early design of the structure already identified the necessity of through holes in the Service Module, in order to allow mirror-cube viewing from the alignment stand during spacecraft integration. Design provisions for alignment corrections were also implemented, e.g. shims and eccentric mounting plugs.

The Mirror Module tests, conducted at the Panter X-ray facility in Munich, Germany, and in the UV facility at the Centre Spatial Liège in Belgium, demonstrated that we were indeed on course to meet the requirements.

In a similar fashion, all other spacecraft constituents like the telescope tube and the mirror and instrument platforms were characterised in order to refine and confirm the predicted alignment budget.

A detailed set of alignment procedures at spacecraft-integration level were developed, debugged and verified already during the spacecraft structural-thermal model test campaign. The mature status of these procedures ensured that the tight integration schedule for the flight-model spacecraft could be maintained.

Figure 3 (right) shows the alignment set-up used during final checking at spacecraft level of the relative axial positioning of all of the units.

The final payload-alignment activities at spacecraft level were carried out in July 1999 at ESTEC, within the scheduled time and to the satisfaction of all parties involved: the scientific experimenters, the Prime Contractor and ESA.

Predicted In-obit Performance

All the results of the unit and subsystem tests, analysis and simulations, together with the results of the spacecraft thermal-balance test and alignment activities, have finally been assembled into the pointing and alignment predictions. These predictions show very promising performances for the telescope. All 'requirements' are met with comfortable margins, and 'goals' will be met for up to ~90% of all observations. As an example, the Table 3 shows the predictions for the measurement accuracy for the RGS instrument and the short-term pointing stability for the OM instrument:

Table 3

Errors in arcsec	*Requirement goal*	*Predicted worst case*	*Predicted ~90% of obs.*
AMA	10	5	
for RGS	4		3.1
RPE	5	1	
for OM	0.25		0.33

Acknowledgement

The authors wish to acknowledge the team effort by all personnel in the groups involved, i.e. the Dornier team, the teams at Centre Spatial de Liège, and at the MPE-Panter facility in Garching and the ESTEC metrology group. They are to be congratulated on their success in the timely and accurate design, implementation and determination of the optical performance of the XMM telescope. esa

XMM's Electrical Power Subsystem

B. Jackson
XMM Project, ESA Directorate for Scientific Programmes,
ESTEC, Noordwijk, The Netherlands

The XMM Electrical Power Subsystem (EPS) is 'conventional' in design in that it follows the ESA Power Standard. This article describes the subsystem's main features and performances, and the steps that have been taken in implementing the lessons learnt from the highly successful SOHO spacecraft recovery efforts, which were described in detail in ESA Bulletin No. 97.

EPS design drivers

The principal mission and spacecraft characteristics influencing the design of XMM's Electrical Power Subsystem (EPS) were:

- Power requirements: 1600 W in Sun, and 600 W in eclipse
- Spacecraft geometry: Two separate Power Distribution Units (PDUs) to reduce harness mass, and to simplify system testing and assembly, integration and verification (AIV), the Service and Focal-Plane Assembly Modules have dedicated PDUs
- Mirror stability: Leading to a dedicated Mirror Thermal Control Unit (MTCU)
- Orbit: (a) 255 eclipses, with a maximum duration of 1.7 h. The eclipses occur when the spacecraft is close to perigee, when the instruments are turned off. This leads to a lower eclipse power requirement and allows smaller batteries to be used; (b) Incomplete ground coverage requires the design to be failure tolerant. It was also a design requirement that the spacecraft should be able to survive for up to 36 h with a failure and without ground intervention.
- Lifetime 10 years: Component total radiation dose levels of 75 krad were taken as a reference, and maximum use was made of spacecraft shielding and rad-hard components. Solar-array degradation is also affected by radiation.
- Telescope: Telescope pointing requirements result in a maximum off-pointing of the solar array from the Sun of 28 deg.

In addition, during the XMM Service Module design phase, the technical requirements were harmonised with those of ESA's gamma-ray observatory spacecraft Integral, leading to a common Service Module design for the two spacecraft.

The resulting EPS design is comprised of the following elements:

- A fixed two-wing deployable solar array for power generation.
- Two nickel-cadmium batteries.
- A Main Regulator Unit (MRU) providing a main bus regulated to 28 V.
- Two independent Power Distribution Units: one for the Focal-Plane Assembly (FPA-PDU) and the other for the Service Module (SVM-PDU).
- A Mirror Thermal Control Unit (MTCU) dedicated to the thermal control of the mirror platform, Mirror Modules and Reflection Grating Assemblies.
- A Pyrotechnic Release Unit (PRU) for automatic activation of the release mechanisms for the solar arrays, and for the initial transmitter and AOCS activation.

XMM's EPS

The overall layout of the EPS is shown in Figure 1, where it can be seen that the Main Regulator Unit (MRU) controls the electrical power generation from the two solar-array wings, the energy storage within the two batteries, and provides the main bus regulation. The power distribution to the various 'users' is performed by the SVM-PDU for the Service Module (SVM) and Mirror Support Platform (MSP) units, and by the FPA-PDU for the units located in the telescope's Focal-Plane Assembly (FPA). Each PDU user outlet is protected by either a Latching Current Limiter (LCL) for switchable users, or by a Foldback Current Limiter (FCL) for permanently powered users.

The MTCU provides thermal control for the three Mirror Modules and the two Reflection Grating Assemblies. In addition, to meet the spacecraft autonomy requirements, it provides a self-monitoring function, which in the event of a failure to respect critical temperature limits performs an automatic switchover to the redundant channel.

The PRU activates the solar-array deployment mechanisms and spacecraft pyrotechnics, as well as automatically configuring the spacecraft into a predefined status at launcher separation.

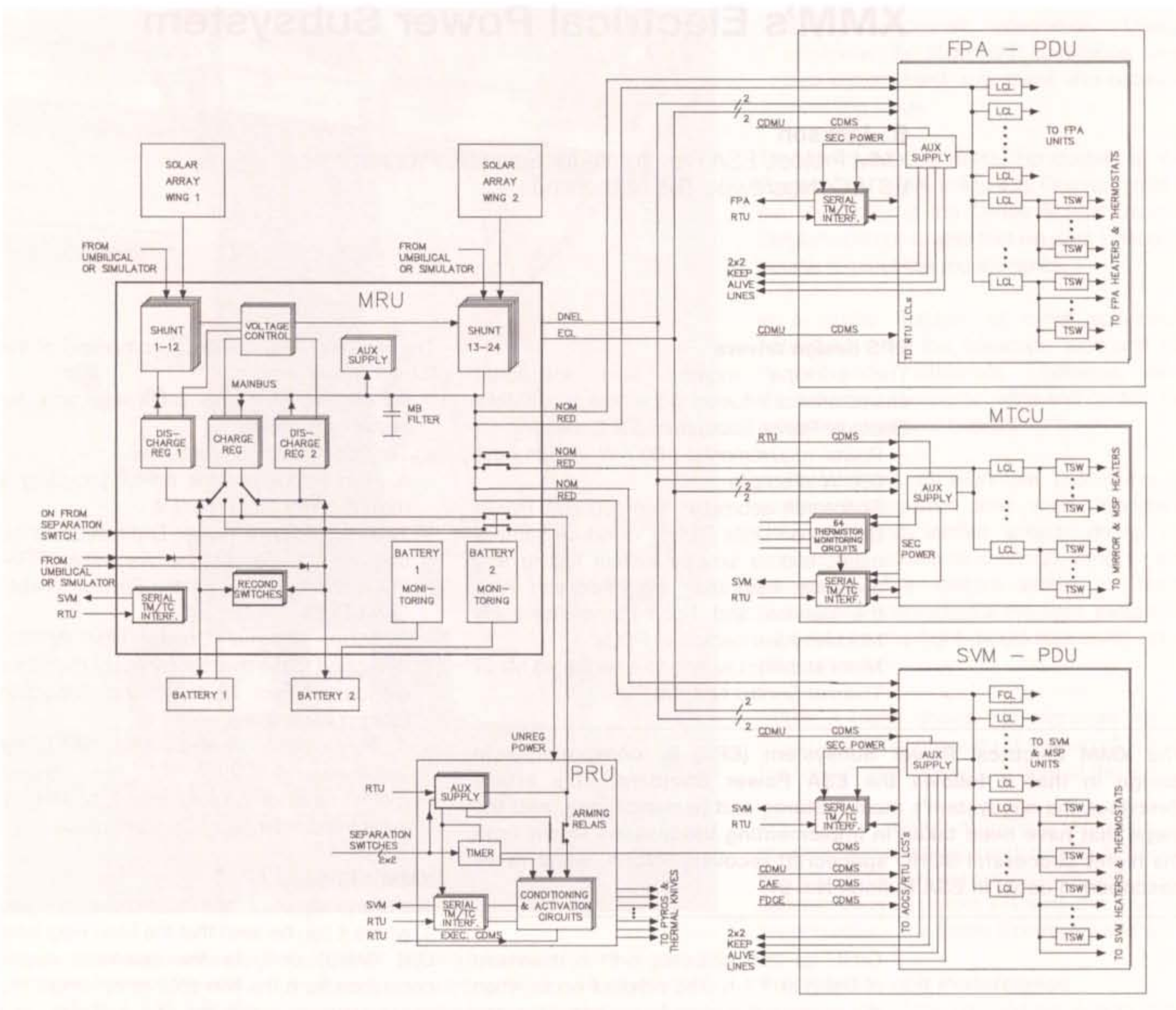

Figure 1. Overview schematic of XMM's Electrical Power Subsystem (EPS)

The solar array

The solar array has two wings (Fig. 2), each with three rigid 1.94 m x 1.81 m panels, giving a total area of 21 m^2 and a mass of 81.4 kg. The two wings are body-fixed and have a Sun incidence angle variation around normal of up to 28 deg. At end-of-life (EOL = 10 years), in the worst case, including one failed section, the solar array is required to provide 1600 W at 30 V at the interface connectors.

During the launch and the early orbit phase, the three panels of each wing are folded and stowed on four hold-down points on the spacecraft. Kevlar restraint cables keep the solar array in this folded position until they are cut on a command from the PRU.

Each wing carries 12 power sections with four sections per panel. The solar-cell strings are interconnected by blocking diodes and discrete panel wiring on the rear of the panel. Power delivery is divided equally between the 24 sections of the array. The 2 ohm.cm silicon Back-Surface Reflector (BSR) solar cells (210 microns), with 300 micron CMX cover glasses, are mounted on CFRP panels. To prevent electrostatic discharges, the cover glasses are coated with conductive indium-tin oxide.

The batteries

XMM has two identical 24 Ah nickel-cadmium batteries (Fig. 3), each with 32 cells. Each 573 x 188 x 222 mm^3 battery weighs 42 kg. To allow for cell short-circuits, the nominal energy budget is calculated with 31, rather than the full 32 cells. To allow for high peak power demands, a battery voltage higher than the bus voltage has been chosen, and battery reconditioning will be performed before each eclipse season.

The MRU

The Main Regulator Unit provides a 28 V regulated main bus voltage, with protection to

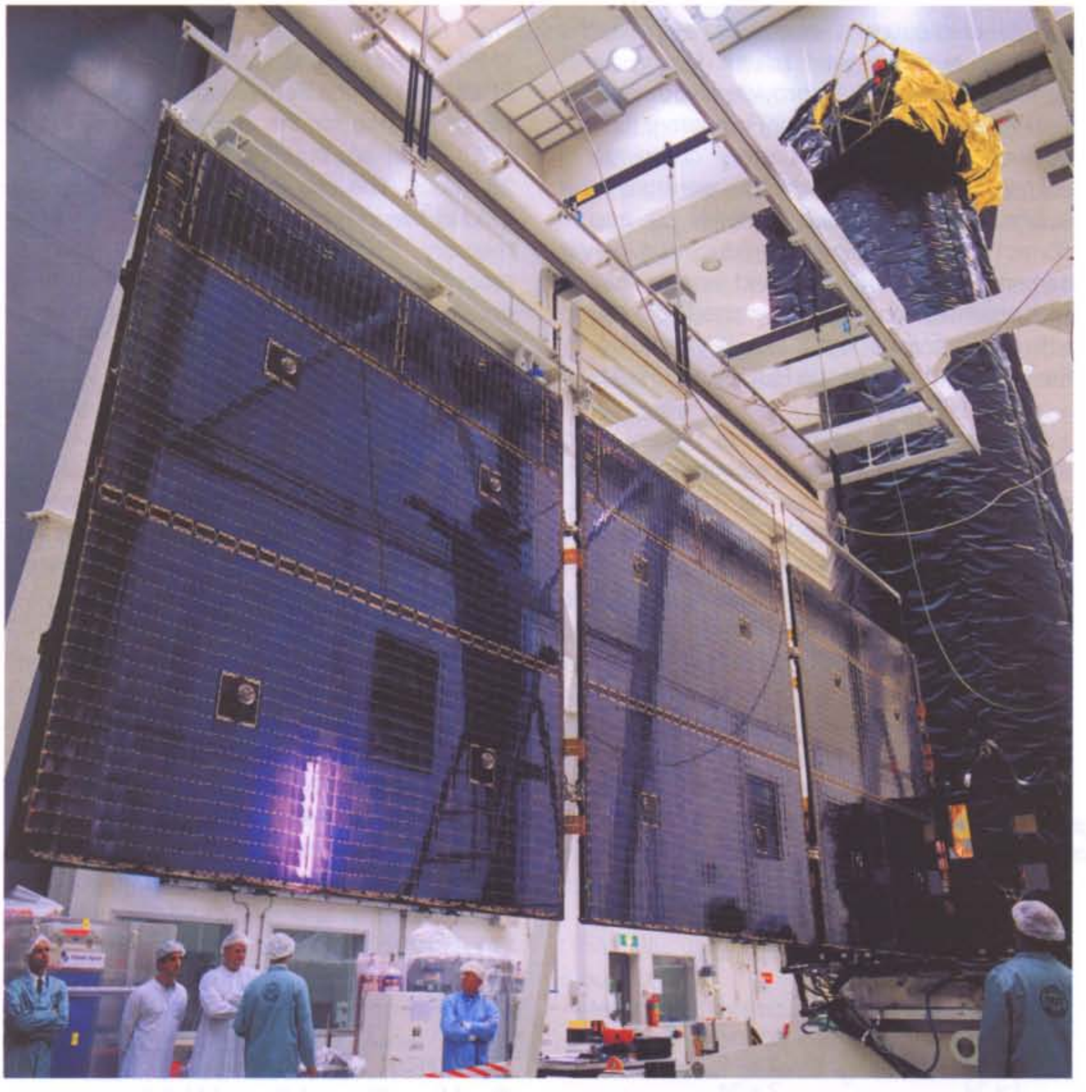

Figure 2. One of XMM's two solar-array wings (flight model), each of which has three folding rigid panels

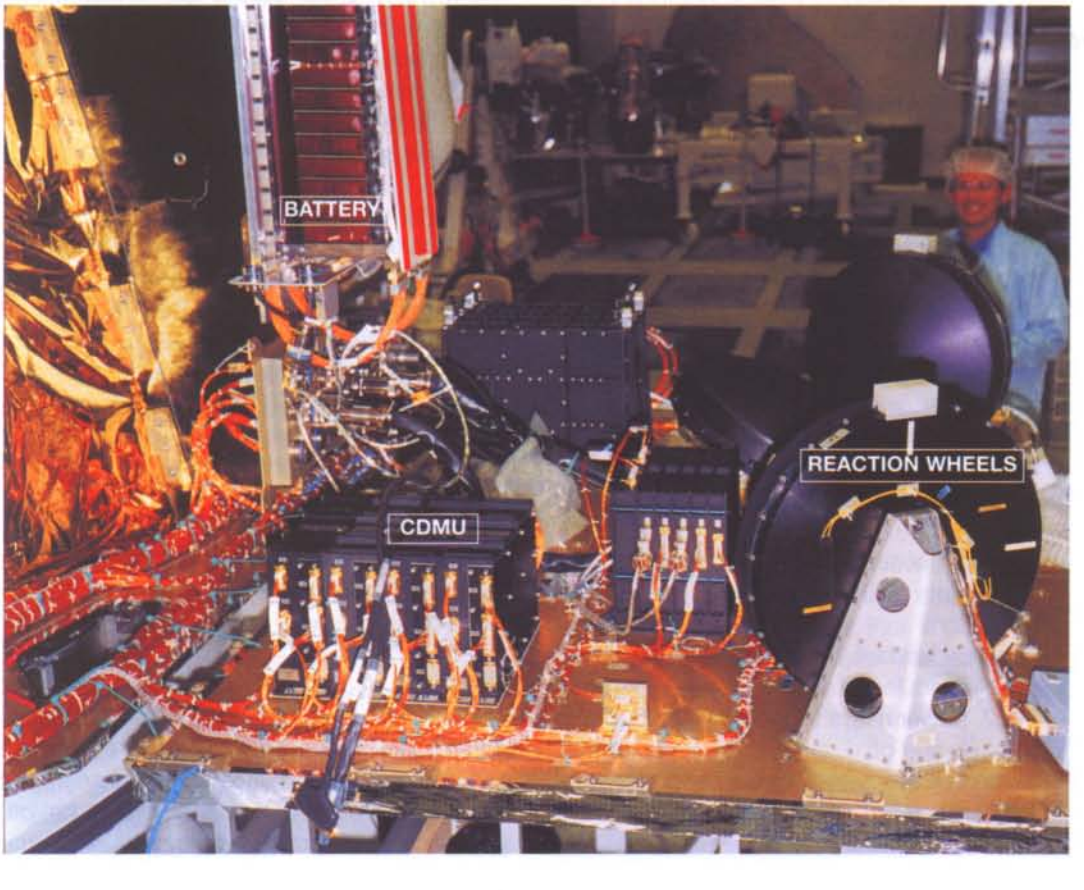

Figure 3. One of XMM's four equipment panels, carrying items powered by the Electrical Power Subsystem: front left, the Command and Data Management Unit (CDMU) and, far right, the AOCS Reaction Wheels; in the upper left corner, one of XMM's two onboard batteries is visible

ensure uninterrupted operation even in the event of a single-point failure. During sunlit periods, the MRU provides power via Sequential Switching Shunt Regulators (S3Rs), as well as managing battery charging. In eclipse mode, the MRU controls the discharging of the two batteries to ensure correct current sharing. To reduce the power demand on the batteries and ensure that all non-essential loads are switched off during eclipse, an eclipse signal ECL is generated by the MRU and sent to the PDUs and MTCU.

To provide protection against a battery over-discharge that could lead to a cell voltage inversion, a Disconnect Non Essential Loads (DNEL) signal is generated by the MRU and can be sent to the PDUs and MTCU. A DNEL signal will be issued as soon as the voltage from one group of four cells of either battery falls below 3.9 V.

Table 1. Key MRU features

Dimensions	540 x 520 x 180 mm^3
Mass	24 kg
Output voltage	28 V +1%-2%
Max bus load demand in sunlight	2100 W
Maximum output power in eclipse	1680 W

Table 2. Key PDU features

	SVM PDU	FPA PDU
Dimensions	455 x 270 x 200 mm^3	312 x 270 x 200 mm^3
Mass	16 kg	11kg
LCL/FCL solid-state switches	2 x 24	2 x 12
TSW heater switches	2 x 24	2 x 24
Keep-alive lines	2 x 2	2 x 2
Maximum continuous load current	25 A	20 A
Maximum peak load current	50 A	30 A

The MRU provides 2 x 2 power lines for the SVM-PDU and the FPA-PDU, and 1 x 2 switched lines for the MTCU. For ground testing, it provides interfaces with solar-array and battery simulators.

The MRU is composed of the following elements:
- bus capacitor and Main Error Amplifier (MEA)
- 24 non-redundant S3R sections (sunlit regulation)
- 2 x 2 hot-redundant Battery Discharge Regulator (BDR) modules for eclipse regulation
- 2 hot-redundant Battery Charge Regulator (BCR) modules to control battery charging
- 2 x 2 power relays to switch the MTCU and PRU on and off
- redundant telemetry/telecommand interfaces
- hot-redundant DC/DC converters for MRU auxiliary supplies.

The PDUs

XMM has two independent and fully redundant PDUs, one for the Focal-Plane Assembly (FPA-PDU) and one for the Service Module (SVM-PDU). Both are supplied from the spacecraft 28 V bus. The outputs can be configured by ground telecommanding, or using a read-only memory (ROM). The PDUs are able to reconfigure their outputs to a predefined configuration, for example in the case of an eclipse or a low battery voltage (ECL, DNEL).

The PDUs provide power distribution via two types of solid-state current limiters:
- Fold-Back Current Limiters (FCLs): for powering receivers, decoders, and essential AOCS units that are always powered on. In the event of an overload, these current limiters enter a fold-back mode.
- Latching Current Limiters (LCL): which operate as telecommanded switches with current limitation protection (thresholds 1A, 2A, 3A, 4.5A or 7A). The switch automatically trips off if the current limitation period exceeds a maximum time limit. The PDUs also provide groups of heater outlets, each outlet being controlled by a transistor switch (TSW) and protected by an LCL.

In addition, the PDUs provide keep-alive lines to maintain instrument memories during eclipse.

The MTCU

The Mirror Thermal Control Unit is responsible for controling and monitoring XMM's Mirror Assemblies (MA) and their support platform (MSP) in order to maintain thermal stability. It operates from the MRU regulated bus and is protected against output line short-circuits.

Latching Current Limiters (LCLs), each of which drives three transistor switches, perform the MSP and MA heater control. An 8 bit telecommand controlling the pulse-width modulation of the TSWs controls the power fed to the individual heaters. In addition, for failure management, the MTCU monitors four critical temperatures and provides automatic switch-over to the redundant side in the event of a temperature-limit failure.

At power on, eclipse and DNEL transitions, the MTCU will automatically configure the heaters into a default status.

The PRU

The Pyrotechnic Release Unit provides sequential activation of the spacecraft subsystems and release mechanisms. The PRU is internally redundant, and it will be 'off' until the spacecraft's separation from the

Table 3. Key MTCU features

Dimensions	402 x 274 x 220 mm^3
Mass	15.8 kg
LCL (3A) solid-state switches	2 x 8
TSW heater switches	2 x 24
Maximum continuous load current	24 A

Table 4. Key PRU features

Dimensions	250 x 250 x 200 mm^3
Mass	5.5 kg
LCL (3A) solid-state switches	2 x 8
Thermal-knife outputs	8 + 8
EED outputs	8 + 8

launcher. It will then be connected to the unregulated battery supplies and will autonomously trigger a timer to power-up basic spacecraft subsystems (AOCS and transmitter) and activate the thermal knives for deploying the solar arrays. Via arming relays and arm/fire switches operated by telecommand, the PRU will fire the Electro-Explosive Devices (EEDs) needed to activate the spacecraft subsystems.

Lessons learnt from SOHO's recovery

Following the successful recovery of the SOHO satellite, the XMM design was re-examined to see how, even in the case of a catastrophic failure, including the loss of the spacecraft main power bus, the probability of recovering the spacecraft could be improved. As a starting point it was assumed that the spacecraft would be in a worst-case configuration, that it would have totally-discharged batteries, would have lost attitude, and that the solar arrays would no longer be Sun-pointing, and with most subsystems cold. In this case, main-bus recovery could only occur when the solar arrays came into sunlight and provided sufficient power to support all connected spacecraft loads. At such a time, it can be assumed that:

- the spacecraft is spinning and not stable and Sun-pointing
- at least some parts of the reaction control system are frozen
- survival thermostats are closed, connecting main (and redundant!) heaters to the spacecraft bus.

Significant lessons learnt from SOHO were:

- to switch on the transmitters as soon as possible (to provide a 'beacon') to show the ground control centre that the spacecraft is powered, and its location
- to minimise power consumption at switch-on and to power up spacecraft units sequentially, allowing time for ground intervention; it is even desirable not to instantly power on the AOCS for example, in case the RCS is frozen. On XMM, the bus load at power up is now limited to 'essential units' only (MRU, receivers, transmitter, Command Data Unit) to maximise the probability that the spacecraft main bus will recover
- to ensure that if sufficient power is available, the spacecraft will recover even without ground intervention
- to ensure that the batteries can be charged as quickly as possible; e.g. to recover a spinning spacecraft, the batteries would be required to power the spacecraft whenever the solar arrays were shadowed and for long enough to process commands and ultimately for the AOCS to stabilise the spacecraft.

Throughout all of the investigations into possible improvements, great care was taken not to create new failure modes that might jeopardise the mission. The changes were to be implemented at a late stage in the programme, when most flight units had already been built and were being integrated. However, the inherent flexibility of the design and the timely work by the spacecraft contractors involved allowed it to be done with minimum impact on the overall schedule.

Ultimately, the following modifications were made to XMM:

- New timer units were added, which generate pulses to the PDU control inputs.
- The ROMs controlling the PDU output configurations were modified.
- The harness was modified so that direct commands (commands from the CDU which are available directly at switch-on without the need to load software or power-on RTUs) were routed to allow the ground to power-off the MTCU and Timer units.
- In addition, the MRU was modified to ensure that the batteries went into full charge mode at power-on (using excess power only!).

The modifications were successfully tested on the integrated flight-model spacecraft and showed that, for example, initial spacecraft power-on now occurs at less than 300 W, compared to a power-on figure prior to modification of more than 1500 W. This provides increased confidence that, even in the unlikely event of a total power loss, the probability of recovering the spacecraft is significantly increased and that it would now begin to recover for Solar Aspect Angles (SAAs) of up to 80 deg.

XMM's Data-Handling Subsystem

A. Karlsson
XMM Project, ESA Directorate for Scientific Programmes,
ESTEC, Noordwijk, The Netherlands

Scaling the XMM data-handling system to the specific needs of the mission has resulted in a flexible and relatively uncomplicated On-Board Data-Handling (OBDH) Subsystem. The XMM spacecraft is operated in real-time and is fully compliant with the ESA packet data-handling standards. Packets are of variable length and presented to the OBDH when available. The OBDH telemetry/telecommand cycles are asynchronous to the instrument and subsystem cycles. The telemetry rates can easily be reallocated to cope with unforeseen spacecraft configurations, e.g. lost telemetry sources. The absence of requirements for automatic reconfiguration has contributed to the reduced subsystem complexity.

XMM's OBDH Subsystem

The On-Board Data-Handling (OBDH) Subsystem for XMM is implemented in three internally redundant physical units: the Central Data Management Unit (CDMU) and two Remote Terminal Units (RTUs). The CDMU and one RTU are located on the Service Module of the spacecraft. The second RTU is installed on the Focal-Plane Assembly (FPA). In addition to the RTUs and the CDMU, the OBDH includes six Data Bus Units (DBUs), which provide the scientific instruments with a digital interface to the data-handling services.

The data processing in the CDMU is performed by the Central Terminal Unit (CTU) based on a MIL-STD-1750 microprocessor with 256 kwords of RAM. The packet handling functions, i.e. telemetry frame generation and telecommand frame decoding, are implemented in standard ASICs developed under ESA contracts, Virtual Channel Assemblers (VCAs), Virtual Channel Mutiplexers (VCMs) and Packet Telecommand Decoders (PTDs).

The users and all of the OBDH units are interconnected by the ESA OBDH bus, comprising a redundant set of interrogation bus and mono-directional response bus. The OBDH bus can transfer, depending on the command rate, approximately 200 kbps of telemetry data, which is roughly three times the XMM downlink data rate of 69.4 kbps (source-packet level).

The bus activities are governed by the Polling Sequence Table (PST), which has a 4 sec cycle and is subdivided into 184 windows of equal duration. These windows are programmable to be either: telecommand distribution, telemetry acquisition from intelligent bus terminal, telemetry acquisition from RTU, or memory patch or dump of a memory on the bus.

The default Polling Sequence Table on XMM has 36 windows for telecommand distribution, 129 windows for telemetry acquisitions from the instruments, 9 windows for AOCS telemetry, 7 windows for RTU acquisitions, and some spares.

The bus is used for both low-level word-oriented data acquisitions and control, as well as for high-level packet transfers. The low-level protocol is used for data transfers to and from the RTUs, while the high-level protocol is used in the communication with the Packet Terminals.

Packet protocol

Packet Terminals are connected to the OBDH via dedicated Data Bus Units. The interface to the DBU, and thus the OBDH bus, is realised by an ASIC Remote Bus Interface (RBI). In order to have a common interface to all Packet Terminals, this specific RBI was imposed on all instruments and the Attitude and Orbit Control Subsystem (AOCS).

The RBI provides the CDMU with Direct Memory Access (DMA) to the processor memory of the Packet Terminals. In addition, the RBI accommodates registers for communication between the Packet Terminal and the OBDH and a register holding a copy of the onboard time.

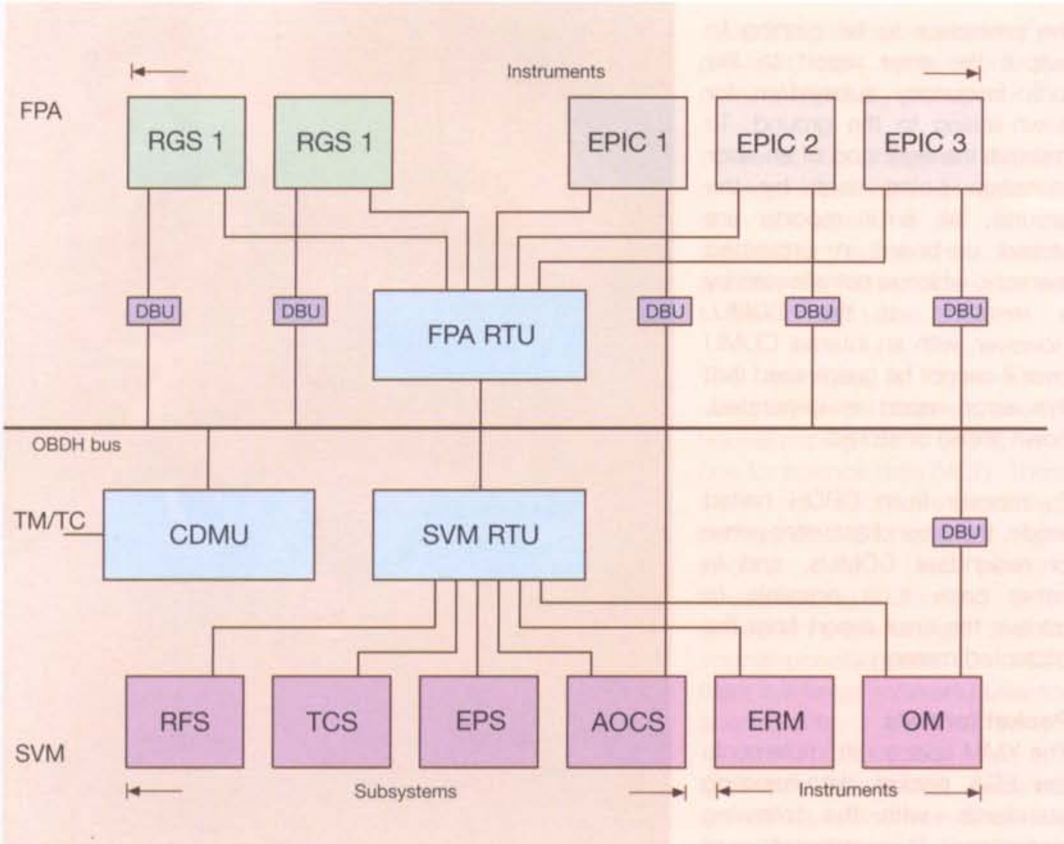

Figure 1. Architecture of XMM's OBDH Subsystem

Packet Terminals receive telecommand packets via DMA in a telecommand buffer in memory. When the OBDH has delivered a telecommand packet, the microprocessor of the Packet Terminal will receive an interrupt as a notification that the telecommand should be processed and removed from the buffer. By setting a flag, the Packet Terminal indicates that it is ready to receive a new telecommand packet.

Whenever the Packet Terminal has a telemetry packet to deliver, it indicates this by setting another flag. This flag is read by the OBDH at each poll of the Packet Terminal, as programmed in the Polling Sequence Table. When the OBDH detects that the flag is set, it will transfer the telemetry packet to a telemetry buffer in the CDMU and downlink it according to its priority.

In order to allow the users to design their scientific instruments without detailed knowledge of the OBDH interface and to fully exploit packet telemetry, the OBDH bus protocol is designed with Packet Terminals being asynchronous to the OBDH data acquisition cycle. This is made possible by datation of the telemetry packets and the direct memory access to the users' memories. The Packet Terminals are free to choose packet production profiles that match the scientific objectives of the instrument, within the constraints of data-rate allocation and the telemetry poll rate.

Autonomy

XMM is required to survive three days of ground-station outage. The autonomy on XMM is decentralised, meaning that all subsystems should manage their own survival and supply essential services to allow other subsystems to survive. Thus the central spacecraft autonomy function, often implemented in the data-handling subsystem, was not required for XMM. Recognising this has allowed a substantial reduction in design and test expenditure by limiting the OBDH autonomy to protection against OBDH internal failures.

Since all autonomous functions are implemented in the various subsystems without relying on services from the data-handling subsystem, it was permissible to cease data-handling services on the detection of an internal OBDH anomaly. As a result, whenever the OBDH detects an anomaly, e.g. an uncorrectable error in memory, it will terminate execution and enter a halt mode. The users of the OBDH services will detect that the OBDH has entered the halt mode by, for example, an accumulation of telemetry packets. The user has to take appropriate measures to operate without OBDH services until they are resumed.

Before entering the halted mode, the OBDH generates an error report describing the reason for the mode transition and forwards it to the telemetry system. Since the telemetry system is implemented in hardware, it does not require the processor to be running to output the error report to the radio-frequency subsystem for down-linking to the ground. To improve the likelihood of an error message being seen by the ground, all error reports are stored on-board in protected memory, which is not affected by a resetting of the CDMU. However, with an internal CDMU error it cannot be guaranteed that this error report is generated, down-linked or stored.

To recover from OBDH halted mode, the ground activates prime or redundant CDMUs, and in either case it is possible to retrieve the error report from the protected memory.

Packet formats

The XMM spacecraft implements the ESA packet data-handling standards, with the following restrictions: (i) segmentation of source packets is not supported, and (ii) the lengths of telemetry packets and telecommand packets have been limited to 518 octets and 248 octets, respectively. It should be noted that 'grouping' is allowed for the science data telemetry packets.

Telemetry and telecomand packet types and subtypes, allowed on XMM, are specified in the Packet Structure Definition, derived from a draft version of the Packet Utilisation Standard. It defines a reduced set of packets tailored to the needs of the average ESA spacecraft, and XMM specifically.

The Packet Structure Definition identifies the packet types and subtypes as derived from the operations concept and the on-board functions required. Furthermore, it specifies the format of the packets, i.e. packet data field headers, identifiers and data records, and parameter formats including, for example, the format of the time and error control words. The following telemetry packet types are defined:

TM(1,x)	Periodic Telemetry Reports
TM(3,x)	Telecommand Verification Reports
TM(4,x)	Non-Periodic Telemetry Reports
TM(5,x)	Task Maintenance Reports
TM(6,x)	Memory Management Reports
TM(7,x)	Time-Tag Buffer Reports
TM(8,x)	On-Board Monitoring Reports
TM(9,x)	Telemetry Management Reports
TM(10,x)	On-Board Time Management Reports
TM(15,x)	Science Telemetry Reports

The following telecommand packet types are defined:

TC(2,x)	Device Commanding
TC(5,x)	Task Management
TC(6,x)	Memory Maintenance
TC(7,x)	Time-Tag Commanding
TC(8,x)	On-Board Monitoring
TC(9,x)	Telemetry Management
TC(10,x)	On-Board Time Management
TC(11,x)	Retrieval Stored Non-Periodic Packets
TC(13,x)	Test Telecommands

Obviously, the users need to specify the packet formats corresponding to their own needs. This is done via packet definitions produced by the users based on the types and formats provided in the Packet Structure Definition.

Telemetry system

The main scientific instruments on board XMM have a data-generation rate proportional to the strength of the observed X-ray target. This will result in time-variable demands from the users on the data-handling services. Responding to this inherent user need, it was decided to implement packets with variable length.

In having variable length packets, the telemetry service to the Packet Terminals is specified by: (i) the number of polls per bus cycle, where polls are evenly distributed over the bus cycle

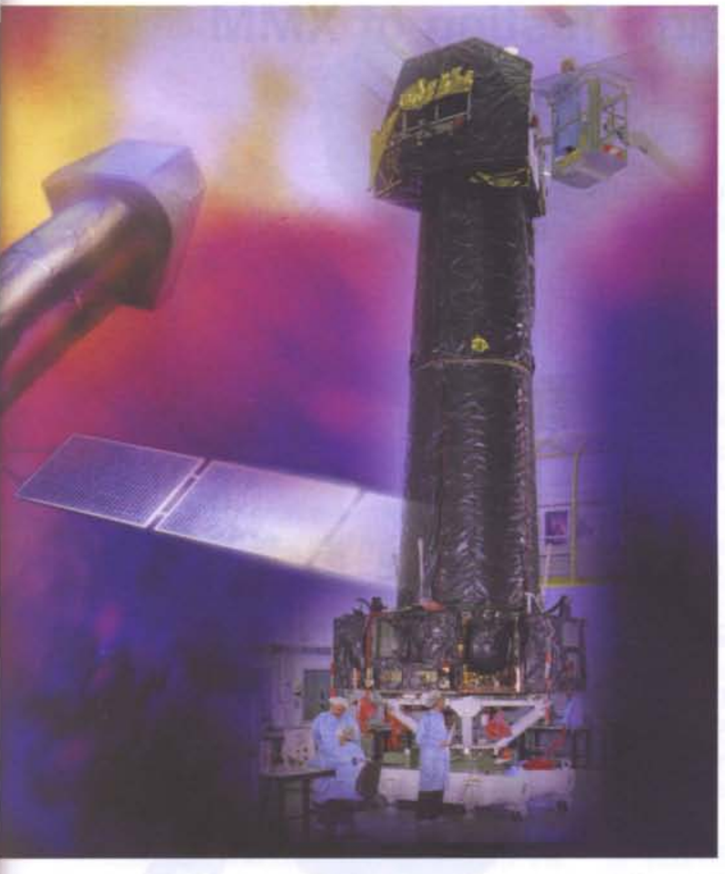

with a certain tolerance, and (ii) the maximum amount of data that may be transferred from a Packet Terminal during a bus cycle. The former is specified in the Polling Sequence Table, and the latter in the Bit Rate Allocation Table. Both tables are programmable from the ground.

To allow the Packet Terminals to produce short telemetry packets, they are polled more frequently than strictly necessary. If all Packet Terminals deliver maximum-size packets at all polls, the total data rate would be 142 kbps, while an average of only 65.6 kbps from the Packet Terminals can be accommodated on the down link. It is therefore essential that the output data rate from the Packet Terminals be controlled.

The control is performed after each telemetry packet read-out. The CDMU verifies how much data it has received from the Packet Terminal during the current bus cycle and compares it against the telemetry threshold of the Packet Terminal. Whenever the threshold has been exceeded, the OBDH will cease acquisition of any further packet from that particular Packet Terminal until the end of the current bus cycle. Note that the read packet is accepted for transfer by the CDMU. The maximum excess data delivered by a Packet Terminal will be a fraction of a telemetry packet.

At the beginning of the next bus cycle, the CDMU will calculate the new threshold by subtracting the excess data of the previous bus cycle from the nominal telemetry allocation.

However, if the Packet Terminal provides less than its allocation in one bus cycle, it will not be credited for the loss of bandwidth, and the next threshold will be set to the nominal value.

The telemetry is down-linked using two virtual channels, one for housekeeping data (VC0), and one for science data (VC7). There are two software-controlled buffers on VC0, one for high-priority data, i.e. periodic housekeeping data and time-correlation packets, and one for normal-priority data. On VC7, there is a single software buffer for science data.

Whenever the packet terminals do not fully utilise their down-link rates, Idle Telemetry Frames will be generated automatically, maintaining a fixed bit rate on the down link.

Conclusion

The benefits of the XMM data-handling architecture and its packet data-handling approach are demonstrated by:
- very smooth integration of the different data-handling systems onboard the spacecraft, and
- the fact that, late in the programme, two Visual Monitoring Cameras could be integrated without any changes to the onboard software.

Acknowledgements

The successful development of XMM's Data-Handling Subsystem is an achievement of several individuals and companies, contributing in various ways. The contributing companies are Laben SpA (I) for the CDMU and RTUs, Alcatel Espacio (E) for the DBUs, and Dornier (D) for the subsystem engineering. Without underestimating the efforts of any individual, I wish to acknowledge the valuable work performed by K. Günthner (Dornier), G. Aranci and G. Rosani (Laben) who worked towards the common goal of developing a reliable data-handling subsystem to meet XMM's requirements.

The Integration and Testing of XMM

Ph. Kletzkine
XMM Project, ESA Directorate for Scientific Programmes,
ESTEC, Noordwijk, The Netherlands

The XMM (X-ray Multi-Mirror) spacecraft, a spaceborne X-ray observatory to be launched by Ariane-5, stands 10 m high and measures over 4 m in diameter in launch configuration, for a launch mass of just under four tons. Such a tall spacecraft challenges the capabilities of existing European environmental testing facilities. Provisions were made in the design for a split according to geometry into an Upper Module and a Lower Module for environmental test purposes. Optical testing of the X-ray Mirror Modules – the core technological challenge – required the use of several existing and custom-built test facilities. In the face of strict schedule requirements, spacecraft-level test flows were organised around extensively parallel flows and all tests were scrutinised for their potential for early problem identification. This article briefly introduces the XMM configuration and schedule constraints, explains the spacecraft-level model philosophy, discusses the consequences for each category of test in terms of facility and test specimen configurations, and summarises the spacecraft test flows and the results achieved.

Configuration and schedule

The XMM satellite (Fig. 1) is configured in a modular manner, described in detail elsewhere in this issue. The Focal-Plane Assembly (FPA) can be fully integrated and tested independently from the Service Module (SVM). However, it is readily apparent that splitting the satellite into Service Module and Payload Module (PM) does not solve the problem of size limitations in environmental testing facilities, since the payload is distributed throughout the length of the spacecraft.

Furthermore, analysis determined that mechanical qualification of the SVM alone was unrealistic. The mechanical behaviour of the lower part of the spacecraft is largely determined by the presence of the three Mirror Modules (MMs), which together and with the two Reflection Grating Assemblies (RGAs) account for a mass of more than 1300 kg mounted into the Mirror Support Platform (MSP). Proper load introduction into the SVM from the MSP fully equipped with Mirror Modules is indispensable.

For environmental test purposes, the spacecraft is therefore split at roughly mid-height. This requires the introduction of an internal bolted interface between the Lower and Upper Telescope Tubes (LTT and UTT), but results in a configuration which lends itself to accommodation in the largest existing European test facilities, namely those at ESTEC.

The Lower Module (LM) consists of: SVM with MSP, Mirror Modules, RGA, Lower Telescope Tube and a closure plate. The Upper Module (UM) consists of FPA and Upper Telescope Tube.

The Lower Module and Upper Module dimensions are compatible with:
- the ESTEC Large Space Simulator solar beam size (6 m diameter) for thermal testing
- the ESTEC 280 kN electrodynamic shaker for vibration testing
- the ESTEC Mass Properties measurement machine with its latest L-4600 arm.

The fully assembled spacecraft is compatible with ESTEC's Large European Acoustic Test Facility (LEAF). Besides acoustic testing, the LEAF was also used to conduct a Modal

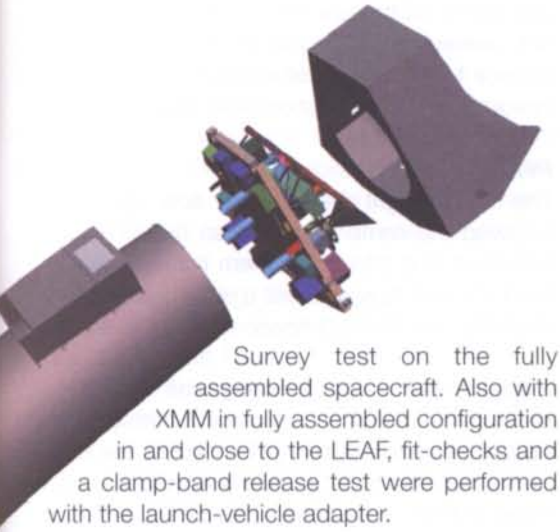

Figure 1. Exploded view of the XMM spacecraft. From top to bottom: FPA thermal tent, FPA with 3 EPIC cameras and 2 RGS cameras, Telescope Tube upper and lower parts, MSP with 3 Mirror Modules and Optical Monitor, SVM

Survey test on the fully assembled spacecraft. Also with XMM in fully assembled configuration in and close to the LEAF, fit-checks and a clamp-band release test were performed with the launch-vehicle adapter.

The spacecraft development schedule had to be compatible with delivery of the Flight Model experiments to the spacecraft in 1998 and with a budget-dictated duration imposing that launch take place no later than early-2000. Phase-B (preliminary design) was performed in 1995, Phase-C/D (detailed design, manufacturing and test) was initiated in March 1996. This translated into the obligation to perform the Structural and Thermal Model (STM) programme and Electrical Model (EM) programme in parallel, and to start the Proto-Flight Model (PFM) assembly before the end of the STM and EM programmes.

Spacecraft-level model philosophy

The Structural and Thermal Model was used to qualify by test the complete spacecraft primary structure and thermal design. The STM can be separated into Lower Module and Upper Module as described above, and the structural and thermal designs take into account the fact that the two are tested separately. The STM was also used to prove the LM-to-UM mating/de-mating procedures, verify the behaviour of the LM-to-UM interface, verify alignment and light-tightness design and test procedures, verify compatibility with the shock inputs, and exercise assembly and handling procedures and Mechanical Ground-Support Equipment.

The Electrical Model was used to verify the electrical design, internal interfaces, software, EMC/ESD, checkout procedures, and Electrical Ground-Support Equipment (EGSE). The EM units are flight-model representative in 'form, fit and function', but are not required to meet as stringent part-reliability standards as the flight units. The EM has no Telescope Tube and no Mirror Modules. The EM Focal-Plane Assembly and EM Service Module are each built around structures representative of the flight layout, so as to achieve good representation for EMC and harness layout.

As soon as their respective test programmes were completed, the STM and EM Service Modules were separated from the rest of their respective satellites and delivered for re-use to Integral, another ESA scientific satellite project that uses the same Service Module design.

The Proto-Flight Model is the actual satellite to be flown. The structural qualification had been acquired on the STM; the 'Proto' part of the name therefore concerns only limited electrical aspects and minor qualification gaps left by configuration changes. The PFM does not re-use any part of the STM nor EM models. However, because the flight Mirror Modules are extremely sensitive to contamination, testing of the PFM spacecraft was mostly carried out with the three STM Mirror Modules installed. This is possible because the STM Mirror Modules' representativeness is excellent in all respects, except of course in terms of optical properties. The flight Mirror Modules were installed at the last mating of the two modules, after thermal and vibration tests and just before acoustic testing.

In addition, the RF Suitcase Model was provided to check RF compatibility between the spacecraft and the ground stations. The RF Suitcase re-uses parts of the EM (Central Data Management Unit and Transponder).

Test flows

All three test flows make use of the schedule optimisation made possible by the modular splitting of the spacecraft by conducting parallel testing whenever the two modules are not assembled together. For each of the three spacecraft models, integration of the Upper Module and Lower Module took place separately.

STM tests

Once the two modules of the Structural and Thermal Model (Fig. 2) were integrated, they were mated, aligned, submitted to light-tightness and alignment checks, de-mated, and shipped to ESTEC for environmental testing.

Each Module underwent, in turn, mass properties measurement, thermal-balance, and sine-vibration testing. The rest of the tests could be carried out on the complete spacecraft and therefore the Upper Module and Lower Module were mated and the assembled STM spacecraft underwent modal-survey testing, acoustic testing, clamp-band release (which also served as a spacecraft-level shock test), and a mechanisms functional test.

EM tests
Testing on the Electrical Model proceeded along with integration in the classical sequence, i.e. electrical integration tests (pin-to-pin, signal presence and shape) and Integrated System Tests (ISTs: all functionalities) were conducted after integration of each electronic unit and each major subsystem. After completion of the tests on both the Lower and Upper Modules, the two were linked by a harness representative of the harness running along the Telescope Tube in the PFM situation. Tests were conducted on the EM satellite to verify Electro-Magnetic Compatibility (EMC) behaviour, both radiated and conducted, and Electro-Static Discharge (ESD) behaviour, also both conducted and radiated. The software logic and code of all major subsystems were checked, exercised and debugged, including both open-loop and closed-loop testing of the Attitude and Orbit Control Subsystem (AOCS) and ISTs of the scientific experiments. The sophisticated Electrical Ground-Support Equipment was also put to the test, the architecture and interfaces between the core computer, the various items of front-end equipment, subsystem checkout computers and scientific instrument stations were exercised and their software debugged. After completion of the EM programme, those items not delivered to Integral as part of the EM Service Module were refurbished as Assembly, Integration and Verification (AIV) spares.

Figure 2. The XMM STM Lower Module (left) and Upper Module (right) at ESTEC

PFM tests
The Proto-Flight Model test flow generally followed the same principles as the STM and EM flows and combined them both. However, the PFM test flow was not a simple addition of the STM and EM test flows.

After completion of its integration along the mechanical and electrical integration procedures validated on STM and EM, the PFM Lower Module was tested for conducted and radiated EMC, then shipped to ESTEC where it first underwent sine vibration testing at acceptance levels in the axial (i.e. longitudinal) direction. Thermal tests (thermal balance, and thermal vacuum at acceptance temperature levels) in the ESTEC Large Space Simulator followed. The Lower Module was opened to permit the removal of several electronic units. They underwent minor modifications as a result of either component alerts or non-conformances, or hard-wired logic changes in the power subsystem decided upon after consideration of the lessons learnt from the recent in-orbit problems experienced by the joint ESA/NASA Solar and Heliospheric Observatory (SOHO). Other activities included the removal of one scientific experiment, the Optical Monitor telescope, to exchange the telescope optics for a higher-performance set; and to exchange, as scheduled, the STM Mirror Modules for the FM Mirror Modules. Exchange operations for the Optical Monitor and Mirror Modules took place in a Class-100 environment because of the sensitivity of the optics to contamination. After all flight units had been mechanically and electrically re-integrated, the Lower Module was mated to the Upper Module and the assembled spacecraft underwent acoustic testing.

The integration schedule for the PFM Upper Module was driven by the delivery schedules for the five focal-plane scientific cameras. The Upper Module went through conducted EMC and was shipped to ESTEC. For reasons of test-facility availability, it first went to thermal testing (thermal balance, and thermal vacuum at acceptance temperature levels) in the ESTEC Large Space Simulator. Mass properties, limited to weighing and determination of centre-of-gravity offset to the longitudinal axis, were measured. A sine vibration test in the lateral direction followed. Two electronic units were removed and were modified, for the same reasons as described for the Lower Module. Meanwhile, software debugging of the scientific cameras proceeded. The two modules were then mated, as described above.

Beyond the electrical integration tests and subsystem-specific Integrated System Tests, the PFM was submitted to functional testing between the major environmental tests and at major system milestones. To cut down on redundant testing, all flight procedures (both nominal and emergency) were distributed into six 'Spacecraft Functional and Performance Test' (SFPT) series that were used instead of specific functional tests. The potential risk was that tests before and after an environmental test or integration step were not always one-to-one identical, potentially making test-result comparison more difficult. All six SFPT series were run, and this drawback has not materialised; the few test deviations have been correctly diagnosed. The advantages of this approach are a significant time saving and the possibility to stagger the very labour-intensive preparation and verification of flight procedure software in an efficient manner. One of the SFPT series was run during thermal-balance/thermal-vacuum testing in addition to subsystem-specific ISTs.

Communication interfaces with the ground segment, located in this case at ESA's European Space Operations Centre (ESOC) in Darmstadt, Germany, were verified by use of the RF Suitcase Model, without having had to wait for completion of the PFM spacecraft. Communications were also checked at intervals by allowing the ground segment to listen-in on the PFM electrical testing being performed at ESTEC. These Listen-In Tests were followed by System Verification Tests (SVTs), i.e. full-fledged end-to-end (spacecraft-to-Mission Operations Centre) tests to exercise all telemetry and telecommand and all flight procedures.

Thermal testing

In total, four environmental spacecraft-level thermal tests were performed, all in the Large Space Simulator (LSS) at ESTEC, the largest solar-simulator facility in Europe: thermal-balance tests on the STM Upper and Lower Modules, and thermal-balance/thermal-vacuum tests on the PFM Upper and Lower Modules.

The purpose of the thermal-balance tests was to validate the thermal mathematical models and to verify the ability of the Thermal Control Subsystem to keep payloads and spacecraft equipment within specified temperature limits under simulated extreme expected orbital conditions. The Upper Module was mounted upright (as it will stand on top of the Ariane-5 launcher) inside the chamber. The Lower Module was 'upside-down', with the 2700 kg mass of the Service Module and Mirror Modules on top of the lower half of an extremely lightweight telescope tube. This unusual set-up (Fig. 3) offered the possibility of simulating very realistically the thermal environment of the bottom part of the spacecraft where the Mirror Module apertures had an unobstructed view to cold space. The correct simulation of the heat fluxes lost into space was of paramount importance for the verification of the temperatures and gradients of the Mirror Modules and the Mirror Support Platform. This would not have been possible if a more conventional mounting of the spacecraft by means of its launch-vehicle interface flange had been selected.

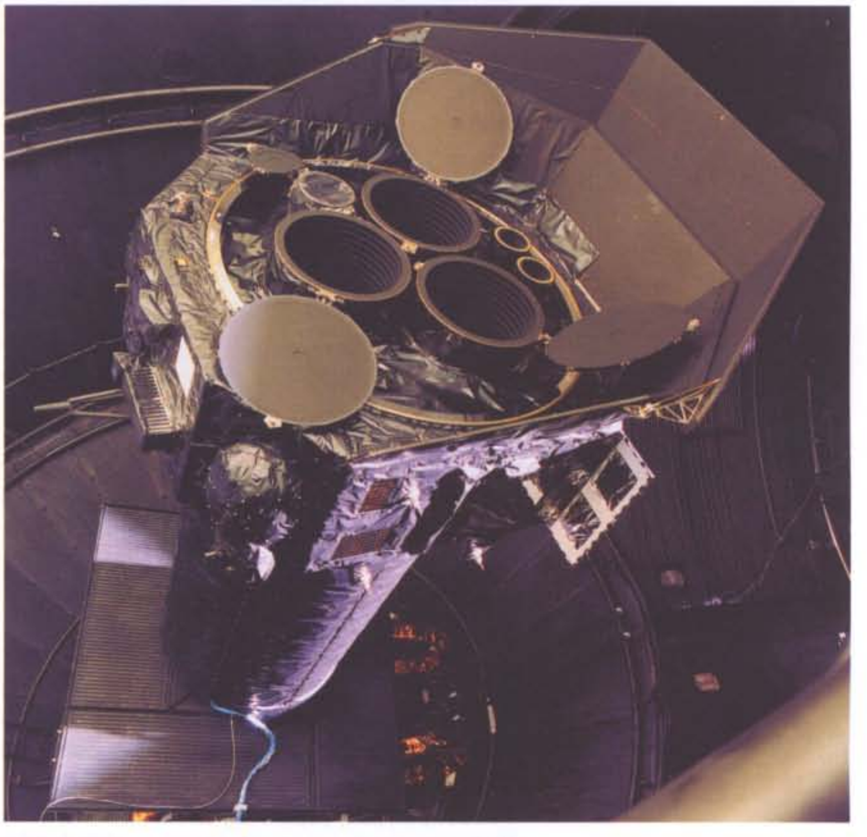

Figure 3. The XMM PFM Lower Module in the Large Space Simulator at ESTEC (January 1999). The Telescope Sun Shield is deployed. The three Mirror Module doors and the Optical Monitor door are open

Due to the architecture of XMM, it was simple to simulate the thermal interface provided by the missing spacecraft module. Because of the low thermal conductance of the long thin-walled Telescope Tube entirely made of carbon-fibre composite, the two modules cannot exchange heat by conduction. The flux exchanged by radiation was simulated by controlling the temperature of a plate inside the test adapter. The two modules were mounted by means of the same test adapter on the LSS gimbal stand, which provided the possibility of changing the spacecraft's attitude with respect to the solar beam direction as required by the simulation of the various orbital phases.

Because of the stringent cleanliness requirements imposed by the optics of the telescope system, a pure nitrogen purge line was located inside the test adapter and used for directly venting the interior of the telescope tube during the re-pressurisation phases. The cryo-panels inside the facility were used to trap contaminants. The STM thermal-balance test also had to verify the effectiveness of the cleanliness measures and procedures adopted in providing the cleanliness level required for the thermal-vacuum testing of the PFM spacecraft, which was then performed with the same set-up, configuration and adapter.

The objective of the PFM thermal-vacuum tests was to verify that the fully integrated spacecraft performed correctly in all operational modes at the expected extreme temperatures induced by the orbital conditions. In addition, some thermal-balance test phases were inserted into the thermal-vacuum programme in order to verify the Thermal Control Subsystem performance after minor modifications had been introduced between the STM design and the final FM design. For cleanliness reasons (even though eventually the cleanliness levels achieved were very good and well within contamination budget), the tests were carried out with the STM Mirror Modules installed in the PFM spacecraft Lower Module, instead of the Flight Model Mirror Modules. In addition to revealing the need for minor trimming of radiators and minor repairs to defective heater lines, the thermal tests have been fully successful in verifying the thermal-control performance and the thermal predictions.

Structural testing

Static strength tests

Strength verification of the primary structure was achieved by statically loading each of the major constituents (SVM central cone, SVM upper and lower platforms, upper and lower Telescope Tube) separately at their own level by their respective manufacturers, i.e. before system-level structural testing. These tests were performed at qualification levels on the STM elements, and at acceptance levels on the PFM elements.

Vibration tests

One test objective was to validate the structural mathematical models used to predict the spacecraft's behaviour during test and in flight as calculated by the Launch vehicle Dynamic Coupled Analysis. Another test objective was to provide proof-of-strength for those parts that did not see a strength verification beforehand, namely: Focal Plane Platform, Service Module equipment panels and their interfaces to the equipment, Focal Plane Assembly secondary structure, Service Module shear walls, Service Module secondary structures such as thruster brackets and Telescope Sun Shield (TSS).

In each of the three orthogonal axes, each STM module was sine-vibration tested following the classical sequence: low-level, intermediate level to define notch profiles, qualification level followed by low-level again in order to check that modal characteristics had not been affected by the tests.

Shaker input levels for the STM Upper Module could not be taken directly from the Ariane-5 User's Manual because of the transfer characteristics of the Lower Module. A system-level response analysis was run to determine these transfer characteristics and the resulting inputs from the Lower Module into the Upper Module at the interface between the Lower Telescope Tube and the Upper Telescope Tube. These levels were used as inputs for the Upper Module testing.

For the STM Lower Module testing, the input levels to be found in the Ariane-5 User's Manual were taken. Despite the absence of the Upper Module, the Lower Module has many modes corresponding to the complete system dynamics, so that a system-level notch profile could be established. This notch profile was acceptable also to the launch authorities.

The testing of both STM modules has demonstrated that the desired response levels have been reached at the resonances as foreseen.

For PFM acceptance testing, the levels were determined by first dividing the levels actually achieved during qualification on the STM by a factor of 1.25. Manual and automatic notch levels were then corrected down in two narrow frequency bands to account for possible shaker control overshoot, thereby making sure sensitive flight hardware was not endangered. The levels were then checked against the results of the Launch Vehicle Dynamic Coupled Analysis and it was verified that acceptance levels showed positive margins throughout the frequency spectrum. This conservative approach both ensured safety of the flight hardware and conserved significant margins to the flight environment, at the time known only as measured values on the first two Ariane-5 flights. Later, the results of measurements aboard the third Ariane-5 flight confirmed the suitability of this approach.

The PFM Lower Module (with about 80% of the total mass, the heavier of the two) was sine-vibration tested with input only in the longitudinal direction (Fig. 4). This saved significant test time and cost. This approach was possible because the successful experience acquired during STM qualification had drawn attention to the fact that cross-coupling alone was sufficient to induce the responses that would have been sought in a test with lateral input. Also, correlations of STM test results with mathematical test predictions were very good and provided confidence in the modelling. The modifications from STM to PFM were few and minor, except for one change of location for one of the two batteries; even this change was not significant at spacecraft level and the panel affected was tested separately to validate the change locally.

The PFM Upper Module was sine-vibration tested only with input in the lateral (z-axis) direction. The rationale was similar to that applied for the Lower Module, with the difference that the results of the Launch vehicle Coupled Dynamic Analysis show less substantial margins in lateral accelerations than in axial. It was therefore decided to test in the more critical lateral direction.

Modal survey
The modal-survey testing was performed on the STM spacecraft by a team from DLR-Göttingen (D). It has shown that the overall lateral mode corresponds very well with computer predictions (11.7 Hz measured, against 11.8 Hz calculated) and has confirmed the recurrence, on the complete spacecraft, of local Service Module modes as found in the Lower Module test. The objective of identifying below 100 Hz all modes with effective mass above 5% of the total mass has been met. This test has been rounded off with a so-called 'boosted' run in which high lateral inputs were given to the Focal Plane Platform such that response levels reached flight levels times a qualification factor. This dwell test at 11.7 Hz demonstrated the load capacity of the fully built-up central core in both lateral directions, as well as the stability of the first lateral resonance under increased loading. This also confirmed qualification of the Lower-to-Upper Module bolted interface.

The excellent results obtained from the STM Modal Survey, together with the fact that the changes from STM to PFM were minor and with the availability of sine-vibration results for both the PFM Lower and Upper Modules, led to a decision not to perform such a modal survey on the PFM spacecraft. The workmanship of the Lower-to-Upper Module interface was checked by inspection (the bolted flange is of a simple design) and by the acoustic test performed on the complete spacecraft.

Figure 4. The XMM PFM Lower Module during axial sine-vibration testing on the ESTEC 280 kN shaker (December 1998)

Acoustic testing
Acoustic testing particularly involved the structures with low mass per surface area such as the Telescope Sun Shield, Service Module upper and lower platforms, Telescope Tube and Focal-Plane Assembly secondary structures.

For STM qualification, dummies represented the solar arrays. Flight solar panels were submitted to separate acoustic tests. The Telescope Sun Shield had gone through an acoustic verification at unit level.

Responses at the level of the Service Module units were recorded for comparison with the unit-level specifications.

The Ariane-5 specified launch environment (plus 4 dB qualification margin for the STM test) determines the qualification and acceptance test levels. Additional STM qualification runs were performed to solve facility control questions, to assess margins available and to take into consideration the acoustic environment measured on the first two Ariane-5 launches. The maxima measured in each octave on the two flights were taken as flight environment plus margins for uncertainty and for qualification. This approach was thus conservative, but realistic in view of flight experience. Compared to the Ariane-5 User's Manual, it led to an increase of several dBs in the low frequency bands, but also to a substantial decrease in the high-frequency bands, where the original User's Manual specification was unnecessarily constraining. The launch-vehicle authority also welcomed this approach, since it adequately covered all concerns about uncertainties above the User's Manual specification in the low frequency bands.

This STM spacecraft-level acoustic-test series was successful in demonstrating qualification of the structure and also in identifying those units for which more unit-level qualification data had to be acquired, which was subsequently done.

For PFM spacecraft acceptance, the acoustic test was performed on the complete PFM spacecraft, including FM solar arrays and Telescope Sun Shield, with the same realistic spectrum, but of course without the addition of the 4 dB qualification margin.

Adapter fit-check and clamp-band release

An Arianespace team performed this test, with the complete STM spacecraft clamped to its launch-vehicle adapter. After a fit-check with the adapter, it involved the pyrotechnic release of the 2624 mm-diameter clamp band. One objective was to prove correct fit to the adapter including accessories (e.g. clamp band, clamp-band extractors and catchers, umbilical connectors, purge ports, release springs, separation switches). Another objective was to demonstrate the feasibility of mating the Telescope Sun Shield to the spacecraft after clamp-band installation and to show proper clamp-band release without interference with any part of the spacecraft, including the Sun Shield. A third objective was to measure the shock levels induced by the clamp-band pyrotechnic release on both sides of the separation plane and further at selected equipment levels. Subsequently, a release of the Telescope Sun Shield was performed to verify proper functioning of its deployment mechanism, even after clamp-band release shock and under adverse thermal gradients. This series of STM qualification tests was completely successful and the results gave rise to no particular concerns.

Shock testing had been performed at unit level, on EQM of FM units as determined on a case-by-case basis, on all those units of the Lower Module for which susceptibility to shock could not be excluded simply by design. Upper Module units are located too far from the launch-vehicle interface to be of any concern.

For PFM spacecraft acceptance, another fit-check with the flight adapter was performed. A pyrotechnic clamp-band release on the PFM was not performed, since all of the useful information that it could provide had been successfully gathered during the STM test*.

Physical checks

Mass properties

The mass, the Centre of Gravity (CoG) and Moments of Inertia (MoI) of both the Lower and Upper Modules (separately) were measured on the STM spacecraft along all three axes. These measurements agreed very well with the predictions.

For PFM acceptance, the mass, CoG location in the horizontal plane and MoI around the longitudinal axis of both Lower and Upper Modules (separately) were measured. This was just to double-check that no gross error had slipped into the calculations and to correct the inevitable small errors due to, for example, test harnesses or minor equipment exchanges. This kept the test configuration simple. Values around the other two axes, while much more cumbersome and costly to measure, need not be known with high accuracy. The STM testing had sufficiently validated the prediction of their value.

Alignment and light-tightness

At regular intervals between STM satellite tests, checks have verified that the spacecraft was able to maintain full integrity, alignment and light tightness – which are crucial to the scientific mission – throughout the gruelling qualification environment (Fig. 5). Custom-designed equipment was built to meet the size, configuration and accuracy requirements of XMM, for both the alignment and the light-tightness measurements.

Between major environmental steps, alignment and light-tightness were checked on the PFM spacecraft in accordance with the procedures verified during STM qualification. Because of the excellent performance of the structure, the checks were somewhat less extensive than on the STM. The major alignment activity consisted of positioning the five scientific cameras located at the telescope focal plane, while taking into account the measured characteristics of the Mirror Modules and

* To account for uncertainties concerning the frequency spectrum and level of shocks imparted by Ariane-5 during the flight, a thorough complementary unit-level shock analysis and test programme was conducted on EQM units in parallel with the launch campaign, as a double-check.

Figure 5. The STM XMM spacecraft assembled on the alignment rotary table. The alignment stand is on the right

Reflection Grating Assemblies. This was done at the time of the mating of the two satellite modules to form the assembled spacecraft, with the actual flight-model Mirror Modules installed.

The accuracies required are only millimetric, but the large size of the spacecraft and the criticality of the positioning – and its stability – for the scientific mission make the time-consuming and delicate alignment activities critical for PFM acceptance. Light-tightness of the telescope is similarly critical, since even minute amounts of stray light would blind the exquisitely sensitive CCD detectors of the experiment cameras, which are able to count X-ray photons one by one and are not completely insensitive to visible light.

EMC testing

All units were fully EMC tested, radiative and conductive, for emissions and for susceptibility. XMM is not a particularly difficult satellite EMC-wise, as it does not carry very powerful sources. The results from unit-level tests had shown considerably wider margins than the required 6 dB between worst-case emissions and susceptibility. However, because of spacecraft size, just as for environmental testing, full-fledged EMC testing in an anechoic chamber would have been next to impossible for the complete satellite, at least if cleanliness requirements were to be observed. It would still have been very cumbersome even if performed on the two separate modules. Nevertheless, self-compatibility and compliance with the launch-vehicle radiative environment had to be demonstrated.

The active electronics are located on the Focal-Plane Assembly and Service Module. The Telescope Tube along which the harness is strapped holds the FPA and SVM about 7 m apart. In electromagnetic terms, the active electronics represent EMC sources, while the interconnecting harness acts like an antenna. Additionally, the parallel routing of different signal cabling could be susceptible to cross-talk. On the other hand, radiated coupling between the Focal-Plane Assembly and the Service Module is minimal.

On the EM satellite, the Lower and Upper Modules were connected by a harness. Conducted emissions and susceptibility were checked. Electrostatic discharges were tested, first conducted (which uncovered malfunctions on two units, later corrected) and then radiated. Radiated emissions and radiated susceptibility were then measured.

All of these tests, even the radiated ones, were performed in a clean room and not in an anechoic chamber. This was only possible because the environment had been measured and verified to be quiet and because the test was performed during the evenings, with little activity around. Despite the very low limit imposed by the launch-vehicle compatibility requirements in the critical 420–480 MHz band, the influence of ambient noise was demonstrated to be small enough to obtain clear and positive results. This is indeed true provided the measurements are performed in a sufficiently narrow bandwidth, i.e. 100 kHz as required by the Ariane-5 User's Manual. Compliance is also made easier by the fact that during launch few units are on, namely the batteries, main supply bus and regulation equipment and telecommand receivers. Susceptibility testing also took into account the relatively high field strength measured at the launch base and originating from various sources other than the launch vehicle itself.

For the PFM testing, the Electrical Model approach was reproduced and even simplified somewhat. For schedule and configurations reasons, it was impractical to perform the tests on the assembled satellite because it would have meant putting off the EMC tests until the end of the programme. For the purposes of acceptance, and in view of the good results obtained on the EM plus good knowledge of all equipment from unit-level tests, PFM tests were carried out separately on the two modules. In addition, to take into account the requirement to verify radiated emissions towards the launch vehicle, the PFM Lower Module radiated EMC test was carried out on the Lower Module equipped with the Telescope Tube harness and the two FPA units that will be powered during launch preparations. These are the FPA Remote Terminal Unit (RTU) for data handling, and the FPA Power Distribution Unit (PDU) for power. Similarity to the behaviour observed on the EM was confirmed for both modules. The measured radiated emissions comply with the launch-vehicle requirements. Performing the measurements in the usual clean room at quiet times again provided usable results at a comparatively low cost.

ESD testing would have been risky on the flight model; it could have caused inadvertent failures or reductions of lifetime. Therefore ESD testing was not performed on the PFM.

Mirror module testing

The core of the XMM X-ray focussing optics is made up of three highly nested Wolter-1 grazing-incidence X-ray telescopes. They provide a large photon collecting area: each 1420 cm^2 at 1.5 keV and 600 cm^2 at 8 keV. Their spatial resolution is better than 16 arcsec. To obtain such an area and resolution while still keeping the mass reasonable, it was necessary to develop the technology for manufacturing thin mirror shells, assembling them into telescopes, called Mirror Modules (Fig. 6) in this context, without loss of performance, testing them thoroughly, and assembling them into a spacecraft while keeping contamination low so as to avoid performance degradation.

It was soon realised that a large amount of Mirror Module testing had to be performed. The 'Panter' X-ray facility at the Max Planck Institute (MPE) in Neuried, Germany, was available to XMM. However, several aspects pleaded for the creation of a new test facility. In addition to the sheer amount of testing of the Mirror Modules that was needed, the Panter facility was to be used for testing the scientific cameras of XMM. The fact that the Mirror Modules tested at Panter had to be in the horizontal position was not insignificant for such thin mirror shells, so parasitic gravity effects could not be excluded. Most important

Figure 6. An XMM Mirror Module

Figure 7. The XMM PFM spacecraft assembled and attached to the container chassis before closure of the container lid

for the measurement of optical performance, a third of the mirror shell surface could not physically be properly illuminated because of the slight divergence of the X-ray beam. The XMM Project Office therefore decided in 1994 to complement the Panter facility by building a custom-designed, vertical facility equipped with an 800-mm EUV collimator and two thin X-ray beams, specially adapted to the dimensions of the XMM Mirror Modules. This facility, called 'Focal-X', is located at Centre Spatial de Liège (CSL), in Belgium.

Nine Mirror Modules have been tested at the Panter facility and at CSL since the completion of Focal-X in 1996: one Qualification, three Structural and Thermal, and five Flight models. Each Mirror Module underwent a sequence of optical tests (EUV full illumination image quality, X-ray local measurements of reflectivity and scattering). Specific tests in Focal-X investigated stray-light characteristics for sources close (up to 7 deg) to the field of view. To validate the stray-light modelling of the telescope, stray-light characteristics at higher angles were measured on two Mirror Modules (one of them equipped with its Reflection Grating Assembly) in a custom-built test set-up at a Daimler-Benz Aerospace facility in Ottobrunn, Germany. At CSL, the sequence continued with sine and random vibration tests on the CSL shaker, thermal-vacuum tests in another CSL vacuum chamber, and final optical tests according to a sequence similar to the first one. For the STM Mirror Modules, the optical tests were of course omitted, but the environmental tests cleared them for further use in the spacecraft-level test programme as described above. They also trained staff, procedures and equipment in advance of the delicate testing of the Flight Models. After the second Flight Model, the test sequence was optimised to take advantage of the learning curve achieved. The optical checks in-between vibration and thermal tests were omitted, some image quality checks were speeded up, the number of time-consuming X-ray reflectivity check points was decreased, and the number of thermal cycles was reduced from 6 to 3. On the other hand, extra test sequences were added to verify the behaviour and performance of the Mirror Modules equipped with their X-ray baffles and, for two of them, with their Reflection Grating Assembly. All Mirror Modules passed the tests and demonstrated consistently better-than-specified performance. The testing also provided the mass properties and alignment values (focal length, orientation of optical axis) needed for the PFM spacecraft alignment activities. Since XMM carries three Mirror Modules, two FM Mirror Modules are full-performance flight spares.

Onwards to launch

The spacecraft launch-preparation campaign is a continuation of the integration and test activities. In this respect, operations such as the assembly of appendages, battery charging,

Figure 8. XMM in flight configuration (artist's impression)

virtually all electrical checkout, alignment stability check, light-tightness check, and camera door checks have been performed just as they were performed during PFM acceptance. The complete end-to-end telecommand and telemetry chain from the Control Centre at ESOC to the spacecraft has been exercised during a System Validation Test, similar to those performed when the spacecraft was still at ESTEC. However, a number of operations have novel aspects:

- The complete spacecraft was transported in one piece (Lower and Upper Module assembled; Fig. 7) to the launch site in one very large container, whereas all previous transportations were in three parts, each in their own container. The spacecraft and its ancillary equipment were transported by sea on a ship that also carried Ariane launch-vehicle stages, parts and equipment from Europe to French Guiana.
- The Reaction Control System tanks are for the first time fuelled with real hydrazine, rather than the water that was used once on the STM spacecraft and twice on the PFM spacecraft to fill the tanks before the vibration and acoustic tests.
- The second flight battery has been installed (one was already installed in the spacecraft before shipment).
- The Telescope Sun Shield has been installed on the spacecraft *after* mating of the spacecraft to the launch vehicle, to allow access to the adapter and clamp band.

The eleven-week launch-preparation campaign is scheduled to lead to the spacecraft's launch in December 1999 and commissioning in early 2000 (Fig. 8).

Conclusion

Large spacecraft such as XMM stretch or surpass the capabilities of existing environmental test facilities in Europe. The XMM test programme has combined testing on the complete spacecraft wherever possible with modular testing where unavoidable. It has made optimal use of existing test facilities for both environmental and electrical testing. While full-illumination, collimated, end-to-end optical tests on the complete satellite at X-ray energies in representative flight conditions was not possible, a combination of optical and alignment tests at Mirror Module level, scientific-camera level and spacecraft level has come as close as possible to an end-to-end verification. This has permitted satisfactory qualification and acceptance and has been possible thanks to the favourable split into modules taken into account from the beginning of the XMM design process.

Acknowledgements

The author would like to thank the staff of the ESTEC Test Centre, the staff of Centre Spatial de Liège, and the XMM Prime Contractor Daimler Benz Aerospace/Dornier, whose work formed the basis for some of the material of this article. The author also gratefully acknowledges the considerable contributions from the other members of the ESA XMM Project Team.

Product Assurance on the XMM Project

J.P. van Dooren
XMM Project, ESA Directorate for Scientific Programmes,
ESTEC, Noordwijk, The Netherlands

Product Assurance has both a preventative and a corrective role in terms of quality control in a spacecraft project. This article summarises how it was approached within the XMM project, what unforeseen problems were encountered, and what lessons can be learned from our experience.

Product Assurance Management

The main elements of Product Assurance (PA) management are manpower, requirements, information flow, configuration control, risk and reviews.

In the case of XMM, ESA project manpower for PA was limited to 1 PA manager and 1 PA engineer. The Prime Contractor provided 1 PA manager and 5 PA engineers and technicians. Each of the subcontractors has at least 1 PA staff member assigned to the project, and each experimenter has at least 1 PA engineer on their team. Functional support has been provided by ESTEC.

The XMM PA requirements are based on the ESA PSS-01 series of Product Assurance and Safety Standards, tailored to XMM needs. They are applicable to the entire spacecraft, with the exception of X-ray mandrel and mirror production and the instruments (OM, RGS, EPIC and RAD). For the mirror production at Medialario (I), ISO-9000 certification was obtained. The facility was built practically from scratch and several Quality Assurance (QA) and other procedures needed to be written.

Dornier, the Prime Contractor for the XMM spacecraft, expanded the ESA PA requirements into their own 'PA Requirements for Subcontractors', which specify the details of XMM PA management for their subcontractors. ESOC organised a new QA structure, following the ISO-9000 standard, and obtained ISO certification. PSS-05-0 is applicable to software.

XMM documents and correspondence have nearly all been generated, stored, transmitted and received electronically. Minutes of meetings are still mostly written by hand. Besides local PC storage, central storage is provided in the form of a Document Management System (DMS) that is accessible via the ESA Intranet. The DMS stores and provides access to faxes, E-mail, reports, technical notes, drawings, etc. Many documents are still faxed, but the E-mail portion is growing. The possibility to attach just about any word-processed text, database file, Non-Conformance Report (NCR) form, scanned photograph or graph, scanned hand-written minutes, etc. to an E-mail message, and the expedient transmission make this technique far superior to faxing. Large documents are sent under the Internet FTP protocol. DMS documents can be searched with keywords. Some discipline is therefore needed from the authors in formulating the title and the abstract. XMM still keeps a paper file, both at ESTEC and at the Prime Contractor, as a backup. Many documents (XMM User Manual, system NCRs) are copied and distributed on CD-ROM.

Some lessons can be learned from the XMM information-handling experience. The use of electronic mail (E-mail, FTP) should be maximised and fax and paper mail must be minimised. Hand-written minutes of Materials Review Board (MRB) meetings should be replaced by electronic text using portable PCs. Teleconferences and video-conferencing (over the Web) should be encouraged. Sub-contractors must be requested to provide their NCRs directly in electronic format. Hand-written notes and drawings must be scanned and electronically linked to the NCR database. Digital photography and videotaping should be encouraged for Mandatory/Key Inspection Point (MIP/KIP) or configuration inspections. All review documents should be on CD-ROM and on the Project Internet web site, with the necessary access limitations, encryption and password protection.

The PSS-01-11 requirements are applicable to Configuration Management (CM). In general,

Figure 1. The Reaction Control System fault tree (loss of human life)

Loss of Life
caused by

- **or — explosion in contained pressurized environment**
  caused by
  - **or — contamination**
  - **or — hot spot**
  - **or — overheating due to jammed closed valve**
  - **or — material incompatibility**
  - **or — other causes**
- **or — fire in non-contained ambient environment**
  caused by
  - **or — erroneous, un-coordinated thruster operation**
    caused by
    - **or — procedural error**
    - **or — other causes**
  - **or — loss of containment — ---AND--- ---------- ignition**
    - **loss of containment caused by**
      - **or — rupture**
        caused by
        - **or — collision**
        - **or — pressure peak**
          caused by
          - **or — wrong temperature**
          - **or — wrong loading**
            caused by
            - **or — procedural error**
            - **or — GSE pressure regulator failure**
            - **or — human error**
            - **or — other causes**
          - **or — other causes**
        - **or — other causes**
      - **or — leak**
        caused by
        - **or — spacecraft (see RCSFTR0.WK4)**
        - **or — GSE**
        - **or — other causes**
      - **or — spillage**
        caused by
        - **or — human errror**
        - **or — wrong procedure**
        - **or — other causes**
      - **or — other causes**
    - **ignition caused by**
      - **or — static discharge**
      - **or — electric switch spark**
      - **or — lightning induced current**
      - **or — other causes**
  - **or — other causes**
- **or — poisoning**
  caused by
  - **or — loss of containment (see above)**
  - **or — contaminated wastes in supply and waste containers**
  - **or — other causes**
- **or — other causes**

CM worked quite well on XMM, although some problems were encountered with software CM, because the many software designers used their own design tools and the interfaces and design methods were insufficiently standardised.

Some lessons can be learnt from our experiences here too. Configuration inspections should be included during MIP and Delivery Review Boards. Standards for software CM should be imposed on all software sub-contractors, including operations and experiments. Interface standards must be defined early in the design phase, and software transferability should be carefully tested. Standards for satellite databases must be imposed on all contributors, including the experimenters.

Formal risk management was not an XMM requirement, but an XMM Safety Review was held that achieved roughly the same result. This review used Fault-Tree Analysis (FTA), starting from an overall 'loss of mission', down to the general system functions. Every function was further divided into subfunctions, and into causes that could lead to a subsystem failure which could lead in turn to the loss of the mission. The Reaction Control System fault tree is shown as an example (Fig. 1).

FTA uses a 'top-down' approach, whereas Failure Mode Effects and Criticality Analysis (FMECA) follows a 'bottom-up' method. In this sense, FTA provides a clearer relationship between cause and effect. It encompasses not only hardware effects, but also software, processes, procedures, and everything that could cause a failure when done incorrectly. The XMM project used FTA extensively to analyse the causes of important non-conformances.

XMM had to deal with a number of non-conformances, as chronicled in Figure 2. Minor NCRs were handled at local level, while major ones involved the Prime Contractor, with the ESA PA and specialised project engineers maintaining an overview and taking action whenever necessary. This delegation of quality handling has resulted in very efficient and fast NCR processing. All NCRs that are still open, relating mainly to operations software and database issues, will probably be closed before the Flight Acceptance Review. Waivers have been handled by a Configuration Control Board (CCB), both at the Prime Contractor and at ESA. This approach has prevented 'creeping design changes'.

The flow of NCR data could have been improved by requesting subcontractors to write their NCRs directly in database format and E-mail them (within the required 24 hours) to the Prime Contractor and to ESA. ESOC opted for consequent database processing of NCRs and their system is working excellently.

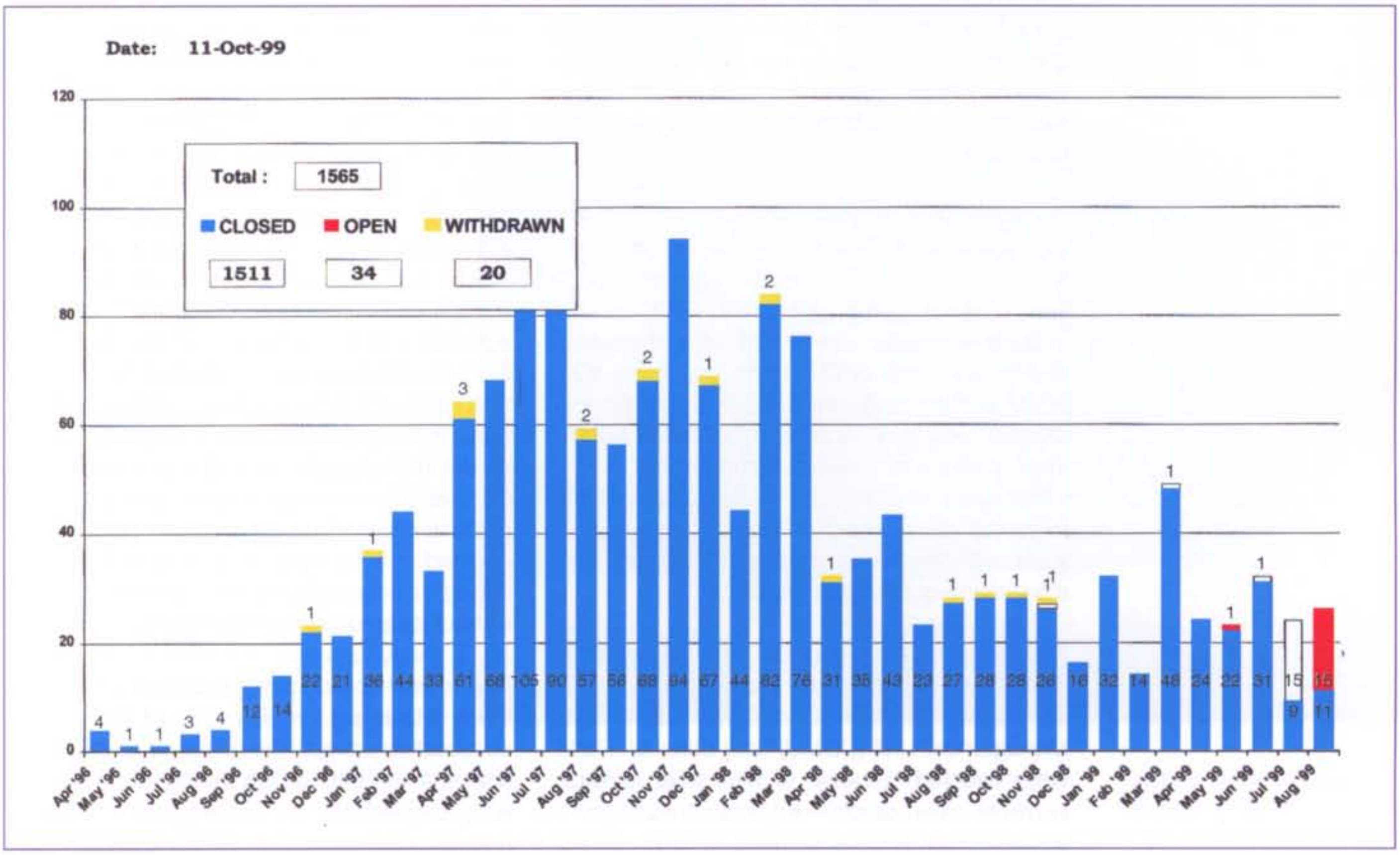

Figure 2. History of major XMM non-conformances

EEE Parts Procurement
As is customary at ESA, PA runs the procurement of electronic, electrical and electro-mechanical (EEE) parts. The reason for this is that testing and quality control is the most important aspect of parts procurement. IGG of Fareham (UK) was selected as the Co-ordinated Parts Procurement Agent for both the XMM and Integral spacecraft in early 1995. They collected the parts' orders from all users, combined them, proposed alternate choices to reduce the number of types, ordered the parts from the manufacturers, performed inspections and functional and parametric tests, and dispatched the parts, with the appropriate number of spares, to the users. Parts known to be radiation-hard above 100 krad were not total-dose-tested again, those between 20 and 100 krad were radiation tested (three pieces per lot), and parts that did not withstand a total dose of 20 krad could not be used. A few waivers were accepted for parts violating this requirement, but which are sufficiently shielded to achieve a low total dose.

Decisions were made during a monthly Parts Co-ordination Board (PCB) meeting at IGG. Most parts were bought against SCC specifications, some against MIL-STD class S, and some against JANTX that were upgraded. The total volume of EEE parts bought by IGG (XMM and Integral) was about 730 000 pieces, divided over 2686 'line items' (different parts). Their quality was controlled through 592 NCRs, which were all closed. 21 NCRs resulted in lot rejection. The main problems encountered were radiation sensitivity, logic IC delivery, and the general quality of some parts.

A major problem occurred with ASICs (VCA and VCM SOS) from one manufacturer, which are used in the Command and Data Management Unit (CDMU) data channel. Parts were rejected because of excessive leakage currents. We discovered that these parts accumulated an electrostatic charge during burn-in, because of some floating pins due to bad contacts. The charges could be removed by a bake-out, which removed the leakage currents. The lot was eventually accepted and the parts caused no further problems.

Materials and Processes Engineering
The XMM Project has pioneered the use of several materials and processes for novel applications. Because of their criticality, they were subjected to rigorous qualification tests.

For the telescope tube, cyanate ester prepreg. mats have been used instead of the better-known epoxy mats. The cyanate CFRP has better mechanical properties and much lower outgassing than epoxy. In order to achieve the specified cleanliness requirements inside the tube, an aluminium vapour barrier was necessary to prevent outgassing towards the inside. The internal surface had to be black for stray-light suppression, and smooth to minimise the effective surface to which contamination molecules could adhere. Both requirements were satisfied with the selection of black Kapton as the innermost layer. It has similar optical absorption characteristics to rough black paint, such as Electrodag 501, but it is very smooth and shiny, which is actually an advantage for stray-light suppression.

A ray of stray light is reflected from the Kapton surface in a specular pattern, whereas from the black paint it reflects in a spherical pattern. This means that for the black Kapton, the telescope tube is only filled with stray light after several reflections, and from the paint in only one. Since at every reflection about 95% of the stray light is absorbed, the suppression is more effective for black Kapton than for black paint, despite or rather thanks to its shiny appearance. It is also slightly conductive. From a cleanliness point of view, the Kapton also proved to be vastly superior to any other inner lining. One important problem was the adherence to the aluminium vapour barrier foil. Several adhesives were evaluated for adhesive strength and low outgassing. Problems with air bubbles occurred during structural and thermal model manufacture. A large air bubble was discovered in the flight-model tube just before the final integration of both tube halves. It was decided not to repair it, but to deflate it by drilling three small holes into it from the outside, without puncturing the inner liners.

The mirror production processes revealed many interesting problems, all of which were successfully solved. The mirror mandrels at one time suffered from a high density of pores. This was caused by an inadequate choice of material (cast aluminium versus forged), which was sensitive to micro-corrosion. This caused tiny pits on the surface on which nickel was deposited. From these pits, pores started to grow around hydrogen bubbles that were not readily removed by the electrolyte flow. A change of material eliminated this problem. Initially, a great deal of effort went into the process of mirror separation from the mandrel. Many small improvements eventually resulted in a mirror shell and module quality well within specification.

An unexpected group of materials and process problems showed up with adhesives. The cells on the spacecraft's solar panels are protected against ultraviolet light and micrometeorites by cover glasses. These are covered with a conductive layer of Indium Tin Oxide (ITO), to prevent electrostatic charging. The ITO is electrically connected with the neighbouring cells' ITO with a dot of conductive RTV silicone rubber. To prevent a short-circuit to the solar cell, a layer of non-conductive RTV is applied first. It turned out to be very difficult to get a low resistance from the ITO layers to ground. Eventually, we settled for a resistance of better than 2 MOhm, which was shown to be more than adequate to remove any charges induced by radiation-belt electrons or protons.

A similar problem occurred with the Optical Solar Reflectors (OSRs), small mirrors that are glued to a Sun-facing surface to keep it cool. They are also covered with a thin layer of conductive ITO to prevent electrostatic charging, on the top and on the sides. The electrical contact with the spacecraft structure, which is the 'ground', is made via conductive RTV at the metallised back, which is connected to the ITO layer at the top through the sides. The main difficulty is making the RTV sufficiently conductive, by adding silver powder. In our case, it did not work. A solution needed to be found by grounding the ITO from the top. Several conductive adhesives were applied on test samples, thermally cycled and tested. The best results were obtained with Electrodag 501, applied at the OSR edges, because it was discovered that the ITO did not extend into the mirror corners.

Another adhesive problem occurred with heaters inside the p-n camera, which see severe thermal cycling. The solution was to mechanically clamp the heater strips to the structure, and not to rely on adhesive strength at all. Yet another adhesive problem showed up with the Delrin stand-offs used to keep the Multi-Layer Insulation (MLI) thermal blankets at a few centimetres distance from the tube, to minimise damage from possible micro-meteoroid impacts. Many stand-offs separated from the tube at the acrylic glue-to-Delrin interface. They were perforated and an epoxy glue was applied that protruded through the holes in the feet, creating a kind of rivet effect. This improvement successfully passed thermal-vacuum and acoustic testing.

An important lesson to be learned from our experience with adhesive problems is that thorough training, and possibly certification, is needed for technicians working with adhesives, to the same degree as with hand-soldering and other vital skills. This is a task for the specialist ESTEC laboratories.

A serious problem occurred during electrical testing (SVT-1): the CDMU showed bootstrap oading errors in some parts of the memory, on both redundant units. Suspect memory chips were removed and tested at ESTEC, but proved fault-free. The most likely cause was one or more open circuits in the multi-layer printed-circuit boards (PCBs). These were sent to ESTEC's laboratories for cross-sectioning. Two open-circuited 'vias' (plated-through holes) were discovered, which explained the failures (Fig. 3). More than fifty vias were cross-sectioned at ESTEC and at the PCB manufacturer, without discovering any further opens. The root cause of the problem was traced back to the manufacturing process. During the cleaning of PCBs with very fine vias, the procedure called for a powerful vibrator to be switched on, in order to remove any air bubbles from the holes. This had been forgotten for the XMM and Integral flight boards, which were in the same lot. For the spare-board lot, the vibrator had been switched on. These boards were thermally cycled to simulate the reflow soldering process, and thoroughly visually inspected, and they were fine. The boards were completely assembled, environmentally tested, and passed without problem. They have been used since then and passed acoustic testing without a glitch.

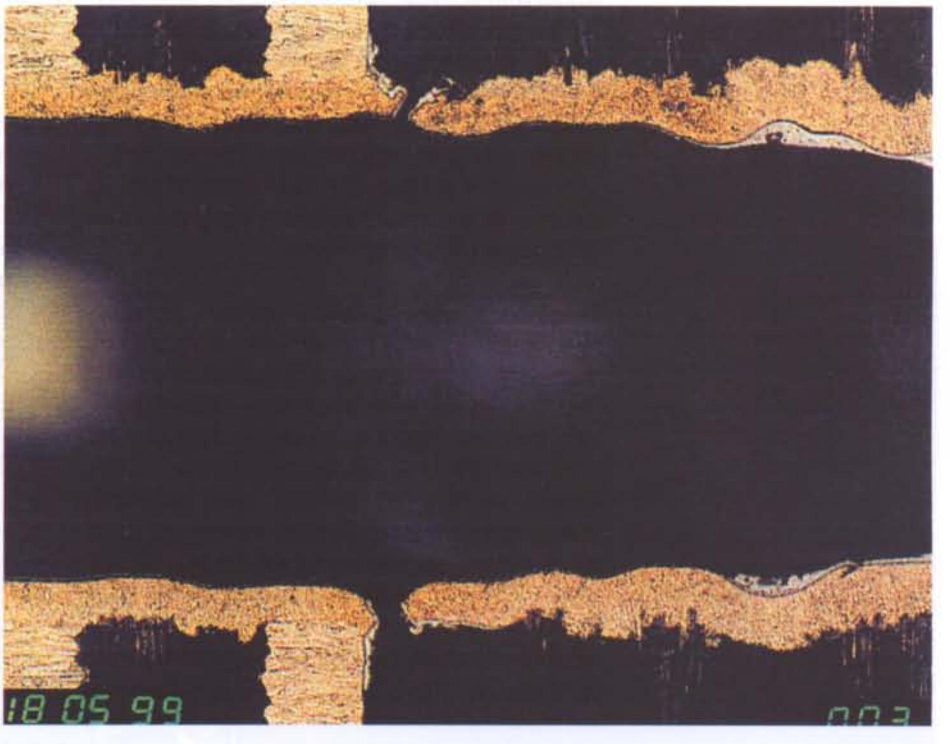

Figure 3. Detail of a via (plated-through) hole from a failed area, showing the gap in the barrel copper

During X-ray testing of the propellant tanks, a handling error caused deformation of a titanium tube. Since it happened very close to the tank inlet fixture, it was impossible to weld. The manufacturer proposed to use a 'Cryofit' memory metal shrink sleeve, which is used extensively on fighter aircraft, where it is subjected to high stress, and on some NASA spacecraft. We decided to perform a series of evaluation tests on it, namely vibration, thermal-cycling, and static-bending and torsion-load testing until failure. The devices turned out to be very robust and it was very difficult to cause a leak under high mechanical stress. We declared it qualified for the repair. ESTEC is currently engaged in a qualification programme for this repair technique's general use.

Cleanliness

The cleanliness requirements for XMM are very strict, with a maximum of 200 ppm at end-of-life for particulate contamination, and 2×10^{-7} g/cm^2 for molecular contamination. These requirements apply inside the telescope tube, which is a Class-100 environment, to the mirrors and to the experiments. The rest of the spacecraft is a Class-100 000 environment, at the level of a normal Assembly, Integration and Verification (AIV) Clean Room.

In the design phase, these stringent requirements were taken into account by making the mirror modules, the telescope tube, and the experiments separately closed units, with their own doors and purging devices. The tube and mirror modules had to be always closed, except for relatively brief moments during optical testing. Special mirrors are used for alignment, so that the mirror module did not need to be opened for this purpose. The mirror modules, telescope tube and optical monitor were continuously purged with pure nitrogen or synthetic air. The EPIC MOS and p-n cameras were evacuated, whilst the RGS cameras were pressurised with nitrogen.

The telescope tube is sealed from CFRP outgassing towards the inside by a continuous aluminium foil, acting as a vapour barrier. For stray-light suppression, the inner surface needs to be black. It also needs to be super-clean. Both requirements were satisfied by choosing a black kapton foil, 25 micron thick, as the innermost layer, glued to the aluminium foil with low-outgassing adhesive. The kapton foil could be cleaned, but this was never necessary thanks to the above-mentioned contamination prevention measures.

Overall cleanliness conditions were kept under control through a detailed measurement programme. AIV room particulate cleanliness was continuously measured with fixed particle counters. The ESTEC and Dornier Clean Rooms have an elaborate air-conditioning system with electrostatic and high-efficiency particulate air filters. A mobile counter was set up next to the satellite. Particle fall-out mirrors (PFOs) were installed before each important test phase and evaluated for particle count. Molecular witness plates were also regularly used.

Tape lifts were taken from inside the telescope tube and sometimes on the outside. Wipe tests were performed on the inside of the tube to measure molecular contamination. For both the structural and thermal model and for the flight model, the measurement results were always well within specification, proving that our contamination prevention programme worked. After thermal-vacuum testing in the Large Space Simulator (LSS) at ESTEC, tape-lifts measured 50 ppm average inside the tube. Wipe tests measured $<0.1 \times 10^{-7}$ g/cm^2.

The most serious cleanliness problem occurred with the EPIC p-n camera's flight model. Noisy signals were read from part of the 4-inch wafer CCD, which is not passivated. At first, it was believed that a coronal discharge due to ice formation was responsible, caused by insufficient vacuum during cooling down. We used the fault-tree technique to identify all possible (imaginable) causes of failure, and possible contamination was listed a number of times. The ESTEC quality-control laboratories tried to provoke such a discharge by cooling test CCDs down in weak vacuum conditions, but that proved to be impossible. Tape lifts had been taken from the flight-spare camera, and a large number of metallic and non-metallic particles were identified with a Scanning Electron Microscope (SEM) (Fig. 4). The failure symptoms were very closely reproduced by randomly shedding metallic particles of different sizes and shapes over the (uncoated) rear side of the CCD.

The lessons learned regarding cleanliness, mainly during the structural and thermal model campaign, can be summarised as follows:
- Keep all sensitive surfaces closed and enclosed volumes purged as long as possible.
- Use all existing techniques for measuring particulate and molecular contamination extensively throughout the programme, and take immediate action if cleanliness deteriorates.
- Test contamination-control procedures during the structural and thermal model programme.
- Perform regular cleanliness inspections involving the materials laboratory.
- Coat or passivate vulnerable surfaces.

Quartz crystal monitors had been installed on the mirror modules to measure molecular contamination, but they turned out to be unreliable.

Radiation

Like every space project, XMM has an extensive radiation-control programme. The space radiation environment was estimated by ESTEC experts, and summarised as a total dose curve versus shielding thickness. Dornier (D) performed a sector analysis, in which the expected total dose was estimated for every electronic unit, assuming a certain amount of shielding from the spacecraft. Every unit designer did his own sector analysis, taking the spacecraft's and his own unit's shielding into account. He provided a list in which the total dose seen during the satellite's ten-year orbital lifetime by every electronic part was listed.

The Central Parts Procurement Agent (IGG) conducted total dose testing, with the standard cobalt-60 test, on those parts that were known to be sensitive to less than 100 krad. Parts sensitive to less than 20 krad were, in principle, rejected. Late in the project, a controversy emerged regarding the radiation hardness of 3C91 opto-couplers. Several laboratories had irradiated these parts with protons, and this showed that they were degrading much faster than with the standard cobalt-60 test. We started a thorough analysis effort on all circuits where this device was used. Monte-Carlo simulation was used to assess what the real failure rate would be, using the actual measured Current Transfer Ratios (CTRs) for the procured parts, as measured by IGG, the actual shielding thickness for the unit, realistic assumptions for the other parameters, and a statistic of the CTRs after proton irradiation versus shielding thickness. The results indicate that in some worst cases on some circuits there may be a problem after several years in orbit. We decided that the risk was small enough to leave the circuits as they were, and to fly them as is. In the critical circuits (FDCE, ACC, PDU) a very large amount of de-rating had been applied, reducing the failure risk almost to zero.

Figure 4. SEM images of a contaminant particle in XMM's p-n camera

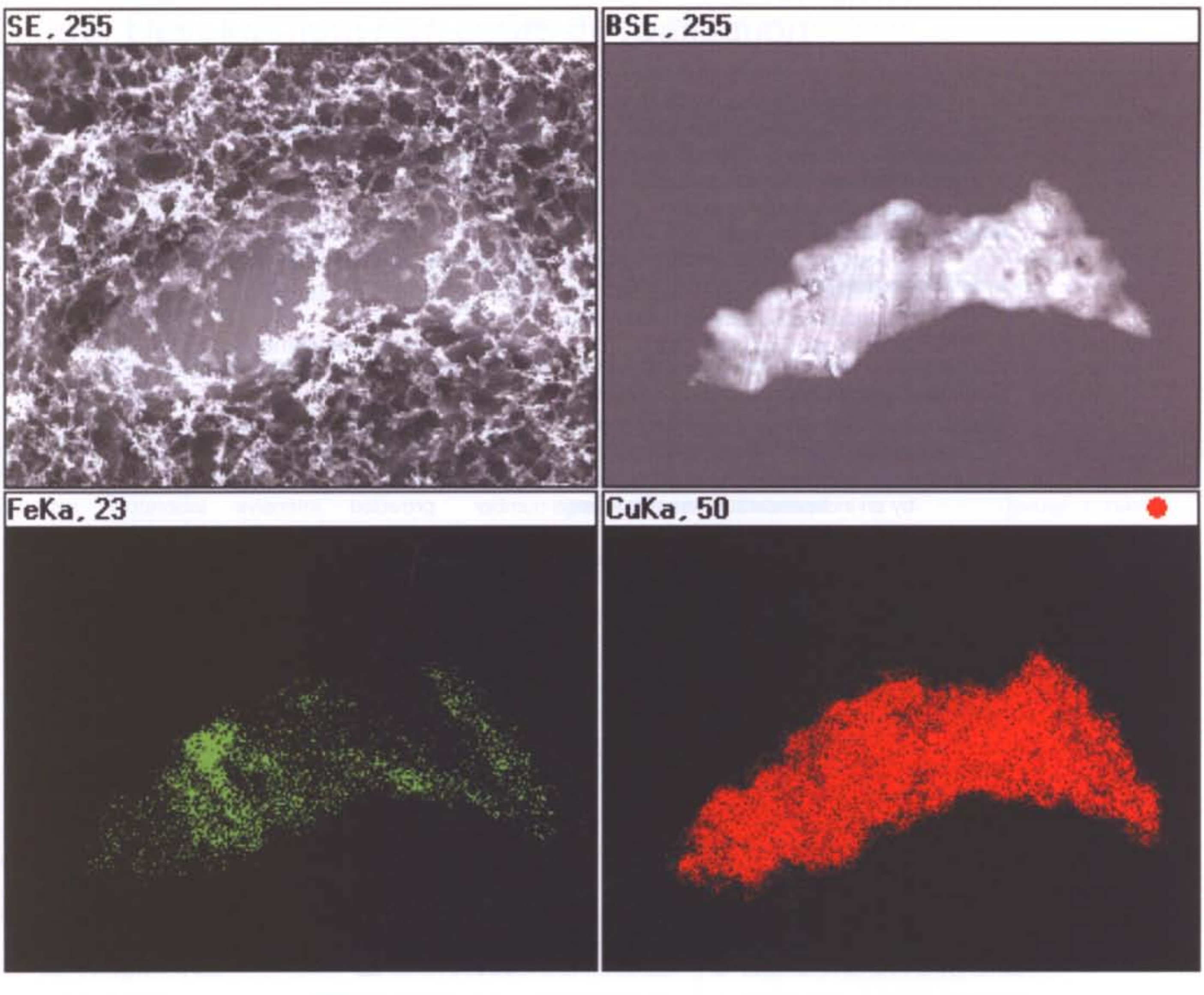

Much effort has been spent to evaluate the sensitivity to Single Event Upsets (SEUs) of a number of XMM's components. The driving factor behind this effort was the temporary loss of the SOHO spacecraft in 1998. A number of phenomena had been recorded before contact was lost that could be explained by SEUs in several circuits. We had already carried out a number of SEU tests on parts used in the (non-redundant) FDCE unit. Test circuits were built and the tests themselves were carried out by Hirex at the University of Louvain-la-Neuve (B) on their synchrotron facility.

The devices under test are irradiated with diverse species of ions, corresponding to energy levels of 1 to more than 100 MeV. The electrical transients in the circuit are counted and recorded. By repeating the test at several energy levels, an upset rate against energy curve is obtained. From this graph, a threshold energy is derived at which the part starts to get upset, and a 'cross-section', which is a measure of the upset rate at threshold. A mathematical convolution of this graph with the distribution function of heavy-ion particles in orbit versus their energies yields the expected upset rate for the tested part in orbit.

Several parts turned out to be quite sensitive. If they were in a critical circuit, performing a critical function, we decided to modify the circuit to make it more immune to SEUs. This can be readily done by slowing the circuit down with RC low-pass filters. The XMM team has in fact done some pioneering work in the field of SEU immune design, which now needs to be expanded into a standard procedure and made available to all projects.

Software

The XMM software requirements are according to ESA PSS-05-0 and ESA PSS-01-21, tailored to project needs. Flight software was validated by an independent contractor. A large number of Non-Conformance Reports were written on Electrical Ground-Support Equipmant (EGSE) software. Problems were encountered due to weak configuration control, and too little standardisation of development tools.

RAMS

Reliability block diagrams and FMECAs were made at system level and at unit level, and also for the complete Attitude and Orbit Control Subsystem (AOCS). A reliability budget was not required for XMM. Reliability analysis is most useful in the initial design phase (Phase-A) of a project, when the overall architecture and concepts are defined. If it is done later, it becomes too much of an academic exercise. Fault-tree analysis was used extensively throughout the project, both for failure analysis and design reviews. Safety is limited to compliance with launch-safety (CSG) requirements.

Ground operations

ESOC started a programme in 1998 to gain ISO-9000 certification for the Centre, which is about to be finalised. The XMM project has benefitted from this effort, by co-operating to set up a non-conformance management procedure, which is working very well. Doubtless, XMM will also benefit from this quality awareness during its operation in orbit.

Conclusions

Product Assurance has proved to be a vital discipline for the XMM project. Important progress was made in materials engineering, especially regarding telescope tube and mirror materials.

EEE parts procurement was well within schedule and cost, and is a guarantee of quality. Hundreds of parts' problems were solved accurately and expediently. The XMM safety review, using top-down Fault-Tree Analysis, was a novel approach to design assurance. Cleanliness control was rigorously enforced, with outstanding results. ESA PA assistance to Experimenters was greatly appreciated, although somewhat late. Important efforts were made in Single-Event Upset analysis and prevention. The ESOC ISO-9000 certification process was very helpful in improving quality assurance for the ground operations for XMM.

Acknowledgements

The XMM Product Assurance effort was mainly carried out by the Dornier PA team, headed by U. Gageur, whose work is greatly appreciated. P. Glaude did the PA on the mirror modules and experiments. The ESTEC QM and QC divisions provided intensive laboratory support, specifically T. de Rooij, D. Adams, D. Collins, M. van Eesbeek, J. Guyt. J. Minnee supported the EEE parts procurement effort with total dedication. R. Harboe-Soerensen of ESTEC and W. Keil of Dornier were responsible for the SEU and radiation analyses. H. Hartmann of Dornier did the contamination control planning and most of the analysis. R. Stritter of Dornier was responsible for contamination measurement and control. It is not possible to mention here all of the PA staff who have contributed to XMM, but all of their efforts are very much appreciated.

Programmes under Development and Operations
Programmes en cours de réalisation et d'exploitation

(status end September 1999)

In Orbit / En orbite

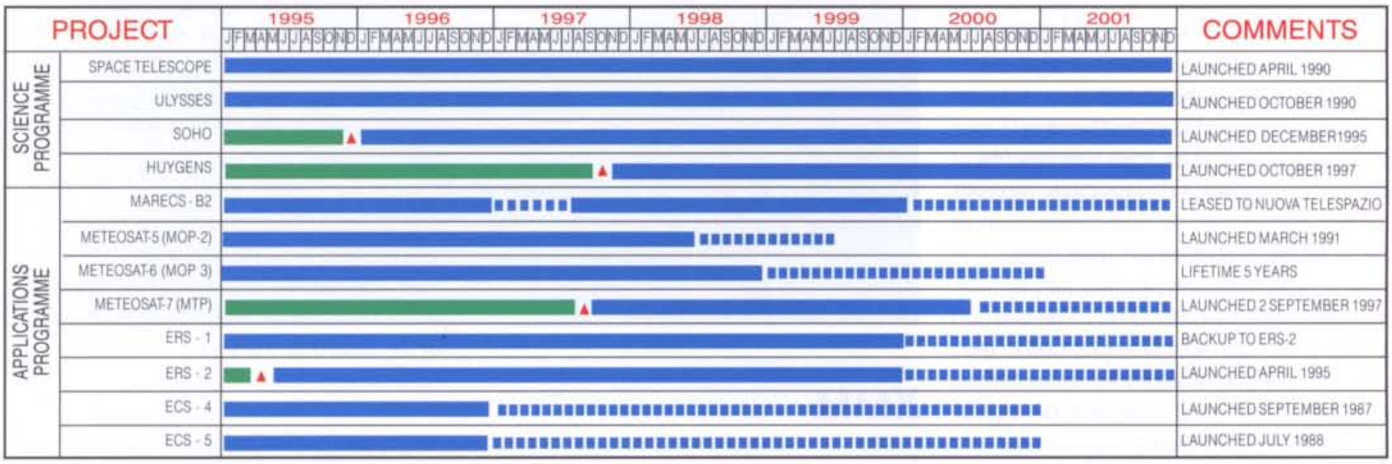

Under Development / En cours de réalisation

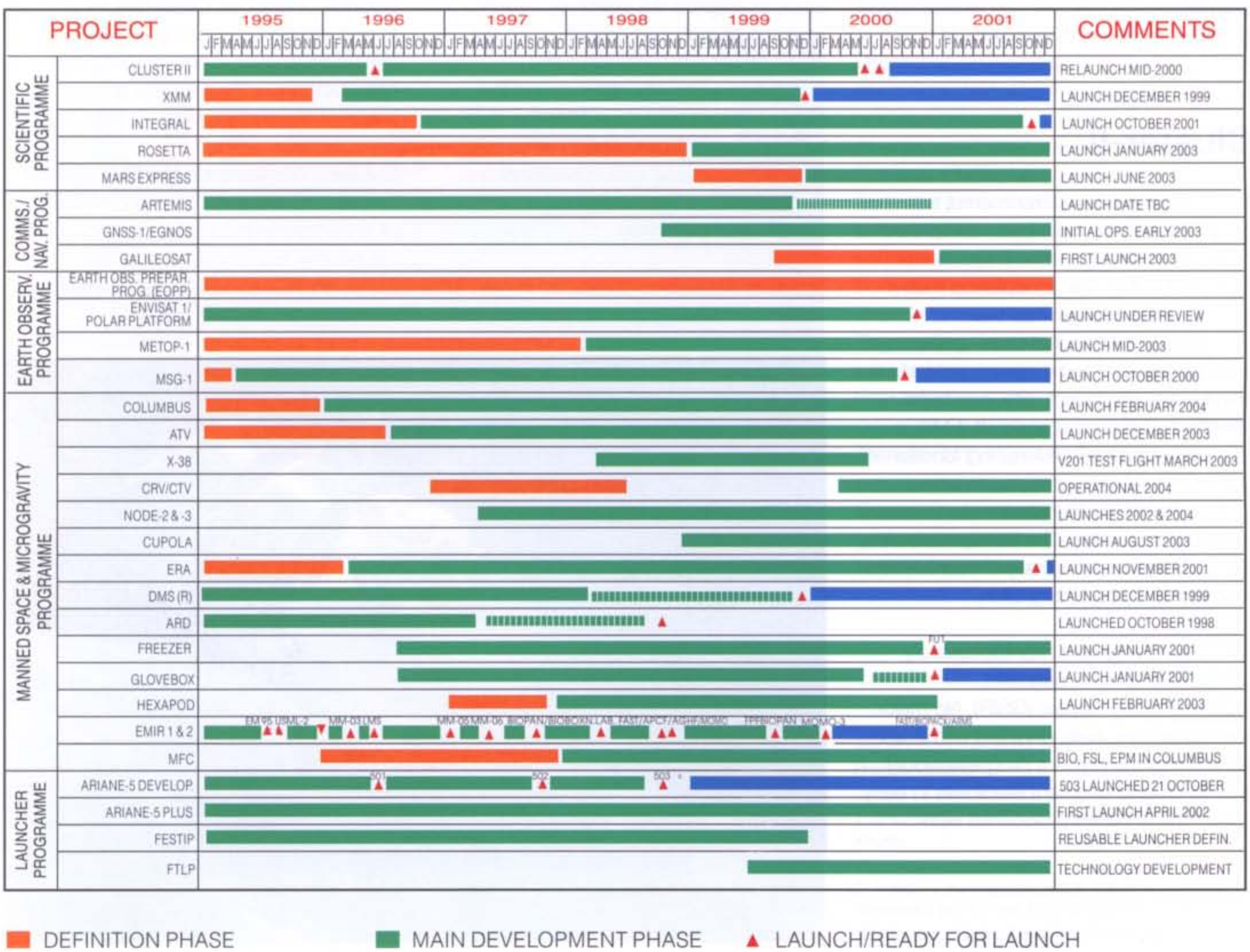

DEFINITION PHASE — MAIN DEVELOPMENT PHASE — ▲ LAUNCH/READY FOR LAUNCH

OPERATIONS — ADDITIONAL LIFE POSSIBLE — ▼ RETRIEVAL — STORAGE

ISO

A major milestone was reached on 7 August when the last of the ISO data entered the public domain. All ISO data are now available to the worldwide astronomical community via the ISO Data Archive, located at <www.iso.vilspa.esa.es>. This archive contains nearly 30 000 scientific observations of all classes of astronomical objects, ranging from the Solar System to very distant extragalactic sources, plus another 70 000 data sets including calibration and engineering observations, and data from instruments operated in parallel and serendipity modes.

The scientific community is using this archive very intensively; in July, for example, more than 8000 observations (a third of the scientific observations in the archive) were downloaded. An incremental development of the archive and its facilities is being followed, with a major release for calibration users having successfully been made in July. Results from ISO data continue to feature prominently in the scientific literature. Examples of ISO results can also be found on the Web via the above URL.

Cluster-II

The functional and environmental test programmes have now been completed on the first two flight-model spacecraft (FM6 and FM7). The acceptance review for the first spacecraft has been successfully held and all open work, which is required to be completed before shipment to the launch site, has been identified. The third spacecraft (FM8) is fully integrated and undergoing functional testing before being shipped in late October to IABG, Munich for its environment testing. The last spacecraft (FM5), which was originally 'Phoenix', has started its payload integration.

The ground segment has successfully passed the Ground Segment Implementation Review (GSIR). No major show-stoppers were identified and it was agreed that the present progress would lead to ground-segment readiness in early 2000. The activities associated with moving the 15 m antenna dish from the Odenwald in Germany to Villafranca in Spain have almost been concluded.

The ground qualification for the new Fregat upper stage for the Soyuz launch vehicle has now been successfully completed. The modifications to the launch tower for Fregat are also now ready and the production of all parts of the launch vehicle for the first vehicles is in hand, consistent with the launch of the first demonstration flight of Soyuz/Fregat in January 2000.

In conclusion, all elements of the Cluster-II mission are on schedule for the launching of the four spacecraft by two launches in June and July 2000.

XMM

Ahead of schedule, the spacecraft left Rotterdam harbour on 12 September for its sea trip aboard the 'Toucan' to Kourou. A first team travelled at the same time by plane to prepare the premises so that work could start immediately upon the ship's arrival. The unloading and installation work was done during the night, and less than 48 h after the ship had moored in Kourou harbour, all necessary material was operational and the first test on the reaction control system was underway.

The spacecraft is now installed in the Final Assembly Building. Mechanical assembly has been completed and functional checks on the onboard systems and scientific payload have been performed successfully. The spacecraft is currently undergoing system validation testing, during which it is operated from ESOC in Darmstadt (D). After completion of this test, further functional checks will be conducted and the alignment of the satellite will be verified. Early November will see commencement of the propellant loading activities, after which the combined operations involving both launch vehicle and satellite will commence.

The satellite flight-acceptance review is progressing well. No major problems have been discovered and the review team is now compiling its report for a final meeting of the Board at the end of October in Kourou.

All ground control software has been delivered and software/hardware integration has been completed. The ground segment is currently involved in the system validation test, after which the Science Operations Centre will be shipped to and installed in Vilspa (E). The ground station hand-over is now rescheduled for early October, in time for the ground-segment readiness review.

The tests conducted in the first phase of the launch campaign have confirmed that all experiments installed on the spacecraft are healthy. Experiment teams are supporting the system validation testing in Kourou and in Darmstadt.

Artist's impression of two of the Cluster-II spacecraft on the Fregat upper stage

1

2

3

XMM will be launched on flight Ariane-504. The launch-vehicle technical acceptance review is currently taking place at Arianespace/Evry, the last formal step before entering into the final phase of launch preparation. The current schedule leads to a launch on 10 December.

Rosetta

Integration of the spacecraft Structural and Thermal Model (STM) has made significant progress since the delivery of the main spacecraft structure in early August. Integration of the harness and propulsion subsystems, including the internal thermal blankets, has been completed. A proof pressure test has been successfully performed. All of the instrument STM models have been integrated. Following the vibration and thermal-vacuum test at IABG in Munich (D), the Lander STM was delivered as planned in mid-August. After its integration on the spacecraft, a separation test has been successfully completed. The programme is on schedule for the delivery of the STM spacecraft to ESTEC in December 1999, ready for the start of the environmental test campaign.

At equipment level, the Preliminary Design Reviews (PDRs) have been completed. Software reviews are now being carried out, addressing all of the avionics software. Overall within the Programme, both on the spacecraft and payload sides, attention is now focussed on the Engineering Qualification Model (EQM) programme, which is due to start in the near future.

As regards the Ground Segment, the industrial contractors for the Mission Control System software and the Rosetta ground simulator have been selected and activities in these areas have started.

Transport of the XMM spacecraft to Kourou, French Guiana

1. Shipment by the "Toukan" from Rotterdam (NL) to Kourou

2. Arrival by truck at the Launch Base

3. Unloading XMM from its transport container

Mars Express

The payload, spacecraft and mission-level requirements review activities were successfully completed just before the summer period. The Board met on 28 June and it concluded that the review had been successful, provided that certain actions are closed out in due time.

The Principal Investigators met in late June to initiate the detailed planning of their instruments. That planning is complicated by the fact that that several instruments could generate more data than the spacecraft can transmit to Earth. Compromises will therefore have to be worked out to ensure that all instrument teams get a sufficient share of the data volume over the mission's lifetime.

The preparations for the Preliminary Design Review (PDR) have started with instrument-level reviews in September. Several Principal Investigators have already submitted their data packages in preparation for these reviews.

After signature of the contract with Starsem for the provision of the launch services, normal work on the detailed definition of all requirements and interfaces has started. The Prime Contractor will be responsible for all technical interfaces, while ESA retains responsibility for all contractual matters.

Artemis

Following the virtual completion of testing of the Artemis satellite, the Pre-Shipment Review has been held. This major Agency review has concluded that, while some documentation still needs to be finalised, when the few remaining tests are completed the satellite will be ready for shipment to the launch site. However, NASDA has experienced some technical problems with the launch campaign (H2F8) preceding the Artemis launch, and has consequently announced some delay. A new launch date will be fixed as soon as the situation on H2F8 is clarified. In the meantime, it is planned to place the Artemis satellite in storage.

With the exception of some baseband equipment at the Telemetry, Tracking and Command (TTC) station, the ground facilities needed to operate Artemis are ready and activities are now concentrating upon preparation of the flight-operation procedures and on simulations to exercise these procedures and to train the operations personnel.

Work is also proceeding at Redu (B) on the facilities to be used by NASDA to receive data from their spacecraft via Artemis. The radio-frequency equipment to be provided by ESA has been delivered to Redu and is being installed and tested, while NASDA is implementing its baseband equipment.

EOEP

Strategy and future programmes

Following agreements in May to initiate the first slice of the Earth Observation Envelope Programme (EOEP), in June the Earth Observation Programme Board (PB-EO) selected the first Earth-Explorer Core Missions. The first mission to be funded is 'Cryosat', which is designed to measure and monitor the volume of ice over the polar regions. The second mission, SMOS, is designed to determine ocean salinity and soil moisture. A third mission, ACE, is to be maintained in 'hot-standby' in case of unforeseen problems with either of the first two.

Future missions

The Phase-A studies of the first four candidate Earth-Explorer Core Missions have been completed and subjected to extensive, independent technical and programmatic evaluation prior to the final selection procedure, which will take place in October/November 1999.

Envisat/Polar Platform

Envisat system

The system activities have been focused on two areas: ensuring completeness of the system verifications before launch, including Ground Segment Overall Verification (GSOV), and preparation of the calibration/validation activities for the in-orbit commissioning of the satellite.

Satellite activities

All the flight-model instruments or instrument assemblies delivered in recent

Artemis during acoustic testing at ESTEC in Noordwijk (NL)

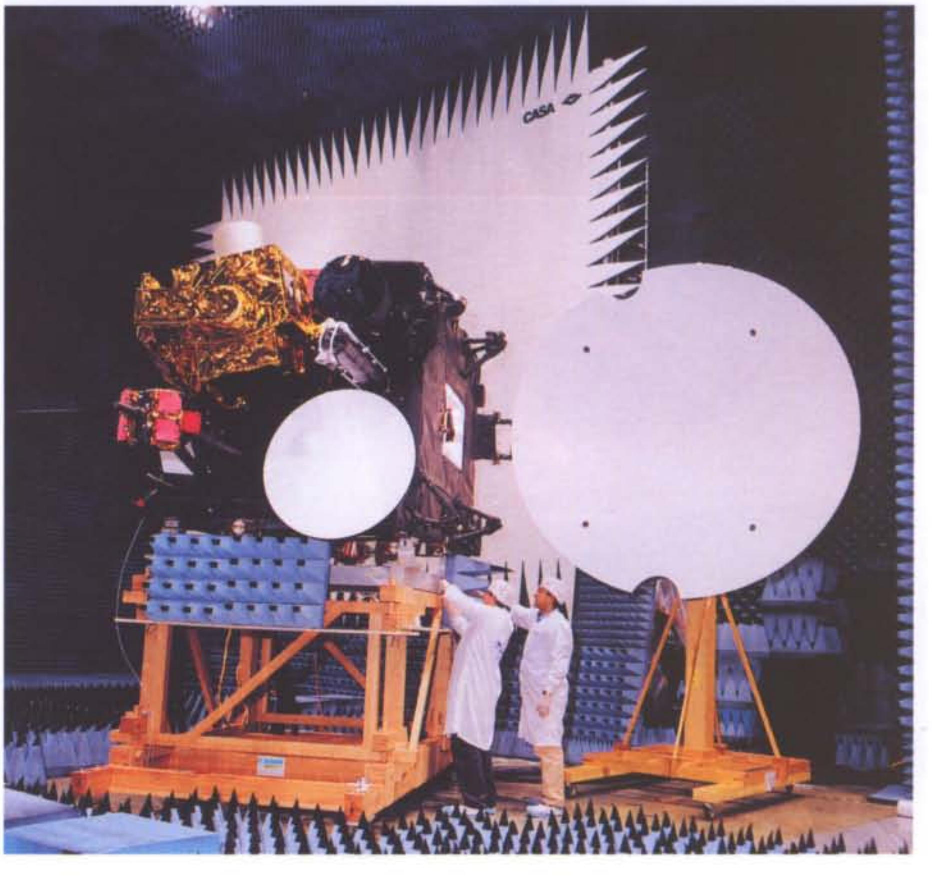

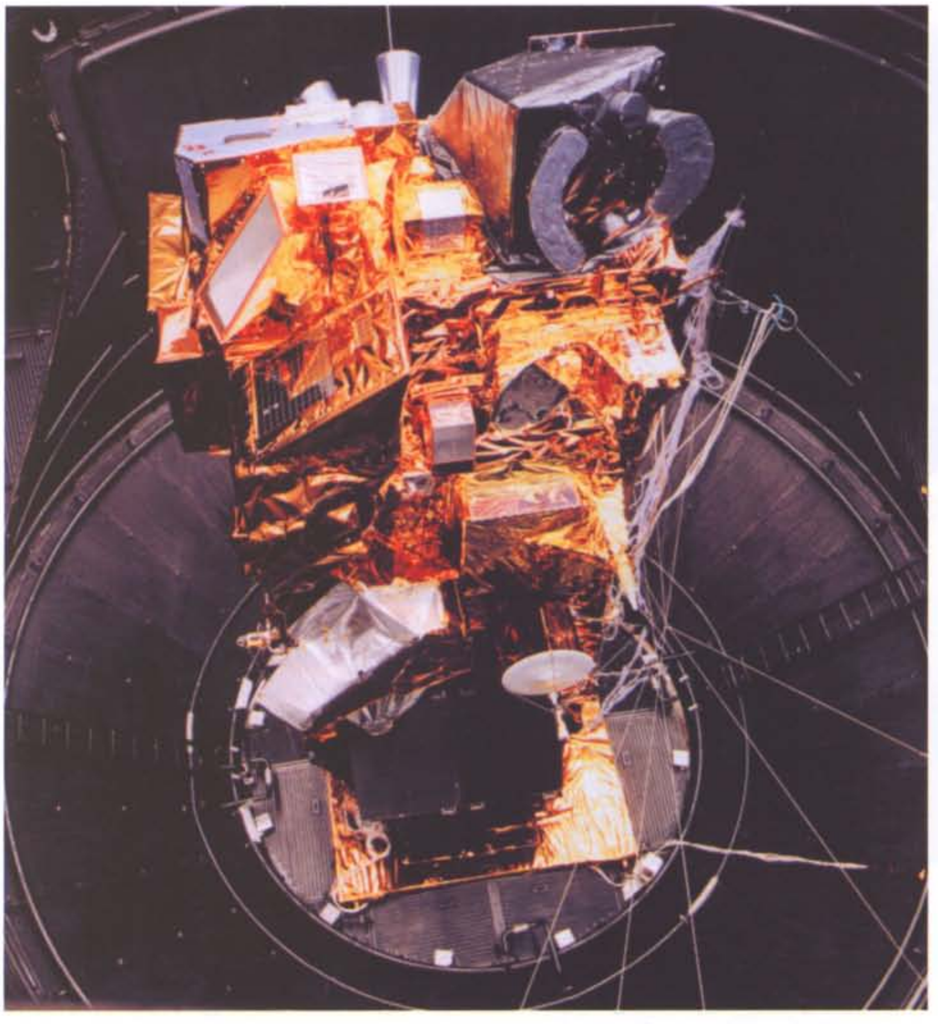

Envisat in the Large Space Simulator (LSS) at ESTEC in Noordwijk (NL)

months have been integrated successfully, and the complete flight-model Payload Module, accompanied by an impressive amount of Electrical and Mechanical Ground-Support Equipment (EGSE and MGSE) was shipped to ESTEC (NL) at the beginning of June. A large part of the Matra Marconi Space team has moved from Bristol (UK) to ESTEC to continue the Assembly, Integration and Test (AIT) activities.

In August, the flight-model Payload Module was transferred, after final preparation, into the ESTEC Large Space Simulator (LSS) for thermal testing. The thermal-balance and thermal-vacuum tests were executed and completed with just a few minor problems, which are currently being addressed. In parallel, the Service Module flight model has been prepared for a qualification shock test with Ariane-5-provided test equipment.

As one of the outcomes of the Envisat Satellite Qualification Review (ESQR), completed in July 1999, the installation of a second Solid-State Recorder has been decided upon and initiated.

Envisat payload

The verification activities on the MIPAS Instrument Optical (MIO) flight-model assembly have been completed successfully and consent to ship it to ESTEC for integration on the satellite was given at the end of September.

The MERIS flight model has been re-integrated, final testing of the instrument is in progress, and delivery is expected before the end of November.

The ASAR antenna has been accepted, following successful completion of the beam-forming tests, and the complete instrument is currently undergoing final integration testing. These tests are expected to be completed at the end of the year.

The repair programme for the ultraviolet-straylight problem on the SCIAMACHY Optical Assembly has been validated and implemented. Final acceptance activities have resumed and delivery of the instrument is expected in early 2000.

Envisat ground segment

The development and integration of the main elements of the Flight Operations Segment (FOS) is progressing according to plan. The operating strategy for the two onboard Solid-State Recorders has been finalised and the associated modifications are being implemented in both FOS and PDS in parallel. The deployment of the Payload Data Segment (PDS) version V2 has been completed and the corresponding acceptance tests are planned for November. A PDS V3 version is currently being defined to cope primarily with updates in the satellite-to-ground interfaces and corresponding evolution/refinement of the instrument-processing algorithms.

Meetings have been held with the potential National and Foreign Station Operators following release of the corresponding applicable specifications. The Processing and Archiving Centre (PAC) implementation activities are in progress with most of the assigned PACs. The Invitation to Tender (ITT) for the commercial distributors is planned to be released in the near future; a briefing for potential tenderers was organised in early September.

Meteosat Second Generation

The engineering-model satellite has been fully integrated and is now undergoing radiated Electro-Magnetic Compatibility (EMC) tests.

The MSG-1 flight-model satellite received its mission communications subsystems in July. The accompanying photograph shows the antenna farm prior to its shipment from Alenia Aerospazio in Rome (I) to Alcatel Space Industries in Cannes (F).

The flight-model SEVIRI Optical Instrument has also been delivered and is presently undergoing acceptance testing. Its measured performance confirms the good quality data already obtained with the SEVIRI engineering model.

The predicted launch date for the MSG-1 spacecraft remains October 2000. MSG-2 and MSG-3 also remain on schedule, with a predicted launch date of 2002 for MSG-2, and an anticipated storage date in 2003 for MSG-3.

Investigations into how to overcome the Ariane-5 shock problem are in progress. Representative flight data from two other satellites on a SYLDA-5 frame are expected in early 2000.

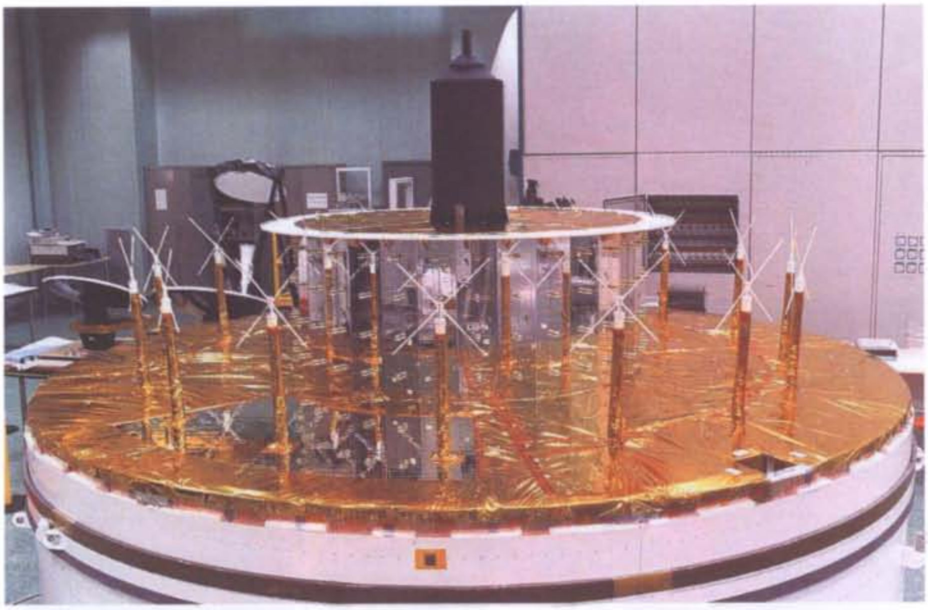

The Meteosat Second Generation antenna subsystem

ERS

Mission operations

During the previous quarter, the ERS system has been operated continuously, with a high level of performance from both the satellite and the ground segment. ERS-2 has ensured the nominal mission, with the ERS-1 payload in hibernation as the mission backup.

The real-time mission was interrupted during four orbits to test the readiness of the overall ERS system for the year-2000 transition. The results demonstrated that the system has indeed been correctly upgraded for that purpose and it is Y2K-compliant.

ERS-1 status

As noted above, the ERS-1 payload continues in hibernation and its performance remains unchanged with respect to the previous report. The SAR is activated twice per day, without data transmission, to maintain the battery capabilities.

ERS-2 status

The platform, the Instrument Data Handling and Transmission (IDHT) system and the payload operated nominally throughout the reporting period. The satellite pointing remains within specification. The close monitoring of gyroscope performance showed an improvement in the noise levels on gyros nos. 5 and 6, but a small degradation in gyro no. 1. Gyro no. 1 has therefore been replaced in the 'piloting triplet' by gyro no. 4, to avoid further degradation and to keep it in operational condition for future use. This piloting triplet will remain in operation until next December when a new Attitude, Orbit and Control System (AOCS) software package will be up-linked to the spacecraft. This newly developed software, which pilots the satellite using just one gyro instead of three, is currently under test.

Metop

With the objective of achieving contract signature before the end of the year, both the Metop industrial partners and the customers, ESA and Eumetsat, have focussed their attention on closing out all of the remaining open points in the contractual and technical baseline. One major element of this has been the firm incorporation of the GRAS instrument within the overall contract, given that at the start of Phase-C/D this instrument, introduced late into the programme, was still an allocation within the industrial proposal.

In parallel with this activity, ESA and Eumetsat have been finalising the details of the documents defining their relationships in this joint programme.

In terms of the industrial development effort, the Preliminary Design Review (PDR) cycle has been completed and many items of equipment are in the final testing stages before delivery of the engineering models for integration. Customer-Furnished Instruments (CFIs) from the United States have been delivered and are in pre-integration with the NOAA (instrument) Interface Unit (NIU) at the Payload Module integrator Dornier (D).

Definition of all elements that will interface with the ground segment has been a priority, so that Eumetsat could issue its Invitation to Tender (ITT) for the core ground segment. This was achieved at the end of August.

PROBA

The spacecraft electrical-model test campaign has been concluded. Integration of the Proto-Flight Model (PFM) spacecraft is ready to start at the end of October with the delivery of the primary structure. The engineering models of the spacecraft computer and power subsystem will support the spacecraft integration before the delivery of the flight units, planned for the end of the year. The other platform flight units have already been delivered, with the exception of the receivers and transmitters, which will also be delivered at the end of the year. The payload-instrument deliveries are planned in November and December after completion of the calibration campaign for the CHRIS spectrometer and after the environmental testing for the DEBIE debris sensor. They will be integrated on the spacecraft with the engineering model of the payload processor unit.

The software development continues in parallel, and the Software Validation Facility has been delivered. The electrical-model test campaign has allowed the reduced version of the software needed to support the spacecraft integration effort to be finalised and validated. The automatic generation of the attitude-control software is now starting following the first delivery of the control models.

As part of the validation of PROBA's attitude-control performance, particularly during the manoeuvres required for the spectrometer measurements, functionality tests have been performed on the wheels and the dual-head star sensor.

The current planning will allow environmental testing of the spacecraft in March and a Qualification and Design Review in December 2000, after the delivery of the last PFM unit.

The first release of the Operations Control Centre software has been delivered and the procurement of the portable ground station initiated. The operations activities at Redu (B) have been initiated.

A second meeting has taken place with the Principal Investigators of the CHRIS instrument, and it has been decided to release an Announcement of Opportunity (AO) to enlarge the exploitation of the CHRIS observations. The observations will be coordinated by ESA's Earth Sciences Division.

The CHRIS spectrometer for PROBA during acceptance testing

International Space Station

European Participation in the ISS Exploitation Programme

The Executive has continued to pursue co-ordination and assessment activities with industry and the User Community. Meetings with industry on the cost and technical references have taken place and a commercial utilisation workshop will be held on 28 October 1999. A first meeting of the multilateral ISS working group on commercialisation will take place in Washington DC on 2 November with the aim of establishing common ground-rules among the Partners for the commercialisation of their respective segments.

ISS Overall Assembly Sequence

Investigations are still continuing to bring the Columbus launch date forward from February 2004 to September 2003, and a Space Station Control Board (SSCB) will be held in end-November/early-December to baseline Assembly Sequence flights for the year 2000.

The launch-preparation testing of the Service Module systems, which include the ESA-furnished DMS-R, is continuing at Baikonur. It was agreed to delay the launch from November to a launch window between 26 December and 16 January, and a more precise launch date will be established at a General Designers' Review (GDR) meeting in Moscow end-October/early-November.

Columbus laboratory

The system-level Electrical Test Model (ETM) testing is proceeding according to plan and Critical Design Reviews (CDRs) at equipment level are about 65% complete, with no major showstoppers evident. Flight-model manufacture is underway with the primary structure pressure shell welding completed.

Columbus Launch Barter

Nodes-2 and -3

Node-2 design has progressed well and flight-unit assembly will start in the first half of next year. The accommodation requirements for Node-3 have continued to change throughout the period, but a Reference Configuration Review in July re-established a baseline for this node and design work has now recommenced.

Software Deliveries/DMS-R items/ Associated Sustaining Engineering for NASA

The last period of sustaining engineering is nearing completion; all other obligations for this element of the Barter have been completed.

Crew Refrigerator/Freezer Racks

The technology study is proceeding as planned, but changes to the agreed Barter requirements, which were expected to be available by end-September, have not yet been received.

Cryogenic Freezer Racks

Following a meeting held by NASA with scientific utilisation representatives and experts of different disciplines, a new release of the Cryosystem Specification was issued and is being reviewed by ESA.

Cupola
Industrial work has progressed well and on schedule, and a full-scale mock-up has been completed and used to conduct a crew review with the participation of ESA and NASA astronauts. Following the announcement of the cancellation of the requirement for the second Cupola and potential changes to the design characteristics of the remaining flight unit, an estimate of the programmatic effects on the scope of the Barter is being prepared.

Automated Transfer Vehicle (ATV)
Preliminary Design Reviews (PDRs) for the Propulsion and Re-boost Subsystems, the Spacecraft Structure Subsystem and the Integrated Cargo Carrier Subsystem have been completed successfully. The overall Phase-C/D planning is under revision and will likely result in a five- to six-month shift in the launch of the first ATV, to end-2003.

Investigations have taken place on the possibility of launching the ATV on the Ariane-5 versatile version with re-startable EPS (Etage Propergols Stockables); a decision on this approach is expected in October 1999.

X-38/CRV and Applied Re-entry Technology (ART)
At the end-July closing date for subscription to the European participation in the ISS Crew Return Vehicle programme, six Member States had confirmed their subscriptions. Two other Member States intend subscribing as soon as a number of arrangements have been formalised. The level of subscription achieved, approximately 190 MEuro, will allow Europe to play a major role in this programme.

The second B52 drop test with X-38 Vehicle V132 was successfully performed in July. For this test, the ESA-provided GNC software for the parafoil descent phase was active. The CDRs for all European hardware for the X-38 orbital test vehicle (V201) have been successfully completed and the manufacture of flight hardware is on schedule.

Atmospheric Re-entry Demonstrator (ARD)
The contract for ARD data exploitation was kicked-off in Bordeaux (F) on 21 July, and its completion is expected within less than a year.

Ground-segment development and operations preparation
More than 20 responses have been received from industry following the Announcement of Opportunity for declaring interest in the Columbus Control Centre subsystem procurements. Invitations to Tender (ITTs) are planned to be released in January 2000.

Utilisation
Promotion
External peers have evaluated the proposals received in response to the 1998/99 Announcements of Opportunity (AO) and made recommendations. Due to their identified application potential, thirty-one of the proposals that were recommended qualify for funding from the Microgravity Application Promotion (MAP) budget. Most of the qualifying projects have been proposed by teams with a strong European dimension and with identified industrial partners. Further new proposals are expected in response to the recently issued Life Sciences AO.

The Programme Committee charged with the preparation of the Global ISS Utilisation Conference 'ISS Forum 2000 - Berlin 13-15 June 2000' will meet in early-November. All ISS Partner Countries and key personalities in Research and Development (R&D) as well as from education and the media, are expected to be present.

Preparation
Although at the end of July the future of DLR's participation in FOCUS was in doubt, a solution has been found allowing activities to continue. At the same time, confirmation from a German industrial consortium regarding their contribution to Phase-C/D of FOCUS has been received. A statement of work is now being prepared to cover a bridging phase, which will be co-financed by ESA, DLR and German industry.

Hardware development
Phase-C/D for the four Express Pallet Adapters (ACES, EUTEF, EXPORT and SOLAR) is now expected to start early next year. The NASA-provided Express Pallet System is experiencing significant delays and, consequently, the Express Pallet Programme is experiencing a delay of more than one year.

Astronaut activities
The CNES Perseus mission with ESA Astronaut J.P. Haigneré on board was successfully completed on 28 August, with the landing in Kasakstan. J.P. Haigneré spent 189 days onboard Mir, which is the longest stay in space by a non-Russian astronaut.

A first group of seven candidates from industry and DLR have started the ISS Instructor Training Course.

Early deliveries
Data Management System for the Russian Service Module (DMS-R)
Modifications to overcome the problems identified in the ESA ground system during the 'four-box test' in Houston in May have been provided to RSC-Energia in accordance with the agreed schedule, and have been verified during the latest 'four-box test' completed in Moscow in October. A software patch to eliminate another DMS-R related problem (boot problem) has also been provided.

MPLM Environmental Control and Life Support Subsystem (ECLSS)
All deliveries have now been completed and the first part of formal 'Transfer of Ownership' protocols between ESA and ASI has been signed by both parties.

The equipment sets for the first two MPLM flight units have been integrated into 'Leonardo' and 'Raffaello' and have been delivered to NASA/KSC for pre-launch ground processing. To date, no problems with the ECLSS hardware have been reported.

European Robotic Arm (ERA)
The ERA CDR was closed-out in October. Initial 'flat-floor' testing with the ERA Engineering/Qualification Model (EQM) has been conducted and the EQM has been delivered to ESTEC for thermal heat-balance tests. Following these tests, it is planned to carry out further flat-floor testing. Assembly of the subsystem flight models is well underway and final assembly of the flight arm is now expected to be complete in May 2000, with delivery to Moscow targeted for end-2000.

Laboratory Support Equipment (LSE)
The CDR for the MELFI -80°C Freezer was formally closed in July. The cooling-performance issue was resolved, with no impact on the specification or design. The Laboratory Ground Model was tested for thermal mathematical model correlation

and will be delivered to NASA in December.

The Ground Unit of the Material Science Glovebox (MSG) was delivered to NASA at the end of August. NASA provided a Crew Test Report in September, which includes some crew-requested modifications that are currently being assessed.

NASA accepted the High Fidelity Avionics and Mechanical Simulators for Hexapod. The Mechanical Simulator is currently undergoing system-level configuration checks.

Microgravity

EMIR-1 and EMIR-2

Eleven ESA microgravity experiments were flown and processed onboard the retrievable Russian capsule Foton-12 from 9 to 24 September. These included three fluid-physics experiments in the FluidPac/Telesupport assembly; four exobiology/radiation experiments in the Biopan; one material-science experiment in the AGAT furnace; two biological experiments in their dedicated and investigator-provided instruments; and one meteorite simulation experiment embedded with three samples in the heat shield of the re-entry capsule.

The PDRs for the European Modular Cultivation System (EMCS) and the Percutaneous Electrical Muscle Stimulator (PEMS) have been completed and authorisation for the development (Phase-C/D) of these facilities has been given.

Phase-C/D for the exobiology facility EXPOSE has been kicked-off.

Following hardware acceptance in October, the facility for studies of the Morphological Transitions in a Model Substance (MOMO) will be delivered to Kennedy Space Centre in November for integration into Spacehab. The flight on Shuttle mission STS-101 is now scheduled to take place in February 2000.

Preparations are continuing for the flight of the Advanced Protein Crystallisation Facility (APCF), Biobox and Biopack, the Facility for Adsorption and Surface Tension (FAST) studies, and the Advanced Respiratory Monitoring System (ARMS) on the STS-107/Spacehab flight in early-2001.

Microgravity Facilities for Columbus (MFC)

For Biolab, nearly all of the subsystem CDRs have been initiated, and the engineering-model manufacturing is almost complete.

Proposals for Phases-B/C/D for the Experiment Preparation Unit (EPU) have been received; their evaluation is in progress and the contract is expected to be awarded by end-October 1999.

The engineering-model manufacturing for the Fluid Science Laboratory (FSL) is 50% complete.

The discussion concerning the introduction of the Microgravity Vibration Isolation System (MVIS) developed by the Canadian Space Agency (CSA) has been shifted to November, due to a delay incurred in the completion of the MVIS PDR.

The Letter of Agreement (LoA) with NASA for the Materials Science Laboratory (MSL) in the US Lab has been signed in September. The absence of a signed LoA had led to a hiatus in the technical exchange between ESA and NASA (due to export-control issues) of about six months. This has introduced a delay into the MSL development, the extent of which is presently being assessed.

The European Physiology Modules (EPM) Phase-B is progressing, with the mid-term review planned in October 1999. Phase-B is foreseen to end by early-2000.

The LoA between NASA and ESA concerning the co-location of the EPM and the NASA Human Research Facility (HRF), as well as the exchange of other physiological experiments, is not yet finalised.

The 2.2 m-diameter Foton-12 reentry capsule carrying Biopan, soon after landing

In Brief

Mercury Mission Named 'BepiColombo' in Honour of Space Pioneer

Meeting in Naples on 20-23 September, ESA's Science Programme Committee recognised the achievements of the late Giuseppe Colombo of the University of Padua by adopting his name for the planned ESA Mercury project. Almost everything known until now about the planet Mercury comes from three passes by NASA's Mariner 10 in 1974-75 and inspired by Colombo's calculations. He suggested how to put a spacecraft into an orbit that would bring it back repeatedly to Mercury. The Italian scientist also explained, as an unsuspected resonance, Mercury's peculiar habit of rotating three times in every two revolutions of the Sun.

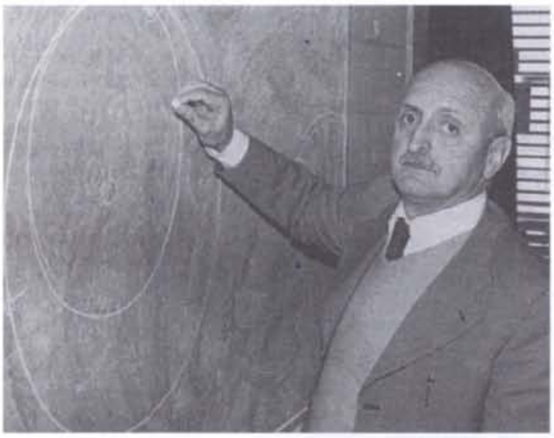

Giuseppe (Bepi) Colombo (1920-1984)

ESA's mission to Mercury is one of ESA's science programme 'Cornerstones'. In the course of the comprehensive Horizon 2000 Plus review of the programme five years ago, it was identified by Europe's space scientists as one of the most challenging long-term planetary projects. Mercury is the least known of the inner planets. Its orbit close to the Sun makes it difficult to observe from a distance and hard to reach by spaceflight. As a result, questions raised by the Mariner 10 fly-bys of a quarter of a century ago remain unanswered.

"I am very pleased we have given the name of BepiColombo to our Mercury cornerstone. Bepi was a great scientist, a great European and a great friend; we could do no better than name one of our most challenging and imaginative missions after him" said Roger Bonnet, Director of the ESA Science Programme.

Scientists cannot claim to fully understand the origin and history of the Earth itself until they can make sense of Mercury. Why is the planet surprisingly dense? Where does its magnetic field come from? What were the effects of massive collisions suffered by Mercury, apparent in shattered zones seen by Mariner 10? Is Mercury geologically active? How does its close proximity to the Sun affect its surface, its tenuous atmosphere and the small magnetic bubble, or magnetosphere, which surrounds it? BepiColombo will seek the answers to these and other questions with three separate sets of scientific instruments. According to preliminary studies completed in April 1999, a Planetary Orbiter will examine the planet from an orbit over the poles, using two cameras and half a dozen other remote-sensing instruments. Seven detectors in a smaller Magnetospheric Orbiter will observe Mercury's magnetic field and its interactions with the solar wind.

A Surface Element dropped by BepiColombo will land near one of the poles of Mercury, where the temperature is milder. Here the instruments will include a camera, a seismometer, a detector for chemical elements, and a package for assessing the temperature, heat capacity, density and hardness of Mercury's 'soil'. The Surface Element is expected to operate for at least a week and the two orbiters for about 12 months.

When ESA began contemplating a mission to Mercury, the journey time was expected to be nearly four years, with a complex series of manoeuvres around Venus and Mercury designed to bring the spacecraft into an orbit similar to Mercury's. Now BepiColombo's journey will be cut to about 2.5 years with the aid of a solar-electric propulsion module, which ejects heavy xenon ions at high speed to provide a small but continuous acceleration over many months. Swing-bys of Venus and Mercury are still part of the mission profile, and a chemical propulsion module will finally put BepiColombo's main spacecraft into orbit around Mercury.

Giuseppe (Bepi) Colombo (1920-1984) was a mathematician and engineer of astonishing imagination, whose bald head and grey moustache were familiar in the corridors of both ESA and NASA. Apart from his work on Mercury, Colombo invented tethers for tying satellites together. As one of the initiators of ESA's mission to Halley's Comet he suggested its name, Giotto, but he died before that project was accomplished. At the University of Padua his work continues in CISAS, the Centro Interdipartimentale Studi ed Attività Spaziali 'G. Colombo'.

In 1985, to commemorate this great scientist, ESA created a 'Colombo fellowship' to be granted to European scientists working in the fields of science explored by G.Colombo.

XMM Draws Youthful Interest

Recently, ESA has been actively promoting a series of activities addressing the younger generation, in a concerted effort to stimulate their interest in space and involve as many young Europeans as possible in the Agency's activities.

In line with these activities, and to celebrate the December launch of XMM, two competitions for European schools in the ESA Member States were announced in September: 'Draw me a Telescope' and 'What's new Mr Galileo?'

Draw me a Telescope

This competition invited school children aged 8 to 12 to draw a telescope as a class activity. Out of over 350 entries received, one per Member State was selected to be included in the official XMM logo. This logo was displayed for the first time on the fairing of the Ariane-5 rocket launching the XMM spacecraft. Additionally, ESA invited one child per country, representing the winning class, to French Guiana to see the launch.

The winning classes come from the following schools:

AUSTRIA:	Bundesgymnasium, Baden bei Wien
BELGIUM:	Gesubsideerde Vrije Basisschool, Brugge
DENMARK:	Nordstrandsskolen, Dragor
FINLAND:	Mäntysalon Koulu, Klaukkala
FRANCE:	Ecole du Vieil Orme, Rambouillet
GERMANY:	Gerhart Hauptmann Schule, Griesheim
IRELAND:	North Dublin National School Project, Dublin
ITALY:	Scuola Elementare "5 giornate", Milano
THE NETHERLANDS:	International School of Amsterdam, Amstelveen
NORWAY:	Kringsjå skole, Oslo
SPAIN:	Colexio Apóstol Santiago (Jesuitas-Vigo), Vigo
SWEDEN:	Hubertusgården, Lund
SWITZERLAND:	Ecole Primaire de La Roche, La Roche
UNITED KINGDOM:	The School of St. Helen and St. Katherine, Abingdon.

What's new Mr Galileo?

This competition was open to youngsters aged 13 to 15 whose classes had to write, in English, a one-page vision of astronomy and its benefits for humanity. In one month's time, ESA received and assessed over 100 essays. The winning classes, one per Member State, were invited to Kourou to visit the launch facilities.

The winning schools are:

AUSTRIA:	Bundesrealgymnasium, Graz
BELGIUM:	Lycée Emile Jacqmain, Bruxelles
FINLAND:	Helsingin Suomalainen Yhteiskoulu, Helsinki
FRANCE:	Collège Buffon, Paris
GERMANY:	Ignaz Kögler Gymnasium, Landsberg A. Lech
IRELAND:	Malahide Community School, Dublin
ITALY:	Istituto Michelangelo Buonarroti, Verona
THE NETHERLANDS:	Niftarlake College, Maarssen
NORWAY:	Enebakk Ungdomsskole, Enebakk
SPAIN:	Colegio El Ave Maria, Benimamet (Valencia)
SWEDEN:	Hökarängsskolan, Farsta
SWITZERLAND:	Cycle d'Orientation du Gibloux, Farvagny
UNITED KINGDOM:	Haggerston School for Girls, Shoreditch, London

Ariane-4 launches

The 118th Ariane launch (V118) took place successfully on Thursday 12 August at 19:52 Kourou time. An Ariane 42P vehicle (equipped with two solid strap-on boosters) lifting-off from the Guiana Space Centre – the European Spaceport in Kourou, French Guiana – placed into geostationary transfer orbit the Indonesian telecommunications satellite TELKOM 1.

Ariane V120, again using a 42P vehicle, was launched on Saturday 4 September at 19:34 Kourou time, delivering the Korean telecommunications satellite, Koreasat 3, into geostationary transfer orbit.

Ariane V121 was launched on Saturday 25 September at 03:29 Kourou time. The 44LP vehicle (equipped with 2 liquid and 2 solid strap-on boosters) lifted off with the American telecommunications satellite, TELSTAR 7.

The 122nd Ariane launch (V122) took place on Tuesday 19 October at 03:22 Kourou time, successfully placing into super-synchronous transfer orbit the American telecommunications satellite ORION 2.

Ariane V123 lifted off on Saturday 13 November at 19:54 Kourou time carrying the American telecommunications satellite, GE4, into geostationary transfer orbit.

50th IAF Congress

The 50th Congress of the International Aeronautical Federation (IAF) took place on 4-8 October 1999 at the RAI Conference Centre in Amsterdam (NL), bringing together over 2000 space community professionals under the theme 'Space – an integral part of the information age'. The exhibition was opened on Monday, 4 October, by His Royal Highness Wilhelm-Alexander, Prince of Orange.

ESA played a major role in the Congress providing information on current and future programmes with presentations and demonstrations of space technology, Earth observation, space science, navigation and telemedicine. Particular highlights included a 3-D presentation of the International Space Station, the original capsule of the Atmospheric Reentry Demonstrator (ARD) and the X-ray mirrors developed for the XMM spacecraft.

A total of 464 students from ESA Member States were sponsored by the Agency's Education and Outreach Office to attend the Congress. This was the first time that such a significant number of students were given the opportunity to follow the various sessions, and to exchange views and ideas with experts from all over the world.

Bus trips to ESTEC were organised on two afternoons, providing Congress participants with the opportunity to see the Artemis and Envisat flight units, and visit the Erasmus User Centre. A number of ESA staff were on hand to welcome the visitors and answer their questions.

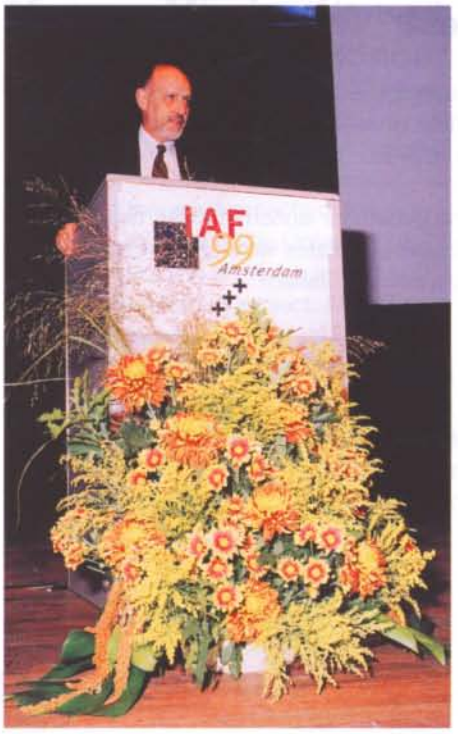

An inaugural speech was given by ESA's Director General, Antonio Rodotà

ESA's DG, Antonio Rodotà, gave an inaugural speech on Monday, 4 October, responding to the address by Annemarie Jorritsma-Liebink, Dutch Minister of Economic Affairs. On Wednesday, 6 October, he opened the plenary session on the 'Future of European Space'. On the evening of 7 October, Mr Rodotà addressed the 464 invited European students and congratulated the winners of the lottery prizes.

Hans Kappler, ESA's Director of Industrial Matters and Technology Programmes, spoke at the plenary session on 'Space Technology needs for the 21st century', as did his counterparts from NASA, NASDA, the Canadian Space Agency and Ball Aerospace. Jörg Feustel-Büechl, Director of Manned Spaceflight and Microgravity programmes, announced the winners of 'Success', ESA's Student Competition for the best ISS Experiment Proposal and handed out prizes at a special event opened as well to the general public.

Altogether, ESA's representatives included fourteen session chairmen or co-chairmen, one symposium coordinator, two rapporteurs and twenty-eight speakers.

The next IAF Congress and Exhibition (51st) will be held on 2-6 October 2000 in Rio de Janeiro. For more information visit the IAF website at <http://www.iafastro.com/>

His Royal Highness Wilhelm-Alexander, Prince of Orange, and Annemarie Jorritsma-Liebink, Dutch Minister of Economic Affairs (centre)

The ESA exhibition provided information, presentations and demonstrations of current and future space technology

The interest and enthusiasm the students demonstrated throughout the Congress were rewarded with a prizes at a special student social event. Prizes were drawn by Antonio Rodotà (centre) and Wubbo Ockels (left), Head of Office for Educational Project Outreach Activities. Charly Pache (right), Ecole Polytechnique Fédérale de Lausanne (CH), was the second prize winner of a trip to Kourou to witness an Ariane launch.
The third prize was a special Internet account received by: Luigi Adamo, University of Palermo (I), Joost van Leeuwen and Wouter Jonker, TU Delft (NL), Mario Roberto Carraro, University of Bologna (I), and Raffaele de Amicis, University of Bologna (I).
The lucky first prize winners were Erik Wouters and Stephan Ullmann, TU Munich (D), who each received a trip to Rio de Janeiro to attend the 51st IAF Congress next year

464 students were sponsored by ESA to participate in the Congress

A True SUCCESS Story

The 50th IAF Congress also saw the presentation of prizes to the winners of another contest launched by ESA last year (November 1998). Dubbed SUCCESS (Space Station Utilisation Contest Calling for European Students' IdeaS), the contest was designed to introduce students and their ideas to space and non-space industries in order to stimulate potential for future industrial research and technology development on the International Space Station.

ESA received 103 experiment proposals from 126 students in Austria, France, Germany, Ireland, Italy, The Netherlands, Norway, Spain and the United Kingdom, spanning the fields of technology, life sciences, physics, materials science, and Earth observation.

Under the aegis of ESA's Director for Manned Spaceflight and Microgravity programmes, Jörg Feustel-Büechl, prizes were awarded to:
1st prize: José Mariano López-Urdiales, Fernando Mancebo-Ordóñez, Daniel Meizoso-Latova and Pablo Valls-Moldenhauer, Instituto Universitario "Ignacio da Riva", Universidad Politécnica de Madrid, Spain
2nd prize: Paolo Ariaudo, Università degli Studi di Napoli "Federico II", Italy.
3rd prize: Alexander Roger and Anna Glennmar, University of Glasgow, UK.

The Spanish students will each be granted a 3-month fellowship at ESA's Research and Technology Centre, ESTEC, to work on their experiments and get ready to test them on a parabolic flight campaign. The Italian student won a laptop computer, while the British students will be able to choose a trip to either KSC to attend a Shuttle launch or to Kourou to witness an Ariane launch.

Finalists of the SUCCESS contest

The first prize, 3-month fellowships at ESTEC, was awarded to four students from the Universidad Politécnica de Madrid

ESA Parabolic Flights to Prepare for the International Space Station

On 25 October, a specially adapted Airbus A-300, took off from Bordeaux-Mérignac airport in France on the first day of a week-long (25-29 October) campaign of parabolic flights designed to carry out experiments in weightlessness, and to test instruments and equipment before they embark on a real spaceflight. These campaigns observe how technical systems and biological, chemical and physical processes function in the absence of gravity. This campaign, the 27th organised by ESA, will focus mainly on how the human respiratory system works and how new materials can be produced.

During a parabolic flight, the aircraft performs a nose-up manoeuvre to put it into a steep climb. This creates a centrifugal force of 1.8 g (1.8 times the force of gravity on the ground) for about 20 seconds. Then the pilot reduces engine thrust to almost zero, injecting the aircraft into a parabola. The plane continues to climb till it reaches the apex of the parabola, then it starts descending. This condition lasts for about 25 seconds, during which the passengers and all unstrapped equipment in the cabin float in the weightlessness resulting from the free fall of the aircraft. When the angle below the horizontal reaches 45°, the pilot accelerates again and pulls up the aircraft to come back to a steady horizontal flight. These manoeuvres are repeated 30 times per flight.

During the weigthlessness periods, the 28 scientists on this flight – from research institutes in six European countries and the US – carried out their work: measuring blood pressure under various conditions, monitoring a newly-developed instrument or heating metals in a purpose-built furnace, in order to confirm a hypothesis, test instruments or replicate results obtained during an earlier spaceflight. The 26 previous campaigns that ESA has conducted since 1984 have produced a total of 2650 parabolas and almost 15 hours of weightlessness, the equivalent of flying around the Earth (in low-Earth orbit) nearly 10 times. A total of 360 experiments have been carried out.

With Europe and its international partners now building the International Space Station, where research will be carried out for the next 15 years, parabolic flights are crucial to the preparation of experiments, equipment and astronauts, and allow scientists to have their experiments tested before they are actually flown on a space mission.

Over the coming four years, ESA will run two parabolic campaigns a year. Scientists are regularly invited to submit experiment proposals for review and selection by peers. Those whose experiments are selected have the possibility to participate in an ESA parabolic flight campaign. In each of its future campaigns, ESA will also include experiments proposed by students to encourage the scientists of tomorrow to learn all about experimention in weightlessness and the extensive research opportunities the International Space Station is going to offer.

Further information on ESA parabolic flights can be found at ESA's special parabolic flight Internet pages at <http://www.estec.esa.int/spaceflight/parabolic>.

Experiments and scientists involved in the 27th ESA parabolic flight campaign

1. "Gravity and lung function, first use of ARMS in microgravity", Prof. D. Linnarsson (Karolinska Institute, Stockholm, S), Prof. M. Paiva (University of Brussels, B) and Dr G.K. Prisk (University of California, San Diego, USA). Focuses on the quantitative relationship between lung geometry, gas diffusion and convective gas transport.
2. "Does weightlessness induce peripheral vasodilatation?", Dr P. Norsk and Dr R. Videbaek (DAMEC, Copenhagen, DK). Tests hypothesis on the dilatation of the heart and the peripheral vascular system that could be caused by weightlessness.

Experiments 1 and 2 above make use of ESA's "Advanced Respiratory Monitoring System" built by Innovision (DK) and Alcatel Space (CH) which is to be flown on the Shuttle in January 2001.

3. "Respiratory mechanics under 0g", Prof. P. Vaïda (University of Bordeaux 2, F) and Prof. G. Miserocchi (University of Milan, I). Studies pulmonary mechanics.
4. "Otolithic control of the cardiovascular system during parabolic flights", Drs P. Denise, H. Normand (University of Caen, F) and Dr P. Arbeille (University of Tours, F). Tests the hypothesis that otolithic receptors, part of the inner ear balance system, affect the cardiovascular system.
5. "In vivo monitoring of the mechanical environment of fractures in microgravity", Prof. M. Hinsenkamp and Prof. F. Burny (University of Brussels, B). Measures mechanical constraints in healing bones in subjects having recently fractured tibia.
6. "The effects of a change in gravity on the dynamics of prehension and the kinematics of the upper limb during cyclic arm movements with a hand-held load", Profs. J.L. Thonnard, N. Heglund and P. Willems (University of Louvain-La-Neuve, B). Measures the grip force and total load force of test subjects.
7. "The effect of short-duration microgravity on leukocyte early signal transduction events and cytoskeleton dynamics", Drs J. Hatton, J.P. Breittmayer (Hôpital Archet, Nice, F) and Dr B. Hashemi (National Space Biomedical Research Institute, Houston, USA). Leukocytes are white blood corpuscles found in suspension in human blood plasma; this experiment will help explain the mechanisms of leukocyte sensitivity to gravity.
8. "Investigations of metallic foam production under microgravity conditions", Dr S. Odenbach (ZARM, University of Bremen, D) and Dr J. Banhart (IFAM, Bremen, D)". Studies metallic foams, new materials with interesting properties of high firmness and low weight with potential applications in lighter car shock absorbers, for instance.
9. "Thermal analysis of pure silicon and aluminum-silicon alloys by mirror furnace experiments", Prof. H. Fredriksson (Royal Institute of Technology, Stockholm, S). Investigates samples of pure silicon and aluminum-silicon alloys using a special furnace developed by the Swedish Space Corporation and flown several times on previous ESA campaigns.
10. "Critical velocities in open capillary flow (choking)", Dr M.E. Dreyer, U. Rosendahl and Prof. H.J. Rath (ZARM, University of Bremen, D). This fluid physics experiment aims at determining the maximum flow rate, which can be established in a capillary channel.
11. "Completion of fault arc investigations at cable bundles under weightlessness conditions", Prof. König, J. Hanson and F. Hörtz (Darmstadt University of Technology, D). This technological investigation looks at the characteristics of insulated cables after exposure to the thermal effect of different electrical powers in microgravity.

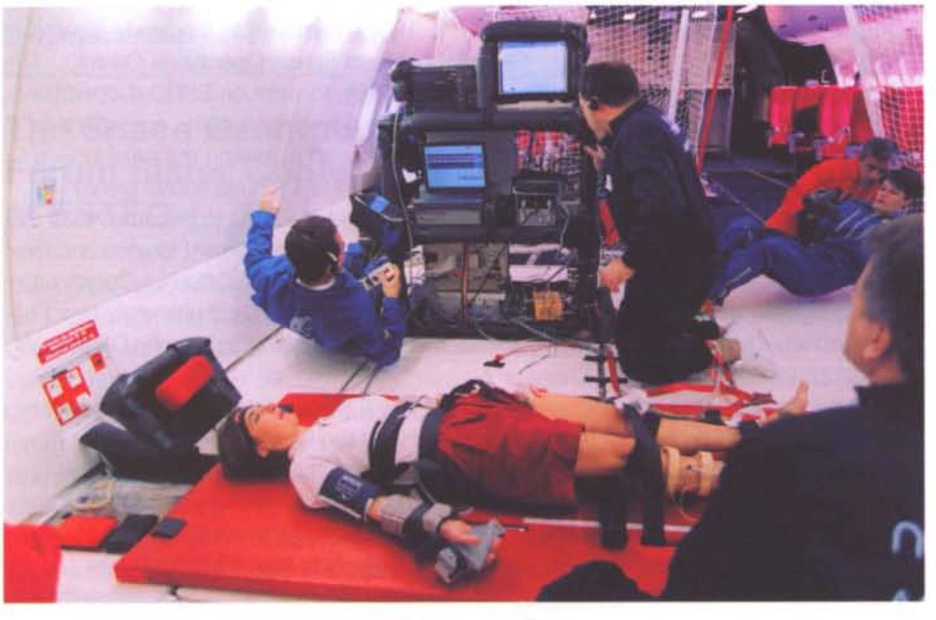

Foton-12 Success

The international Foton-12 mission, carrying a record-size Agency payload, was launched from Russia's Plesetsk Cosmodrome on 9 September. After 14.6 days in orbit, its descent capsule landed safely in southwest Russia; the ESA payload was retrieved within hours and carried back to Europe. Foton's 11 ESA experiments covered fluid physics, biology, radiation dosimetry, material science and meteoritics – another first.

Making its debut was the FluidPac facility, with its associated Telesupport unit, which, for the first time, provided scientists with online monitoring of their experiments. Two fluid physics experiments (MAGIA and TRAMP) were successfully performed, while BAMBI suffered a technical failure and had to be aborted.

ESA's Biopan external exposure facility, completing its fourth flight, performed well. The unit's lid was opened 20 hours after launch, by telecommand from the Moscow control centre, to expose the four radiation and exobiology experiments directly to the space environment. It was closed after 303 hours. Biopan was returned to ESTEC and the experiments extracted on 28 September.

Like Biopan's experiments, the standalone ALGAE (cell biology) and SYMBIO (botany) went as planned and were safely recovered after landing. The novel reentry study, STONE, with simulated-meteorite rock samples embedded in the capsule's heatshield, went well, although one of the three samples was lost during descent.

Another ESA experiment processed three samples in the Agat furnace to investigate the diffusion coefficients of tellurium and indium in gallium antimonide. Other payloads, from France, Germany and Russia, were also flown. Throughout the mission, Foton-12's status could be closely followed on the Web, where a special homepage was updated daily. Further information can still be found at <http://www.estec.esa.nl/spaceflight/foton/>; see also page 95 of this issue.

Plastics and Space Meeting the Challenges to Mankind

ESA and the European plastics industry have presented new research showing how plastics and space research will help address some of the future challenges facing mankind. A joint press conference on the subject, organised by ESA's Technology Transfer Programme headed by Pierre Brisson of the Directorate of Industrial Matters and Technology Programmes, was held on 7 October at ESTEC's Erasmus User Centre.

The proceedings, opened by Jörg Feustel-Büechl, ESA's Director of Manned Spaceflight and Microgravity, were followed by representatives of the European plastics industry, environment and sustainability experts, and over forty journalists working for the international media

The report 'Coming of Age: Plastics and Space Meeting the Challenges to Mankind', commissioned by the European plastics industry and the ESA Technology Transfer Programme, was presented. It highlights some of the key issues facing mankind, such as climate change, pressure on finite resources and terrestrial habitat, and shows how transferring technologies developed for space applications could provide some of the required solutions.

Numerous examples illustrated in the report include:

- water purification systems, based on technology for use on the International Space Station, are currently under development to deliver fresh water to millions of needy people in India and the Far East
- lightweight vehicle construction techniques, applied to components of the Space Station, Space Shuttle and other space systems, are integral to new generations of eco-efficient aircraft and automobiles
- the use of solar light, and the efficient use and retention of energy on board spacecraft, are opening up the development of alternative energy sources on Earth and ensuring efficient use of fossil fuels through improved domestic insulation.

Pierre Brisson, Directorate of Industrial Matters and Technology Programmes

For further information about ESA's Technology Transfer Programme, visit the website <http://www.esa.int/technology/>.

On 7 October, ESA's Technology Transfer Programme organised a joint press conference with the European plastics industry on the benefits of plastics and space research, at ESTEC's Erasmus User Centre

New Head of ESA Cabinet

The new Head of Cabinet, Mr Brian Walker, took up duty on 1 August 1999. His Office provides the Secretariat to the ESA Council, manages planning, information, representational and operational requirements for the Director General, and is responsible for the Agency's official record and the management of its archives.

A long-serving ESRO and ESA staff member, Brian Walker joined ESTEC (NL) in October 1964 to work on the ESRO-2 satellite project, as deputy Project Manager with specific responsibility for checkout and orbital operations. In 1967, he moved on to the TD1A project to manage checkout design and procurement.

In 1968, he moved to the newly created European Space Operations Centre, ESOC (D), to work on ESRO-1 operations and the preparation of the operations for the re-launch (following the initial launch failure) of ESRO-2. He subsequently progressed at ESOC to become Head of the Mission Management Branch and later Division, Head of the Office for Coordination and Management, and ultimately Head of the Ground System Engineering Department.

In 1989, he moved to ESA Headquarters to Head the Coordination and Management Office, where one of his many functions was to Chair the Agency's Adjudication Committee (1989 to 1994). In 1994, he was appointed Associate Director for Information Systems, with additional responsibility from 1997 for the reform of Purchasing, Records Management, and Information and Documentation Services.

In his new role as Head of the ESA Cabinet, Brian Walker will also be responsible for the Agency's Central Management Support Unit.

Brian Walker

Mercure Project Successfully Completed

On 6 October, the Mercure project was formally concluded during a meeting of its Governing Board, held at the Ministry of Foreign Affairs in Madrid. The project was created in Madrid on 25 November 1994 when six ESA Member States – Austria, Belgium, Norway, Spain, Switzerland and the United Kingdom – signed a Memorandum of Understanding, together with the Agency, to participate in and to contribute to the project. Mercure is a European response to the importance that the United Nations Conference on the Environment, UNCED, held in Rio de Janeiro in June 1992, placed on the need to improve the availability of and access to environmental information in achieving sustainable development.

The project is elaborated by the United Nations Environment Programme, UNEP, in partnership with ESA. Under the auspices and technical coordination of ESA and the leadership of the Spanish Company INDRA in Barcelona, a consortium of industry from the participating States, including Newtec CY (B), Nera (N), Softlab (A) and CIR SA (CH), has provided satellite earth stations and associated equipment, installed at several of UNEP's world-wide centres. Global capacity on the Intelsat system is used to interconnect the earth stations. The overall Mercure network is controlled by a Master Station operated by Swisscom Telecom in Leuk (CH).

The Mercure network is now an integral part of UNEPnet, which is a dedicated global Internet for environment and sustainable development. Its role is to improve environmental data and information exchange and to address the 'widening gap' between the industrialised and developing worlds. Responsibility for the technical implementation and day-to-day operation of the UNEPnet/Mercure programme rests with the UNEPnet Implementation Centre in Arendal, Norway.

UNEP's ability to operate as a UN centre from Kenya is entirely dependent on reliable and cost-effective communications not only with other UN centres, but also with UNEP's own offices around the World and the national governments served by the programme. High-capacity Internet services, video conferencing and electronic publication of UNEP's products would simply not be feasible without Mercure. In fact, Mercure has greatly increased UNEP's ability to collaborate effectively with other centres around the World.

The Space Generation Forum Sister Conference at ESTEC

The Third United Nations Conference on the Exploration and Peaceful Uses of Outer Space (UNISPACE III) was held in Vienna, Austria from 19-30 July 1999. The UN had agreed that an international youth forum for university students, graduate students and young professionals, called the 'Space Generation Forum (SGF)' and organised by International Space University (ISU) alumni, should be held in conjunction with UNISPACE III.

It was proposed by the Forum committee that local brainstorming sessions, known as Sister Conferences, should be held around the World before the Vienna meeting to collect and assimilate ideas and thereby provide as meaningful an input as possible for the Forum. To involve the younger staff at ESA in the above activities, it was decided to hold one of the SGF Sister Conferences at ESTEC, in Noordwijk (NL).

The ESTEC Sister Conference, held on the morning of 3 June, was built around two main discussion groups: Education & Public Outreach and Science & Technology. The event was supported by the ESA Office for Education Projects and Outreach Activities. Seventeen people participated, seven of whom chose to be in the Education and Public Outreach discussion group, and ten in the Science and Technology group.

The Education and Outreach group focused on eight topics:
1. Education and Outreach: present concerns
2. NASA versus ESA Experiences
3. Europe's Needs
4. Added-value of a European Approach
5. Organisation of a European Effort
6. Use of ISS for Education and Public Awareness
7. Pan-European Student Micro-satellite Programme
8. Our Future in Education and Outreach.

The Science and Technology group also had eight main topics as a starting point:
1. Microgravity
2. Physiology
3. Breakthroughs in Propulsion Systems
4. How to Develop Innovative Technology using Space Missions?
5. Space Weather
6. Astrophysics, Astronomy
7. Planetology
8. From the Smallest to the Largest (fractal geometry?).

One of the most important results of the Education and Outreach discussion group was the concept of the added-value of a European approach, using all of our cultural differences to our advantage. The importance of high-level communication between institutions, academia, industry, etc. was highlighted. The creation of 'space projects' with the capacity to involve a large number of young Europeans, and the use of the International Space Station for education and public outreach, were just two of the recommendations to emerge.

Participants at ESTEC

Education & Public Outreach Discussion Group:
- Cedric Bouvry
- Ana Colorado McEvoy
- Viney Dhiri
- Christian Henjes
- Tobias Horn
- Paul Tucker
- Sander Van Dijk

Science &Technology Discussion Group:
- Antonio Manuel Araujo
- Nicolas Boulant
- Anne Cizeron
- Patrick Couta
- Jean-Christophe Dunat
- Annette Jaeckel
- Sandra Mingot
- Esther Martinez
- Oscar Martinez
- Erik Nijs

Basically two topics stood out in the Science and Technology discussion group: how to use the effects of microgravity to our advantage, and how to avoid hazardous space-weather effects. The participants were intrigued by how microgravity might be used to benefit science, technology and physiology research. It was suggested that more new materials (e.g. medicines, polymers, computer chips, crystals, etc.) with very pure properties could be developed (as yet unknown types of atomic binding might be possible in microgravity?). It was emphasised that these new materials should be developed for peaceful purposes! Also, it was suggested that microgravity could be used to test some of our basic theories about, for example, atomic structures. The need for more research into the effects of microgravity on the human organism (bone loss and muscle weakness) was emphasised. Could research in microgravity lead to new immunisation possibilities against disease?

The participants also found the subject of space weather highly important for the advancement of the utilisation of the space environment. 'Space weather' (i.e. how the space environment may have unwanted effects on both technological and biological systems in space and on Earth) is becoming a topic of world-wide interest due to the fact that it directly and/or indirectly influences everybody on Earth. It was agreed that improved prediction techniques for the radiation and particles coming from the Sun is essential. Also the growing problem of debris (natural and man-made) in space was deemed to be a very important issue in this context.

The Space Generation Forum in Vienna
The Space Generation Forum was funded mainly by the Austrian Government, the UN and commercial sponsors, such as Boeing and Lockeed Martin. The available budget was used to promote the event and to finance approximately 200 young people (students and young professionals) from all over the World to participate.

The areas that the SGF delegates in Vienna focussed on were:
- Public Awareness and Outreach
- Education
- Development of Society & Meeting Basic Needs
- Arts and Humanities
- Philosophy, Religion, Ethics/Morality
- International Co-operation
- Transmission of Knowledge

The SGF Participants at UNISPACE III in Vienna, July 1999

- Environment
- International Security and Peacekeeping
- Military
- Commercialisation
- Science and Technology
- Access to Space.

Forty-nine recommendations were drawn up by the SGF participants and ten of them, representing the younger generation's vision for the future of space, were selected by democratic vote for presentation to the official Delegations to UNISPACE, representing 60 countries:

Recommendations:
1. Education without Frontiers: a Global Education Curriculum: indicating that education is a priority for young people.
2. Priority Access to Mobile Satcom Network for Disaster Emergency Relief: indicating that direct benefits of space technology to humankind is a concern.
3. International Space Authority: indicating that young people expect leadership.
4. SGF Follow-up: indicating that the SGF participants appreciated the Forum as a means of expressing their opinions and their vision.
5. Establishment of an International Centre for Space Medicine (ICSM): indicating that health is a main concern.
6. International Space Chamber of Commerce: indicating that young people would like to see an official institution that would provide funding for space activities all over the World.
7. Action Plan for Meeting the World's Basic Needs through Technology: indicating the same conclusion as for R-3.
8. Nobel Space Prize: indicating a common desire to increase awareness of space among the general public and to raise its status in the scientific community.
9. UN Space Youth Advisory Council (YAC): indicating that young people want to have a voice and to participate actively in long-term policy making.
10. Planetary Defence/Protection: indicating that there is a common awareness, among young people, that our species needs a global understanding of such natural threats as possible impacts of Near Earth-Objects with the 'Blue Planet'.

Five of these ten recommendations – R1, R2, R4, R8 and R9 – were integrated into the so-called 'Vienna Declaration' emanating from UNISPACE III. Further information concerning these Recommendations can be found under 'Declaration of the SGF Conference', at www.spacegeneration.org.

Many ESA staff were involved in the SGF conference in Vienna, and several former and present ESTEC employees were on the event's Local Organising Committee. Mr Clovis de Matos presented the results of the ESTEC SGF Sister Conference during the poster exhibition.

C.J. de Matos, C. De Vos, N. Crosby & J. Kraemer *Local SGF Organising Committee, ESTEC*

SOHO Rescuers Honoured

On 16 July, during the 1999 NASA Honor Awards Ceremony at Goddard Space Flight Center (GSFC) in Maryland (USA), ESA's Francis Vandenbussche was presented with the NASA Medal for Public Service by Mr A.V. Diaz, Director of GSFC, and Dr Edward Weiler, NASA Associate Administrator for Space Science, *"in recognition of his inspiring leadership, engineering insight and diplomatic skills, which were the key to the successful recovery of the ESA/NASA Solar and Heliospheric Observatory (SOHO)"*.
On the same day, Mr Vandenbussche also received, on behalf of the European SOHO Recovery Team, the NASA Group Achievement Award, *"in recognition of the outstanding achievements of the ESA/ NASA Recovery Team who successfully restored operation to the disabled Solar and Heliospheric Observatory."* esa

Francis Vandenbussche with Mr A.V. Diaz (left) and Dr Edward Weiler (right)

European Satellite Technology Helps Fight Forest Fires

In managing emergency situations, such as forest fire fighting, modern organisations require real-time communications between command centres and those 'in the field', as well as deployment over the affected region of, for example, helicopters, vehicles and heavy fire-fighting equipment.

Newly emerging and existing space-based technologies such as navigation satellite systems, satellite communications and Earth observation methods could satisfy many of today's emergency management requirements. But a gap currently exists between these technologies and their operational use. How can this gap be bridged?

ESA has come up with an answer by promoting a new initiative for REal-time Management of emergency situations via SATellite. REMSAT makes maximum use of existing space technologies (telecommunications, positioning, Earth observation systems) as well as hand-held terminals carried by firemen, in order to provide communications with central Emergency Management Control Centres via transportable Intermediate Satellite Terminals.

REMSAT not only provides improved communications between fire crews in the field and the fire-fighting control centres, but also data, video images and geographical location capabilities, through to the positioning and status information of all resources. It also allows additional background information on the fire area, in the form of satellite imagery, aerial photography and meteorological data – essential aids to fire modelling, prediction and suppression.

A pilot demonstration of REMSAT capabilities was conducted in Canada last September. Under an ESA contract, MacDonald Dettwiler & Associates (CDN) – a company with extensive expertise in space-based operations and transportable equipment – teamed up with the British Columbia Forest Service. The BCFS is charged with fighting forest fires in B.C, protecting communities and timber resources in an area of over 1 million square kilometres. The protection programme is deployed for an average of over 3000 fires annually.

Under the demonstration scenario, a nominal fire lasting 19 days was simulated. Positioning functions were provided by GPS, messaging by the Orbcomm LEO satellite system and low/high data rate voice and video services by the Canadian GEO satellite system Anik. The results met with an enthusiastic response from Provincial Government Minister of Forests, Mr David Zirnhelt and the BCFS. A further two (full-scale) simulations are planned in spring 2000, followed by full operational deployment of the system in a real fire that summer.

Forest fire fighting was the selected application for the pilot demonstration, but REMSAT can be adapted to meet the needs of many other types of emergencies such as earthquakes, floods, exceptionally heavy winter conditions and those involving hazardous materials. It can also be made compatible with various satellite systems currently available. esa

Planets, Planets Everywhere

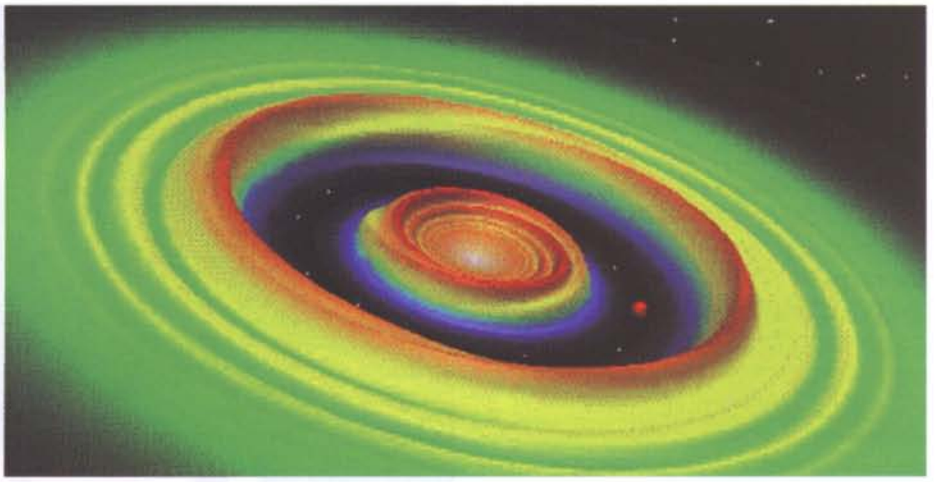

Computer rendering, based on a hydrodynamic model which calculates the evolution of a protostellar disk as a giant protoplanet forms (Image courtesy: Geoffrey Bryden, Lick Observatory, University of California, Santa Cruz)

More than a dozen planets orbiting other 'suns' have been found in the last few years, but are they the rule or the exception? ESA's Infrared Space Observatory (ISO) has shown that the formation of extra-solar planets must be a very common event. As explained in the journal Nature (30 September 1999), ISO has found that almost all young stars are surrounded by a disc of debris – a requisite for planet making – while most above a certain age are not. Correlating these data and certain events in the history of our own Solar System, such as the formation of the Moon's craters, astronomers postulate that the discs of older stars have vanished because they have already condensed into planets.

The authors, an international team led by Harm Habing, from Leiden University (NL), wanted to know if stars belonging to a particular class were more likely than others to form planets. In our own Solar System, planets formed out of a disc of small particles of dust, so every star surrounded by such a disc is a potential planet-forming star. The astronomers therefore chose a sample of 84 nearby stars, all of them very common and in the most stable phase of their lives – the 'main sequence' – but of different ages. Which ones would have discs?

Discs are difficult to see because they emit very faintly; only a few have been positively detected so far. Using ISO, the international team found that 15 stars in their sample did have a disc. Then they analysed the ages of the stars: it turned out that most of those younger than 400 million years had discs, while the great majority of the older ones did not.

"We show for the first time that the presence of a disc around a main sequence star depends strongly on the star's age. Why do those above a precise age not have discs? We searched for clues in our own Solar System, and realised that it was just when the Sun was that age (about 400 million years) that planets were forming", Habing says.

In our Solar System, several facts demonstrate that very soon after the formation of the planets the disc orbiting the Sun disappeared. Some evidence comes, for instance, from Moon craters. These 'scars' on the lunar surface were made while the planets were completing their formation phase and the Sun was losing its own disc of debris, during the 'clean-up phase' of the Solar System. The newly-born planets scattered the remaining planetesimals, which were ejected from the system, fell into the Sun or collided with other large bodies, such as the Moon. The age determinations of lunar rocks brought back by the Apollo missions prove that all this happened when the Sun was 300 to 400 million years old.

In the light of these facts, the authors postulate that the young stars in their sample – those with a disc – are now undergoing their 'heavy bombardment' period. When this process finishes, the disc will vanish and proto-planets will orbit the star instead.

Does this theory mean that all stars for which a disc cannot be observed are surrounded by planets?

"This is something we cannot say. That's where the knowledge barrier is", Habing answers. *"However, we think the Sun has the same history as the other planetary systems. When the planets form they destroy the disc"*.

World Experts on Space Debris Meet

Space debris experts from around the globe gathered from 11 until 13 October 1999, at the European Space Agency Operations Centre (ESOC), Darmstadt (D) for the 17th meeting of the Inter-Agency Space Debris Coordination Committee (IADC).

IADC is concerned with all technical issues of the space debris problem. The main objectives of IADC are to exchange results of research in the field of space debris, to cooperate in research activities and to identify debris mitigation options.

The 17th IADC discussed ways and methods to control the growing amount of orbiting debris. Radar and optical telescopes regularly track over 10 000 artificial objects in space. The number of untrackable objects in the size range from 1 cm to 10 cm that could seriously damage an operational spacecraft, is estimated at between 100 000 and 150 000. The International Space Station (ISS) will be equipped with about 200 shields in order to defeat impacts of particulates about 1-2 cm size.

Some recent and current topics of the IADC include:
- guidelines for the disposal of spacecraft in the geostationary orbit
- data exchange procedure and communications for reentry of risk objects
- common database of space objects
- risk assessment for the 1999 Leonids and countermeasures
- measures to reduce the growth of the debris population in low-Earth orbit.

The results from the work of the IADC will provide a technical basis for deliberations on space debris at next meeting of the Scientific and Technical Subcommittee of UNCOPUOS in February 2000.

Focus Earth

The Izmit Earthquake: A Quick Post-Seismic Analysis with Satellite Observations

M. Barbieri, J. Lichtenegger & G. Calabresi
Earth Observation Department, ESRIN, Frascati, Italy

Buildings were razed to the ground and electric and telephone lines cut in Izmit, in northwest Turkey, by the strong earthquake that shook the region on 17 August 1999. The National Earthquake Information Centre reported a quake of magnitude 7.8, almost as strong as the 7.9-magnitude San Francisco quake that claimed 700 victims in 1906. In Turkey, four days after the event, the death toll had risen to more than l0 000, with 45 000 reported injured and thousands of people still missing.

The earthquake's epicentre was identified as being between Izmit and Bursa (Fig. 1), about 100 km east of Istanbul. High casualty figures were reported not only in Golcuk, but also in the towns of Derince and Darica, both situated to the west of Izmit. The large town of Adapazari, northeast of Sapanca Lake, was also severely damaged by the quake.

Since this devastating first shock, there has been a second series of tremors further east, but along the same fault line, peaking on 12 November and bringing death and destruction to the towns of Kaynashli and nearby Duzce.

Geological setting of the area

Turkey's North Anatolian Fault Zone (NAFZ) is the most active in the country. Historically, it is here that most of the biggest earthquakes have originated. The NAFZ zone splays out into three strands at about 30.5 deg E. The northern strand crosses the Bay of Izmit and the Marmara Sea, and reappears in the Gulf of Saros. Many researchers believe that the Marmara Sea region is a depression that is slowly widening, due to two fault systems running in parallel.

The tectonic activity in the area is basically explained by movements of the Eurasian, Arabic and African plates activating different portions of the Anatolian fault system (Fig. 2). The NAFZ is a close analogue of the San Andreas fault in California. Both structures are active, have similar slip rates, lengths and straightnesses, but earthquakes occur five times more frequently in the NAFZ (M > 6.7!).

Figure 1. Geographical map of the earthquake area

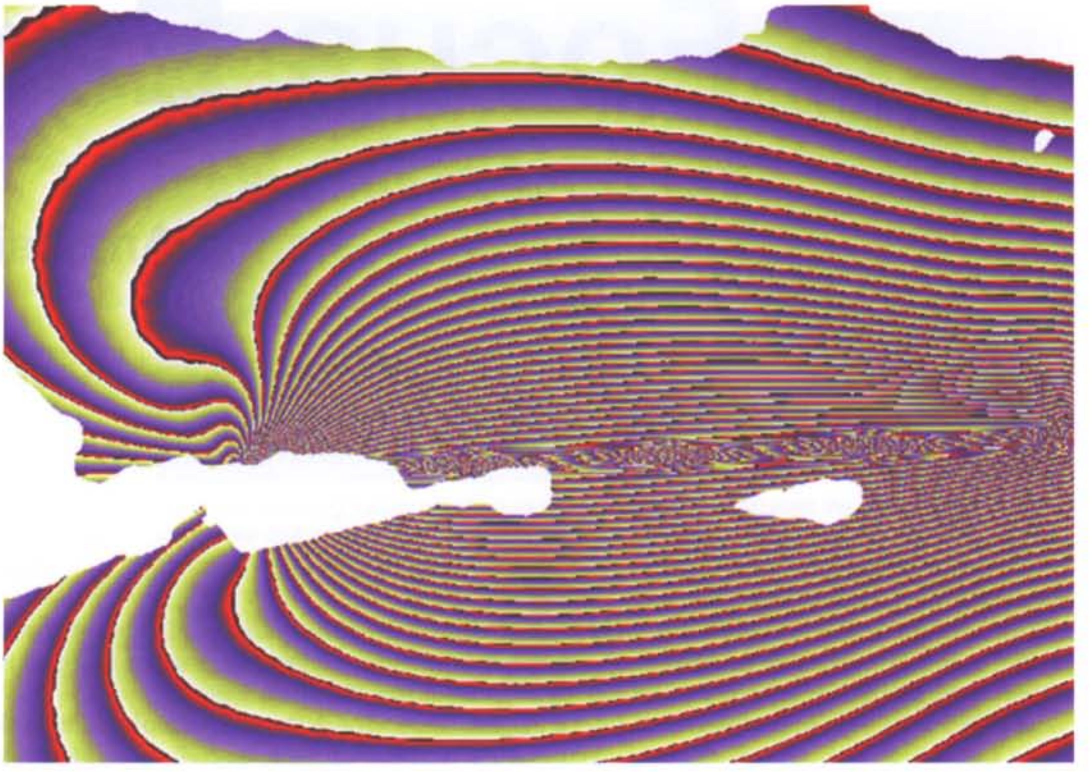

Figure 3. Theoretical surface deformation model based on geophysical data. The comparison with Figure 4 demonstrates the possibility to reconstruct the effects of a seismic event through the interpretation of ERS SAR interferometric fringes

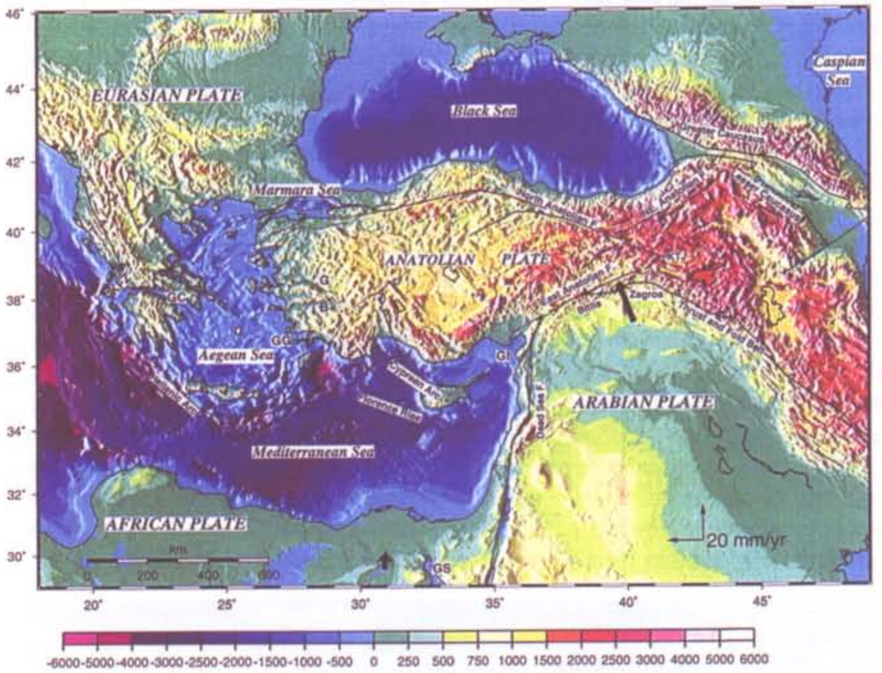

Figure 2. Overview of the main geological and morphological features evidencing the tectonic plate relationships in the eastern Mediterranean region

Seismic-event analysis

The 17 August earthquake originated at a depth of between 10 and 16 km along almost vertical ruptures. Four different fault segments became active during the two consecutive shocks: the first shock lasted 12 seconds and affected the western part, i.e. Golcuk, Izmit – Sapanca and Arifiye – Akyazi. Eighteen seconds later, the Earth shook again for 7 seconds, this time along the Golyaka rupture to the east-northeast of Sapanca. The surface displacement reached a maximum of 5 m near the town of Arifiye. The average offset along the active fault system was 2 to 4 m.

Earthquake effects as observed by ERS SAR

ERS-1 and 2 data were used to obtain a SAR differential interferogram showing the surface deformation in an area between Istanbul and the Lake of Sapanca. A theoretical deformation model (Fig. 3) derived from geophysical data was compared with the ERS SAR-derived phase interferogram (Fig. 4). The result of the modelled earthquake movement can be recomputed and displayed as fringes. The geophysical interpretation of the model is that the rupture occurred along an east-west fault, causing a predominantly horizontal movement (right-lateral strike).

In the interferogram (Fig. 4), each colour cycle from red to yellow corresponds to a ground displacement of 28 mm in the slant range direction (ERS satellite's viewing direction). By counting the number of fringes, one can calculate the co-seismic deformation. In the present case, 28 ± 2 fringes can be observed across the image. They suggest a deformation of about 81cm in the ERS viewing direction. The horizontal component of this measurement can be simply computed based on the viewing incidence angle (see Fig. 7).

With this approach, SAR interferometry can be used to quantify the dislocation produced by an earthquake. Basically, three measurements are needed to define the spatial displacement vector. Hence, three observations or interferograms from different viewing angles are required. In practice, the SAR data from ERS's ascending and descending passes would provide two of the three observations needed; the third might

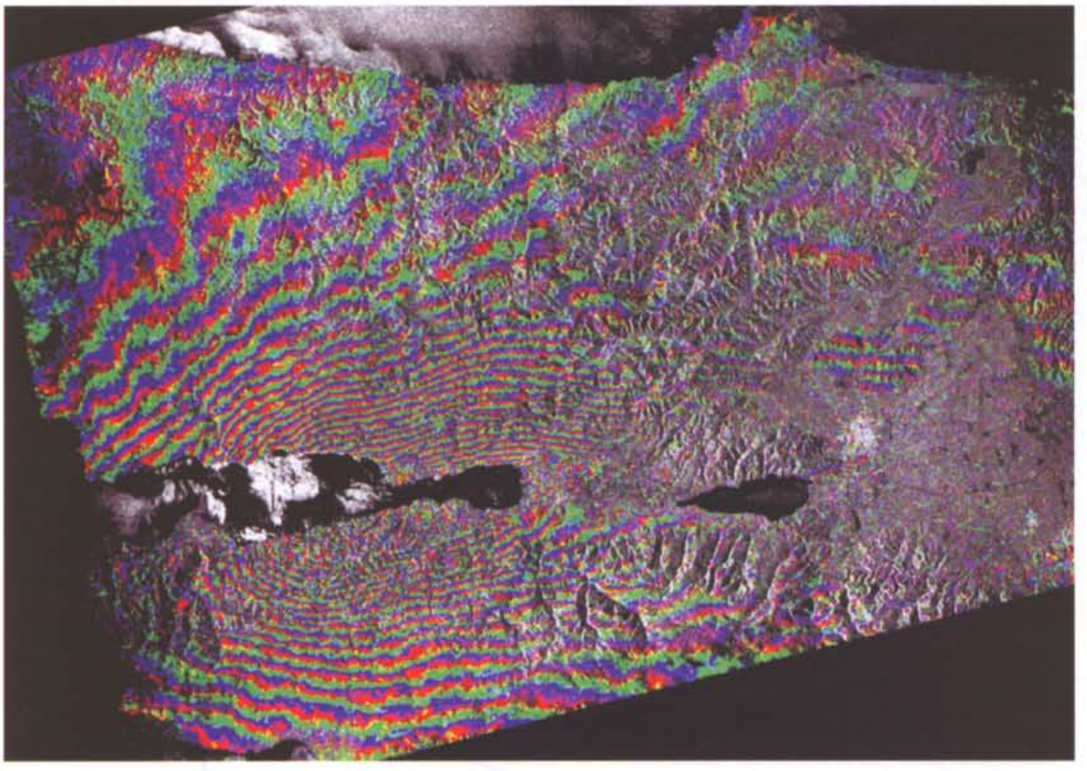

Figure 4. Interferometric fringes computed from an ERS-1/ERS-2 data pair acquired before and after the earthquake. The fringes are superimposed on a SAR amplitude image

be retrieved from historical data and from a tectonic analysis of the area.

In the Turkish case, we find ourselves with an exceptional view of events in being able to observe a nearly horizontal movement, occurring in an east-west direction that is almost parallel to the sensor observation direction. In this particular case, one observation can be sufficient. In fact, the displacement so-derived (207 cm) is in good agreement with both ground measured and modelling results.

Successful application of SAR interferometry is highly dependent on the satellite's orbit. For differential interferometry, the smaller the separation between the two observations (perpendicular baseline), the better will be the result. Small baselines are optimal to preserve the coherence; at the same time, the influence of ground topography in the interferogram becomes negligible. In the case of the ERS SAR image pair used here, the perpendicular baseline was about 18 m over Izmit. This low figure was obtained thanks to the careful satellite orbital monitoring and manoeuvering performed by the ESA ground controllers at ESOC in Darmstadt (Germany).

Interferometric/optical image product

Figure 5 shows an attempt to superimpose the ERS-derived interferometric fringes on a Landsat Thematic Mapper (TM) image.
This might well be

Figure 5. The interferometric fringes shown in Figure 4 were superimposed on a Landsat Thematic Mapper (TM) image. Urban areas are shown in red/magenta. The intensity of the ground deformation is proportional to the fringe density. This image product enables a first assessment of damage, even for remote locations

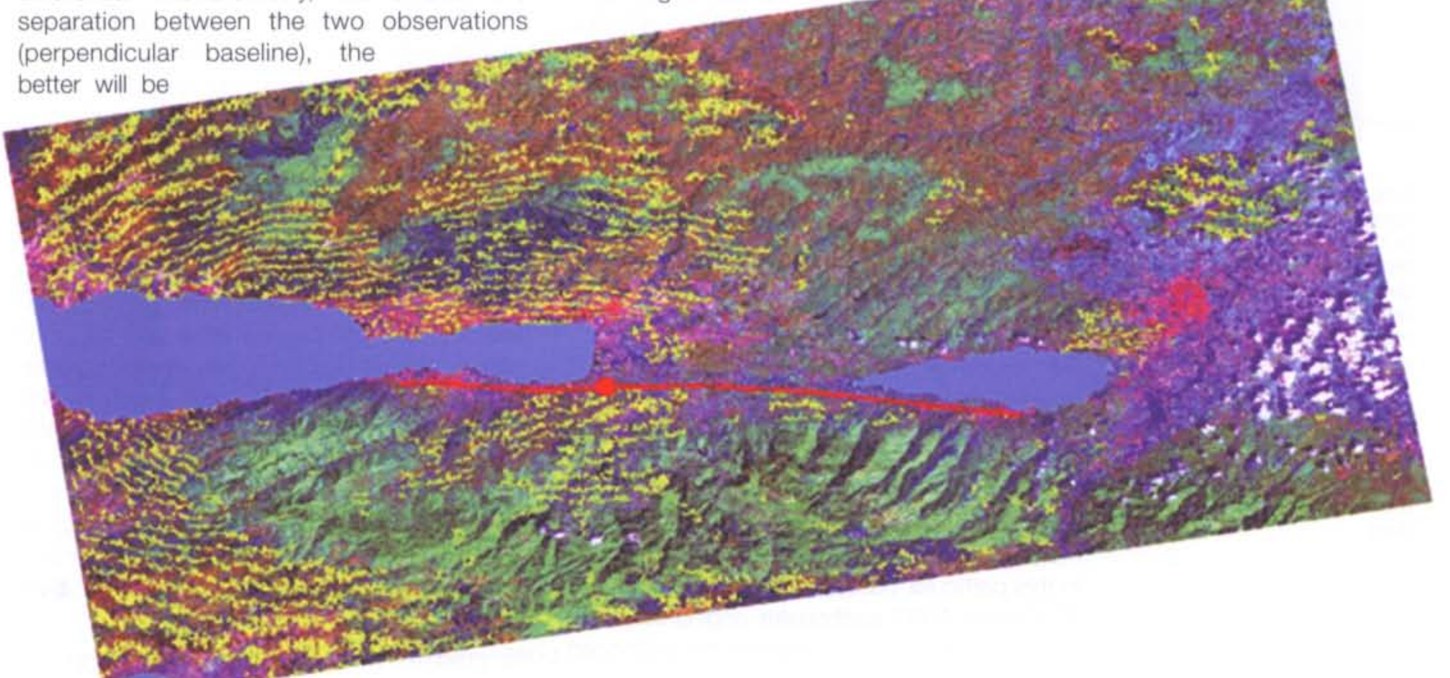

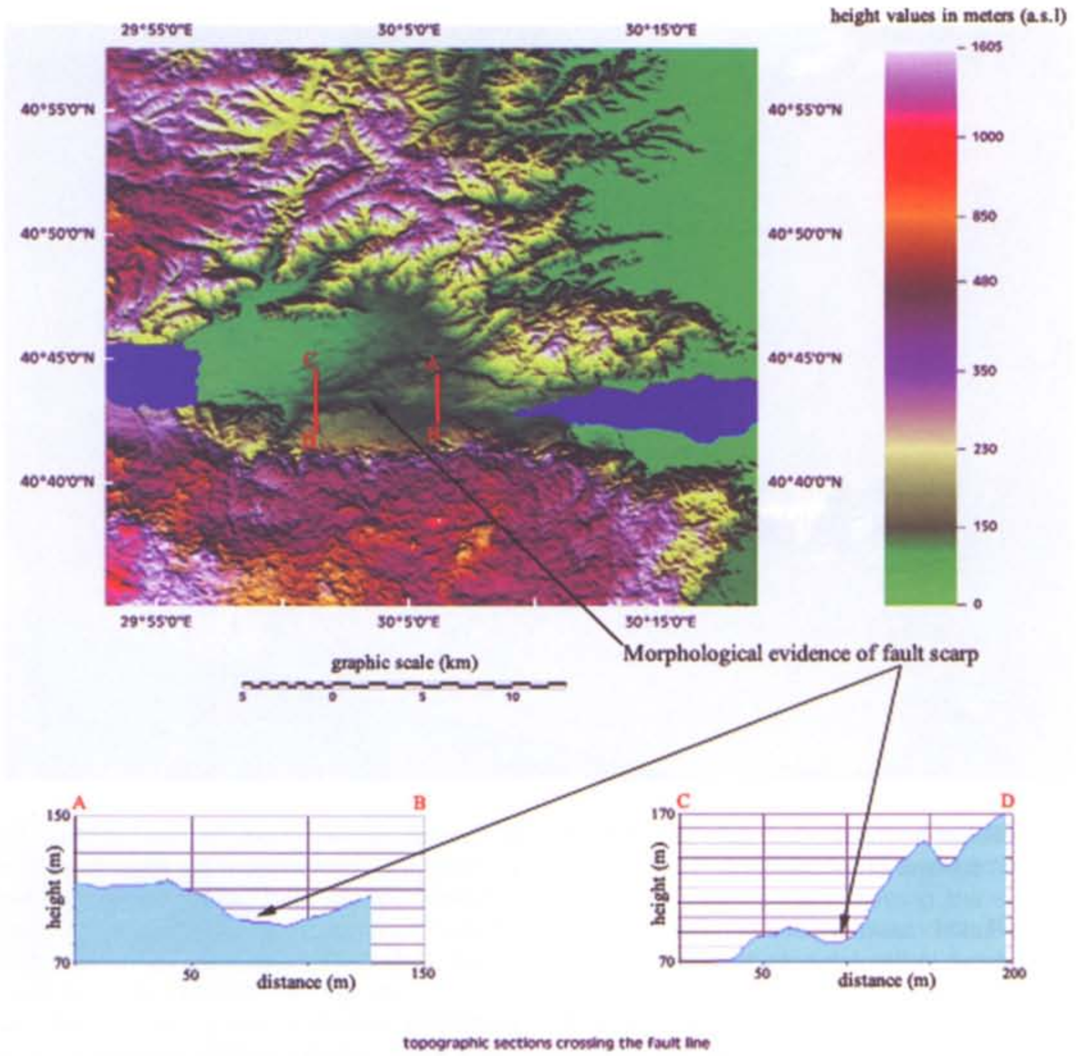

Figure 6. The shaded-relief image was obtained from an ERS SAR interferometric DEM. Height values are colour-coded. The image product can be used in studies relating to the recognition of tectonic and morphological lineaments

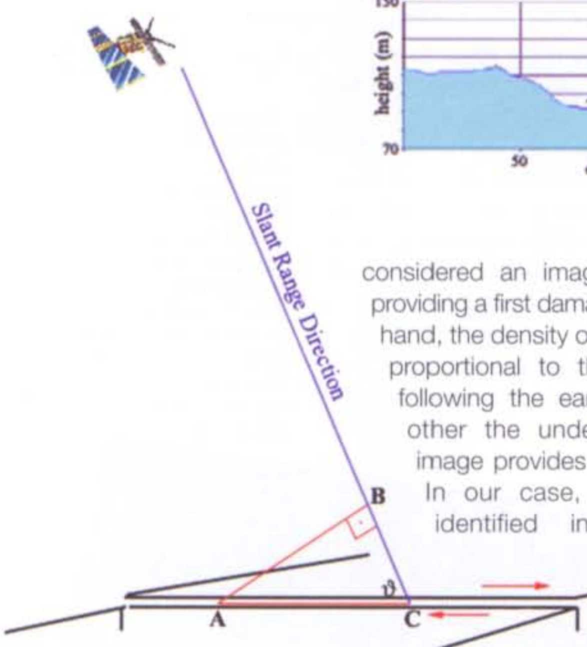

Figure 7. ERS SAR slant-range viewing with respect to the geological fault movement. A simple geometrical function can be used to determine the movements horizontal component.

BC = slant-range deformation of approx. 81cm
AC = fault-plane horizontal deformation of approx. 81/cos ϑ = 207 cm (ϑ = 67 deg)

considered an image product suitable for providing a first damage assessment. On one hand, the density of the fringes (in yellow) is proportional to the degree of damage following the earthquake, while on the other the underlying optical satellite image provides land-cover information. In our case, urban areas can be identified in magenta: relevant damage data are retrievable from the fringe density. The active fault location (red line) was performed by using conventional geological maps and was further refined with satellite image interpretation. The epicentre is marked with a solid red circle.

Geological analysis enhanced by ERS SAR interferometry

A altitude colour-coded and shaded Digital Elevation Map (DEM) generated from the ERS tandem pair of 12 - 13 August 1999 is shown in Figure 6. This image clearly shows the morphological and tectonic features in the area. In this particular case, the fault from which the 17 August 1999 earthquake originated could be easily identified by analysing the enhanced morphology shown by the DEM. This kind of ERS InSAR product can be used by specialists to study tectonically active areas not only in this region, but also elsewhere in the World. One of the most significant outputs from such an analysis is 'risk maps'.

Conclusions

For the Izmit earthquake, as for previous similar events all over the World, ERS SAR interferometry has provided extremely useful results. A quantitative analysis was performed to assess the overall displacement on the surface. It is believed that an image pair from an ascending and a descending pass might be sufficient, together with tectonic information, to estimate the movement quantitatively. In this particular case, the favourable situation with respect to both satellite orbit and tectonics allowed the dislocation to be determined using a single interferometric pair, together with geological information. A SAR interferometric/optical image product has been worked out which might well meet the requirement of gaining immediate access to information on land cover and earthquake intensity whenever and wherever such natural disasters occur.

Applications are invited for the position of

Director of Neuchâtel Observatory

(for Spring 2001)

Founded in 1858, Neuchâtel Observatory has the main mission to perform research and development in the area of Time and Frequency (T/F) and its applications, including pre-industrial development and technology transfer to industry.
The position involves the accomplishment of the Observatory's mission, insure its funding as well as its future development. Teaching at the University is an additional task envisaged. Activity fields range from space applications, atmospheric studies, metrology through to telecommunications.
The holder of the post will also be responsible for the relationship with the scientific, industrial and political communities, media relations, budget and personnel management. The ideal candidate will have a sound management experience in a T/F or related environment based on a Ph.D or equivalent in Physics, Electronics or Engineering. Previous experience in managing an institution or a research group is required. The ability to teach at the University will be an additional advantage.

Excellent remuneration as well as above average benefits reflecting the seniority of this position are offered.
For further information please contact Giovanni Busca:
tel. ++41 32 889 68 70
fax ++41 32 889 62 81
e-mail giovanni.busca@ne.ch or visit http://www.ne.ch/adm/dep/ocne
Please forward your application to :
Service du personnel, rue du Musée 1, case postale 563,
2001 Neuchâtel, Switzerland

Application deadline 29th February 2000.

Publications

The documents listed here have been issued since the last publications announcement in the ESA Bulletin. Requests for copies should be made in accordance with the Table and Order Form inside the back cover

ESA Newsletters

REACHING FOR THE SKIES, NO. 20 (AUGUST 1999)
WILLEKENS P. (EDS. T.D. GUYENNE & D. DANESY)
NO CHARGE

EARTH OBSERVATION QUARTERLY NO. 63 (SEPTEMBER 1999)
GUYENNE T.D. & DANESY D. (EDS.)
NO CHARGE

PREPARING FOR THE FUTURE, VOL. 9, NO. 2 (SEPTEMBER 1999)
BRISSON P. (ED. M. PERRY)
NO CHARGE

EUROCOMP (AUTUMN 1999)
SPACE COMPONENTS STEERING BOARD
(ED. B. BATTRICK)
NO CHARGE

EARTH OBSERVATION QUARTERLY NO. 64 (DECEMBER 1999)
GUYENNE T.D. & DANESY D. (EDS.)
NO CHARGE

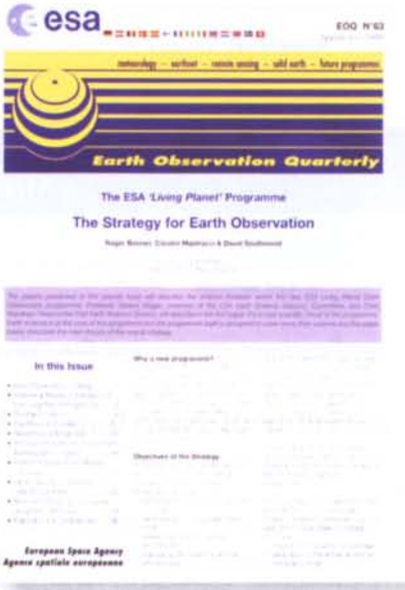

ESA Brochures

COLUMBUS: EUROPE'S LABORATORY ON THE INTERNATIONAL SPACE STATION (OCTOBER 1999)
THIRKETTLE A. & GULPEN J. (ED. A. WILSON)
ESA BR-144 // 41 PP
PRICE: 20 DFL / 9 €

UNA STORIA DI SUCCESSI – 30 SCOPERTE DALLE MISSIONI SCIENTIFICHE NELLO SPAZIO DELL'ESA (1999)
TESTO GRUPPPO COMUNICAZIONI SCIENTIFICHE (COMPILATORE N. CALDER)
ESA BR-147 // 32 PP
PRICE: 15 DFL / 5 €

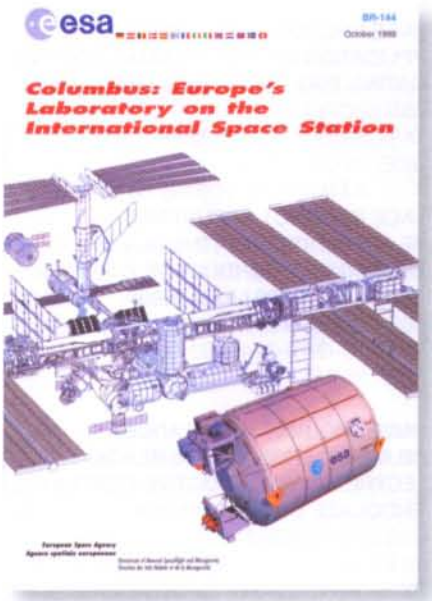

LA HISTORIA DE UN ÉXITO – 30 DESCUBRIMIENTOS DE MISIONES ESPACIALES DE LA ESA (1999)
SERVICIO DE COMUNICACION DE CIENCIA (COORDINADOR N. CALDER)
ESA BR-147 // 32 PP
PRICE: 15 DFL / 5 €

METEOSAT SECOND GENERATION (MSG) – THE SATELLITE DEVELOPMENT (NOVEMBER 1999)
WEYMIENS B. & OREMUS R.
(ED. B. BATTRICK)
ESA BR-153 // 55 PP
PRICE: 50 DFL / 20 €

ESA Special Publications

INVESTING IN SPACE – THE CHALLENGE FOR EUROPE
INVESTIR DANS L'ESPACE – LE DEFI LANCE A L'EUROPE
INVESTIEREN IM WELTRAUM – DIE HERAUSFORDERUNG EUROPAS
ESA LONG-TERM SPACE POLICY COMMITTEE (LSPC)
(EDS. B. BATTRICK & G. NAJA)
ESA SP-2000 // **CD-ROM**

PRICE: 25 DFL / 10 €

THE ULYSSES MISSION: LAUNCH – SEPTEMBER 1995, INCLUDING JUPITER FLY-BY (APRIL 1999)
MARSDEN R.G., SMITH E.J. & TRANQUILLE C. (ED. B. BATTRICK)
ESA SP-1230 // **8 CD-ROMS**
PRICE: 200 DFL / 80 €

EXOBIOLOGY IN THE SOLAR SYSTEM AND THE SEARCH FOR LIFE ON MARS (OCTOBER 1999)
BRACK A., FITTON B. & RAULIN A.
(ED. A.WILSON)
ESA SP-1231 // 188 PP
PRICE: 70 DFL // 30 €

REPORT ON THE ACTIVITIES OF SPACE SCIENCE DEPARTMENT 1997-1998 (AUGUST 1999)
HUBER M.C.E., TAYLOR B.G., WENZEL K.-P. & READINGS C. (ED. A. WILSON)
ESA SP-1232 // 242 PP

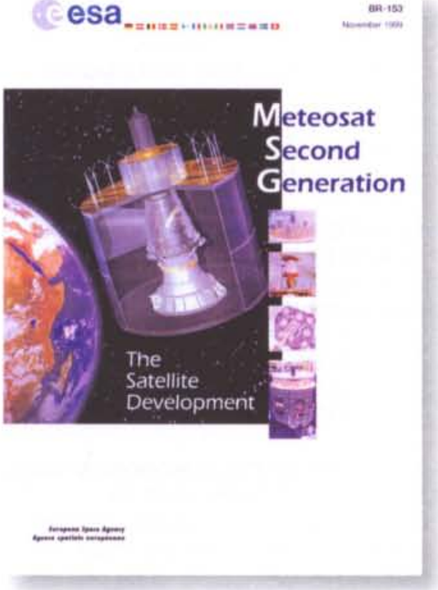

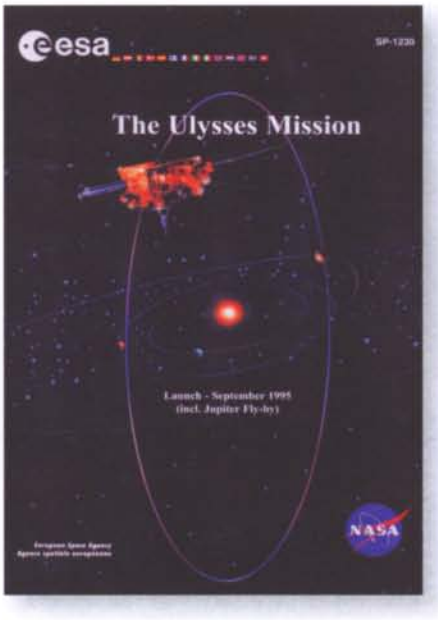

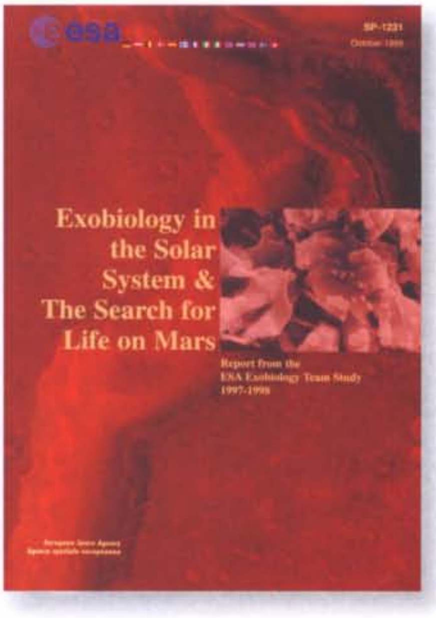

PRICE: 70 DFL / 32 €
ESA-INDUSTRY SPACE DAYS – ASSESSMENT REPORT, ESTEC, NOORDWIJK, 26-27 MAY 1999 (AUGUST 1999)
BAUGHAROUAT N. (ED. T.D. GUYENNE)
ESA SP-1236 // 45 PP
PRICE: 30 DFL / 10 €

INES GUIDE NO.1 – INTERNATIONAL ULTRAVIOLET EXPLORER IUE NEWLY EXTRACTED SPECTRA / HERBIG – HARO OBJECTS (SEPTEMBER 1999)
GOMEZ DE CASTRO A.I., ROBLES A. & WAMSTEKER W. (ED. R.A. HARRIS)
ESA SP-1237 // 166 PP
PRICE: 70 DFL / 30 €

THE HISTORY OF THE EUROPEAN SPACE AGENCY – PROCEEDINGS OF AN INTERNATIONAL SYMPOSIUM, LONDON, 11-12 NOVEMBER 1998 (JUNE 1999)
HARRIS R.A. (ED.)
ESA SP-436 // 252 PP
PRICE: 70 DFL / 30 €

EUROPEAN ROCKET AND BALLOON PROGRAMMES AND RELATED RESEARCH – PROCEEDINGS OF THE 14TH ESA SYMPOSIUM, POTSDAM, GERMANY 31 MAY – 3 JUNE 1999 (SEPTEMBER 1999)
SCHÜRMANN B. (ED.)
ESA SP-437 // 620 PP
PRICE: 100 DFL / 60 €

SPACE MECHANISMS AND TRIBOLOGY – PROCEEDINGS OF THE 8TH EUROPEAN SYMPOSIUM, TOULOUSE-FRANCE, 29 SEPTEMBER – 1 OCTOBER 1999 (SEPTEMBER 1999)
DANESY D. (ED.)
ESA SP-438 // 345 PP
PRICE: 75 DFL / 34 € (CD VERSION 25 DFL / 11 €

ESA Procedures, Standards & Specifications

SPACE PRODUCT ASSURANCE – THE MANUAL SOLDERING OF HIGH-RELIABILITY ELECTRICAL CONNECTIONS (AUGUST 1999)
ECSS SECRETARIAT
ESA ECSS-Q-70-08A // 94 PP
PRICE: 50 DFL / 20 €

SPACE PRODUCT ASSURANCE – THE APPLICATION OF THE BLACK COATING AEROGLAZE Z306 (JULY 1999)
ECSS SECRETARIAT
ESA ECSS-Q-70-25A // 32 PP
PRICE: 35 DFL / 10 €

SPACE PRODUCT ASSURANCE – THE DETERMINATION OF OFFGASSING PRODUCTS FROM MATERIALS AND ASSEMBLED ARTICLES TO BE USED IN A MANNED SPACE VEHICLE CREW COMPARTMENT (JULY 1999)
ECSS SECRETARIAT
ESA ECSS-Q-70-29A // 26 PP
PRICE: 35 DFL / 10 €

SPACE PRODUCT ASSURANCE – THE APPLICATION OF THE THERMAL CONTROL COATING PSG 120FD (JULY 1999)
ECSS SECRETARIAT
ESA ECSS-Q-70-33A // 34 PP
PRICE: 35 DFL / 10 €

SPACE PRODUCT ASSURANCE – THE APPLICATION OF THE BLACK ELECTRICALLY CONDUCTIVE COATING AEROGLAZE H322 (JULY 1999)
ECSS SECRETARIAT
ESA ECSS-Q-70-34A // 32 PP
PRICE: 35 DFL / 10 €

SPACE PRODUCT ASSURANCE – THE APPLICATION OF THE BLACK ELECTRICALLY CONDUCTIVE COATING AEROGLAZE L300 (JULY 1999)
ECSS SECRETARIAT
ESA ECSS-Q-70-35A // 32 PP
PRICE: 35 DFL / 10 €

ESA Scientific & Technical Memoranda

AN INVESTIGATION INTO BALL GRID ARRAY INSPECTION TECHNIQUES (SEPTEMBER 1999)
WICKHAM M., HUNT C., ADAMS D.M. & DUNN B.D.
ESA STM-261 // 59 PP
PRICE: 50 DFL / 16 €

CODE-DIVISION MULTIPLE ACCESS FOR SATELLITE PERSONAL COMMUNICATION SYSTEMS (OCTOBER 1999)
DE GAUDENZI R. (ED. B. BATTRICK)
ESA STM-262 // 442 PP
PRICE: 110 DFL / 50 €

DIGITAL SIGNAL-PROCESSING TECHNIQUES FOR PERSONAL AND BROADCASTING SATELLITE COMMUNICATION SYSTEMS (OCTOBER

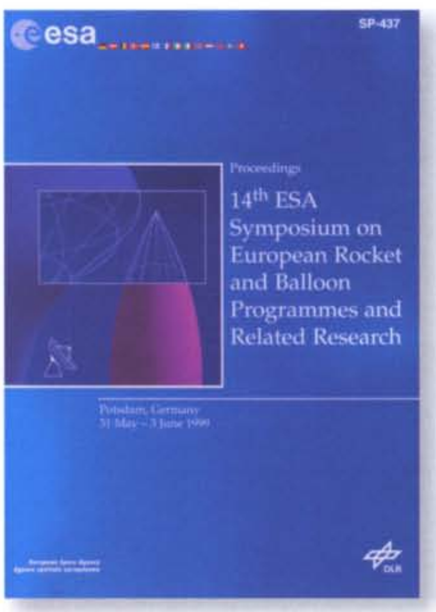

1999)
COLZI E. (ED. B. BATTRICK)
ESA STM-263 // 249 PP
PRICE: 90 DFL / 40 €

ESA Contractor Reports

ATV ENHANCEMENT FOR ADDITIONAL MISSIONS ANTENNA STUDY – EXECUTIVE SUMMARY (FEBRUARY 1999)
DAIMLER CHRYSLER AEROSPACE, GERMANY
ESA CR(P)-4248 // 45 PP
PRICE: 25 DFL / 10 €

STUDY OF PRECISE RELATIVE POSITIONING USING GNSS THREE-CARRIER AMBIGUITY RESOLUTION (TCAR) – FINAL REPORT (MARCH 1998)
SPECTRA PRECISION, GERMANY
ESA CR(P)-4249 //82 PP
PRICE: 50 DFL / 20 €

PRODUCT ASSURANCE FOR NEXT-GENERATION SPACE SYSTEMS – FINAL REPORT (MAY 1999)
MATRA MARCONI SPACE, FRANCE
ESA CR(P)-4250 // 261 PP
PRICE: 90 DFL / 40 €

COST REDUCTION PROGRAMME FOR GAAS SUBSTRATES REQUIRED FOR SOLAR CELL MANUFACTURING – FINAL REPORT (NOVEMBER 1998)
FREIBERGER COMPOUND MATERIALS GMBH, GERMANY
ESA CR(P)-4251 // 33 PP
PRICE: 25 DFL / 10 €

METEOROIDS & DEBRIS FLUX AND EJECTA MODELLING – FINAL REPORT (DECEMBER 1998)
UNISPACE KENT, UK
ESA CR(P)-4252 // 499 PP
PRICE: 110 DFL / 50 €

TRIBOLOGY ADAPTATION SURFACE ADHESION – FINAL REPORT AND EXECUTIVE SUMMARY (NOVEMBER 1998)
CSEM, SWITZERLAND
ESA CR(P)-4253 // 36 PP AND 20 PP
PRICE: 25 DFL AND 25 DFL / 10 € AND 10 €

FIBRE OPTIC GYROS FOR SPACE USE – FINAL REPORT (APRIL 1999)
EUROFOG, FRANCE
ESA CR(P)-4254 // 89 PP
PRICE: 50 DFL / 20 €

SIMULATION TOOL FOR MANOEUVRING OF A SERVICING/INSPECTION VEHICLE – MIV TOOL – EXECUTIVE SUMMARY (APRIL 1999)
ALENIA, ITALY
ESA CR(P)-4255 // 29 PP
PRICE: 25 DFL / 10 €

MICROCONTROLLER FOR ON-BOARD DATA HANDLING – FINAL REPORT (MARCH 1999)
ADV ENGINEERING, FRANCE
ESA CR(X)-4256 // 11 PP
PRICE: 25 DFL / 10 €

FEASIBILITY STUDY OF HIGH SPATIAL RESOLUTION RADAR ALTIMETER (HSRRA), – FINAL REPORT (APRIL 1999)
ALENIA, ITALY
ESA CR(P)-4257 // 552 PP
PRICE: 110 DFL / 50 €

FREE-FLYING MICRO OPERATOR STUDY – EXECUTIVE SUMMARY (JULY 1999)
ALENIA, ITALY
ESA CR(P)-4258 // 28 PP
PRICE: 35 DFL / 10 €

MICRO-ROBOTS FOR SCIENTIFIC APPLICATIONS – EXECUTIVE SUMMARY (MARCH 1999)
VON HOERNER & SULGER GMBH, GERMANY
ESA CR(P)-4259 // 47 PP
PRICE: 35 DFL / 10 €

HIGH-RESOLUTION STANDARD PROXIMITY SENSOR – FINAL REPORT (SEPTEMBER 1999)
VIBRO-METER, SWITZERLAND
ESA CR(P)-4260 // 43 PP
PRICE: 35 DFL / 10 €

32-BIT MICROPROCESSOR AND COMPUTER DEVELOPMENT PROGRAMME – FINAL REPORT (MAY 1997)
SAAB ERICSSON SPACE, SWEDEN
ESA CR(P)-4261 // 101 PP
PRICE: 50 DFL / 20 €

DIGITAL SWITCHED ISL AND BURSTY ACCESS TECHNOLOGY – EXECUTIVE SUMMARY (MAY 1999)
NORTEL TELECOM, BELGIUM
ESA CR(P)-4262 // 15 PP
PRICE: 35 DFL / 10 €

Contractor Reports

There are two types of Contractor Reports: CR(P) and CR(X) reports.

ESA CR(P) documents are available on microfiche from either of the following addresses:

British Library - Doc. Supply Centre
Customer Service
Boston Spa
Wetherby, West Yorkshire
LS23 7BQ
England

Universitaetsbibliothek und TIB
Welfengarten 1B
D-30167 Hannover
Phone: (+49) 511/762-2268
Fax: (+49) 511/715936

ESA CR(X) documents have restricted distribution and are not available on microfiche. Printed copies can be requested via ESA Publications Division

Credit Card Payments for ESA Publications

It is possible to purchase the Agency's publications from the ESA Publications Division 'Bookshop' using your corporate or your personal credit card (Eurocard/Mastercard, Visa or American Express).

You can telephone or telefax your orders to the numbers given below, quoting your card's number and its expiry date.

The Bookshop (attn. Mr Frits de Zwaan)
ESA Publications Division
ESTEC
Keplerlaan 1
2200 AG Noordwijk
The Netherlands

Telephone: (31) 71 5653405
Telefax: (31) 71 5655433

Other methods of payment are also accepted. Please call or fax for details.

A list of the latest publications can be accessed via the ESA Publications Division's Home Page at the following Internet/WWW address:

http://esapub.esrin.esa.it/

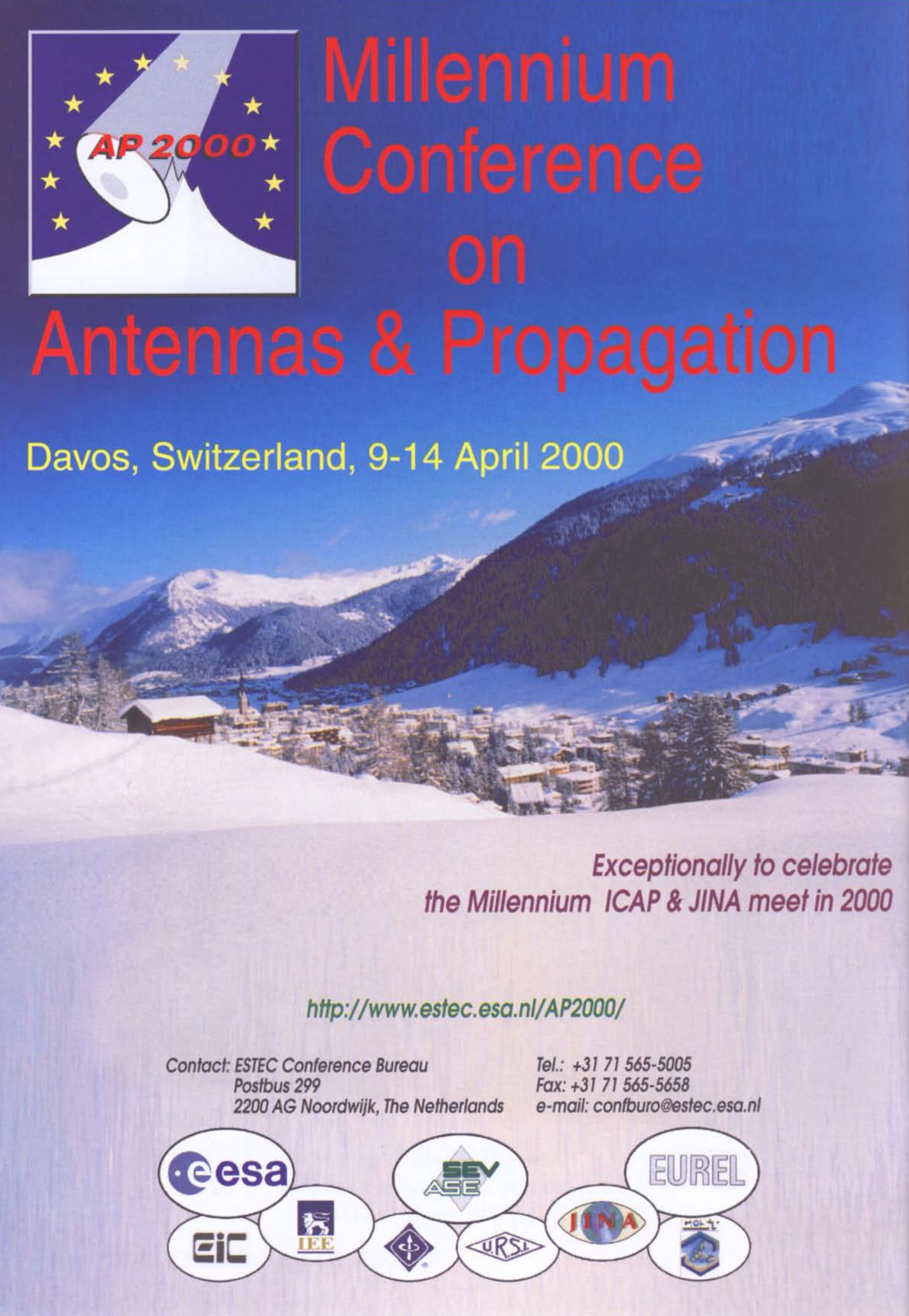
AP 2000
Millennium
Conference
on
Antennas & Propagation
Davos, Switzerland, 9-14 April 2000
Exceptionally to celebrate
the Millennium ICAP & JINA meet in 2000
http://www.estec.esa.nl/AP2000/
Contact: ESTEC Conference Bureau
Postbus 299
2200 AG Noordwijk, The Netherlands
Tel.: +31 71 565-5005
Fax: +31 71 565-5658
e-mail: confburo@estec.esa.nl
esa
SEV ASE
EUREL
EIC
IEE
U.R.S.I.
JINA

Publications Available from ESA Publications Division

Publication	Number of issues per year	Scope/Contents	Price	Source
Periodicals				
ESA Bulletin	4	ESA's primary magazine	Free of charge	ESA Publications Division, c/o ESTEC, 2200 AG Noordwijk, The Netherlands
Earth Observation Quarterly	4	Remote-sensing news	"	"
ECSL News	4	News from the European Centre for Space Law (under the auspices of ESA)	"	"
Reaching for the Skies	4	ESA's Space Transportation Systems news	"	"
Microgravity News	3	Microgravity Programme news	"	"
Preparing for the Future	4	Technology Programme news	"	"
Monographs	**Code**			
Conference Proceedings	(SP-xxx)	Collection of papers presented at an ESA conference	Prices vary	ESA Publications Division, c/o ESTEC, 2200 AG Noordwijk, The Netherlands
Special Publications	(SP-xxxx)	Detailed monographs on post-graduate level subjects	"	"
Brochures	(BR-xxx)	Concise summaries on specific subjects	"	"
Scientific & Technical Reports	(STR-xxx)	Graduate level — reflecting ESA's position on a given subject	"	"
Scientific & Technical Memoranda	(STM-xxx)	Graduate level — latest but not finalised thinking on a given subject	"	"
Procedures, Standards & Specifications	(PSS-xxx)	Definitive requirements in support of contracts	"	"
Training Manuals	(TM-xxx)	Series for education of users or potential users of ESA programmes, services or facilities	"	"
Public-relations material		General literature, posters, photographs, films, etc.		ESA Public Relations Service 8-10 rue Mario-Nikis 75738 Paris 15, France

All periodicals are also available via the Internet at:

http://esapub.esrin.esa.it/

Selected public-relations material and other ESA information is available at:

http://www.esrin.esa.it

Order Form for ESA Publications

Without receipt of payment no publications are sent. All payments in Dutch Guilders (Dfl). Within Europe, mailing is free of charge. Outside Europe, airmail is free of charge for orders over Dfl. 100; smaller orders are sent sea mail.

No. of copies	ESA reference	Title	Price per copy Dfl.	Total Dfl.
			Order Subtotal:	
			Discount for orders over Dfl. 100: less 10% of subtotal:	
			Total amount:	

MAILING ADDRESS *(please print carefully):*

Name

Function Organisation

Address

Town & Postal Code Country

Date Signature

PAYMENT *please tick one box:*

O Cheque enclosed (made payable to ESA Publications Division)
return order form with cheque to: ESTEC - Finance Division (EFA/P)
P.O.Box 299 - 2200AG Noordwijk - The Netherlands

O Items ordered are all free of charge

Credit Card: O Eurocard/Mastercard O Visa O AmEx

Card No. expires:

Name Card Holder

return form to: The Bookshop (attn. Mr. Frits de Zwaan) - ESA Publications Division - ESTEC
P.O.Box 299 - 2200AG Noordwijk - The Netherlands; FAX: +31 - (0)71 565 5433

Telephone orders (and further information) : *+31 (0)71 565 3405*

Information via e-mail: FDEZWAAN@ESTEC.ESA.NL
Internet - list of the latest publications: http://esapub.esrin.esa.it/esapub.html
Printed annual catalogues of ESA publications are available free of charge from the bookshop.

Member States

Austria
Belgium
Denmark
Finland
France
Germany
Ireland
Italy
Netherlands
Norway
Spain
Sweden
Switzerland
United Kingdom

Etats membres

Allemagne
Autriche
Belgique
Danemark
Espagne
Finlande
France
Irlande
Italie
Norvège
Pays-Bas
Royaume-Uni
Suède
Suisse

European Space Agency
Agence spatiale européenne

Contact: ESA Publications Division
c/o ESTEC, PO Box 299, 2200 AG Noordwijk, The Netherlands
Tel (31) 71 565 3400 - Fax (31) 71 565 5433
Visit ESA Publications at: http://www.esa.int